Dietary regulation of microRNA expression in colorectal cells

Karen Joy Humphreys

Bachelor of Medical Science

Bachelor of Nutrition and Dietetics (Honours)

Department of Gastroenterology and

Department of Nutrition and Dietetics

School of Medicine

Faculty of Health Science

Flinders University

A thesis submitted for the degree of

Doctor of Philosophy

2012

Table of Contents

List of Figures

List of Tables

List of Abbreviations

Ac	acetylation
ACTB	beta actin
ACVR2	activin type 2 receptors
AGO2	argonaute-2
AKT (PKB)	v-akt murine thymoma viral oncogene homolog 1
ANOVA	analysis of variance
APC	adenomatous polyposis coli
APS	ammonium persulfate
Arg	arginine
BAX	BCL2-associated X protein
BCL2L11 (Bim)	BCL2-like 11 (apoptosis facilitator)
BR	butyrate-resistant
BRAF	v-Raf murine sarcoma viral oncogene homolog B1
C13ORF25	C13 open reading frame 25
CAS	cellular apoptosis susceptibility
CCDC88A	coiled-coil domain containing 88A
CCND1	cyclin D1
CCNE1	cyclin E1
CDK19 (CDC2L6)	cyclin-dependent kinase 19
CDK8	cyclin-dependent kinase 8
CDKN1A (p21)	cyclin-dependent kinase inhibitor 1A
CDKN2A	cyclin-dependent kinase inhibitor 2A
cDNA	complementary DNA
CDX2	caudal type homeobox 2
ChIP	chromatin immunoprecipitation
CHX	cycloheximide
CIMP	CpG island methylator phenotype
CIN	chromosomal instability
CRC	colorectal cancer
CSIRO	Commonwealth Scientific and Industrial Research Organisation
CTGF	connective tissue growth factor
CTNNB1	catenin (cadherin-associated protein), beta 1
DALY	disability-adjusted life year

DGCR8	DiGeorge syndrome critical region gene 8
DMSO	dimethyl sulfoxide
DNA	deoxyribonucleic acid
DNMT1	DNA (cytosine-5-)-methyltransferase 1
DNMT3A	DNA (cytosine-5-)-methyltransferase 3 alpha
DNMT3B	DNA (cytosine-5-)-methyltransferase 3 beta
dsRNA	double stranded RNA
DTT	dithiothreitol
E2F	E2F transcription factor family
E2F1	E2F transcription factor 1
E2F2	E2F transcription factor 2
E2F3	E2F transcription factor 3
ECL	enhanced chemiluminescence
EDTA	ethylenediaminetetraacetic acid
EGR2	early growth response 2
EMAST	elevated microsatellite instability at selected tetranucleotide repeats
EPIC	European Prospective Investigation into Cancer and Nutrition
ESR1	estrogen receptor 1
FAP	familial adenomatous polyposis
FBXW7	F-box and WD repeat domain containing 7, E3 ubiquitin protein ligase
FDA	US Food and Drug Administration
FOS	v-fos FBJ murine osteosarcoma viral oncogene homolog
FSANZ	Food Standards Australia New Zealand
GAB1	GRB2-associated binding protein 1
GAB2	GRB2-associated binding protein 2
GADD45A	growth arrest and DNA-damage-inducible, alpha
H1/H5	histone 1/ histone 5
H2A and 2B	histone 2A and 2B
H3	histone 3
H4	histone 4
HAT	histone acetyltransferase
HER2 (ERBB2)	human epidermal growth factor receptor 2
HDAC	histone deacetylase
HDI	histone deacetylase inhibitor

HDM	histone demethylases
His	histidine
HMT	histone methyltransferase
HNPCC	hereditary nonpolyposis colorectal cancer
hnRNPA1	heterogeneous nuclear ribonucleoprotein A1
HRAS	v-Ha-ras Harvey rat sarcoma viral oncogene homolog
IgG	immunoglobulin G
IP	immunoprecipitation
IPA	Ingenuity Pathway Analysis
JARID1B	histone demethylase jumonji, AT rich interactive domain 1B
K	lysine
KRAS	v-Ki-ras2 Kirsten rat sarcoma viral oncogene homolog
LIN28A	lin-28 homolog A
Lys	lysine
MAP	mitogen-activated protein
MAPK7 (ERK5)	mitogen-activated protein kinase 7
MAPK12	mitogen-activated protein kinase 12
MCC	mutated in colorectal cancers
me	methylation
me2	di-methylation
me3	tri-methylation
MGMT	O6-methylguanine-DNA methyltransferase
MIR17HG	miR-17-92 cluster host gene
miRNA	microRNA
MLH1	DNA mismatch repair protein MLH1 (MutL protein homolog 1)
MLH2	DNA mismatch repair protein MLH2 (MutL protein homolog 2)
MSH2	mutS homolog 2
MSH3	mutS homolog 3
MSH6	mutS homolog 6
MSI	microsatellite instability
MSS	microsatellite stable
MYB	v-myb myeloblastosis viral oncogene homolog
MYC (C-MYC)	myelocytomatosis oncogene
NC	negative control
NEDD9 (HEF1)	neural precursor cell expressed, developmentally down-regulated 9

NF-κB	nuclear factor kappa-light-chain-enhancer of activated B cells
NHMRC	National Health and Medical Research Council
NR	not reported
NRAS	neuroblastoma RAS viral (v-ras) oncogene homolog
NRM	normal rectal mucosa
NSP	non-starch polysaccharide
O6CMG	O6-carboxymethylguanine
O6MeG	O6-methyl-2-deoxyguanosine
PACT	protein activator of PKR
PBS	phosphate buffered saline
PcG	polycomb group
PDCD4	programmed cell death 4
RHOB	ras homolog family member B
PI3K	phosphatidylinositol 3-kinases
PIC	protease inhibitor cocktail
PIK3CA	phosphoinositide-3-kinase, catalytic, alpha polypeptide
PMS2	postmeiotic segregation increased 2
PMSF	phenylmethylsulfonyl fluoride
pre-miRNA	precursor miRNA
pri-miRNA	primary miRNA
PTEN	phosphatase and tensin homolog
RISC	RNA-induced silencing complex
RM	red meat
RNA	ribonucleic acid
RNAi	RNA interference
RNU6B	U6B small nuclear RNA
RPL30	ribosomal protein L30
RS	resistant starch
RTCA	real-time cell analysis
RT-PCR	reverse transcription polymerase chain reaction
SDS-PAGE	sodium dodecyl sulfate polyacrylamide gel electrophoresis
SAHA	suberoylanilide hydroxamic acid
SCFA	short-chain fatty acid
SD	standard deviation
SEM	standard error of the mean
shRNA	short hairpin RNA

siRNA	small interfering RNA
SIS (PDGFB)	platelet-derived growth factor beta polypeptide
SMAD2	SMAD family member 2
SMAD3	SMAD family member 3
SMAD4	SMAD family member 4
SP1	Sp1 transcription factor
SP3	Sp3 transcription factor
TBS	tris-buffered saline
TCF4	transcription factor 4
TEMED	tetramethylethylenediamine
TGFBIIR	transforming growth factor beta, receptor type II
TNM	Tumour Node Metastasis (TNM) Classification of Malignant Tumours
TP	target protector
TP53	tumour protein p53
TPM1	tropomyosin 1
TRBP	human immunodeficiency virus transactivating response RNA-binding protein
TRxG	trithorax group
TS	thymidylate synthase
TSA	trichostatin A
TSP1	thrombospondin-1
TSS	transcription start site
TXNIP	thioredoxin-interacting protein
UTR	untranslated region
WCRF	World Cancer Research Fund
WNT	wnt signalling protein
XPO5	exportin 5
YLL	years of life lost

Summary

Colorectal cancer (CRC) development is associated with epigenetic modifications, including DNA methylation changes, altered histone modification patterns, and dysregulated microRNA (miRNA) expression. While some dietary compounds can alter colorectal cell behaviour through epigenetic mechanisms, their role in modifying miRNA expression in CRC cells and normal colorectal tissue has been less studied. The diet-derived compound butyrate, with its known role in histone modification, is a plausible candidate for altering miRNA expression. This study examined dietary regulation of miRNA expression in colorectal cells, and explored the role of butyrate and other histone deacetylase inhibitors (HDIs) in modulating CRC risk through altered miRNA expression. The down-stream consequences of these miRNA changes, and the roles of miRNAs in the context of the anti-proliferative effects of HDIs, were determined. In addition to exploring the action of butyrate, a potentially protective dietary component, the study also investigated whether factors that possibly increase CRC risk, such as high red meat intake, alter miRNA expression.

In vitro, butyrate and other HDIs altered levels of some miRNAs that are dysregulated in CRC, including the oncogenic miR-17-92 miRNA cluster which is over-expressed in CRC. Butyrate decreased miR-17-92 miRNA levels in CRC cells, with a corresponding increase in expression of miR-17-92 targets, including cell cycle inhibitors and pro-apoptotic genes. Mechanisms for this decrease included changes in regulators of miR-17-92 host gene transcription, and altered histone acetylation and methylation patterns centred around the transcription start site and promoter of the miR-17-92 host gene. Decreased miR-17-92 expression may be partly responsible for the anti-proliferative effects of HDIs, with introduction of miR-17-92 cluster miRNA mimics reversing this effect and decreasing target gene transcript levels. Of the cluster members, miR-19a and miR-19b were primarily responsible for promoting proliferation, while in a novel finding, miR-18a acted in opposition to other members to decrease growth. Two pro-proliferative genes, *NEDD9* and *CDK19*, were identified as novel miR-18a targets. This study presents the first evidence of competing roles for miR-17-92 cluster members, in the context of HDI-induced changes in CRC. miR-18a may play a homeostatic role in containing the oncogenic effects of the entire cluster, but may be selectively decreased in CRC compared with other cluster members.

SUMMARY

In addition to the capacity of butyrate to reverse the dysregulation of miR-17-92 miRNAs in CRC cells *in vitro*, this action was demonstrated with resistant starch supplementation *in vivo*, in rectal biopsies from healthy human volunteers exposed to high red meat levels. High red meat intake raised levels of miRNAs with oncogenic potential, particularly miR-17-92 cluster miRNAs and miR-21. Resistant starch supplementation raised faecal butyrate concentrations, and decreased miR-17-92 cluster miRNAs to baseline levels. *In vivo* modulation of miRNAs in colorectal cells by dietary compounds has not previously been demonstrated in humans. Regulation of miRNA expression demonstrates a plausible mechanism to explain some of the chemo-protective effects of butyrate, and potentially carcinogenic properties of other dietary components. Understanding how dietary compounds alter miRNA expression, and how miRNAs modulate the action of HDIs, may provide new opportunities for CRC therapies and prevention strategies.

Declaration

I certify that this thesis does not incorporate without acknowledgment any material previously submitted for a degree or diploma in any university; and that to the best of my knowledge and belief it does not contain any material previously published or written by another person except where due reference is made in the text.

Karen J Humphreys

Publications and Presentations

Peer-reviewed Publications

Humphreys KJ, Cobiac L, Le Leu RK, Van der Hoek MB, Michael MZ. Histone deacetylase inhibition in colorectal cancer cells reveals competing roles for members of the oncogenic miR-17-92 cluster. *Molecular Carcinogenesis*. 5 February 2012. [Epub ahead of print].

Poster Presentations

Humphreys KJ, Le Leu RK, Cobiac L, Michael MZ. Butyrate alters microRNA expression in colorectal cells. 31st Lorne Genome Conference, Mantra Erskine Resort, Lorne, Victoria, Australia, 14 – 16 February 2010.

Humphreys KJ, Le Leu RK, Cobiac L, Michael MZ. Butyrate alters microRNA expression in colorectal cells. MicroRNAs and Non-Coding RNAs and Cancer Keystone Symposia Conference, Fairmont Banff Springs, Banff, Alberta, Canada, 11 – 16 February 2011.

Humphreys KJ, Cobiac L, Le Leu RK, Van der Hoek MB, Michael MZ. Histone deacetylase inhibition in colorectal cancer cells reveals competing roles for members of the oncogenic miR-17-92 cluster. Epigenetics 2012 4th Australian Scientific Conference, the National Wine Centre of Australia, Adelaide, South Australia, Australia, 7 – 9 May 2012. **Best conference poster prize.**

Oral presentations

Humphreys KJ, Le Leu RK, Cobiac L, Michael MZ. Butyrate alters microRNA expression in colorectal cells. Australian Society for Medical Research Annual Scientific Meeting, the Entertainment Centre, Adelaide, South Australia, Australia, 9 June 2010.

Various presentations at the Flinders Centre for Innovation in Cancer annual research days, Adelaide RNA special interest group meetings, and the Flinders Clinical and Molecular Medicine cluster seminar series.

Acknowledgements

I would like to sincerely thank my PhD supervisors for their advice and support throughout my PhD. I would particularly like to thank Dr Michael Michael for allowing me to undertake research in his laboratory, and for passing on his expert knowledge in the field of miRNAs. I would like to thank Dr Richard Le Leu for giving me the opportunity to be an investigator in the human dietary intervention trial, and Professor Lynne Cobiac for providing assistance on the dietary aspects of my project. Special thanks go to all my supervisors for the time they have given me during my PhD and during the final production of this thesis.

I would also like to thank Professor Graeme Young for his vision and commitment to enabling diet and colorectal cancer research at Flinders University. I am grateful to the Flinders Foundation and the NHMRC for funding during my PhD research.

My laboratory colleagues also deserve thanks for the support they have provided over my PhD, and I am particularly grateful to Letitia Pimlott and Veronika Bandara for their advice and helpful conversations.

I would like to thank Mark Van der Hoek and Rosalie Kenyon from the Adelaide microarray facility for assisting with the miRNA microarray, and researchers at CSIRO for sharing ideas and material. Dr Leah Cosgrove and Dr Kim Fung generously provided the butyrate-resistant cell lines, and collaborators at CSIRO involved in the human dietary intervention trial kindly allowed me to use the collected tissue for miRNA specific investigations.

Finally, a very large thank you goes to my family and friends for their love and support through my PhD journey. Thank you to Dave Mutton for all his support and for enabling me to complete my PhD. Thank you to my mum and dad for always being there to encourage me and provide assistance, and for inspiring me to pursue a career in science.

Chapter 1. Introduction

1.1 Epigenetic modulation of gene expression

Colorectal cancer (CRC), which includes cancer of the colon, the rectosigmoid junction and the rectum, is a major cause of morbidity and mortality worldwide (AIHW 2012, IARC 2012). The majority of CRC cases occur sporadically, and their development may be influenced by environmental and lifestyle factors, including diet (WCRF 2007). Multiple epigenetic events are responsible for the onset and progression of CRC, in addition to genetic changes (Toyota et al 1999, Esteller et al 2001, Zhu et al 2004, Enroth et al 2011).

Epigenetic modulation is the alteration of gene expression or cellular phenotype without changes to the underlying DNA sequence (WCRF 2007). One classic epigenetic mechanism is the remodelling of chromatin leading to altered gene expression. Genomic DNA is wrapped around histone proteins to form nucleosomes, which collectively form a structure known as chromatin. Various levels of chromatin remodelling occur, and include DNA methylation, histone modification, exchange of core histones with variant histones, and disruption of basic nucleosome structure and histone DNA contacts (Hake et al 2004).

Histone modifications largely occur along the tails of core histones that protrude from the chromatin unit. These are subject to multiple post-translational modifications, including methylation, acetylation, phosphorylation and other processes (Luger et al 1997, Strahl & Allis 2000). These histone modifications can open or compact the chromatin structure and affect levels of transcription and gene expression (Luger et al 1997, Strahl & Allis 2000, Hake et al 2004, Campos & Reinberg 2009, Guil & Esteller 2009). Numerous enzymes are involved in histone modifications (Allis et al 2007, Kouzarides 2007). Histone methyltransferases (HMT) and histone demethylases (HDM), for example, control levels of histone methylation, while histone acetyltransferases (HATs) and histone deacetylases (HDACs) are responsible for increasing and decreasing histone acetylation respectively. Increased histone acetylation generally promotes a more relaxed chromatin structure, allowing transcriptional activation, while decreased acetylation can lead to transcriptional repression (Turner 1998, Strahl & Allis 2000). Additional layers of complexity exist, however, with distinct patterns of specific histone modifications shown to play particular roles in gene activation or silencing. This complexity gave rise to the 'histone code' hypothesis, which

proposed that one modification or combination of histone modifications could determine a particular functional output (Strahl & Allis 2000, Jenuwein & Allis 2001). The outcomes of histone modifications can be to initiate transcriptional activation, silencing or other cellular responses, and are reviewed in more detail in Chapter 7 (Strahl & Allis 2000, Jenuwein & Allis 2001).

DNA methylation, which is catalysed by DNA methyltransferase enzymes, can also result in chromatin reconfiguration and transcriptional repression (Nan et al 1998). DNA methylation involves the addition of a methyl group to cytosine residues at adjacent cytosine and guanine nucleotides (CpG di-nucleotides). CpG di-nucleotides occur in high concentration in certain areas of the genome, and are referred to as CpG islands. CpG islands are often found at the 5' promoter region of genes, and around 60% of genes have a CpG island at their promoter (Bird 2002). DNA methylation of a CpG island at a gene promoter can lead to silencing of this gene, by directly inhibiting binding of transcription factors and by recruiting transcription co-repressor complexes that can cause chromatin reconfiguration (Boyes & Bird 1991, Cross et al 1997, Nan et al 1997, Nan et al 1998).

In addition to chromatin remodelling, another common epigenetic machinery is the regulation of gene expression by non-coding RNAs such as microRNAs (miRNAs). miRNAs are small non-coding RNA sequences that post-transcriptionally regulate the expression of target genes by binding to complementary target mRNAs. They can cleave complementary mRNAs, or where there is imperfect complementarity, can act through translational inhibition and transcript destabilisation (Hutvagner & Zamore 2002, Filipowicz et al 2008, Guo et al 2010). miRNAs have a unique place in the field of epigenetics; they can be classified as epigenetic regulators of gene expression, but can themselves experience altered transcription via epigenetic mechanisms. As outlined in the sections below, epigenetic machineries play a vital role in the development and progression of CRC, and may be influenced by dietary components.

1.2 Development and progression of colorectal cancer

1.2.1 Epidemiology of colorectal cancer

Worldwide, CRC is the third most common cancer, with around 1.2 million new cases recorded in 2008 (IARC 2012). There is large geographical variation in the global distribution of CRC, with the highest incidence in the USA, Australia, New Zealand, and parts of Europe, the lowest incidence in Africa and Asia, and intermediate levels in

South America (IARC 2007, Jemal et al 2011, IARC 2012). Incidence can vary up to 10-fold between countries with the highest and lowest rates, with almost 60% of cases occurring in developed regions (IARC 2007, IARC 2012). While incidence may be stabilising in long-standing developed countries, it is increasing rapidly in economically developing countries (Center et al 2009, Jemal et al 2011). CRC is a major contributor to both morbidity and mortality, particularly in countries which have the highest incidence of the disease (IARC 2012). Mortality is approximately half that of incidence, with around 600,000 deaths recorded in 2008 worldwide, making CRC the fourth most common cause of death from cancer (IARC 2012). Mortality rates are decreasing in some developed countries, due to improved treatment and early detection, but are increasing in many developing countries (Center et al 2009, Jemal et al 2011).

In Australia, CRC is the second most frequently occurring cancer in the population, with 14,255 people diagnosed with the disease in 2008 (13% of all cancer cases) (AIHW 2011). The age-standardised incidence rate in 2008 was 61.8 per 100,000, with risk of diagnosis before age 85 at 1 in 12 (AIHW 2011). While cancer incidence projections to 2020 indicate that the number of new CRC cases per year may be stabilising, CRC will remain among the most common cancers diagnosed in Australia in 2020 (AIHW 2012). CRC is the second most common cause of cancer death in Australia, with 4,047 deaths in 2007, accounting for 2.9% of all person deaths and 10.1% of all cancer deaths (AIHW 2011). The age-standardised mortality rate in 2007 was 17.8 per 100,000, with risk of dying from CRC before age 85 at 1 in 41 (AIHW 2011). In 2010, CRC was estimated to be the second leading cause of the burden of disease due to cancer (37,800 disability-adjusted life years (DALYs) in males (13% of cancer burden) and 30,300 DALYs in females (12% of cancer burden)). It was also the second highest cancer contributing to years of life lost (YLL) due to premature death (55,800 YLL) (AIHW 2010). The total health expenditure in 2000 – 01 for CRC was $235 million (AIHW 2005).

1.2.2 Characteristics of colorectal cancer development

The colon and rectum are the final sections of the digestive system in humans and most vertebrates. Functions of the colon include storage of waste, absorption of water, salts and some nutrients, and bacterial-aided fermentation of undigested material, before elimination from the body (Cummings 1975, Ruppin et al 1980). The transformation of normal colonic mucosa into invasive cancer can often take years to decades (Al-Sohaily et al 2012). This development generally involves multiple steps, from aberrant crypt cells

and epithelial hyperplasia, to adenomatous polyps, carcinoma, and metastasis (Muto et al 1975, Fearon & Vogelstein 1990).

In a healthy colorectum there exists a balance between proliferation, differentiation, migration and apoptosis. The adult colorectal epithelium undergoes constant regeneration as differentiated cells at the epithelial surface are shed and replaced by new cells (Booth & Potten 2000, Mariadason et al 2002, Kosinski et al 2007). The lining of the colon consists of millions of crypts, which each contain thousands of cells, including multiple stem cells that maintain the crypts through continual division and differentiation (Booth & Potten 2000, Yatabe et al 2001, Kim & Shibata 2002, Kosinski et al 2007, Powell et al 2012). The stages of cell division include a resting phase (G_0), growth and preparation of chromosomes for replication (G_1), DNA replication (S), preparation of cells for division (G_2), and mitosis (M), with several checkpoints to check for DNA damage or errors in replication (WCRF 2007). Stem cell division can yield more stem cells, and also cells that migrate upward through the crypt, proliferate and differentiate (Snippert et al 2010). Differentiated epithelial cells have a rapid turnover, while stem cells that are maintained at the base of the crypt can accumulate alterations in the copied DNA over time, if not recognised by DNA repair mechanisms (Yatabe et al 2001, Kim & Shibata 2002). Most alterations will be lost, but sometimes in a clonal selection process a single crypt may sequentially collect multiple alterations that provide a growth advantage (crypt niche succession); rarely, this combination of alterations collectively confers a tumour phenotype (Kim & Shibata 2002, Barker et al 2009). Alterations may lead to novel or increased function of oncogenes, or loss of function of tumour suppressor genes, leading to the visible start of a growth advantage and phenotypic progression (Fearon 2011).

Aberrant crypts can progress to lesions that project above the surrounding mucosa, and are termed polyps. Small hyperplastic polyps will only rarely progress to CRC, while adenomatous polyps (adenomas), which are characterised by dysplastic morphology and altered differentiation, are more likely to be precursors to CRC (Winawer et al 2006). Some polyps, identified as serrated polyps, have a distinct development pathway not seen in traditional adenomas, and progress to cancer via a different pathway, the serrated neoplasia pathway (Torlakovic et al 2003, Konishi et al 2004, Spring et al 2006). Only a fraction of adenomas will ever progress to CRC (Winawer et al 2006). CRC tumours are characterised by uncontrolled growth and evasion of apoptosis, sustained angiogenesis, and eventual tissue invasion and metastasis (WCRF 2007). The process of invasion and metastasis involves detachment of tumour cells from the primary site,

migration, invasion of blood or lymphatic vessels, dissemination, and finally settlement in the distant site (Al-Sohaily et al 2012).

CRC may be detected through routine screening, such as a faecal occult blood test, sigmoidoscopy or colonoscopy, or may first present with the development of symptoms. Symptoms are common in advanced CRC when prognosis is poor but are less common and obvious early in the disease (Cappell 2008). A two-step process is commonly employed to detect early stage CRC, with a colonoscopy performed when an initial faecal occult blood test is positive (Levin et al 2008). Besides serving as a detection method, a colonoscopy allows biopsies to be performed, and pre-cancerous polyps to be removed, thereby preventing CRC development (Winawer et al 1993, Cappell & Friedel 2002). CRC diagnosis and staging can incorporate clinical and pathologic examination. The TNM staging system, developed by the American Joint Committee on Cancer (AJCC) and the International Union Against Cancer (UICC), is commonly used, and is based on the extent of the tumour (T), the extent of spread to the lymph nodes (N), and the presence of metastasis (M). Overall cancer staging can classify cancers as Stage 0 (carcinoma in situ), Stage I (localised cancer), Stage II or III (locally advanced cancer, with degrees of lymph node involvement), or Stage IV (cancer is metastasised, or spread to other organs) (AJCC 2010).

Treatment strategies for CRC are dependent on tumour stage (Crea et al 2011). Early stage CRC that is confined to the sub-mucosa can be treated by surgical resection with curative intent. Surgical excision is the preferred option for localised tumours, while adjuvant chemotherapy may be employed after surgical resection, particularly in patients with lymph node invasion (Cunningham et al 2010). Metastatic CRC patients may be treated with chemotherapeutic agents and best supportive care. While a five-year survival rate of approximately 90% is possible when CRC is detected and treated early, when metastatic disease is detected the median survival is approximately six months (Kohne & Lenz 2009).

1.2.3 Genetic and epigenetic events in colorectal cancer development

Normal colorectal regeneration requires balanced molecular control, with multiple gene expression pathways involved in creating and maintaining this balance. Examples of pathways that maintain a normal colorectal phenotype include the WNT-β-catenin signalling pathway which is involved in maintaining proliferation (Mariadason et al 2001, Batlle et al 2002, van de Wetering et al 2002), the TGF-β superfamily signalling pathway

which plays a role in tissue homeostasis (Becker et al 2004, Bellam & Pasche 2010), and the Notch signalling pathway which influences cell fate and differentiation (Fre et al 2005, Okamoto et al 2009, Zheng et al 2009). CRC progression generally requires multiple genetic and epigenetic events resulting in the loss-of-function of tumour suppressor genes and gain-of-function of oncogenes, and dysregulation of signalling pathways involved in cellular metabolism, proliferation, differentiation, survival and apoptosis (Fearnhead et al 2002, Al-Sohaily et al 2012). Approximately 5% of CRC cases are caused by inherited genetic mutations. Known inherited conditions that predispose to CRC include, among others, familial adenomatous polyposis (FAP) which is an autosomal dominant disorder caused by germ line mutations of the adenomatosis polyposis coli (*APC*) tumour suppressor gene (Kinzler et al 1991), and hereditary non-polyposis colorectal cancer (HNPCC) or Lynch syndrome which is also an autosomal dominant disorder caused by germ line mutations in DNA mismatch repair genes (Fishel et al 1993, Bronner et al 1994, Papadopoulos et al 1994). The remaining 95% of CRC cases occur sporadically via a series of genetic and epigenetic changes, brought about by intrinsic and extrinsic forces. Of this majority, a percentage (~20%) will have a positive family history but cannot be categorised as having any known hereditary CRC syndrome; these cases may have an underlying inherited predisposition, or common environmental and lifestyle factors (Power et al 2010).

The first molecular model of CRC development was offered by Fearon and Vogelstein (1990), which proposed that the mutational activation of oncogenes and inactivation of tumour suppressor genes, and the mutation of at least four or five genes, were required for cancer development. The total accumulation of changes, rather than their order, was seen as responsible for determining the tumour's biologic properties (Fearon & Vogelstein 1990). Since this model, multiple genes have been investigated for their link to CRC development, but only a limited number of gene mutations have been found in a sizable proportion of CRCs, and their combination in the same cancer is less common (Fearon 2011). One common genetic change often associated with adenomatous polyps is loss of function of the tumour-suppressor gene *APC*. Approximately 70 – 80% of sporadic colorectal adenomas and carcinomas have somatic mutations that inactivate *APC* (Fearon 2011). In one CRC model, *APC* has been described as a 'gatekeeper' gene due to its responsibility in maintaining balance in colon cell numbers (Kinzler & Vogelstein 1997). In this model, other genes that maintain genetic integrity, such as DNA mismatch repair genes, may be referred to as 'caretaker genes' (Kinzler & Vogelstein 1997). *APC* assists in the control of cell adhesion, migration, chromosomal

segregation, and apoptosis in the colonic crypt, and is a regulator of the β-catenin-dependent WNT signalling pathway (He et al 1998). Loss of *APC* function leads to accumulation of β-catenin, which in turn binds to transcription factors and alters the expression of multiple genes affecting cell cycle progression, proliferation, differentiation, migration, apoptosis, and angiogenesis (He et al 1998, Tetsu & McCormick 1999). Mutations of the potential oncogene *KRAS* (v-Ki-ras2 Kirsten rat sarcoma viral oncogene homolog) are also found to occur in many early to late adenomas, while mutations of the tumour suppressor p53 (tumour protein p53 or *TP53*) will tend to occur later, and may promote the change from adenoma to carcinoma (Vogelstein et al 1988, Fearnhead et al 2002). Other oncogenes that have altered function in a significant fraction of sporadic CRCs include *PIK3CA*, *BRAF*, *NRAS*, *EGFR*, *CDK8*, *C-MYC*, *CCNE1*, *CTNNB1*, *ERBB2*, and *MYB*, while other tumour suppressors that are commonly mutated include *PTEN*, *FBXW7*, *SMAD2*, *SMAD3*, *SMAD4*, *TGFβIIR*, *TCF7L2*, *ACVR2*, *BAX* and *MCC* (Fearon 2011). Various molecular pathways of CRC have been demonstrated, which lead to different cancer phenotypes. Currently three distinct molecular pathways have been identified, including the Chromosomal Instability (CIN) pathway, the Microsatellite Instability (MSI) pathway, and the CpG Island Methylator Phenotype (CIMP) pathway, although these pathways are not mutually exclusive (Jass 2007).

In the CIN pathway, defects in chromosome segregation lead to loss or gain of chromosomes or chromosome regions containing genes important in the cancer development process (Lengauer et al 1997, Wang et al 2004). This pathway is associated with chromosome number imbalance (aneuploidy), chromosomal genomic amplifications, and loss of heterozygosity (Thiagalingam et al 2001). A large fraction of sporadic CRCs, approximately 65 – 70%, present with altered chromosome number or structure (Al-Sohaily et al 2012). Broad chromosome amplifications and deletions have been observed in CRC, in addition to focal gains or losses in regions containing important cancer genes (Thiagalingam et al 2001, Wang et al 2004). Specific mutations in oncogenes and tumour suppressor genes can occur in addition to these karyotype abnormalities. Common chromosomes and genes affected in the CIN pathway include the 5p allele which harbours the *APC* and *MCC* (mutated in colorectal cancers) genes, the 8p allele, the 17p allele which contains p53, and the 18q allele (Vogelstein et al 1988, Jen et al 1994, Chughtai et al 1999).

Another molecular pathway for CRC development is the MSI pathway. Microsatellites are short repeat nucleotide sequences prone to errors, particularly base-pair mismatches,

during DNA replication. Normally, these errors are recognised and repaired by the DNA mismatch repair system. MSI occurs when the mismatch repair system is unable to recognise and correct these errors (Ionov et al 1993, Thibodeau et al 1993). Defects in mismatch repair genes such as *MLH1*, *PMS2*, *MSH2*, *MSH3* and *MSH6* can occur in hereditary conditions, and in a subset of sporadic CRC (Fishel et al 1993, Bronner et al 1994, Papadopoulos et al 1994, Yin et al 1997, Nicolaides et al 1998). Approximately 15% of sporadic CRC are characterised by MSI, resulting from genetic or epigenetic inactivation of mismatch repair function (Ionov et al 1993, Thibodeau et al 1993, Suraweera et al 2002). In sporadic CRC cases with MSI, epigenetic inactivation of the DNA mismatch repair protein MutL homolog 1 (*MLH1*) is more frequent (Herman et al 1998, Toyota et al 1999). Specific microsatellite loci are usually examined to identify MSI, and define tumours as MSI-high, MSI-low, or microsatellite stable (MSS), or with elevated microsatellite instability at selected tetra-nucleotide repeats (EMAST) (Suraweera et al 2002, Haugen et al 2008). MSI is essentially an indication of defective mismatch repair function. Cells with mismatch repair gene mutations cannot repair spontaneous DNA errors and progressively accumulate mutations throughout the genome, resulting in tumour development. A number of genes have coding repeats that are susceptible to mutations when mismatch repair is defective, including cancer-relevant genes involved in DNA repair, cell cycle control, apoptosis, and signal transduction (Al-Sohaily et al 2012).

The role of epigenetics in the development of CRC was acknowledged with the description of the CIMP pathway for CRC development, which specifically refers to the epigenetic modification of DNA methylation that can occur at CpG islands. In CRC, promoter-specific CpG island hypermethylation is an alternative mechanism to genetic mutations for the silencing of tumour suppressor genes; this is likely an early event in tumourigenesis, and can be more frequent than genetic changes (Toyota et al 1999, Esteller et al 2001, Weisenberger et al 2006, Schuebel et al 2007). Genes with tumour suppressor function that are commonly hypermethylated in CRC include cyclin-dependent kinase inhibitor 2A (*CDKN2A*), the DNA mismatch repair protein *MLH1*, and the DNA repair protein O-6-methylguanine-DNA methyltransferase (*MGMT*) (Toyota et al 1999, Shen et al 2005). CIMP refers to the presence of hypermethylation of multiple genes, and specific markers are examined to identify CIMP positive (CIMP-high) tumours. CIMP-high tumours account for 15 – 20% of sporadic CRC. While there is some debate as to whether the CIMP represents a truly distinct pathway, CIMP tumours have been shown to have unique clinical and pathologic features (Hawkins et al

2002, Jass 2007). The CIMP classification has some overlap with MSI; for example, the silencing of the *MLH1* mismatch repair gene in sporadic MSI-high CRC is usually caused by hypermethylation (Herman et al 1998). There are several examples of the same genes being affected in CRC regardless of the underlying molecular pathway, for example loss of *APC* function is common in many CRC, but this can occur through various mutations, chromosomal abnormalities and loss of heterozygosity, and/or promoter methylation (Miyoshi et al 1992, Huang et al 1996, Hiltunen et al 1997, Sturlan et al 1999, Fodde et al 2001).

Besides the recognised role of promoter DNA hypermethylation in CRC development, other epigenetic mechanisms including global DNA hypomethylation, histone modifications and alterations in miRNA expression can also contribute to CRC development. In contrast to the high levels of gene promoter methylation present in many tumours, global DNA hypomethylation has also been observed in CRC, which may also predispose to genomic instability and disruption of normal gene expression patterns (Matsuzaki et al 2005, Rodriguez et al 2006). CRC is also associated with altered patterns of histone modifications, and dysregulation of proteins responsible for these modifications (Zhu et al 2004, Wilson et al 2006, Enroth et al 2011). Disruption of normal miRNA expression levels has also been shown in CRC, with increased levels of some miRNAs with oncogenic potential, and decreased levels of some miRNAs with tumour suppressor roles, as detailed in Section 1.3 (Michael et al 2003, Cummins et al 2006, Slaby et al 2007).

1.2.4 Risk factors in colorectal cancer development

CRC risk is a combination of genetic predisposition and lifestyle and environmental factors. A small fraction of CRCs result from inherited germ line mutations in genes associated with cancer; while the remaining majority involve alterations accumulated over time, due to genetic mutations or epigenetic changes (WCRF 2007). Increasing age is one of the most important risk factors for CRC, with over 90% of sporadic CRCs occurring in individuals over the age of 50 (Al-Sohaily et al 2012). In addition to the accumulation of mutations over time, epigenetic changes also accelerate with age; increased DNA methylation, for example, has been shown to correlate with advanced age (Toyota et al 1999, Fraga et al 2005a). Family history is also an important risk factor, even when a known hereditary syndrome is not present (Power et al 2010). Internal factors likely to modify risk include oxidative stress, inflammation, and hormonal changes. Environmental and lifestyle risk factors include obesity and physical inactivity,

tobacco and cigarette smoke, and alcohol consumption, as well as excess consumption of potentially carcinogenic food substances and inadequate consumption of protective dietary components (WCRF 2007, Mathers et al 2010, Al-Sohaily et al 2012). While aging and genetic susceptibility are irreversible, some CRCs may be prevented by altering environmental risk factors, in order to minimise inflammation and exposure to mutagens, reduce epithelial cell proliferation, and support the apoptotic removal of damaged cells (Lund et al 2011).

1.3 Diet and colorectal cancer

1.3.1 Dietary influences on the colon

Dietary components can directly affect the genome, and can also epigenetically alter gene expression without altering the DNA sequence (WCRF 2007). The latter is termed nutritional epigenetics, which is the non-coding modification of genes through changes in DNA methylation, histone homeostasis, miRNA levels and DNA stability, in response to nutrition (WCRF 2007). Colonic epithelial cells are directly exposed to dietary compounds, and a significant proportion of CRCs may be diet related. Carcinogens ingested as part of, or with, foods and drinks can interact directly with the cells lining the colon and rectum if they are not metabolised or absorbed in the small intestine (WCRF 2007). Links between diet and cancer risk are complex, and a typical diet may provide more than 25,000 bioactive food constituents (Craig 1997, Liu 2004). Diet components may affect gut mucosa directly from the luminal side, or indirectly through whole-body metabolism (Nystrom & Mutanen 2009). Dietary constituents can modify a multitude of processes in both normal cells and cancer cells, and different cells may vary in their response to bioactive food components. Dose, timing, and duration of exposure are also important in determining the response (WCRF 2007).

One of the first links between a food component and CRC risk was proposed several decades ago, with Burkitt (1971) noting that a lack of fibre in the diets of the Western world may contribute to changes in bowel health. The link between diet and CRC development is supported by evidence for substantial geographical variations in CRC incidence rates and trends, with long-standing economically developed countries having higher incidence rates of the disease (Center et al 2009). Factors associated with economic development or Westernisation include a diet characteristically high in red or processed meat and refined carbohydrates, and low in fibre, fruits and vegetables, accompanied by lifestyle changes such as a reduction in physical activity levels (Center et

al 2009). There is evidence that populations moving from low-incidence areas to high-incidence areas take on the disease profile of the new country within one generation, suggesting a strong environmental link (Flood et al 2000). The adoption of Western dietary and lifestyle practices in developing countries has led to rapid increases in CRC rates; while incidence rates stabilised in the majority of developed countries, there was significant increases in Eastern European countries, most parts of Asia, and select countries of South America (Center et al 2009).

The geographical indication of a role of diet in CRC fits with evidence from case series and prospective cohort studies in humans. The authors of the latest report of the World Cancer Research Fund, for example, conducted systematic reviews of cohort and case-control studies to judge that there was convincing evidence that red meat, processed meat, alcoholic drinks, and body fatness increased risk of CRC (WCRF 2007). Alternatively, garlic, milk, and foods containing dietary fibre or calcium were judged to probably protect against this cancer (WCRF 2007). There was more limited evidence to suggest that non-starchy vegetables, fruits, fish, and foods containing folate, selenium or vitamin D may decrease risk, and limited evidence to suggest that cheese, and foods containing iron, animal fats or sugars may increase risk (WCRF 2007).

There is substantial evidence from cohort and case-control studies that high intake of red or processed meats may increase CRC risk, as discussed in Chapter 8. The largest human cohort study to date, the European Prospective Investigation into Cancer and Nutrition (EPIC) study, used data from 478,040 individuals to identify that CRC risk was positively associated with intake of red and processed meat, with a hazard ratio per 100 g increase in intake of red and processed meat of 1.55 (95% confidence interval (CI) 1.19 – 2.02, *P* trend = 0 .001) (Norat et al 2005). Systematic reviews of available cohort and case-control studies have found high red meat or processed meat intake to be a convincing risk factor for CRC (Larsson & Wolk 2006, WCRF 2007, Chan et al 2011); in the review by the WCRF (2007), intake of more than approximately 500 g of cooked meat per week was associated with significantly increased risk of CRC. Isolating the independent effects of red meat on CRC is difficult, and current evidence may suffer from potential confounding from other dietary and lifestyle factors (Alexander & Cushing 2011). There are, however, plausible mechanisms by which red meat can increase CRC risk. Red meat has been shown to increase DNA damage and induce DNA strand breaks (Toden et al 2006, Toden et al 2007). The generation of potentially carcinogenic N-nitroso compounds can increase DNA alkylation and enhance formation of pro-mutagenic DNA adducts (Lewin et al 2006), the production of

heterocyclic amines and polycyclic aromatic hydrocarbons through cooking at high temperature can also induce DNA damage (Rohrmann et al 2009), while the haem iron and free iron in red meat can lead to the production of free radicals, which can also be damaging (Glei et al 2006).

Dietary fibre can be defined as the fraction of the edible parts of plants or their extracts, or synthetic analogues, that are resistant to digestion and absorption in the small intestine, usually with complete or partial fermentation in the large intestine (FSANZ 2012). This definition encompasses the traditional forms of dietary fibre, such as soluble and insoluble non-starch polysaccharides (NSP), and also includes resistant starches and other food materials that are resistant to digestion (Cummings et al 1996, Topping & Clifton 2001). Evidence from cohort and case-control studies has generally shown that high intake of dietary fibre may decrease CRC risk, as discussed in Chapter 8. The EPIC study, for example, found that in 519,978 individuals dietary fibre intake was inversely related to incidence of CRC, with an adjusted relative risk for the highest versus lowest quintile of fibre from food intake of 0.58 (95% CI 0.41 – 0.85) (Bingham et al 2003). This association was substantiated by systematic review evidence from the WCRF (2007) which identified a clear dose-response relationship from generally consistent cohort studies, and concluded that foods containing dietary fibre probably protect against CRC. Interventional studies examining the effect of fibre on CRC risk in humans usually use biomarkers or adenomas as surrogate endpoints, and have presented less conclusive evidence. A systematic review of interventional studies concluded that increasing fibre in a Western diet for two to four years did not lower the risk of CRC (Asano & McLeod 2002). It was noted that longer-term trials and higher dietary fibre levels may be needed to reproduce the effect of dietary fibre shown in the observational studies, while the source of the dietary fibre may also influence its effect (Asano & McLeod 2002, Young et al 2005, Schatzkin et al 2007).

Possible mechanisms for a protective effect of dietary fibre include the dilution of faecal contents, increased stool weight and decreased transit time, binding of carcinogens and bile salts, increased colonic microbiota and altered species balance, and production of fermentation products including short chain fatty acids (SCFAs) (Young et al 2005, WCRF 2007). The fermentation of fibre and resistant starch to produce SCFAs such as butyrate offers a plausible mechanism for a protective effect of this dietary component (Young et al 2005). Butyrate is a known histone deacetylase inhibitor (HDI) with chemoprotective effects, and is reviewed further in Section 1.3.2 and Chapter 4.

Dietary components may alter cancer risk through both genetic and epigenetic mechanisms. The DNA damage induced by red meat is an example of a genetic mechanism for modifying CRC risk (Toden et al 2006, Toden et al 2007). One example of an epigenetic mechanism is the modification of histones by dietary factors that can act as HDIs, such as butyrate from fibre (Mariadason et al 2000), diallyl disulphide from garlic and other allium vegetables (Druesne et al 2004, Druesne-Pecollo et al 2007, Altonsy & Andrews 2011), and sulphoraphane, a glucosinolate from cruciferous vegetables (Myzak et al 2004, Myzak et al 2006a, Myzak et al 2006b, Myzak et al 2007, Clarke et al 2011a). DNA methylation is another example of epigenetic change influenced by diet. Appropriate gene expression is maintained by appropriate patterns of methylation, and dietary factors such as folate, a methyl-donor, are important determinants of normal methylation (Wallace et al 2010). Imbalanced intake of specific dietary constituents such as folate may increase risk of cancer (Motiwala et al 2003, Wallace et al 2010). Dietary compounds may also exert additional epigenetic influences by altering miRNA expression in various cell types, as reviewed in Section 1.5.

1.3.2 Butyrate and colorectal cancer

Butyrate is a prime example of a diet-derived substance with an epigenetic mechanism for altering CRC risk. Dietary fibre residues that reach the colon in animals and humans are metabolised by anaerobic bacteria to produce SCFAs, plus lactate, ethanol, hydrogen, methane, and carbon dioxide (Young et al 2005). The major SCFAs produced are acetate, propionate and butyrate. While all SCFAs have some beneficial effects on gut health, butyrate has particular chemoprotective effects and is preferentially taken up by the colonic epithelium (Cummings et al 1987). Besides being a preferred energy source for colonic epithelia (Roediger 1982, Scheppach et al 1992, Young et al 2005), butyrate also plays a role in cell cycle regulation, apoptosis, proliferation, differentiation, inflammation, and DNA repair in CRC cells (Mariadason et al 2000, Iacomino et al 2001, Daly & Shirazi-Beechey 2006). A number of *in vitro* studies have investigated the effect of butyrate on gene expression in CRC cells; the results of a systematic search for such studies are presented in Chapter 4. An early key study in a human colorectal adenocarcinoma cell line found that gene expression changes began as soon as 30 min after butyrate treatment, and continued to progress over 48 h (Mariadason et al 2000). Larger microarray studies support this early work and indicate that a substantial number of genes experience altered expression with butyrate treatment. One large study in HT29 CRC cells, for example, showed that 1984 genes (10.2%) had a >2-fold variation above or below control levels with 5 mM butyrate treatment for 24 h (Daly et al 2005,

Daly & Shirazi-Beechey 2006). Of these, 796 genes were up-regulated (4.1%) and 1187 were down-regulated (6.1%). Many butyrate-responsive genes are associated with the regulation of colonic tissue homeostasis, and have been shown to be deregulated in colon cancer tissue compared to normal healthy colonic mucosa. Genes up-regulated with butyrate include tumour suppressors associated with cell cycle arrest and induction of apoptosis, such as *CDKN1A* (cyclin-dependent kinase inhibitor 1A or p21), *GADD45A* (growth arrest and DNA-damage-inducible, alpha), *MAPK12* (mitogen-activated protein kinase 12 or p38), *FOS* (v-fos FBJ murine osteosarcoma viral oncogene homolog), *PTEN* (phosphatase and tensin homolog), and *TXNIP* (thioredoxin-interacting protein). Genes down-regulated by butyrate include oncogenes associated with cell cycle progression, DNA replication, proliferation, metastasis, inhibition of apoptosis, and tumour markers (Daly & Shirazi-Beechey 2006).

Butyrate's ability to epigenetically regulate gene expression is often attributed to its action as a HDI leading to histone hyperacetylation and chromatin remodelling, although it can also influence other machineries including acetylation of non-histone proteins, alteration of DNA methylation, and selective regulation of histone methylation and phosphorylation (Boffa et al 1981, Boffa et al 1994, Daly & Shirazi-Beechey 2006). When derived from a high fibre diet butyrate has value as chemopreventive agent and promoter of gut health. In an unmodified state, however, butyrate has less value as a systemic chemotherapeutic agent for various tumours, due to its short half-life (Miller et al 1987). Other structurally distinct but functionally similar HDIs have greater potential in cancer therapy. Suberoylanilide hydroxamic acid (SAHA), for example, is a HDI that is US Food and Drug Administration (FDA) approved for cutaneous T-cell lymphoma (Duvic et al 2007, Olsen et al 2007) and has undergone small clinical trials for solid tumours, including CRC (Vansteenkiste et al 2008, Wilson et al 2010b). Like butyrate, SAHA has been shown to induce histone acetylation, promote cell cycle arrest and apoptosis, and regulate similar genes, including those involved in cell cycle control, DNA replication, recombination and repair, apoptosis, and cell growth and proliferation (Portanova et al 2008, LaBonte et al 2009, Wilson et al 2010a).

1.4 microRNAs and colorectal cancer

The cellular pathways influenced by HDIs, including cell cycle regulation, proliferation, differentiation, and apoptosis, are also regulated by miRNAs. miRNAs represent an additional form of epigenetic gene regulation, and can themselves experience altered transcription through epigenetic mechanisms.

1.4.1 Definition and discovery of microRNAs

miRNAs are small non-coding 19 – 25 nucleotide RNA sequences that post-transcriptionally regulate the expression of target genes by binding to complementary target mRNAs and preventing the translation of mRNA into protein (Mendell 2005, Esteller 2011). They represent one component of a larger collection of various non-coding RNAs with regulatory functions, which also includes endogenous small-interfering RNAs (endo-siRNAs), PIWI-interacting RNAs (piRNAs), and other short and longer non-coding RNAs (Kim et al 2009, Esteller 2011, Mendell & Olson 2012).

The first miRNAs were discovered in the nematode *C. elegans*. The *C. elegans* heterochronic gene lin-4 was found to encode a small RNA that regulated translation of lin-14 and lin-28 via an antisense RNA-RNA interaction (Lee et al 1993, Wightman et al 1993, Moss et al 1997, Olsen & Ambros 1999). The discovery of the lin-4 miRNA was followed by identification of a second miRNA in *C. elegans*, let-7 (Pasquinelli et al 2000, Reinhart et al 2000, Abrahante et al 2003). lin-4 and let-7 were shown to directly control expression of target genes, through binding to complementary elements in the 3' untranslated regions (3'UTR) of the gene transcripts (Reinhart et al 2000). In loss-of-function studies, deletion of lin-4 and let-7 lead to mutants that failed to develop and differentiate at the appropriate larval stages (Lee et al 1993, Reinhart et al 2000). Both lin-4 and let-7 were discovered to be evolutionarily conserved in multiple species, which implied a more universal role for these genes in animals (Pasquinelli et al 2000, Lagos-Quintana et al 2002).

Numerous miRNAs have since been identified in animals, plants, viruses, and other organisms (Lagos-Quintana et al 2001, Lau et al 2001, Lee & Ambros 2001, Mourelatos et al 2002, Reinhart et al 2002, Houbaviy et al 2003, Lim et al 2003). The first release of the miRBase database of miRNAs in 2002 contained 218 entries, and subsequently experienced rapid expansion (Griffiths-Jones et al 2006). The latest release of the miRBase database now contains 18,226 entries representing hairpin precursor miRNAs, expressing 21,643 mature miRNA products, in 168 species. Over one thousand miRNAs have been identified in humans, with 1527 precursors and 1921 mature miRNAs currently listed in miRBase (Griffiths-Jones et al 2006). One miRNA can target hundreds of genes, and a gene can be regulated by multiple miRNAs. Various estimates suggest that one to two thirds of human protein coding genes are regulated by miRNAs (Kim et al 2009, Esteller 2011).

1.4.2 microRNA biogenesis and mechanism of action

Both protein-coding genes and non-coding RNA genes are present in the genome. The general structure of a gene consists of a promoter region and TSS, and a transcribed region that can contain exons (which are found in the mature transcript) and introns (which are removed from the primary transcript). More than half of miRNAs are located in the introns of protein-coding or long non-coding RNA genes. These intragenic miRNAs can share common promoters with their host gene, some of which can be more than 20 kb upstream of the pre-miRNA coding region (Rodriguez et al 2004, Suzuki et al 2011). Other intragenic miRNAs can have their own promoters and can be transcribed independently of the host gene, while other miRNAs and their promoter regions can be entirely intergenic (Ozsolak et al 2008, Suzuki et al 2011).

The canonical miRNA biogenesis pathway is shown in Figure 1.1. Non-canonical miRNA biogenesis pathways have also been identified, which can be Drosha or Dicer independent (Miyoshi et al 2010). In the standard pathway, miRNAs are transcribed in the nucleus as primary miRNA transcripts (pri-miRNAs) by RNA polymerase II or RNA polymerase III (Cai et al 2004, Lee et al 2004, Borchert et al 2006). A typical pri-miRNA contains a hairpin stem of 33 base pairs, a terminal loop, and two single-stranded unpaired flanking regions. The double stranded stem and unpaired flanking regions of the pri-miRNA are important for recognition and processing by components of the microprocessor complex (Zeng & Cullen 2003, Denli et al 2004, Zeng et al 2005, Han et al 2006). The microprocessor complex contains DGCR8 (DiGeorge syndrome critical region gene 8) for binding and stabilization, and a ribonuclease Drosha which cleaves the pri-miRNA. Drosha cleaves the 3' and 5' arms of the pri-miRNA hairpin, to form a precursor miRNA molecule (pre-miRNA) (Gregory et al 2004, Han et al 2004). For some specific miRNAs, other proteins may assist in regulating Drosha-mediated cleavage (Guil & Caceres 2007). The pre-miRNA is then transported to the cytoplasm by Exportin 5 (XPO5) in complex with Ran-GTP (Yi et al 2003, Bohnsack et al 2004). XPO5 may also protect the pre-miRNA against nuclease digestion (Yi et al 2003, Bohnsack et al 2004, Lund et al 2004). Following export to the cytoplasm, the pre-miRNA is then cleaved near the terminal loop by the ribonuclease Dicer, releasing a ~22 nucleotide miRNA duplex (Macrae et al 2006). During this process, Dicer interacts with TRBP (human immunodeficiency virus transactivating response RNA-binding protein) and PACT (protein activator of PKR), and together these molecules mediate the assembly of the miRNA in the RNA-induced silencing complex (RISC), which also incorporates Argonaute-2 (AGO2) (Chendrimada et al 2005, Haase et al 2005, Lee et al

2006). AGO2 can assist in pre-miRNA cleavage (Diederichs & Haber 2007), but its main function is as a RISC effector protein mediating mRNA regulation (Hutvagner & Zamore 2002, Liu et al 2004, Meister et al 2004, Pillai et al 2004). Following Dicer cleavage, the duplex is unwound and one strand remains on the AGO2 as the mature miRNA, while the other less stable strand is degraded (Khvorova et al 2003, Schwarz et al 2003). The two strands may be identified as -5p or -3p, or the less stable strand can also be referred to as the * form. The seed sequences of mature miRNAs (nucleotides 2 – 8) are highly conserved, and it is these sequences which specifically bind to complementary target sites in the 3'UTR of mRNA (Brennecke et al 2005). Mature miRNAs associated with AGO2 can act by cleaving complementary mRNAs. Alternatively, when there is imperfect complementarity, miRNAs can act through translational repression and also transcript destabilisation, for example via mRNA deadenylation (Hutvagner & Zamore 2002, Liu et al 2004, Wu et al 2006, Mathonnet et al 2007, Filipowicz et al 2008, Guo et al 2010). In mammals, imperfect binding to the target mRNA is most typical (Brennecke et al 2005), and destabilization of target mRNAs may be a predominant reason for reduced protein output (Guo et al 2010).

Each miRNA may have hundreds of evolutionary conserved target mRNAs and even more non-conserved targets (Bentwich et al 2005). There are multiple methods available to identify miRNA target genes and confirm their biological efficacy (Kuhn et al 2008). Experimental validation of direct miRNA targeting has been performed for many miRNA and mRNA target pairs, while many more remain undiscovered or unconfirmed (Bartel 2009).

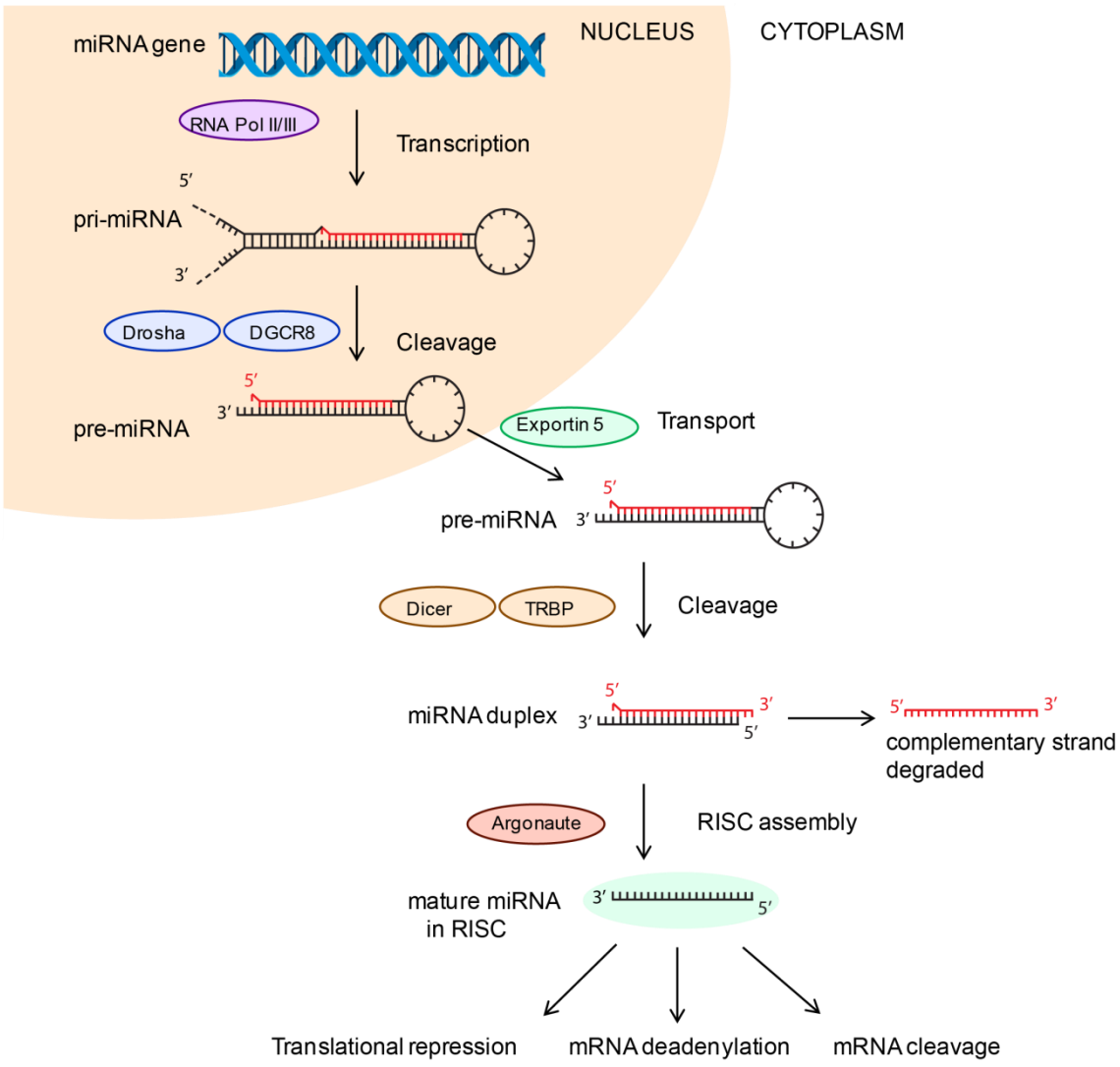

Figure 1.1 miRNA biogenesis pathway

In the canonical miRNA biogenesis pathway, the transcribed primary miRNA (pri-miRNA) is processed by the microprocessor complex which includes Drosha, to form a precursor miRNA (pre-miRNA) which is transported to the cytoplasm. It is then further processed by Dicer, Argonaute and other proteins to form the mature miRNA, which is incorporated in the RNA-induced silencing complex (RISC). Non-canonical miRNA biogenesis pathways can also occur, for example Drosha or Dicer independent processing.

1.4.3 microRNAs in development and disease

miRNAs have been shown to play roles in fundamental biological processes such as cell proliferation, metabolism, differentiation, and apoptosis, and are important regulatory molecules in both normal development and disease progression (Ambros 2004, Mendell & Olson 2012). Some miRNAs have important functions in embryogenesis and early development (Alvarez-Garcia & Miska 2005, Suh & Blelloch 2011). Deletion of certain miRNAs, or defects in miRNA processing such as the deletion of Dicer, can lead to lethal phenotypes or developmental disorders in mouse models (Bernstein et al 2003, Morita et al 2007, Ventura et al 2008, Wang et al 2008). A small number of human developmental disorders have been linked to miRNA defects, including deafness caused by a mutation in the miR-96 gene (Lewis et al 2009, Mencia et al 2009), and microcephaly, short stature and digital abnormalities caused by hemizygous deletions of the miR-17-92 host gene (de Pontual et al 2011).

The indication that miRNAs play important roles in diverse human diseases stems from a large body of evidence on the function of miRNAs in cancer cells (Mendell & Olson 2012). Calin et al (2002) first demonstrated a link between miRNAs and cancer, when they identified frequent deletions of miR-15 and miR-16 genes in chronic lymphocytic leukaemia. Profiling studies in human tissue have revealed multiple miRNAs that are dysregulated in various cancers (Calin et al 2004a, Cummins et al 2006, Volinia et al 2006), and experiments in cancer cell lines and rodent models have shown specific miRNA activity to influence tumourigenesis (He et al 2005a, Mu et al 2009, Olive et al 2009). Expression profiles of miRNAs are altered in many tumours, and miRNA genes often occur in genomic regions that are deleted or amplified in cancer (Calin et al 2004b). miRNAs have been shown to function as tumour suppressors or oncogenes, by altering gene expression and affecting signalling pathways. Reduction or over-expression of certain miRNAs contributes to tumour progression (Guil & Esteller 2009, Mendell & Olson 2012).

Disrupted miRNA expression patterns have also been observed in numerous non-neoplastic diseases (Esteller 2011). miRNAs are important for correct functioning of the nervous system, and dyregulation of miRNAs has been shown in neurological disorders such as motor neuron disease, multiple sclerosis, Parkinson's disease, Alzheimer's disease, and ataxia (Kim et al 2007a, Schaefer et al 2007, Hebert et al 2008, Hebert et al 2009, Shin et al 2009a, Williams et al 2009, Gehrke et al 2010). In cardiovascular disorders, miRNAs are also likely to play an important role, and heart failure and

vascular diseases are associated with distinct miRNA expression profiles (van Rooij et al 2006, Ji et al 2007). Roles for miRNAs have also been implicated in inflammatory disorders, metabolic conditions, viral diseases and other non-neoplastic disorders (Krutzfeldt et al 2005, Esau et al 2006, Zampetaki et al 2010, Brest et al 2011, Reesink et al 2012).

1.4.4 microRNAs in colorectal cancer

Human tumours are often characterised by a general defect in miRNA production, resulting in global miRNA down-regulation (Lu et al 2005, Thomson et al 2006). Despite this, numerous studies have shown specific miRNAs to be commonly elevated in cancer, with some of these miRNAs possessing oncogenic potential. A substantial number of miRNAs are decreased in CRC tissue samples compared to normal tissue, with a number of other miRNAs increased. A systematic search of the literature identified multiple studies characterising miRNA expression in CRC cells, with the findings summarised in Table 1.1. Michael et al (2003) were the first to identify two mature miRNAs, miR-143 and miR-145, that consistently displayed reduced levels in adenoma and CRC tissue compared with normal mucosa. miRNA profiling methods have since allowed the detection of numerous miRNAs that are dysregulated in CRC (Cummins et al 2006). In an approach known as miRNA serial analysis of gene expression (miRAGE), one early study identified 200 known mature miRNAs, 133 novel miRNA candidates, and 112 previously uncharacterised miRNA forms in human CRC cell lines (Cummins et al 2006). A number of large profiling studies have shown similar numbers of miRNAs increased and decreased in CRC (Bandres et al 2006, Cummins et al 2006, Volinia et al 2006, Monzo et al 2008, Schetter et al 2008, Arndt et al 2009, Chen et al 2009, Motoyama et al 2009, Sarver et al 2009, Chang et al 2011b, Knowlton et al 2011, Luo et al 2012, Mosakhani et al 2012). One such profiling study, for example, used microarray analysis and real-time RT-PCR to compare more than 200 miRNAs in CRC and adjacent normal tissue cells and found that 41 miRNAs were up-regulated and 31 down-regulated in CRC cells (Chen et al 2009). There can be more confidence that a miRNA is dysregulated in CRC when this miRNA is identified by multiple profiling studies, and validated using supplementary methods such as real-time qPCR.

Of the miRNAs that are down-regulated in CRC, miR-143 and miRNA-145 are amongst the most commonly reported (Table 1.1). Following on from the initial study which identified reduced accumulation of mature miR-143 and miR-145 in colorectal

adenomas and carcinomas compared to normal colorectal epithelium (Michael et al 2003), this finding has since been confirmed in multiple profiling studies (Table 1.1). miR-143 and miR-145 are likely to possess tumour suppressor activity, and have been shown to inhibit growth in CRC cells by altering gene expression (Akao et al 2006b). miR-143 has been shown to regulate *ERK5*, a component of MAP kinase signalling pathways and a mediator of the activity of several oncogenes (Esau et al 2004, Akao et al 2006b, Wang & Tournier 2006). An inverse correlation between miR-143 and expression of the oncogene *KRAS* has also been found (Chen et al 2009). miR-145 has also been shown to inhibit cancer cell growth by various mechanisms, such as inhibiting *IRS1* (interferon response sequence 1) (Shi et al 2007) and *C-MYC* (myelocytomatosis oncogene) expression (Sachdeva et al 2009), and regulating components of the MAP kinase signalling pathway (Wang et al 2012). Another miRNA decreased in CRC is miR-34a, which has been shown to inhibit cell proliferation, decrease expression of the transcription factor *E2F*, and increase p53 expression (Tazawa et al 2007). miRNAs in the let-7 family are also dysregulated in CRC (Table 1.1). Some miRNAs in this family may also play tumour suppressor roles by altering gene expression, inhibiting cell growth, and decreasing *KRAS* and *C-MYC* expression (Johnson et al 2005, Akao et al 2006a, Sampson et al 2007).

Many other miRNAs are up-regulated in CRC, with some shown to function as oncogenes (Table 1.1). miR-21 and the miR-17-92 cluster are examples of miRNAs with known oncogenic properties that have been shown by multiple studies to be increased in CRCs (Table 1.1). Levels of these miRNAs are also increased in many other cancers (Ota et al 2004, Hayashita et al 2005, He et al 2005a, Volinia et al 2006, Petrocca et al 2008). miR-21 has been shown to repress expression of tumour suppressor genes such as *PTEN*, *TPM1* (tropomyosin 1), *PDCD4* (programmed cell death 4), and *RHOB* (Ras homolog family member B), and to promote tumour development and induce invasion and metastasis (Meng et al 2007, Zhu et al 2007, Asangani et al 2008, Medina et al 2010, Chang et al 2011a, Liu et al 2011b). Higher miR-21 expression has been found in more advanced CRC tumours, and has been linked to poorer survival and therapeutic outcome (Schetter et al 2008, Kulda et al 2010, Shibuya et al 2010, Valeri et al 2010, Chang et al 2011a, Liu et al 2011a, Vickers et al 2012). The miR-17-92 cluster has been designated oncomir -1 due to its oncogenic potential (He et al 2005a), and has been shown to promote proliferation and angiogenesis, inhibit differentiation, and sustain cell survival (Mu et al 2009, Olive et al 2009). The miR-17-92 cluster comprises six mature miRNAs, miR-17, miR-18a, miR-19a, miR-20a, miR-19b, and miR-92a. Validated miR-

17-92 targets include the cell cycle inhibitor *CDKN1A* (p21) and the pro-apoptotic genes *PTEN* and *BCL2L11* (BCL2-like 11 apoptosis facilitator, commonly known as Bim) (Ventura et al 2008, Inomata et al 2009, Mu et al 2009, Olive et al 2009, Wong et al 2010). miRNAs in the miR-17-92 cluster have also been associated with invasion and metastasis of CRC cells (Kahlert et al 2011), and with poorer survival (Yu et al 2012).

There is emerging evidence that certain miRNAs may be used as biomarkers for the presence and stage of CRC (Xi et al 2006, Slaby et al 2007, Diaz et al 2008, Schepeler et al 2008, Schetter et al 2008, Baffa et al 2009, Yamamichi et al 2009, Akao et al 2010). miRNA profiles may also identify different tumour types, such as those with microsatellite stability or instability (Lanza et al 2007, Earle et al 2010, Balaguer et al 2011, Bartley et al 2011, Slattery et al 2011). There is some research to suggest that miRNAs in plasma, serum or faeces may also serve as novel biomarkers for CRC (Ng et al 2009a, Huang et al 2010, Link et al 2010, Cheng et al 2011, Kalimutho et al 2011a, Kalimutho et al 2011b).

Table 1.1: Studies reporting altered miRNA expression in colorectal cancer cells from human tumour tissue samples

Up-regulated miRNAs		Down-regulated miRNAs	
miRNA	**Studies**	**miRNA**	**Studies**
miR-7	(Motoyama et al 2009, Akao et al 2010)	miR-1	(Cummins et al 2006, Schetter et al 2008, Arndt et al 2009, Chen et al 2009, Sarver et al 2009, Chang et al 2011b, Mosakhani et al 2012)
miR-10a	(Volinia et al 2006, Monzo et al 2008, Chen et al 2009)	miR-7	(Chen et al 2009)
miR-10b	(Chen et al 2009)	miR-7-1*	(Mosakhani et al 2012)
miR-15a	(Bandres et al 2006, Monzo et al 2008, Chang et al 2011b)	miR-9	(Bandres et al 2006, Sarver et al 2009)
miR-15b	(Xi et al 2006, Monzo et al 2008)	miR-9-3p	(Volinia et al 2006)
miR-16	(Chen et al 2009, Luo et al 2012)	miR-9*	(Bandres et al 2006, Sarver et al 2009, Mosakhani et al 2012)
miR-17-3	(Chen et al 2009)	miR-10b	(Arndt et al 2009, Sarver et al 2009, Mosakhani et al 2012)
miR-17-3p	(Bandres et al 2006, Monzo et al 2008, Chen et al 2009, Ng et al 2009a, Sarver et al 2009)	miR-16	(Cummins et al 2006, Earle et al 2010)
miR-17	(Volinia et al 2006, Monzo et al 2008, Schetter et al 2008, Arndt et al 2009, Chen et al 2009, Diosdado et al 2009, Motoyama et al 2009, Earle et al 2010, Chang et al 2011b, Luo et al 2012, Yu et al 2012)	miR-20b	(Sarver et al 2009)
miR-18a	(Cummins et al 2006, Arndt et al 2009, Chen et al 2009, Diosdado et al 2009, Motoyama et al 2009, Ng et al 2009a, Wang et al 2010, Luo et al 2012, Yu et al 2012)	miR-22	(Yamakuchi et al 2011)
miR-18b	(Motoyama et al 2009, Wang et al 2010, Luo et al 2012)	miR-23a	(Chen et al 2009)
miR-19a	(Bandres et al 2006, Cummins et al 2006, Monzo et al 2008, Arndt et al 2009, Chen et al 2009, Diosdado et al 2009, Ng et al 2009a, Wang et al 2010, Chang et al 2011b, Luo et al 2012, Yu et al 2012)	miR-23b	(Cummins et al 2006, Chen et al 2009)
miR-19b	(Cummins et al 2006, Arndt et al 2009, Diosdado et al 2009, Ng et al 2009a, Chang et al 2011b, Yu et al 2012)	miR-24	(Cummins et al 2006)
miR-20a	(Bandres et al 2006, Volinia et al 2006, Monzo et al 2008, Schepeler et al 2008, Schetter et al 2008, Arndt et al 2009, Chen et al 2009, Diosdado et al 2009, Motoyama et al 2009, Ng et al 2009a, Earle et al 2010, Chang et al 2011b, Luo et al 2012, Yu et al 2012)	miR-24-1*	(Mosakhani et al 2012)
miR-20a*	(Wang et al 2010)	miR-26a	(Cummins et al 2006, Chen et al 2009, Ng et al 2009b)
miR-21	(Bandres et al 2006, Cummins et al 2006, Volinia et al 2006, Slaby et al 2007, Monzo et al 2008, Schetter et al 2008, Arndt et al 2009, Chen et al 2009, Yamamichi et al 2009, Akao et al 2010, Kulda et al 2010, Shibuya et al 2010, Chang et al 2011a, Chang et al 2011b, Fassan et al 2011, Knowlton et al 2011, Liu et al 2011a,	miR-26b	(Schepeler et al 2008, Earle et al 2010)

	Luo et al 2012)
miR-21*	(Mosakhani et al 2012)
miR-23a	(Luo et al 2012)
miR-23b	(Luo et al 2012)
miR-24-1	(Volinia et al 2006)
miR-24-2	(Volinia et al 2006)
miR-25	(Cummins et al 2006, Monzo et al 2008, Arndt et al 2009, Chen et al 2009, Earle et al 2010)
miR-27a	(Monzo et al 2008, Chen et al 2009, Luo et al 2012)
miR-27b	(Cummins et al 2006, Luo et al 2012)
miR-29a	(Bandres et al 2006, Cummins et al 2006, Monzo et al 2008, Arndt et al 2009, Motoyama et al 2009, Sarver et al 2009)
miR-29b	(Bandres et al 2006, Volinia et al 2006, Arndt et al 2009, Luo et al 2012)
miR-30c	(Volinia et al 2006)
miR-31	(Bandres et al 2006, Slaby et al 2007, Monzo et al 2008, Arndt et al 2009, Chen et al 2009, Motoyama et al 2009, Sarver et al 2009, Wang et al 2009b, Earle et al 2010, Chang et al 2011b)
miR-32	(Cummins et al 2006, Volinia et al 2006, Sarver et al 2009)
miR-33	(Cummins et al 2006, Sarver et al 2009)
miR-34a	(Bandres et al 2006, Monzo et al 2008, Schetter et al 2008, Arndt et al 2009, Chen et al 2009)
miR-34c	(Bandres et al 2006)
miR-92	(Bandres et al 2006, Cummins et al 2006, Monzo et al 2008, Schepeler et al 2008, Schetter et al 2008, Chen et al 2009, Diosdado et al 2009, Motoyama et al 2009, Ng et al 2009a, Earle et al 2010, Yu et al 2012)
miR-93	(Schetter et al 2008, Arndt et al 2009, Chen et al 2009, Earle et al 2010, Chang et al 2011b)
miR-95	(Bandres et al 2006, Monzo et al 2008, Schetter et al 2008, Arndt et al 2009, Motoyama et al 2009, Ng et al 2009a)
miR-96	(Bandres et al 2006, Monzo et al 2008, Arndt et al 2009, Sarver et al 2009)
miR-98	(Monzo et al 2008, Chang et al 2011b)
miR-99a	(Monzo et al 2008)
miR-99b	(Volinia et al 2006, Schetter et al 2008)
miR-103	(Monzo et al 2008, Chen et al 2009)
miR-104	(Bandres et al 2006)
miR-27b	(Mosakhani et al 2012)
miR-28	(Cummins et al 2006, Almeida et al 2012, Mosakhani et al 2012)
miR-28-3p	(Chang et al 2011b, Almeida et al 2012)
miR-29b	(Cummins et al 2006)
miR-29c	(Cummins et al 2006)
miR-30a-3p	(Bandres et al 2006, Monzo et al 2008, Schetter et al 2008, Arndt et al 2009, Sarver et al 2009, Mosakhani et al 2012)
miR-30a	(Cummins et al 2006, Arndt et al 2009, Ng et al 2009b, Sarver et al 2009, Mosakhani et al 2012)
miR-30b	(Schepeler et al 2008, Mosakhani et al 2012)
miR-30c	(Bandres et al 2006, Cummins et al 2006, Arndt et al 2009, Mosakhani et al 2012)
miR-30d	(Cummins et al 2006)
miR-30e-3p	(Motoyama et al 2009, Mosakhani et al 2012)
miR-31	(Mosakhani et al 2012)
miR-31*	(Mosakhani et al 2012)
miR-34a	(Tazawa et al 2007, Lodygin et al 2008, Akao et al 2010)
miR-34b	(Schetter et al 2008, Toyota et al 2008)
miR-34c	(Schetter et al 2008, Toyota et al 2008)
miR-92b*	(Luo et al 2012)
miR-99a	(Bandres et al 2006)
miR-100	(Bandres et al 2006, Chen et al 2009)
miR-101	(Cummins et al 2006, Schepeler et al 2008)
miR-103	(Cummins et al 2006)
miR-107	(Cummins et al 2006)
miR-122	(Mosakhani et al 2012)
miR-124a	(Bandres et al 2006)
miR-125a	(Arndt et al 2009, Chen et al 2009, Ng et al 2009b)

miR-105	(Monzo et al 2008)	miR-125b	(Cummins et al 2006, Monzo et al 2008, Chen et al 2009, Ng et al 2009b)
miR-106a	(Bandres et al 2006, Volinia et al 2006, Monzo et al 2008, Schetter et al 2008, Arndt et al 2009, Chen et al 2009, Ng et al 2009a, Luo et al 2012, Yu et al 2012)	miR-126	(Guo et al 2008, Li et al 2011a)
miR-106b	(Cummins et al 2006, Schetter et al 2008, Arndt et al 2009, Chen et al 2009, Ng et al 2009a, Wang et al 2010, Yu et al 2012)	miR-129	(Bandres et al 2006)
miR-107	(Volinia et al 2006, Monzo et al 2008)	miR-130a	(Chen et al 2009)
miR-122a	(Monzo et al 2008)	miR-130b	(Chen et al 2009)
miR-126	(Volinia et al 2006, Chen et al 2009)	miR-133a	(Bandres et al 2006, Cummins et al 2006, Arndt et al 2009, Ng et al 2009b, Sarver et al 2009, Chang et al 2011b, Mosakhani et al 2012)
miR-127	(Schetter et al 2008)	miR-133b	(Bandres et al 2006, Chen et al 2009, Hu et al 2010, Mosakhani et al 2012)
miR-128a	(Monzo et al 2008, Chen et al 2009)	miR-136	(Chen et al 2009)
miR-128b	(Volinia et al 2006, Chen et al 2009)	miR-137	(Bandres et al 2006, Ng et al 2009b, Sarver et al 2009, Balaguer et al 2010, Mosakhani et al 2012)
miR-130b	(Monzo et al 2008, Arndt et al 2009, Chang et al 2011b)	miR-138	(Sarver et al 2009, Knowlton et al 2011)
miR-132	(Chen et al 2009)	miR-139	(Bandres et al 2006, Monzo et al 2008, Arndt et al 2009, Chen et al 2009, Sarver et al 2009, Chang et al 2011b, Mosakhani et al 2012)
miR-133b	(Schetter et al 2008, Earle et al 2010)	miR-143	(Michael et al 2003, Akao et al 2006b, Cummins et al 2006, Slaby et al 2007, Arndt et al 2009, Chen et al 2009, Motoyama et al 2009, Ng et al 2009b, Wang et al 2009b, Akao et al 2010, Earle et al 2010, Kulda et al 2010, Knowlton et al 2011, Mosakhani et al 2012)
miR-134	(Monzo et al 2008)	miR-143*	(Mosakhani et al 2012)
miR-135a	(Bandres et al 2006, Monzo et al 2008, Nagel et al 2008, Schetter et al 2008, Earle et al 2010)	miR-144	(Chen et al 2009)
miR-135b	(Bandres et al 2006, Monzo et al 2008, Nagel et al 2008, Ng et al 2009a, Sarver et al 2009, Wang et al 2010, Chang et al 2011b)	miR-144*	(Mosakhani et al 2012)
miR-141	(Monzo et al 2008, Chen et al 2009)	miR-145	(Michael et al 2003, Akao et al 2006b, Bandres et al 2006, Cummins et al 2006, Slaby et al 2007, Monzo et al 2008, Schepeler et al 2008, Arndt et al 2009, Chen et al 2009, Motoyama et al 2009, Ng et al 2009b, Wang et al 2009b, Akao et al 2010, Earle et al 2010, Knowlton et al 2011)
miR-142-3p	(Cummins et al 2006, Monzo et al 2008, Chen et al 2009, Chang et al 2011b)	miR-145*	(Mosakhani et al 2012)
miR-142	(Cummins et al 2006, Monzo et al 2008, Chen et al 2009)	miR-147	(Sarver et al 2009)
miR-146	(Bandres et al 2006, Monzo et al 2008)	miR-147b	(Luo et al 2012)
miR-147	(Monzo et al 2008)	miR-148b	(Schetter et al 2008, Song et al 2012)
miR-148a	(Bandres et al 2006, Cummins et al 2006, Monzo et al 2008, Chang et al 2011b)	miR-149	(Bandres et al 2006, Monzo et al 2008, Chen et al 2009, Chang et al 2011b)
miR-150	(Volinia et al 2006)	miR-150	(Chen et al 2009, Knowlton et al 2011,

miR-151	(Monzo et al 2008)
miR-153a	(Schetter et al 2008)
miR-154	(Monzo et al 2008)
miR-154*	(Bandres et al 2006)
miR-155	(Bandres et al 2006, Volinia et al 2006, Chen et al 2009, Shibuya et al 2010)
miR-181a	(Monzo et al 2008, Chen et al 2009)
miR-181b	(Bandres et al 2006, Nakajima et al 2006, Xi et al 2006, Monzo et al 2008, Schetter et al 2008, Arndt et al 2009, Chen et al 2009)
miR-181c	(Monzo et al 2008)
miR-181d	(Motoyama et al 2009)
miR-182	(Monzo et al 2008, Arndt et al 2009, Motoyama et al 2009, Sarver et al 2009, Chang et al 2011b)
miR-182*	(Bandres et al 2006, Sarver et al 2009)
miR-183	(Bandres et al 2006, Monzo et al 2008, Arndt et al 2009, Motoyama et al 2009, Sarver et al 2009, Earle et al 2010, Chang et al 2011b)
miR-185	(Schetter et al 2008)
miR-186	(Monzo et al 2008)
miiR-188	(Chen et al 2009, Sarver et al 2009)
miR-191	(Cummins et al 2006, Volinia et al 2006, Xi et al 2006, Monzo et al 2008, Schepeler et al 2008)
miR-192	(Cummins et al 2006)
miR-193a-3p	(Luo et al 2012)
miR-194	(Bandres et al 2006, Monzo et al 2008)
miR-196a	(Chen et al 2009, Schimanski et al 2009)
miR-196b	(Motoyama et al 2009, Wang et al 2010)
miR-197	(Monzo et al 2008)
miR-199a	(Chen et al 2009)
miR-199b	(Chen et al 2009)
miR-200a	(Cummins et al 2006, Monzo et al 2008, Schepeler et al 2008, Chen et al 2009, Luo et al 2012)
miR-200b	(Bandres et al 2006, Cummins et al 2006, Monzo et al 2008, Chen et al 2009)
miR-200c	(Bandres et al 2006, Nakajima et al 2006, Xi et al 2006, Monzo et al 2008, Chen et al 2009)
miR-203	(Bandres et al 2006, Volinia et al 2006, Monzo et al 2008, Schetter et al 2008, Arndt et al 2009, Chen et al 2009, Earle et al 2010)
	Ma et al 2012)
miR-150*	(Luo et al 2012)
miR-181a	(Cummins et al 2006)
miR-184	(Bandres et al 2006)
miR-187	(Bandres et al 2006)
miR-191	(Earle et al 2010)
miR-192	(Braun et al 2008, Schetter et al 2008, Chen et al 2009, Earle et al 2010, Knowlton et al 2011, Mosakhani et al 2012)
miR-192*	(Mosakhani et al 2012)
miR-193a	(Cummins et al 2006, Chen et al 2009)
miR-193b	(Chen et al 2009)
miR-194	(Braun et al 2008, Chen et al 2009, Knowlton et al 2011, Mosakhani et al 2012)
miR-195	(Cummins et al 2006, Monzo et al 2008, Arndt et al 2009, Chen et al 2009, Liu et al 2010, Mosakhani et al 2012)
miR-196a	(Earle et al 2010)
miR-199a	(Bandres et al 2006)
miR-200c	(Cummins et al 2006)
miR-202	(Knowlton et al 2011)
miR-203	(Chiang et al 2011)
miR-204	(Bandres et al 2006, Ng et al 2009b, Chang et al 2011b)
miR-206	(Knowlton et al 2011)
miR-211	(Bandres et al 2006)
miR-212	(Chen et al 2009)
miR-214	(Bandres et al 2006, Chen et al 2009)
miR-215	(Braun et al 2008, Schetter et al 2008, Chen et al 2009, Ng et al 2009b, Earle et al 2010, Chang et al 2011b, Mosakhani et al 2012)
miR-218	(Cummins et al 2006, Chen et al 2009, Mosakhani et al 2012)
miR-296	(Bandres et al 2006)
miR-299	(Chang et al 2011b)
miR-301	(Schetter et al 2008)
miR-302c*	(Knowlton et al 2011)
miR-320	(Knowlton et al 2011)

miR-205	(Chen et al 2009)
miR-210	(Bandres et al 2006, Monzo et al 2008, Schetter et al 2008, Chen et al 2009)
miR-211	(Schetter et al 2008)
miR-212	(Schetter et al 2008)
miR-213	(Volinia et al 2006, Monzo et al 2008)
miR-214	(Chang et al 2011b)
miR-215	(Monzo et al 2008)
miR-216	(Monzo et al 2008)
miR-219	(Monzo et al 2008, Schetter et al 2008)
miR-220	(Motoyama et al 2009)
miR-221	(Volinia et al 2006, Monzo et al 2008, Chen et al 2009, Ng et al 2009a, Chang et al 2011b, Sun et al 2011)
miR-222	(Monzo et al 2008, Schetter et al 2008, Chen et al 2009, Ng et al 2009a, Luo et al 2012)
miR-223	(Volinia et al 2006, Schetter et al 2008, Chen et al 2009, Ng et al 2009a, Earle et al 2010)
miR-224	(Bandres et al 2006, Monzo et al 2008, Arndt et al 2009, Motoyama et al 2009, Ng et al 2009a, Sarver et al 2009, Wang et al 2010)
miR-287	(Sarver et al 2009)
miR-301	(Monzo et al 2008)
miR-301b	(Wang et al 2010)
miR-302a	(Schepeler et al 2008, Motoyama et al 2009)
miR-302b	(Motoyama et al 2009)
miR-320	(Monzo et al 2008, Schepeler et al 2008)
miR-324	(Monzo et al 2008, Chang et al 2011b)
miR-330	(Monzo et al 2008)
miR-335	(Schetter et al 2008, Wang et al 2010)
miR-338	(Monzo et al 2008, Schetter et al 2008)
miR-339	(Monzo et al 2008)
miR-346	(Schetter et al 2008)
miR-370	(Monzo et al 2008)
miR-373	(Monzo et al 2008)
miR-374	(Monzo et al 2008, Wang et al 2010)
miR-424	(Wang et al 2010)
miR-425	(Luo et al 2012)
miR-429	(Cummins et al 2006)
miR-432	(Schepeler et al 2008)
miR-450	(Cummins et al 2006)
miR-492	(Schepeler et al 2008)
miR-493-3p	(Motoyama et al 2009)
miR-494	(Mosakhani et al 2012)
miR-500	(Mosakhani et al 2012)
miR-503	(Sarver et al 2009)
miR-510	(Schepeler et al 2008)
miR-324	(Schetter et al 2008, Knowlton et al 2011)
miR-328	(Bandres et al 2006, Sarver et al 2009)
miR-330	(Knowlton et al 2011)
miR-331	(Schetter et al 2008)
miR-340	(Bandres et al 2006)
miR-342	(Cummins et al 2006, Grady et al 2008, Schetter et al 2008, Wang et al 2011)
miR-362-3p	(Mosakhani et al 2012)
miR-363	(Sarver et al 2009, Mosakhani et al 2012)
miR-365	(Cummins et al 2006, Luo et al 2012, Mosakhani et al 2012, Nie et al 2012)
miR-370	(Knowlton et al 2011)
miR-375	(Sarver et al 2009, Chang et al 2011b, Luo et al 2012)
miR-376b	(Knowlton et al 2011)
miR-378	(Sarver et al 2009, Wang et al 2010, Luo et al 2012, Mosakhani et al 2012)
miR-378*	(Arndt et al 2009, Wang et al 2010, Mosakhani et al 2012)
miR-382	(Knowlton et al 2011)
miR-422a	(Arndt et al 2009, Chang et al 2011b, Luo et al 2012)
miR-422b	(Arndt et al 2009)
miR-423	(Luo et al 2012)
miR-455	(Schepeler et al 2008)
miR-485-3p	(Chang et al 2011b)
miR-484	(Schepeler et al 2008)
miR-486	(Sarver et al 2009)
miR-490	(Knowlton et al 2011)
miR-490-3p	(Mosakhani et al 2012)
miR-497	(Arndt et al 2009, Sarver et al 2009, Mosakhani et al 2012)
miR-500	(Knowlton et al 2011)
miR-503	(Knowlton et al 2011)
miR-511	(Sarver et al 2009)
miR-516	(Knowlton et al 2011)
miR-517*	(Knowlton et al 2011)
miR-518a-2*	(Knowlton et al 2011)
miR-518b	(Knowlton et al 2011)
miR-518c*	(Knowlton et al 2011)
miR-518f*	(Knowlton et al 2011)
miR-519e*	(Knowlton et al 2011)
miR-526a	(Knowlton et al 2011)
miR-526b	(Knowlton et al 2011)
miR-526c	(Knowlton et al 2011)
miR-527	(Knowlton et al 2011)
miR-551b	(Sarver et al 2009)

miR-512	(Schepeler et al 2008)
miR-513	(Schepeler et al 2008)
miR-513a-3p	(Mosakhani et al 2012)
miR-513b	(Mosakhani et al 2012)
miR-513c	(Mosakhani et al 2012)
miR-526c	(Schepeler et al 2008)
miR-527	(Schepeler et al 2008)
miR-542	(Sarver et al 2009)
miR-550	(Motoyama et al 2009)
miR-552	(Sarver et al 2009)
miR-570	(Motoyama et al 2009)
miR-582	(Chang et al 2011b)
miR-584	(Sarver et al 2009)
miR-675	(Tsang et al 2010)
miR-892b	(Mosakhani et al 2012)
miR-1201	(Luo et al 2012)
let-7f	(Chang et al 2011b)
let-7g	(Nakajima et al 2006, Monzo et al 2008)
let-7i	(Luo et al 2012)

miR-557	(Luo et al 2012)
miR-572	(Luo et al 2012)
miR-582	(Mosakhani et al 2012)
miR-590	(Mosakhani et al 2012)
miR-598	(Mosakhani et al 2012)
miR-602	(Luo et al 2012)
miR-634	(Luo et al 2012)
miR-642	(Sarver et al 2009, Chang et al 2011b)
miR-658	(Luo et al 2012)
miR-663	(Luo et al 2012)
miR-650	(Sarver et al 2009)
miR-744	(Luo et al 2012)
miR-874	(Luo et al 2012)
miR-886-3p	(Chang et al 2011b)
miR-888	(Luo et al 2012)
miR-1204	(Luo et al 2012)
miR-1224-3p	(Luo et al 2012)
miR-1238	(Luo et al 2012)
miR-1246	(Luo et al 2012)
miR-1275	(Luo et al 2012)
miR-1290	(Luo et al 2012)
miR-1298	(Luo et al 2012)
miR-1908	(Luo et al 2012)
let-7	(Akao et al 2006a)
let-7a	(Fang et al 2007, Chen et al 2009, Earle et al 2010)
let-7b	(Cummins et al 2006, Knowlton et al 2011)
let-7c	(Cummins et al 2006, Chen et al 2009)
let-7e	(Chen et al 2009, Knowlton et al 2011)
let-7f	(Cummins et al 2006)
let-7g	(Cummins et al 2006, Chen et al 2009)

1.5 Diet and microRNA regulation

Each step of the miRNA biogenesis pathway is tightly controlled. The dysregulation of miRNAs in CRC can be characterised by differential expression of pre-miRNA sequences and/or mature miRNAs compared to normal cells. miRNA transcription is regulated by a network of transcriptional machineries and transcription factors (Kim et al 2009). miRNA dysregulation at a transcriptional level may be due to genetic mutations in the miRNA region, or due to altered transcriptional regulation via changes in regulatory proteins or epigenetic mechanisms. Expression of some miRNAs can be altered by the degree of DNA methylation (Lujambio et al 2008, Suzuki et al 2011), while another possible epigenetic mechanism for altering miRNA expression is via histone modification (Suzuki et al 2011). Thomson et al (2006) were among the first to show that a large fraction of miRNA genes are also regulated post-transcriptionally, and that expression levels of a primary transcript does not always correlate with levels of the mature miRNA. At a post-transcriptional level, dysregulation may be a result of changes in proteins involved in the processing, maturation and stability of miRNA (Thomson et al 2006, Melo et al 2009, Melo et al 2010, Melo et al 2011).

There is some evidence to suggest that dietary components can modulate miRNA levels, thereby contributing to the cancer-protective or carcinogenic effect of that food component (Davis & Ross 2008). A systematic search of the literature revealed various dietary compounds that can alter miRNA expression in cancer models, with the studies presented in Table 1.2.

While there are no human studies investigating the role of dietary components on miRNA expression in colorectal cells, a limited number of studies have looked at the effects of diet in other *in vivo* models, particularly rats (Table 1.2). Davidson et al (2009) fed rats diets containing corn oil or fish oil with pectin or cellulose. These rats were also injected with azoxymethane, a colon-specific carcinogen, or saline as a control. At an early stage of cancer progression (10 weeks post-azoxymethane injection), five miRNAs (let-7d, miR-15b, miR-107, miR-191 and miR-324-5p) were selectively modulated by fish oil exposure. For these five miRNAs, expression in the fish oil fed animals was not affected by azoxymethane treatment, whereas for the corn oil groups, azoxymethane exposure resulted in a significant down-regulation of expression ($P < 0.05$). At 34 weeks post-azoxymethane injection, the incidence of adenocarcinomas was significantly reduced in fish oil fed animals compared with corn oil fed animals ($P< 0.05$). The fish oil fed rats had the smallest number of differentially expressed miRNAs for the

azoxymethane versus saline treated groups, demonstrating a novel role for fish oil in protecting the colon from carcinogen-induced miRNA dysregulation (Davidson et al 2009). A study by Shah et al (2011) presented similar findings, with rats fed diets containing corn oil or fish oil and pectin or cellulose and injected with azoxymethane or a saline control. Colonic mucosa was assayed at an early time of cancer progression, and global gene set enrichment analysis was used to identify miRNAs significantly enriched by the change in expression of their putative target genes. A number of miRNAs linked to canonical oncogenic signalling pathways, including miR-16, miR-19b, miR-21, miR26b, miR27b, miR-93, and miR-203, were modulated by diet and carcinogen exposure (Shah et al 2011), although the exact dietary components responsible for these changes were unclear. These *in vivo* studies identified that diet could modify miRNA expression in CRC cells, but although a fibre comparison was incorporated in both the study designs, a specific role or mechanism for dietary fibre was not identified.

Other dietary components have also been shown to alter miRNA expression, in cancer types other than CRC, using *in vivo* rat models and cancer cell lines. Some of the food components had a protective effect on cancer risk, including folate, curcumin, vitamin E, and retinoic acid (Table 1.2).

Dietary folate is a methyl donor, and an important epigenetic determinant of normal methylation and gene expression (WCRF 2007, Wallace et al 2010). Several studies used a rat model to determine the effects of a folate, methionine and choline deficient diet on miRNA expression (Kutay et al 2006, Pogribny et al 2008, Tryndyak et al 2009, Wang et al 2009a, Starlard-Davenport et al 2010). Rats fed a folate/methyl deficient diet develop hepatocellular carcinomas after 54 weeks (Motiwala et al 2003). Hepatomas induced by folate/methyl deficiency had significantly altered miRNA expression compared to the livers of rats fed a control diet (Kutay et al 2006, Pogribny et al 2008, Tryndyak et al 2009). miRNAs were also differentially expressed in the livers of rats after several weeks on the folate/methyl deficient diet, with this early alteration indicating that aberrant miRNAs expression may be an important contributing factor in the development of hepatocellular carcinoma (Tryndyak et al 2009, Wang et al 2009a, Starlard-Davenport et al 2010). miRNAs with tumour suppressor roles, such as miR-122, were decreased in the early stages of hepatocellular carcinoma induced by folate/methyl deficiency (Kutay et al 2006, Pogribny et al 2008, Tryndyak et al 2009), while miRNAs with oncogenic activity, such as miR-221 , miR-155, and miR-21, were increased (Kutay et al 2006, Wang et al 2009a, Starlard-Davenport et al 2010). Another study which examined the effects of folate deficiency in human lymphoblastoid cells also found that miRNA expression was

dysregulated; however, when cells were returned to a folate-sufficient medium this expression returned to that of control cells (Marsit et al 2006).

Curcumin is a naturally occurring flavonoid with pro-apoptotic properties (Sun et al 2008). Sun et al (2008) observed that curcumin up-regulated the expression of some miRNAs and down-regulated others, in a human pancreatic carcinoma cell line. miR-22, which was up-regulated by curcumin, inhibited expression of *SP1* (SP1 transcription factor) and *ESR1* (estrogen receptor 1) (Sun et al 2008). *ESR1* gene expression has been linked to breast cancer and other tumour types, while *SP1* is believed to play a role in growth and metastasis (Sun et al 2008).

The effect of dietary vitamin E on miRNA expression in a rat model has also been studied (Gaedicke et al 2008). After six months on a vitamin E deficient or sufficient diet, the livers of rats fed the vitamin E deficient diet had significantly lower levels of miR-122a and miR-125b expression (Gaedicke et al 2008). These miRNAs have been shown to regulate expression of genes associated with lipid metabolism and cancer (Gaedicke et al 2008), with reduced levels of miR-122 found in hepatocellular carcinoma (Kutay et al 2006).

Retinoic acid has also been shown to have an effect on miRNA expression. In acute promyelocytic leukaemia, retinoic acid responsive genes are transcriptionally repressed, unless pharmacological doses of all-trans-retinoic acid are present. In a microarray analysis of an acute promyelocytic leukaemia cell line, the miRNA expression profile was altered after treatment with all-trans-retinoic acid (Garzon et al 2007). These results were confirmed in primary acute promyelocytic leukaemia cells from patients (Garzon et al 2007). miRNAs thought to play tumour suppressor roles, such as miR-15a, miR-16-1 and several let-7 family members, were up-regulated by all-trans-retinoic acid (Garzon et al 2007). Additional studies have observed the effects of retinoic acid in other conditions. For example, in the retinoic acid-induced neural differentiation of human embryonal carcinoma (NT2) cells, miR-23 was found to play a critical role (Kawasaki & Taira 2003). Another study found that retinoic acid treatment dysregulated several miRNAs, and was associated with abnormal development of the spinal cord in a rat spina bifida model (Zhao et al 2008).

Epigenetic regulation of miRNA expression has been described in CRC tissues and cell lines (Lujambio et al 2008, Toyota et al 2008, Bandres et al 2009, Choudhry & Catto 2011, Suzuki et al 2011); however, there is only limited evidence for the role of food components or food-derived substances in the epigenetic modulation of miRNA

expression. While there is some evidence to suggest that dietary components such as folate and curcumin can alter miRNA levels through epigenetic mechanisms, these studies have not been performed in colorectal cells (Davis & Ross 2008). There is also some very preliminary evidence for regulation of miRNAs by fibre (Shah et al 2011). A mechanism for potential miRNA regulation by dietary fibre may be the production of butyrate. In CRC cells, butyrate has been shown to modify expression of multiple genes, thereby affecting cell cycle regulation, apoptosis, proliferation, differentiation, inflammation, and DNA repair (Mariadason et al 2000, Iacomino et al 2001, Daly & Shirazi-Beechey 2006). Butyrate, with its known role in histone modification, is also a plausible candidate for altering miRNA expression through epigenetic changes.

Table 1.2: Studies reporting altered miRNA expression in *in vivo* and *in vitro* cancer models in response to treatment with a dietary component

Study	Cell line/s or species	Methods	Key results
Fish oil and fibre diets			
Davidson et al (2009)	Rat (CRC)	- 2×2×2 factorial design with two types of dietary fat (n-6 PUFA as corn oil or n-3 PUFA as fish oil), two types of dietary fibre (cellulose or pectin) and two treatments (injection with the colon carcinogen, azoxymethane, or with saline). - TaqMan Human MicroRNA Panel Low-Density Arrays	At 10 weeks post-azoxymethane injection, five miRNAs (let-7d, miR-15b, miR-107, miR-191 and miR-324-5p) were selectively modulated by fish oil exposure. For these five miRNAs, expression in the fish oil fed animals was not affected by azoxymethane treatment, whereas for the corn oil groups, azoxymethane exposure resulted in a significant ($P <$ 0.05) down-regulation of expression. At 34 weeks post-azoxymethane injection, the incidence of adenocarcinomas was significantly reduced in fish oil fed animals compared with corn oil fed animals ($P<$ 0.05). The fish oil fed rats had the smallest number of differentially expressed miRNAs for the azoxymethane versus saline treated groups.
Shah et al (2011)	Rat (CRC)	- 2×2×2 factorial design with two types of dietary fat (n-6 PUFA as corn oil or n-3 PUFA as fish oil), two types of dietary fibre (cellulose or pectin) and two treatments (injection with the colon carcinogen, azoxymethane, or with saline). - Global gene set enrichment analysis	A number of miRNAs linked to canonical oncogenic signalling pathways, including miR-16, miR-19b, miR-21, miR26b, miR27b, miR-93, and miR-203, were modulated by diet and carcinogen exposure. The exact dietary components responsible for these changes were unclear.
Folate/ methyl deficient diet			
Kutay et al (2006)	Rat (hepatocellular carcinoma)	- Diet low in L-methionine and devoid of choline and folic acid or methyl-adequate diet for 9, 18, 36, or 54 wks. - Diet switched in some rats. - miR microarray chip containing 368 probes, including 245 human and mouse miR genes.	During folate and methyl deficient diet-induced hepatocarcinogenesis, 23 miRNAs were up-regulated and 3 down-regulated. Up-regulated miRNAs included miR-101b-2, miR-130, miR-130a, miR-172a-2, miR-219-1, miR-23a, miR-23b, miR-24, miR-328-1, let-7a-2, miR-103-2, miR-106, miR-106a-1, miR-106b-1, miR-130a-1, miR-17, miR-20, miR-20-1, miR-21, miR-21-1, miR-320-2, miR-93, miR-99b. Down-regulated miRNAs included miR-122, miR-123, and miR-215.
Marsit et al (2006)	lymphoblast cell line TK-6	- Cell line treated with folate deficient media or control for 6 days. - miR microarray mirVana miRNA Bioarray (Ambion), which examines 385 known human miRNAs. - Confirmed by real-time RT-PCR.	Folate deficiency significantly altered miRNA expression. Up-regulated miRNAs included miR-181b, miR-182, miR-222, miR-345, miR-181a, miR-205, miR-145, miR-99a, miR-125b, miR-130b, miR-221, miR-22, miR-191, miR-103, miR-107, miR-34a, miR-183, miR-146, miR-422b, miR-7037, miR-24, and miR-361. Down-regulated miRNAs included miR-198 and miR-210.
Pogribny et al (2008)	Rat (hepatocellular carcinoma)	- Diet details NR. - Real-time RT-PCR.	During methyl deficient diet-induced hepatocarcinogenesis miR-34a, miR-16, and miR-127 were down-regulated.
Tryndyak et al (2009)	Rat (hepatocellular carcinoma)	- Diet low in L-methionine and devoid of choline and folic acid or methyl-adequate diet for 9, 18, 36, or 54 wks. - Diet switched in some rats. - Real-time RT-PCR.	During methyl deficient diet-induced hepatocarcinogenesis miR-34a, miR-16a, miR-127, miR-181a, and miR-200b were down-regulated.

Starlard-Davenport et al (2010)	Mouse (hepatocellular carcinoma)	- Low methionine diet, lacking in choline and folic acid, or control diet for 12 wks. - miRNA microarray analysis - Confirmed by RT real-time qPCR.	In the livers of methyl-deficient mice 74 miRNAs were differentially expressed (40 up-regulated and 34 down-regulated) ($P < 0.05$). Up-regulated miRNAs included miR-34a, miR-155, miR-200b and miR-221. Down-regulated miRNAs included miR-15a, miR-30a, miR-101a and miR-122.
Wang et al (2009a)	Mouse (hepatocellular carcinoma)	- Choline-deficient and amino acid–defined diet or control diet for 6, 18, 32, and 65 wks - miRNA microarray analysis - Confirmed by real-time RT-PCR.	In mice fed deficient diet, 30 hepatic microRNAs were significantly altered ($P \leq 0.01$). Up-regulated miRNAs included miR-155, miR-221/222, and miR-21. Down-regulated miRNAs included miR-122.
Curcumin			
Sun et al (2008)	Human pancreatic carcinoma cell line BxPC-3	- Cell line treated with 0 or 10 µmol/L curcumin or liposomal curcumin for 72 h. - miR microarray Atactic chip with 300 probes. - Confirmed by real-time RT-PCR.	After 72 h curcumin incubation, 11 miRNAs were significantly up-regulated, and18 were significantly down-regulated ($P < 0.05$). Up-regulated miRNAs included miR-103, miR-181a, miR-181b, miR-181d, miR-21, miR-22, miR-23a, miR-23b, miR-24, miR-27a, miR-34a. Down-regulated miRNAs included miR-140, miR-146b, miR-148a, miR-15b, miR-195, miR-196a, miR-199a, miR-19a, miR-204, miR-20a, miR-25, miR-26a, miR-374, miR-510, miR-7, miR-92, miR-93, and miR-98. At the same concentration, liposomal curcumin significantly up-regulated 5 miRNAs and down-regulated 10 miRNAs ($P < 0.05$). Up-regulated miRNAs included miR0193b, miiR-34a, miR-22, miR-92, and miR-21. Down-regulated miRNAs included mir-199b, miR-199a, miR-25, miR-15b, miR-15a, miR-31, miR-16, miR-24, let-7i, and miR-20b.
Vitamin E			
Gaedicke et al (2008)	Rat (liver)	- Vitamin E deficient or sufficient diet for 6 months. - Real-time RT-PCR.	Vitamin E deficient group had significantly lower levels of miR-122a ($P < 0.05$) and miR-125b ($P < 0.0001$).
Retinoic acid			
Kawasaki and Taira (2003)	Human embryonal carcinoma cell line NT2	- NT2 cells grown in the presence or absence of synthetic siRNA-miR-23 (which reduces intracellular level of precursor and mature miR-23). Cells treated with retinoic acid to differentiate.	Expression of Hes1, a transcriptional repressor, was regulated by miR-23 during the retinoic acid-induced neural differentiation of NT2 cells.
Garzon et al (2007)	Acute leukemia cell lines: NB4, HL-60; Human samples (bone marrow and blood)	- Cell lines treated with 100 nM all-trans-retinoic acid or control for 4 days. - miRNA microarray chip-containing 368 probes, corresponding to 245 human and mouse miRNA genes. - Confirmed by real-time RT-PCR.	During retinoic acid treatment of NB4, miR-15a, miR-15b, miR-16-1, let-7a-3, let-7c, let-7d, miR-223, miR-342, miR-107 and miR-147 were up-regulated. miR-181b was down-regulated. There were similar miR-223 and let-7a expression in HL-60 cells treated with retinoic acid. There were similar let-7d, let-7a-3, miR-223, miR107, miR-15a and miR-16-1 in primary blast cells from three acute leukemia patients treated with retinoic.
Zhao et al (2008)	Spina bifida fetal rat model	- Pregnant rats given single dose (135 mg/kg body weight) of all-trans-retinoic acid and killed 3, 5, 7, or 9 days after treatment. - Northern blot.	miRNAs miR-9/9*, miR-124a, and miR-125b were down-regulated in retinoic acid-treated sacral spinal cord compared to control.

CRC: colorectal cancer; NR: not reported; PCR: polymerase chain reaction; PUFA: polyunsaturated fatty acid; RT: reverse transcription; siRNA: small interfering RNA.

Chapter 2. Aims

2.1 General hypotheses and aims

As shown in Chapter 1, CRC development is associated with epigenetic modifications, including DNA methylation changes, altered histone modification patterns, and dysregulated miRNA expression. While some dietary compounds are likely to alter CRC risk through epigenetic mechanisms, their role in modifying miRNA expression in CRC cells and normal colorectal tissue has been less studied. Diet-derived butyrate, with its known role in histone modification, is a plausible candidate for altering miRNA expression. This study aimed to examine dietary regulation of miRNA expression in colorectal cells. In particular, the study aimed to systematically explore the role of butyrate and other HDIs in modulating CRC risk through altered miRNA expression, in CRC cells *in vitro*, and in rectal tissue *in vivo*. It was hypothesised that modification of miRNA expression may contribute to the chemo-protective effect of butyrate and other HDIs. To address this hypothesis, the study also aimed to examine the down-stream consequences of miRNA changes, and the roles of miRNAs in the context of the anti-proliferative effects of HDIs. In addition to exploring the action of butyrate, a potentially protective dietary component, the study also aimed to investigate whether factors that possibly increase CRC risk, such as high red meat intake, alter miRNA expression. It was hypothesised that increased intake of red meat may alter miRNA expression profiles, but that feeding resistant starch could protect against this dysregulation by increasing butyrate levels in the colorectum.

2.2 Chapter 4 aim

To determine whether butyrate treatment alters miRNA expression in CRC cell lines, through miRNA microarray analysis and subsequent real-time RT-PCR validation.

2.3 Chapter 5 aim

To compare the effect of butyrate and other HDIs on miR-17-92 expression in CRC cells, and to confirm the effect of HDIs on miR-17-92 target gene expression.

2.4 Chapter 6 aim

To examine the roles of members of the miR-17-92 cluster in the context of the anti-proliferative effects of HDIs, and to determine the specific roles of these miRNAs in modulating target gene expression.

2.5 Chapter 7 aim

To determine the effect of butyrate on miR-17-92 host gene transcription, and specifically to investigate the effect of butyrate treatment on the levels of acetylation and methylation at DNA-bound histones surrounding *MIR17HG*, the miR-17-92 host gene.

2.6 Chapter 8 aim

To investigate the effect of high red meat intake and resistant starch supplementation on miRNA expression in the rectal mucosa cells of healthy human volunteers.

Chapter 3. Materials and Methods

3.1 *In vitro* experimental methods

For the following methods, details and suppliers of chemicals and reagents, equipment, primers and oligonucleotides, antibodies, and buffers and solutions are listed in Tables 3.4 – 3.8.

3.1.1 Cell culture

Several stable CRC cell lines were used for *in vitro* experiments.

The HT29 colorectal adenocarcinoma cell line (ATCC, Manassas, VA, USA) is an adherent epithelial cell line, which was derived in 1964 from the diseased colon of a 44 year old Caucasian female. The line is positive for expression of *C-MYC*, *KRAS*, *HRAS*, *NRAS*, *MYB*, *SIS* and *FOS* oncogenes. *N-MYC* oncogene expression was not detected. There is a G -> A mutation in codon 273 of the p53 gene resulting in an Arg -> His substitution (ATCC, Manassas, VA, USA). HT29 cells were maintained in Dulbecco's Modified Eagle's Medium/ F-12 Nutrient Mixture (Ham) Medium (1:1) containing 5% foetal bovine serum.

The HCT116 colorectal carcinoma cell line (ATCC, Manassas, VA, USA) is an adherent epithelial line derived from an adult male. This line has a mutation in codon 13 of the *RAS* proto-oncogene, while p53 is wild-type (ATCC, Manassas, VA, USA). Cells were maintained in McCoy's 5A Medium (modified) containing 10% foetal bovine serum.

HT29 and HCT116 butyrate-resistant cell lines (HT29-BR and HCT116-BR) were developed by Fung et al (2009). These CRC cell lines were made less responsive to the apoptotic effects of butyrate through sustained exposure to gradually increasing concentrations of sodium butyrate. Cultures were initially exposed to 0.5 mM sodium butyrate and concentration was increased by 0.5 mM increments. Cells were maintained at each concentration step for at least two passages until the butyrate concentration reached 5 mM (Fung et al 2009). Cells were maintained in appropriate medium (as outlined above) containing 5 mM sodium butyrate.

Cells were cultured at 37°C and 5% CO_2, and were shown by routine testing to be mycoplasma free. Addition of antibiotics to the culture medium was not required. Cells were maintained at less than 80% confluence, with media renewal two to three times per week.

Cells were subcultured (passaged) approximately once per week, with a sub-cultivation ratio of 1:3 to 1:8. To passage cells, culture medium was removed and discarded, and the cell layer briefly rinsed with 1× PBS to remove traces of serum which naturally contains trypsin inhibitor. PBS was removed, and 1× trypsin-EDTA solution was added to the flask. Cells were incubated at 37°C for approximately 5 min, until observation of the cells under an inverted microscope showed the cell layer to be dispersed. To deactivate trypsin, appropriate growth medium was added, and cells were mixed by gently pipetting. Appropriate aliquots of the cell suspension were added to new culture flasks with additional growth medium for continued culture, or were removed for cell counting and seeding of plates at the commencement of a new experiment. Cells were discarded after a maximum of 10 passages.

Cells were stored in foetal bovine serum and 10% DMSO, in cryovials at -80°C (for short term storage) or liquid nitrogen (for long term storage). Cells were frozen slowly by placing vials in a freezing container with isopropanol, and when required were resuscitated quickly by thawing in a 37°C water bath.

3.1.2 Cell treatments

Adherent cell lines were harvested with trypsin, and a small aliquot was removed for cell counting using a haemocytometer.

Most cell experiments were conducted in 6-well (35 mm) plates, with cells seeded at 3×10^5 per 35 mm well. For 24-well plates cells were seeded at 1×10^5 per well, for xCELLigence RTCA E-plates (equivalent in size to wells in 96-well plates) cells were seeded at 0.2×10^5 per well, and for 15 cm plates cells were seeded at 3×10^6 per plate. With the exception of some transfection experiments, after seeding cells were maintained for 24 h prior to treatment.

To prepare the butyrate treatment, sodium butyrate was dissolved in Dulbecco's Modified Eagle's Medium without foetal bovine serum to make a 1 M stock solution, and filtered using a 0.2 μm filter, before further dilution in appropriate cell culture medium. The trichostatin A (TSA) was a sterile ready-made 5 mM solution which required simple dilution in appropriate cell culture medium. To prepare the suberoylanilide hydroxamic acid (SAHA) treatment, SAHA was first dissolved in DMSO to make a 1 M solution, then diluted in Dulbecco's Modified Eagle's Medium without foetal bovine serum to make a 1 mM stock solution, and filtered using a 0.2 μm

filter. The stock solution was then further diluted in appropriate cell culture medium. All solutions were freshly prepared for each treatment.

Cells were cultured with 1, 5, 10 or 25 mM sodium butyrate, 1, 2, or 3 μM SAHA, 0.3, 0.5 or 0.7 μM TSA, or control medium for 48 h. Additional cells were treated in triplicate with 5 μg/mL cycloheximide, which was added 3 h prior to other treatments, and again when cells were treated with butyrate or maintained in control medium.

3.1.3 RNA extraction and quantification

3.1.3.1 RNA extraction

For cell culture in 6-well or 24-well plates, TRIzol Reagent was used to obtain RNA from samples. Following media removal from the plates, 1 mL (for 6-well plates) or 400 μL (for 24-well plates) of TRIzol Reagent was added directly to the cells in the culture dish. Cells were lysed directly in the culture dish by pipetting the cells up and down several times. Total RNA was extracted according to the manufacturer's instructions, as detailed below.

Homogenised samples were incubated for 5 min at room temperature to permit complete dissociation of the nucleoprotein complex. For phase separation, 200 μL (for 6-well plates) or 80 μL (for 24-well plates) of chloroform was added to a sample, and the tube was shaken vigorously by hand for 15 sec. The sample was then incubated for 2 – 3 min at room temperature, and then centrifuged at 12,000 × g for 15 min at 4°C. This process separated the mixture into a lower red phenol-chloroform phase, an interphase, and a colourless upper aqueous phase, with RNA remaining exclusively in the aqueous phase. Once centrifuged, the aqueous phase of the sample was removed, avoiding any withdrawal of the interphase or organic layer when removing the aqueous phase. The aqueous phase was transferred into a new tube.

For RNA precipitation, 0.5 mL (for 6-well plates) or 200 μL (for 24-well plates) of 100% isopropanol was added to the removed aqueous phase. The sample was incubated at room temperature for 10 min, and centrifuged at 12,000 × g for 20 min at 4°C. The RNA forms a pellet on the side and bottom of the tube. Supernatant was then removed from the tube, leaving only the RNA pellet. The pellet was washed by adding 1 mL (for 6-well plates) or 500 μL (for 24-well plates) of chilled 75% ethanol. The sample was vortexed briefly, then centrifuged at 7,500 × g for 5 min at 4°C. The ethanol wash was then discarded, and the remaining RNA pellet air-dried on ice for 5 – 10 min. The RNA pellet was then resuspended in 20 – 50 μL of RNase-free water, ready for quantitation.

For solid tissue such as human rectal biopsies, the same TRIzol protocol was employed, with minor variation. For solid tissue stored in RNA later, the frozen sample was placed in 300 μL TRIzol and homogenised with brief pulses using a homogeniser with sterile pestle. An additional 200 μL of TRIzol was then added for a total of 500 μL. Processing then proceeded as for the standard TRIzol protocol, using 100 μL chloroform, 250 μL isopropanol, and 500 μL chilled 75% ethanol.

3.1.3.2 RNA quantitation

RNA was quantified using a Nanodrop-8000 spectrophotometer, by first blanking the Nanodrop-8000 pedestals with 1 μL water, then loading 1 μL of each sample on the pedestals to obtain RNA quantity and 260/280 and 260/230 ratios. The RNA integrity was also assessed using agarose gel electrophoresis or using an RNA 6000 Pico Chip run on an Agilent 2100 bioanalyzer. RNA was stored at -80°C.

3.1.4 Protein extraction and quantification

3.1.4.1 Protein extraction

Prior to use, 10 mL of protein lysis buffer was prepared by addition of 10 μL of 1 M DTT and 1 Complete mini protease inhibitor cocktail tablet. Cells were washed in 1 × PBS after media removal, and 300 μL or 60 μL protein lysis buffer was added to obtain whole cell protein extracts from 6-well and 24-well plates respectively. Once the buffer was added, cells were scraped to homogenise, and passed through a fine 26 gauge needle. Protein was stored at -20°C.

3.1.4.2 Protein quantitation

Protein extracts were quantified using the EZQ Protein Quantification kit. For the EZQ protocol, standards were prepared by making serial dilutions of 2 mg/mL ovalbumin stock solution in protein extraction buffer (dilution range from 0.02 – 2 mg/mL). The EZQ assay paper was then inserted into a 96-well microplate cassette. In triplicate, each of the protein standards, samples, and no-protein control (buffer only) were loaded by spotting 1 μL of each onto the assay paper, ensuring the membrane was not scratched or punctured. The protein samples on the paper were allowed to dry completely, and the protein-spotted assay paper was removed from the cassette and placed in tray. The protein-spotted assay paper was then washed with 40 mL methanol, with gentle agitation, for 5 min. After washing, the assay paper was dried, and 40 mL of the EZQ protein quantitation reagent (Component A) was added to the tray. The protein-spotted assay paper in the stain solution was then agitated gently on an orbital

shaker for 30 min. After staining, the assay paper was rinsed for 1 – 2 min in rinse buffer (10% methanol, 7% acetic acid), with this wash repeated twice, for a total of three rinses. The fluorescence from the protein-spotted assay paper was then detected using a Typhoon scanner, and results analysed using Carestream Molecular Imaging Software. The fluorescence values of the experimental samples and standards were determined by subtracting the fluorescence value of the no-protein control. A standard curve was created by plotting the corrected fluorescence values of the standards versus the corresponding protein mass (or concentration).The mass (or concentration) of the experimental samples could then be determined from the standard curve.

3.1.5 Microarray analysis

miRNA expression profiling from HT29 control medium and 5 mM butyrate cells was performed using the Exiqon v11 ready-to-spot probeset. For each sample, 4 μg of total RNA was labelled by the ligation of a fluorescently modified RNA dimer (Thomson et al 2004). Two sample (dual colour) competitive hybridisations were performed using Cy3 and Cy5 labelled sample pairs. Hybridisation was performed for 16 h at 56°C under LifterSlips in 1× Exiqon hybridisation buffer in 25 μL. Slides were placed in Corning hybridisation chambers and protected from light for the incubation. Slides were washed using dilutions of the Exiqon Wash Buffer kit, and scanned at 10 μm resolution with a Genepix 4000B Scanner. Mean pixel intensity values in scanned images were extracted for both channels (Cy3, Cy5) using the Spot v3 plugin (CSIRO, VIC, Australia) within the R statistical software package. After background subtraction, foreground intensities were $\log_2$ transformed and ratios (Cy5/Cy3) were obtained. Ratios were normalised within the Limma plugin (Smyth 2005) using the global Loess normalisation routine. Arrays were normalised to each other, and for each probe across the arrays a linear model was fitted to determine final expression values and associated ranking statistics.

3.1.6 Relative quantitation real-time RT-PCR

3.1.6.1 Real-time RT-PCR for microRNAs

miRNA expression analysis was performed using RNA from HT29 and HCT116 control and treated cells. miRNA expression analysis of normal human rectal mucosa was also performed. This sample was prepared following ethics approval from the Flinders Clinical Research Ethics Committee. cDNA was synthesised from 20 ng total RNA using miRNA-specific primers according to the TaqMan miRNA Assay protocol, using 3.5 μL master mix, 2.5 μL RNA, and 1.5 μL primer. For each reverse transcription (RT) reaction, the master mix contained 0.075 μL 100 mM dNTPs, 0.5 μL multiscribe

RT enzyme, 0.75 μL 10× RT buffer, 0.095 μL RNase inhibitor, and 2.08 μL water. Once the mastermix, miRNA-specific primer, and RNA were added to the wells of eight-strip tubes, samples were incubated on ice for 5 min, then loaded into a thermal cycler. The RT program on the thermal cycler consisted of a 30 min incubation at 16°C, a 30 min incubation at 42°C, a 5 min incubation at 85°C, and finally an incubation at 4°C until ready for use in real-time PCR.

Real-time PCR was carried out according to the TaqMan protocol, using triplicate 10 μL reactions for each biological replicate including 1 μL of reverse transcription product, 0.5 μL miRNA-specific primer and probe assay mix, 5 μL 1× TaqMan Universal PCR Master Mix No AmpErase UNG, and 3.84 μL water. Once all reactions were loaded into four-strip PCR tubes, tubes were loaded into a thermal cycler capable of recording in real-time. Thermal cycling was performed using a Corbett Rotorgene 2000 or a Qiagen Rotorgene Q, and consisted of a 10 min incubation at 95°C, then 50 cycles of a 15 sec denaturing step at 95°C and a 60 sec annealing/ extension step at 60°C.

miRNA levels were normalised relative to the levels of the endogenous small nuclear RNA gene RNU6B. Expression levels were calculated from Ct values using Qgene (Muller et al 2002).

3.1.6.2 Real-time RT-PCR for mRNAs

For mRNA expression analysis, RNA was pre-treated with a DNAfree system, using 1 μL DNase and 2.5 μL DNase buffer in 22.5 μL diluted RNA (0.1 μg/μL), with a 20 min incubation at 37°C. This was followed by deactivation with 2.5 μL DNase deactivation slurry. For cDNA synthesis, 1 μL (100 ng) of random hexamer primers was added to 1 μg total DNase treated RNA (10 μL), with a 5 min incubation at 70°C. Subsequently, to each sample, 1 μL M-MLV Reverse Transcriptase, RNase H minus, Point mutant, 5 μL RT buffer, 1.25 μL dNTP mix, and 6.75 μL water was added to make a 25 μL reaction. Following a 10 min incubation at room temperature, reverse transcription was carried out in a thermal cycler with a 50 min hold at 50°C, followed by a 15 min hold at 70°C. The resulting cDNA was then diluted 1:2.5 for use in real-time PCR. Real-time PCR was carried out according to the TaqMan Gene Expression Assay protocol, using triplicate 10 μL reactions including 2 μL of RT product, 0.5 μL mRNA-specific Gene Expression assay mix, 5 μL 2× TaqMan Gene Expression master mix, and 2.5 μL water. Cycling consisted of a 2 min incubation at 50°C and a 10 min incubation at 95°C, then 50 cycles of a 15 sec denaturing step at 95°C and a 60 sec annealing/ extension step at 60°C.

Transcript levels were normalised relative to levels of endogenous control *ACTB* (β-actin) mRNA. Expression levels were calculated from Ct values using Qgene (Muller et al 2002).

3.1.7 Western blot analysis

Protein extracts from control and treated HT29 and HCT116 cells were resolved by SDS-PAGE gel and electro-blotted onto polyvinylidene difluoride membranes.

3.1.7.1 SDS-PAGE gels

For this protocol, 50 ng of each protein sample was used, in a volume of 25 μL. To this volume, 25 μL of loading dye was added (prepared using 150 μL 2× SDS loading dye and 30 μL 1 M DTT to give a concentration of 200 mM DTT). The sample and loading dye mix were heated at 100°C for 3 min, as was a 20 μL sample of pre-stained broad range (7 – 175 kDa or 10 – 230 kDa) marker.

The SDS-PAGE gel consisted of a 5% stacking gel on top of an 8% or 10% separation gel. The 8% separation gel had 2.5 mL 4× lower buffer, 2 mL 40% acrylamide/ bisacrylamide, 35 μL 10% APS, 15 μL TEMED, and 5.5 mL water. The 10% gel had 2.5 mL 4× lower buffer, 2.5 mL 40% acrylamide/ bisacrylamide, 35 μL 10% APS, 15 μL TEMED, and 5 mL water. Separation gels were allowed to set for 20 min before addition of the stacking gel, which had 1.25 mL 4× upper buffer, 625 μL 40% acrylamide/ bisacrylamide, 35 μL 10% APS, 15 μL TEMED, and 3.1 mL water. Once gels were prepared and placed in a tank with 1× SDS running buffer (prepared from 5× stock), prepared protein samples and marker were loaded. Gel was run at consistent 25 mAmps for 45 – 60 min.

3.1.7.2 Electro-blotting

Once run, gels were soaked in transfer buffer for 10 – 15 min. Twelve pieces of blotting paper were also soaked in transfer buffer, and the polyvinylidene difluoride membrane was soaked in methanol for 15 sec, water for 2 min, and transfer buffer for 5 min. The gel and membrane were then sandwiched between the 12 pieces of blotting paper on a semi-dry blotter, and transferred at 77 mAmps for 2.5 – 3 h.

3.1.7.3 Protein detection with antibodies

After transfer, membranes were blocked using 5% skim milk in 1× TBS-T prior to overnight incubation with primary antibodies: rabbit monoclonal anti-CDKN1A (12D1), rabbit monoclonal anti-PTEN (D4.3), rabbit monoclonal anti-BCL2L11 (C34C5), or mouse monoclonal anti-HEF1/NEDD9 (2G9) (all 1:1000). Rabbit

monoclonal anti-ACTB (1:5000) (ab8227) was used as a loading control. After overnight incubation, membrane was washed four times in 1× TBS-T, before 1 h incubation with secondary horseradish peroxidase-conjugated goat anti-rabbit IgG or donkey anti-mouse IgG. After four more 1× TBS-T washes, the enhanced chemiluminescence (ECL) system was used (5 min dark incubation with 0.5 mL of ECL substrate and 0.5 mL of enhancer) to visualise bands using an ImageQuant LAS 4000 system. Densitometry was performed using Multi Gauge software, with results normalised to ACTB protein levels.

3.1.8 Transfection with microRNA mimics, target protectors and small interfering RNAs (siRNAs)

3.1.8.1 Transfection with microRNA mimics

HT29 cells were reverse transfected with miRNA mimics using Lipofectamine 2000 according to the manufacturer's protocol in 24-well and in xCELLigence RTCA E-plate formats (E-plate wells were equivalent in size to wells in a 96-well plate). miRNA oligonucleotide duplexes (miRNA mimics) were used at 20 nM each in the following combinations: miR-17 family, miR-18 family, miR-19 family, miR-92 family, entire miR-17-92 cluster, miR-17-92 cluster minus miR-18a, or negative control mimic (sham). The reverse transfection protocol for one well of a 24-well plate consisted of dilution of the miRNA mimics in 50 μL Opti-MEM reduced serum medium, and dilution of Lipofectamine 2000 by adding 1 μL to 50 μL Opti-MEM reduced serum medium. For one well of an E-plate, volumes of Opti-MEM were reduced to 25 μL for miRNA mimic dilution and to 25 μL for dilution of 0.25 μL Lipofectamine 2000. Diluted Lipofectamine 2000 was incubated for 5 min, then combined with diluted miRNA mimic/s and incubated for a further 15 min. During this incubation period, cells were prepared for seeding. For 24-well plates, cells were seeded at 1×10^5, while for 96-well E-plates, cells were seeded at 0.2×10^5. The mimic-Lipofectamine 2000 complex solution was added to the well (100 μL in total for one well of a 24-well plate, 50 μL in total for one well of an E-plate), followed by the appropriate number of cells in standard growth medium (500 μL in total for one well of a 24-well plate, 100 μL in total for one well of an E-plate. After 8 h of transfection, cells were treated with 5 mM butyrate, 2 μM SAHA, or control medium and grown for 48 h. For the 96-well plates, proliferation was recorded using the xCELLigence RTCA DP instrument. For the 24-well plates, cells were harvested and RNA extracted for real-time RT-PCR.

3.1.8.2 Transfection with microRNA mimics and target protectors

In additional 24-well plate experiments, cells were reverse co-transfected with miR-18a mimics and also with miScript target protectors designed for miR-18a predicted target genes *NEDD9* and *CDK19*, or with a negative control miScript target protector. Target protectors are single-stranded, modified RNAs that specifically interfere in the interaction between a miRNA and a single target, while leaving the regulation of other targets of the same miRNA unaffected. Target protectors were designed for the four potential miR-18a binding sites in the *NEDD9* 3'UTR and the three potential binding sites in the *CDK19* 3'UTR using a Qiagen algorithm (www.qiagen.com/miDesign [accessed 3 November 2011]), and were reverse transfected at a concentration of 500 nM for each target protector. The target protector sequences are shown in Table 3.6. After 8 h of transfection, cells were treated with 5 mM butyrate or control medium and grown for 48 h. Cells were harvested after 48 h and RNA harvested for real-time RT-PCR.

3.1.8.3 Transfection with small interfering RNAs (siRNAs)

In separate E-plate experiments, two pre-designed small interfering RNAs (siRNAs) for *NEDD9*, two pre-designed siRNAs for *CDK19*, or a negative control siRNA were reverse transfected at a total concentration of 20 nM. After 8 h of transfection, cells were treated with 5 mM butyrate or control medium and grown for 48 h. Proliferation was recorded using the xCELLigence RTCA DP instrument.

3.1.9 Real-time cell growth analysis

Cell proliferation was measured using the xCELLigence RTCA DP instrument and 16-well E-plates, which uses electrical contacts on the bottom of the E-plate wells to continually monitor cell growth over time. Following a blanking step with media only in each E-plate well, HT29 or HCT116 cells were seeded at 0.2×10^5 cells per well of an E-plate. In some experiments, at this seeding stage reverse-transfection was also performed as described above. Growth of the cells was tracked every 30 min for 7 – 8 h before treatment addition. Growth was subsequently tracked every 30 min over 48 h.

3.1.10 microRNA target prediction

Predicted miRNA target genes were determined using miRGen, focusing on genes common to two or more prediction programs (Megraw et al 2007), and analysed using Ingenuity Pathway Analysis (IPA) to identify all genes involved in proliferation and cell cycle control, and expressed in colorectal cells.

3.1.11 Chromatin immunoprecipitation

A chromatin immunoprecipitation (ChIP) experiment was performed in HT29 cells, to determine the effects of butyrate treatment on histone acetylation and methylation pattern around the transcription start site (TSS) of the *MIR17HG* gene, which is the miR-17-92 cluster host gene. ChIP was performed using the SimpleChIP Enzymatic Chromatin IP kit, and was carried out according to the manufacturer's instructions, as detailed below. This kit made use of Micrococcal Nuclease to digest the chromatin, and agarose beads for the immunoprecipitation.

3.1.11.1 Optimization of chromatin digestion

Before performing ChIP on the butyrate-treated and control medium HT29 cells, optimal conditions for digestion of cross-linked DNA to 150 – 900 base pairs in length were determined. For the optimisation, cross-linked nuclei from 4×10^7 HT29 cells were obtained, using the method described in 3.1.11.2. Micrococcal Nuclease was diluted 1:5 in 1× buffer B + DTT. In five tubes each containing 200 µL of the nuclei preparation, 0 µL, 2.5 µL, 5 µL, 7.5 µL or 10 µL of the diluted Micrococcal Nuclease was added, with tubes incubated for 20 min at 37°C with frequent mixing. The digest was stopped by adding 20 µL of 0.5 M EDTA and placing tubes on ice. The nuclei were then pelleted by centrifugation, the supernatant was removed, and the pellet was resuspended in 200 µL of 1× ChIP buffer + protease inhibitor cocktail (PIC) + PMSF. Each tube was then incubated on ice for 10 min, then sonicated to rupture nuclear membrane, using three sets of 20 sec pulses with 30 sec intervals of incubation on ice between pulses. The lysates were clarified by centrifugation, and 50 µL of each sonicated lysate was transferred to a new tube. To each 50 µL sample, 100 µL water, 6 µL 5 M NaCl and 2 µL RNAse A were added, and samples were incubated at 37°C for 30 min. Following addition of 2 µL Proteinase K, samples were incubated at 65°C for 2 h. DNA fragment size was determined by electrophoresis, with 20 µL of each sample loaded onto a 1% agarose gel, with a 1 kb DNA marker also loaded. From the gel, the digestion conditions which produced DNA in the desired range of 150 – 900 base pairs could be determined, and the volume of diluted Micrococcal Nuclease that produced the desired size of DNA fragments was equivalent to the volume of Micrococcal Nuclease stock subsequently used to digest the 4×10^7 cells in the preparative chromatin digestion.

3.1.11.2 *In vivo* cross-linking, nuclei preparation and nuclease S7 digestion of chromatin

For each treatment (butyrate or control medium), 4×10^7 cells were required for the ChIP experiment, to generate one chromatin preparation that could be used for up to ten separate immunoprecipitations. To ensure an adequate supply of HT29 cells, eight 15 cm plates were seeded for each treatment, at a concentration of 3×10^6 cells per plate. Cells were grown for 48 h, then treated with 5 mM butyrate or control medium for 48 h. After 48 h, one plate from each treatment group was treated with trypsin and used for determination of cell number using a haemocytometer, to determine how many plates were required to provide 4×10^7 cells.

To perform cross-linking in the remaining plates (two sets of 4×10^7 cells), various solutions were prepared, as outlined in Table 3.8. To cross-link proteins to DNA, 540 µL of 37% formaldehyde was added to each 15 cm culture plate containing 20 mL medium, with incubation for 10 min at room temperature. This was followed by addition of 2 mL of 10× glycine to each dish, with 5 min incubation at room temperature. Medium was then removed and cells were washed two times with 20 mL ice-cold 1× PBS. To each plate, 2 mL ice-cold 1× PBS + PMSF was added, and cells were scraped into cold buffer. For each treatment, cells were combined into one 15 mL tube, and cells centrifuged at 1,500 rpm for 5 min at 4°C. Supernatant was removed, cells were resuspended in 10 mL ice-cold Buffer A + DTT + PIC + PMSF, and were incubated on ice for 10 min. Nuclei were pelleted by centrifugation at 3,000 rpm for 5 min at 4°C, supernatant was again removed, and the pellet was resuspended in 10 mL ice-cold Buffer B + DTT. Centrifugation and supernatant removal was repeated, and the pellet was resuspended in 1.0 mL Buffer B + DTT and transferred to a 1.5 mL tube. An appropriate amount of Micrococcal Nuclease was added, as determined in section 3.1.11.1, and tubes were incubated for 20 min at 37°C with frequent mixing to digest DNA to approximately 150 – 900 base pair lengths. The digest was stopped by adding 100 µL of 0.5 M EDTA and placing tube on ice. Nuclei were then pelleted by centrifugation at 13,000 rpm for 1 min at 4°C, supernatant was removed, and pellet resuspended in 1 mL of 1× ChIP buffer + PIC + PMSF and split into two tubes of 500 µL. Tubes were incubated on ice for 10 min, then each tube of lysate was sonicated using three sets of 20 sec pulses with 30 sec intervals on wet ice between pulses. Lysates were then clarified by centrifugation at 10,000 rpm for 10 min at 4°C. The supernatant, which was transferred to a new tube, was now the cross-linked chromatin preparation. For analysis of DNA digestion and determination of chromatin concentration, 50 µL of

the chromatin preparation was removed, with the remainder stored at -80°C until further use.

3.1.11.3 Analysis of chromatin digestion and concentration

To each of the 50 µL chromatin samples, 100 µL nuclease-free water, 6 µL 5 M NaCl and 2 µL RNAse A were added, with incubation at 37°C for 30 min. To each RNAse A-digested sample, 2 µL Proteinase K was then added, and samples were incubated at 65°C for 2 h. DNA was purified from samples using spin columns as described in Section 3.1.11.7, and a 10 µL sample was used to determine DNA fragment size by electrophoresis on a 1% agarose gel with a 100 base pair DNA marker. DNA should have been digested to a length of approximately 150 – 900 base pairs (1 to 5 nucleosomes). In addition, DNA concentration was determined using a Nanodrop-8000 spectrophotometer, with DNA concentration ideally between 100 and 200 µg/mL.

3.1.11.4 Chromatin immunoprecipitation

The antibodies used for immunoprecipitation of the control and butyrate-treated chromatin included the positive control rabbit monoclonal Histone H3 (D2B12) XP (ChIP Formulated) and the negative control Normal Rabbit IgG, as well as the antibodies of interest including rabbit polyclonal anti-acetyl-histone H3 (Lys 9/ Lys 14), rabbit polyclonal anti-acetyl-histone H3 (Lys 27), and rabbit polyclonal anti-tri-methyl histone H3 (Lys 4). Enough 1× ChIP Buffer was prepared for ten immunoprecipitations (five for each treatment), with each precipitation containing 400 µL of 1× ChIP Buffer (40 µL of 10× ChIP Buffer + 360 µL water) and 2 µL PIC. To the prepared ChIP buffer, the equivalent of 100 µL (10 to 20 µg of chromatin DNA) of the cross-linked chromatin preparation was added for each immunoprecipitation. For example, for five immunoprecipitations, a tube was prepared containing 2 mL 1× ChIP Buffer (200 µL 10× ChIP Buffer + 1.8 mL water) + 10 µL PIC + 500 µL digested chromatin preparation. For each treatment, a 10 µL sample of the diluted chromatin was removed and stored at -20°C to be used as a 2% input sample. For each immunoprecipitation, 500 µL of the diluted chromatin was transferred to a microcentrifuge tube and the immunoprecipitating antibody was added at an appropriate concentration (Table 3.7). Immunoprecipitation samples were incubated overnight at 4°C with rotation. The following day, 30 µL of ChIP-Grade Protein G Agarose Beads were added to each immunoprecipitation sample, with incubation for 2 h at 4°C with rotation.

3.1.11.5 Washing of immunoprecipitated chromatin

To wash the immunoprecipitation samples, low and high salt washes were prepared, as outlined in Table 3.8. The Protein G Agarose Beads in each immunoprecipitation were pelleted by brief 1 min centrifugation at 6,000 rpm, and supernatant was then removed. To each pellet of beads, 1 mL of low salt wash was added, with incubation at 4°C for 5 min with rotation. Centrifugation, supernatant removal, and addition of low salt wash were repeated two additional times, for a total of three low salt washes. Following the final supernatant removal, 1 mL of high salt wash was added to the beads, with incubation at 4°C for 5 min with rotation.

3.1.11.6 Elution of chromatin from antibody/ Protein G beads and reversal of cross-links

For each washed immunoprecipitation and each 2% input sample, 150 µL 1× ChIP Elution Buffer was prepared. First, 150 µL of the 1× ChIP Elution Buffer was added to the 2% input sample tubes from section 3.1.11.4 and tubes were set aside at room temperature. For the washed immunoprecipitation samples, the Protein G Agarose Beads were pelleted by brief 1 min centrifugation at 6,000 rpm, and supernatant was removed. To each immunoprecipitation sample, 150 µL 1× ChIP Elution Buffer was added. Chromatin was eluted from the antibody/Protein G beads for 30 min at 65°C with gentle vortexing at 1,200 rpm. The Protein G Agarose Beads were pelleted by brief 1 min centrifugation at 6,000 rpm, and each eluted chromatin supernatant was transferred to a new tube. To all tubes, including the 2% input samples, 6 µL 5 M NaCl and 2 µL Proteinase K were added, and tubes were incubated for 2 h at 65°C.

3.1.11.7 DNA purification using spin columns

Before DNA purification, 24 mL of ethanol (96 – 100%) was added to the DNA Wash Buffer before use. One DNA spin column/collection tube was used for each chromatin sample from Section 3.1.11.6. To begin purification, 750 µL of DNA Binding Buffer was added to each sample, and 450 µL of each sample was added to a DNA spin column in a collection tube. The tube was centrifuged at 14,000 rpm for 30 sec, the spin column was removed from the collection tube and liquid discarded, then the spin column was replaced in the collection tube. The remaining 450 µL of sample was added to the spin column in the collection tube and the centrifugation and discarding of liquid was repeated. To the spin column in a collection tube, 750 µL of DNA Wash Buffer was then added, and tubes were re-centrifuged at 14,000 rpm for 30 sec. Liquid in the collection tube was again discarded. A further centrifugation at 14,000 rpm for 30 sec

was performed, the collection tube and liquid were discarded, and the spin column was placed in a new 1.5 mL tube. DNA was eluted in 50 µL of DNA Elution Buffer following centrifugation at 14,000 rpm for 30 sec. The eluate of purified DNA was stored at -80°C.

3.1.11.8 Primer design

To quantify the purified DNA for each immunoprecipitation sample, primer pairs were designed to target intron and exon regions of the *MIR17HG* gene, as well as to target up to 4 kB upstream of the TSS. A search for *MIR17HG* gene primer pairs that had previously been designed and validated identified suitable primer pairs as described by O'Donnell et al (2005) and Pospisil et al (2011). In addition, to cover all regions of the gene and the upstream region, several new primers pairs were designed using Primer Express Software. Primers were designed with close adherence to the following criteria: Primer length: 24 nucleotides; Optimum Tm: 60°C; Optimum GC: 50%; Amplicon size: 80 – 160 base pairs. Details of forward and reverse primers spanning each gene region are shown in Table 3.6. These primer pairs for the *MIR17HG* gene were tested using 30 ng DNA from HT29 cells purified with the DNeasy Blood and Tissue kit. Real-time qPCR for each primer pair was carried out according to the TaqMan Fast SYBR Green protocol, as described in section 3.1.11.9.

3.1.11.9 Quantitation of DNA by relative quantitation real-time PCR

In addition to the histone samples of interest, PCR reactions also included the positive control Histone H3 sample, the negative control Normal Rabbit IgG sample, a tube with no DNA to control for contamination, and a serial dilution of the 2% input chromatin DNA (undiluted, 1:5, 1:25, 1:125) to create a standard curve and determine the efficiency of amplification. Primers used included twelve primer pairs for the *MIR17HG* gene region, and a control primer provided by the manufacturer for Human ribosomal protein L30 (*RPL30*) Exon 3.

Real-time qPCR was carried out according to the TaqMan Fast SYBR Green protocol, using triplicate 20 µL reactions including 2 µL of DNA, 2 µL (300 nM) of forward primer, 2 µL (300 nM) of reverse primer, 10 µL Fast SYBR Green master mix, and 4 µL water. Cycling consisted of a 20 sec incubation at 95°C for DNA polymerase activation, then 40 cycles of a 3 sec denaturing step at 95°C and a 30 sec annealing/ extension step at 60°C.

Real-time qPCR data were normalised using the percent input method. Step one of this method was to adjust the Ct of the input by subtracting 5.64 (i.e. as the starting input fraction was 2%, then a dilution factor of 50 or 5.64 cycles (i.e. $\log_2$ of 50) was subtracted from the Ct value of diluted input). Step two of the percent input method was to perform the following calculation for the Ct value of each immunoprecipitation sample: $100 \times 2^{(\text{Adjusted input minus Ct IP})}$, with this calculation normalising the data to input. In addition, an alternative method of analysis was used, with expression levels normalised to the 2% starting input fraction using Qgene, which took into account the efficiency of amplification using a serial dilution standard curve.

3.1.12 Statistical analysis

Where relevant, results were presented as mean ± standard error of the mean (SEM) of at least three biological replicates. Statistical analyses were performed with PASW Statistics 17 using an unpaired Student's t-test, with a P value < 0.05 considered statistically significant.

It should be noted that cell proliferation and miRNA expression data are presented across several Chapters, to illustrate particular findings pertinent to the subject of that Chapter. To ensure consistency, findings are presented from large experiments, which were conducted at the same time with the same cells using various treatments. For the miRNA data, for example, data are presented from a large experiment which included treatment with various concentrations of butyrate, SAHA, and TSA, with or without cycloheximide treatment; the butyrate results are presented in Chapter 4 and 5, the other histone deacetylase inhibitor results are presented in Chapter 5, and the cycloheximide results are presented in Chapter 7. Similarly, a large cell proliferation experiment was conducted, where the butyrate results from several cell lines are presented in Chapter 4, and the other HDI results are presented in Chapter 5. The data from these large experiments represent robust findings which replicated results from preliminary experiments not shown in full in the main thesis Chapters (see Appendix 1).

3.2 *In vivo* experimental methods – High red meat and resistant starch trial in humans

A randomised cross-over trial was conducted comparing the effects of a control diet, high red meat (RM) diet, and RM diet supplemented with resistant starch (RM + RS) on markers of CRC risk in healthy volunteers aged 50 – 75 years. Within this trial, a sub-study was conducted to determine the effect of the dietary intervention on colorectal miRNA expression patterns.

3.2.1 Study details

Table 3.1: High red meat and resistant starch trial details

Original title: **Dietary protein-induced DNA damage in the colon: the effect of a red meat diet in humans**	
Study design	Randomised, controlled, cross-over trial
Study registration	ANZCTR (Australian & New Zealand Clinical Trials Registry): ACTRN12609000306213, registered 19/05/2009.
Ethics approval	Flinders Clinical Research Ethics Committee/ Clinical Drug Trials Committee (protocol number 155/09)
Study start date	1/07/2009
Duration of study (recruitment, intervention, and sample collection)	12 months
Sources of funding	NHMRC funded project grant #535079

3.2.2 Objectives and hypotheses

The overall study objective was to determine if consumption of a diet high in lean red meat by humans increases toxic fermentation products that could damage DNA, and if supplementation of the diet with RS (as a butyrylated high amylose maize starch, StarPlus™) can ameliorate these effects. The miRNA specific objective was to determine if consumption of a high red meat diet by humans alters miRNA expression in rectal mucosa tissue, and if supplementation of the diet with RS (as a butyrylated high amylose maize starch, StarPlus™) modifies any altered expression.

The overall hypothesis of the study was that increased dietary red meat will increase colonic mutational load and genomic instability in humans which would translate to increased risk of developing CRC but feeding resistant starch will alter fermentation of protein and protect against DNA lesions and their consequences. The miRNA expression hypothesis was that increased dietary red meat may alter miRNA expression profiles, but feeding resistant starch could protect against this dysregulation by increasing butyrate levels in the colorectum.

3.2.3 Participant inclusion and exclusion criteria

Table 3.2: High red meat and resistant starch trial participant inclusion and exclusion criteria

Inclusion criteria	Exclusion criteria
Age 50 – 75 years	Evidence of any active mucosal bowel disease, e.g. colitis, or of malabsorption
Healthy, with no active bowel disease	Intolerance to high-fibre foods
Able to provide informed consent	Any perceived contraindication to consumption of the high protein diet
	Previous bowel surgery (excluding polypectomy)
	Ingestion of regular laxatives or laxative derivatives (excluding regular fibre intake)
	Ingestion of regular probiotic complimentary medicines
	Antibiotic therapy in the previous four weeks

3.2.4 Recruitment

Patients were recruited by advertisement or by invitation from their treating physician during consultation at the Gastroenterology Outpatient Clinics at Flinders Medical Centre. The study protocol was explained to each participant, and written informed consent was obtained prior to study commencement. Participants could withdraw at any time during the study, freely and without prejudice to any treatment at Flinders Medical Centre. Participants were also withdrawn if they developed intolerance to dietary products, intolerance, allergy or any unacceptable reaction to red meat, or onset of any acute diarrhoeal disease. Any samples collected for withdrawn participants could be destroyed according to the patient's wishes.

3.2.5 Sample size determination

A sample size power calculation was based on the anticipated effect on the primary outcome measure of protein fermentation products. A group size of n = 20 in a cross-over design study gave 80% power to detect a 20% change with 95% probability. It was planned for 25 to be recruited to allow for drop-outs. For colorectal biomarkers, the inclusion number was not based on a power calculation, as the size of the effect on the various biomarkers was not known. A study by Rafter et al (2007) recently used the same group sizes (n = 20) in a related study.

3.2.6 Randomisation procedure

Random sequence allocation was generated using a computer generated randomisation sequence and implemented by a trial nurse, to determine whether the RM diet or the

RM + RS diet was received first. Due to the nature of the interventions this was an open trial, with participants not blinded to interventions.

3.2.7 Interventions

Dietary interventions were explained during scheduled clinic visits to Flinders Medical Centre Endoscopy Unit. The study consisted of two intervention periods of four weeks each, preceded by a four-week run-in (control) period and separated by a four-week washout period (Table 3.3). Volunteers were randomised to a RM diet or RM + RS diet for the first intervention, and for the second intervention received the alternative diet.

At the outset of the study, participants' normal diets were assessed using a standard food frequency questionnaire developed by The Cancer Council Victoria (2005) and a study dietitian (Pennie Taylor or Karen Humphreys) gave advice as to study diet requirements. Participants were instructed to maintain their usual diet during the study but to avoid supplementation with any fibre, high-protein, or probiotic supplements, except those protein-containing and RS-containing foods prescribed for the study. Participants were to avoid when possible, or record the use of any medication that could have interfered with bowel function. Participants were also asked to keep their weight stable for the duration of the study, following advice from the study dietitians (KH and PT) as required. Weight was measured at each clinic visit.

Participants were monitored by a trial nurse and a study dietitian (KH) during both interventions periods, to ascertain diet and intervention guidelines were being followed and to provide any assistance needed. Participants were followed up when the study had finished with either a phone conversation or a clinic visit to ascertain the status of their health and well-being. At this time participants were advised on their future red meat consumption with regard to risk factors for this food. Participants could request the overall results of the trial.

3.2.7.1 Run-in and washout periods

For run-in (control) and washout periods, participants were required to follow normal dietary habits for four weeks. No dietary changes were required, except the avoidance of fibre, high-protein, or probiotic supplements.

3.2.7.2 High red meat diet

For the RM diet, participants were required to consume 300 g (raw weight) of lean red meat per day for four weeks. Meat was supplied to the participants in 100 g frozen packs of lean mince, beef strips, or lamb strips, with three packs to be consumed each

day. Participants could spread their meat consumption throughout the day if they preferred (for example, 100 g for lunch, and 200 g for dinner). This level of red meat is tolerated well by humans with studies often using levels of RM at 400 g per day (Lewin et al 2006). Participants were also required to consume two serves of reduced fat milk or orange juice per day, to match the two serves in the RM + RS diet as detailed below.

3.2.7.3 High red meat and resistant starch diet

For the RM + RS diet, participants were required to consume 300 g (raw weight) lean red meat per day for four weeks, with the addition of 40 g of butyrylated high amylose maize starch per day. This butyrylated starch was StarPlus™, which is 50 – 60% RS, and was provided in pre-packed 20 g sachets. Participants were required to consume a total of two sachets daily (one sachet in the morning and one in the evening), by mixing the RS powder into either 250 mL reduced fat milk (flavoured milk was acceptable) or orange juice. Other intervention studies have used RS up to 50 g per day, while 40 g per day has been shown to modify faecal biomarkers significantly (Young & Le Leu 2004).

3.2.8 Outcomes

Outcomes were predefined, with no changes after commencement. For the entire study, primary outcome measures were the effect of protein and RS on formation of colonic fermentation products, and the effect of protein and RS on epithelial consequences. Secondary outcome measures were the effects of protein and RS on bacterial profiles in faeces and rectal mucosa, and on rectal mucosa gene and miRNA expression. This latter outcome measure is of most relevance to this study, and is explored in Chapter 8.

For the entire study, the dietary induced events to be studied included faecal SCFAs, faecal and urine protein fermentation products, faecal and mucosal bacterial population profiles, rectal epithelial responses to protein feeding (specifically DNA strand breaks (comet assay), O6-Methyl-2-deoxyguanosine (O6MeG) DNA adducts, spontaneous apoptosis, cell proliferation, expression of the DNA repair protein *MGMT*, and expression of other markers of DNA repair, carcinogenesis and apoptosis), rectal mucosa miRNA and target gene expression changes, and blood-borne factors (inflammatory and immune markers such as growth factors or immune cells).

Blood samples, rectal pinch biopsy, mucosal swabs and faecal & urine specimens were obtained at the end of each four-week dietary period, with a total of four sample collection visits, at the end of the run-in control diet, first intervention diet, washout diet, and second intervention diet (Table 3.3). Participants were asked to fast for 2 h

prior to their scheduled blood sample collection time. Each participant was also required to fill out a food diary for three days prior to each clinic visit, with a total of four food diaries. Blood collection, rectal biopsies, and mucosal swabs were performed at Flinders Medical Centre Endoscopy Unit. Food diaries were collected during visits. Faecal and urine samples were collected from participants' homes.

3.2.8.1 Demographic data

Details of medical history and medications, weight, bowel health and symptoms, and adverse events were collected by a trial nurse throughout the study. The standard food frequency questionnaire developed by The Cancer Council Victoria (2005) was completed at the first clinic visit.

3.2.8.2 Weighed food diaries

The composition of the participants' diets and their compliance with the dietary interventions was assessed using a weighed food diary. This was completed by participants at the end of each four-week dietary period, three days prior to each clinic visit. Participants were requested to record all food and drink eaten, to be specific and note details and brands of food, and to weigh foods using provided digital kitchen scales for best accuracy. Metric cups and spoons could be used for some items like fluids, sugar or oil. A dietitian (KH) entered the food diaries into Foodworks Professional nutritional calculation software, which calculates energy and macronutrient intake based on Australian food composition tables and food manufacturers' data.

3.2.8.3 Faecal samples

A 24 h faecal collection was conducted by the participant for the 24 h prior to each clinic visit, and placed in the home freezer provided. These samples were collected by a study investigator and analysed for faecal bulk, pH, carbohydrate fermentation products (acetate, propionate, butyrate, and total SCFAs), protein fermentation products (N-nitrosamines, phenols, cresols), and microbiota profile.

3.2.8.4 Urine samples

A SPOT/MSSU urine sample was collected by the participant prior to each clinic visit, on the morning of the visit, and placed in the home freezer provided. These samples were collected by a study investigator and analysed for N-nitrosamines, phenols, cresols and creatinine.

3.2.8.5 Blood samples

A trained nurse collected 30 mL of blood from each subject at each clinic visit. The blood samples were handled according to strict protocols designed to minimise the risk of traumatic injury or infection to the laboratory staff. The plasma/serum were tested by the Flinders Medical Centre SA Pathology diagnostic laboratory for changes in the levels of inflammatory markers including C-reactive protein, inflammatory cytokines, haemoglobin and mean cell volume.

3.2.8.6 Rectal mucosa biopsies

Participants were required to undertake anal examination by an experienced clinician at each clinic visit, at the end of each four-week phase. Four pinch rectal biopsies were taken at each visit with rigid forceps through sigmoidoscopic examination performed without bowel preparation. This was performed by an experienced gastroenterologist who had performed these procedures previously. The procedure has minimal pain or discomfort associated with it, and an unlikely risk of post-procedure bleeding. Colonic biopsies are safe and the investigators were previously involved in projects where this procedure was done without incident (Macrae et al 1997, Worthley et al 2009). Two biopsies of <0.5 cm in any dimension were each placed in 2.5 mL RNA later, stored at 4°C overnight, and subsequently stored at -80°C. Additional biopsies were placed in formalin. Histological analysis of rectal biopsy tissue stored in formalin included testing for DNA strand breaks, O6MeG, baseline apoptosis, cell proliferation, and *MGMT* expression. Analysis of the tissue stored in RNA later included quantitation of miRNA expression profiles, investigation of miRNA target gene changes at the mRNA level, and examination of bacterial DNA profiles.

3.2.8.7 Mucosal swabs of rectum

A mucosal swab was taken at the time of each rectal biopsy, and analysed by a study investigator for surface mucosal bacteria.

Table 3.3: High red meat and resistant starch trial intervention and data collection flow chart

Weeks:	**-4**	**0**	**4**	**8**	**12**
Visit:	**1**	**2**	**3**	**4**	**5**
	RUN IN / NORMAL DIET	RM +/- RS		WASHOUT/ NORMAL DIET	RM +/- RS
Food diary:		XXX	XXX	XXX	XXX
Faecal sample:		X	X	X	X
Urine sample:		X	X	X	X
Blood sample:		X	X	X	X
Rectal biopsy:		X	X	X	X
Mucosal swab:		X	X	X	X

3.2.9 microRNA and target gene mRNA analysis of rectal biopsies

Following storage in RNA-later, rectal biopsy samples were processed to extract total RNA, as detailed in Section 3.1.3. Analysis of miRNA and target gene mRNA levels in these samples was conducted using relative quantitation real-time RT-PCR as detailed in Section 3.1.6.

3.2.10 Maintenance of records

Clinical data sheets were used to record relevant information needed to interpret the end points. These were locked in a secure area where clinical and research records were already stored within the Department of Gastroenterology. Only investigators directly involved in the trial had access to these records. An indication that the person was participating in the study was included in their hospital records where relevant. Records were kept confidential and data was not released in any way that identified an individual.

3.2.11 Statistical methods

Means and standard deviations were calculated for all the outcome variables measured. The cross-over study design with two intervention periods provided two options for analysis of statistical significance; pooling of participant outcome measures by treatment regardless of intervention period with the assumption that period and carry-over effects are not significant, or separate analysis of participant measures based on intervention period, with investigation of treatment effect, period effect, and carry-over effect. A paired Student's t-test was used for initial determination of the significance of changes in outcome variables between treatment groups irrespective of intervention period. To assess differences between treatments with consideration of the intervention period, analysis of variance (two way ANOVA (time and group effect)) was used to compare

changes in outcome variables between RM and RM + RS groups, with the period effect (systematic difference between the two time periods in which treatment was given) and carry-over effect (effect of previous treatment on outcomes of second treatment) also tested. Groups-by-periods plots were also presented. If the carry-over effect was not significant, then the data from two periods could be combined and analysed; in which case the initial Student's t-test was deemed valid. Otherwise, the data only from the first intervention period could be used to estimate the treatment effect. Statistical analyses were performed using STATA statistical software, version 12.0 and R version 2.15.0 (R Development Core Team 2011). A P value < 0.05 was considered statistically significant.

3.3 Reagents and equipment used for experiments

Table 3.4: Chemicals and reagents

Reagent	Supplier
40% Acrylamide/Bis-acrylamide	Sigma–Aldrich, St Louis, MO, USA
Ammonium persulfate (APS)	Sigma–Aldrich, St Louis, MO, USA
Chloroform	Chem-supply, Gillman, SA, Australia
Complete Mini Protease Inhibitor Cocktail Tablets	Roche, Basel, Switzerland
Cycloheximide	Sigma-Aldrich, St Louis, MO, USA
Dimethyl sulfoxide	Sigma–Aldrich, St Louis, MO, USA
DL-Dithiothreitol	Sigma–Aldrich, St Louis, MO, USA
DNA ladders	New England Biolabs, Ipswich, MA, USA
DNA loading dye	New England Biolabs, Ipswich, MA, USA
DNase buffer	Promega, Madison, WI, USA
DNase inactivation slurry	Ambion, Foster City, CA, USA
dNTP mix	Promega, Madison, WI, USA
Dulbecco's Modified Eagle Medium	Invitrogen, Newcastle, NSW, Australia
E-plate 16	Roche, Basel, Switzerland
Enhanced chemiluminescence reagents	SuperSignal West Pico, Rockford, IL, USA
Ethanol	Chem-supply, Gillman, SA, Australia
Exiqon hybridization buffer (208020)	Exiqon, Vadbaek, Denmark
Exiqon v11 ready-to-spot probeset (208210-A v11.0)	Exiqon, Vadbaek, Denmark
Exiqon Wash Buffer kit (208021)	Exiqon, Vadbaek, Denmark
EZQ Protein Quantitation kit	Invitrogen, Newcastle, NSW, Australia
Fast SYBR Green Master Mix	Applied Biosystems, Foster City, CA, USA
F-12 Nutrient Mixture	Invitrogen, Newcastle, NSW, Australia
Foetal bovine serum	Bovogen Biologicals, Essendon, VIC, Australia
Formaldehyde	Chem-supply, Gillman, SA, Australia
Glycine	Sigma–Aldrich, St Louis, MO, USA
Hydrochloric acid	Chem-supply, Gillman, SA, Australia
Immobilon transfer polyvinylidene diflouride membrane	Millipore, Bedford, MA, USA
Isopropanol	Chem-supply, Gillman, SA, Australia
LifterSlips	Erie Scientific, Portsmouth, NH, USA
Lipofectamine 2000 Transfection Reagent	Invitrogen, Newcastle, NSW, Australia
M-MLV Reverse Transcriptase, Rnase H minus, Point mutant	Promega, Madison, WI, USA
McCoy's 5A (modified) Medium	Invitrogen, Newcastle, NSW, Australia
N,N,N',N'-Tetramethylethylenediamine (TEMED)	Sigma–Aldrich, St Louis, MO, USA
Opti-MEM Reduced Serum Medium	Invitrogen, Newcastle, NSW, Australia
Phenylmethanesulfonyl fluoride (PMSF)	Sigma–Aldrich, St Louis, MO, USA
Pre-stained protein markers (broad range 7 – 175 kDa or 10 – 230 kDa)	New England Biolabs, Ipswich, MA, USA
Qiagen DNeasy Blood & Tissue Kit	Qiagen, Valencia, CA, USA
RNA 6000 Pico kit	Agilent Technologies, Santa Clara, CA, USA
RNA later	Ambion, Foster City, CA, USA
RQ1 RNase-Free DNase	Promega, Madison, WI, USA
SimpleChIP Enzymatic Chromatin IP kit (Agarose Beads)	Cell Signaling Technology, Danvers, MA, USA

Contains:	
Glycine Solution (10×)	
Buffer A (4×)	
Buffer B (4×)	
ChIP Buffer (10×)	
ChIP Elution Buffer (2×)	
5 M NaCl	
0.5 M EDTA	
ChIP-Grade Protein G Agarose Beads #9007	
DNA Binding Buffer	
DNA Wash Buffer	
DNA Elution Buffer	
DNA Spin Columns	
Protease Inhibitor Cocktail (200×)	
RNAse A (10 mg/mL)	
Micrococcal Nuclease (2000 gel units/µL)	
Proteinase K (20 mg/mL)	
SimpleChIP® Human RPL30 Exon 3 Primers #7014	
SimpleChIP® Mouse RPL30 Intron 2 Primers #7015	
Histone H3 (D2B12) XP® Rabbit mAb (ChIP Formulated) #4620	
Normal Rabbit IgG #2729	
1M DTT	
Skim milk powder	Fonterra, Mt Waverley, VIC, Australia
Sodium chloride	Chem-supply, Gillman, SA, Australia
Sodium butyrate	Sigma–Aldrich, St Louis, MO, USA
Sodium dodecyl sulfate	Sigma–Aldrich, St Louis, MO, USA
StarPlus™ (50 – 60% RS)	National Starch and Food Innovation, Bridgewater, NJ, USA
Suberoylanilide hydroxamic acid	Selleck Chemicals, Houston, TX, USA
TaqMan Gene Expression Master Mix	Applied Biosystems, Foster City, CA, USA
TaqMan MicroRNA Reverse Transcription Kit	Applied Biosystems, Foster City, CA, USA
TaqMan Universal PCR Master Mix No AmpErase UNG	Applied Biosystems, Foster City, CA, USA
TRIzol Reagent	Invitrogen, Newcastle, NSW, Australia
Trichostatin A Ready Made Solution	Sigma–Aldrich, St Louis, MO, USA
Trizma HCl	Sigma–Aldrich, St Louis, MO, USA
Trizma Base	Sigma–Aldrich, St Louis, MO, USA
TrypLE Express (tryspin)	Invitrogen, Newcastle, NSW, Australia
Tween-20	Sigma–Aldrich, St Louis, MO, USA
Whatman filter paper	Whatman, Maidstone, Kent, UK

Table 3.5: Equipment and software

Equipment	Supplier
Agilent 2100 Bioanalyzer	Agilent Technologies, Santa Clara, CA, USA
Allegra X-22 R centrifuge	Beckman Coulter, Brea, CA, USA
Axiovert 25 light microscope	Ziess, Jena, Germany

Carestream Molecular Imaging Software	Carestream Health, Rochester, NY, USA
CO_2 water jacketed cell incubator	Forma Scientific, Marietta, OH, USA
Corbett Rotorgene 2000	Corbett Research, Sydney, NSW, Australia
modified Dremel Multipro homogeniser	Dremel, USA
Dry block heater	Thermoline L+M, Sydney, NSW, Australia
Multi Gauge software	Fujifilm Corporation, Tokyo, Japan
Gel tank blotting system	Bio-Rad, Hercules, CA, USA
GeneAmp PCR system 9700 thermal cycler	Applied Biosystems, Foster City, CA, USA
Gene Genius Bio imaging System	Syngene, Cambridge, UK
Genepix 4000B Scanner	Molecular Devices, Union City, CA, USA
ImageQuant LAS 4000	GE Healthcare Life Sciences, Uppsala, Sweden
Ingenuity Pathway Analysis Software	Ingenuity Systems, Redwood City, CA, USA
Microcentrifuge 5424	Eppendorf, Hamburg, Germany
Microson Ultrasonic cell disruptor	Misonix, Farmingdale, NY, USA
Nanodrop-8000	Nanodrop Technologies, Wilmington, DE, USA
PASW Statistics 17	IBM Corporation, Somers, NY
Power-Pac Basic	Bio-Rad, Hercules, CA, USA
Primer Express Software	Applied Biosystems, Foster City, CA, USA
Programmable Thermal Controller	MJ Research, Waltham, MA, USA
R statistical software package	R Project, Vienna, Austria
Rocking platform	Ratek, Boronia, VIC, USA
Rotorgene Q	Qiagen, Valencia, CA, USA
STATA statistical software, version 12.0	StataCorp, TX, USA
Tempette Junior TE-85 water bath	Techne, Staffordshire, UK
Typhoon 9400 Variable mode imager	Amersham Biosciences, Piscataway, NJ, USA
Ultra-low temperature freezer (-80°C)	Thermo Scientific Revco, Waltham, MA, USA
Weigh scales	Shimadzu, Kyoto, Japan
xCELLigence RTCA DP instrument	Roche, Basel, Switzerland

Table 3.6: Primers and oligonucleotides

Assay	Catalogue number/ Sequence	Supplier
Random primer 6	S1230S (5' d(N_6) 3' [N=A,C,G,T])	New England Biolabs, Ipswich, MA, USA
Taqman assays:		
hsa-miR-16	#000391	Applied Biosystems, Foster City, CA, USA
hsa-miR-17	#000393	
hsa-miR-18a	#002422	
hsa-miR-19a	#000395	
hsa-miR-20a	#000580	
hsa-miR-19b	#000396	
hsa-miR-92a	#000430	
hsa-miR-106a	#002169	
hsa-miR-18b	#002217	

hsa-miR-20b	#001014	
hsa-miR-21	#000397	
hsa-miR-23a	#000399	
hsa-miR-23b	#000400	
hsa-miR-29b	#000413	
hsa-miR-33a	#002135	
hsa-miR-192	#000491	
hsa-miR-196a	#241070	
hsa-miR-196b	#002215	
hsa-miR-210	#000512	
hsa-miR-215	#000518	
hsa-miR-301a	#000528	
hsa-miR-301b	#002392	
hsa-miR-584	#001624	
hsa-miR-1275	#002840	
hsa-miR-1290	#002863	
RNU6B	#001093	
CDKN1A	#Hs00355782_m1	
PTEN	#Hs02621230_s1	
BCL2L11	#Hs00708019_s1	
E2F1	#Hs00153451_m1	
c-MYC	#Hs00905030_m1	
NEDD9	#Hs00610590_m1	
CDK19	#Hs00292369_m1	
LIN28	#Hs00702808_s1	
CCDC88A	#Hs00214014_m1	
GAB1	#Hs00157646_m1	
ACTB (β-actin)	#Hs99999903_m1	
Primers for ChIP analysis:		
SimpleChIP Human RPL30 Exon 3 Primers 1	#7014	Cell Signaling Technology, Danvers, MA, USA
P1: 17HG -4 to -3kb (-3.9 kb)	F: 5' TTTGGCCCCACTTCTTACCA 3' R: 5' CTTTACAATCAACCAAGAGCCTTTG 3'	Geneworks, Hindmarsh, SA, Australia
P2: 17HG -3 to -2kb (-2.3 kb)	F: 5' AAACGTTCTGAATGTTCTGGATTGT 3' R: 5' CACAGCCTTCTCAAGTCAGCTAAA 3' (O'Donnell et al 2005)	
P3: 17HG -2 to -1kb (-1.8 kb)	F: 5' CGAAACCCTTAAAATGCAACCTACT 3' R: 5' CAGGATTTTGGAAGACGCAAAT 3'	
P4: 17HG -1 to -0.5kb (-0.5 kb)	F: 5' ACCTCGGAAACCCACCAAG 3' R: 5' TCTCCCTGGGACTCGACG 3' (O'Donnell et al 2005)	
P5: 17HG -0.5 to 0kb (-0.1 kb)	F: 5' GCTAATGAGGGAGTGGGGCTTGTC 3' R: 5' CACCTCGAAGGACCATGTGGGTG 3' (Pospisil et al 2011)	
P6: 17HG exon 1 and intron 1 (1.5 kb)	F: 5' AAAGGCAGGCTCGTCGTTG 3' R: 5' CGGGATAAAGAGTTGTTTCTCCAA 3' (O'Donnell et al 2005)	

P7: 17HG exon 2	F: 5' CTCGACTCTTACTCTCACAAATGG 3'	
(1.8 kb)	R: 5' GCTACTGGTGCAGTTAGGTCC 3' (O'Donnell et al 2005)	
P8: 17HG intron 2	F: 5' TTTAAACAGGATATTTACGTTCTGC 3'	
and exon 3 (2.3 kb)	R: 5' GAGGAAATCTTCACATCCACG 3' (O'Donnell et al 2005)	
P9: 17HG intron 3	F: 5' GGCACTTGTAGCATTATGGTGACA 3'	
(2.9 kb)	R: 5' GCACCTTAGAACAAAAAGCACTCA 3'	
P10: 17HG intron 3	F: 5' GCCTGTCGCCCAATCAAA 3'	
(3.4 kb)	R: 5' CAGCAGAATATCACACAGCTGGAT 3'	
P11: 17HG intron 3	F: 5' CCAAGCTGAAGTACAGGCAAACT 3'	
(4.6 kb)	R: 5' TGGGTGGTCTAACCTAGTGTTATGG 3' (O'Donnell et al 2005)	
P12: 17HG exon 4	F: 5' CCAGACTTGGGTTTTCTCCTGTAG 3'	
(6.2 kb)	R: 5' GAGTTGTTCTCCAGGAAGTTGCA 3'	
miRNA oligonucleotide duplexes:		
miR-17:	5' CAAAGUGCUUACAGUGCAGGUAG 3'	GenePharma,
	5' ACCUGCACUGUAAGCACUUUGUU 3'	Shanghai,
miR-18a:	5' UAAGGUGCAUCUAGUGCAGAUAG 3'	China
	5' AUCUGCACUAGAUGCACCUUAUU 3'	
miR-19a:	5' UGUGCAAAUCUAUGCAAAACUGA 3'	
	5' AGUUUUGCAUAGAUUUGCACAUU 3'	
miR-20a:	5' UAAAGUGCUUAUAGUGCAGGUAG 3'	
	5' ACCUGCACUAUAAGCACUUUAUU 3'	
miR-19b:	5' UGUGCAAAUCCAUGCAAAACUGA 3'	
	5' AGUUUUGCAUGGAUUUGCACAUU 3'	
miR-92a:	5' UAUUGCACUUGUCCCGGCCUGU 3'	
	5' AGGCCGGGACAAGUGCAAUAUU 3'	
NC mimic	5' UUCUCCGAACGUGUCACGUTT 3'	
	5' ACGUGACACGUUCGGAGAATT 3'	

miScript target protectors:

	Seed sequence (and location on 3'UTR)	**Target protector context sequence**	
TPNEDD91	Site 1: GCACCTT (nucleotides 338 – 344); Site 2: GCACCTT (nucleotides 350 – 356)	5'AACCATGAATTACGAAGCACCTTAGTA AGCACCTTCTAAT 3'	Qiagen, Valencia, CA, USA
TPNEDD92	Site 3: TCACCTT (nucleotides 485 – 491)	5'AGTTTATTTGCAAGTGTTCACCTTCCAA ATCATGAGGCAT 3'	
TPNEDD93	Site 4: GCACCTT (nucleotides 1055 – 1061)	5'GAATTTATTGCTATCTTGCACCTTCTTT AAAACTCACATA 3'	
TPCDK191	Site 1: GCACCTT (nucleotides 308 – 314)	5'TTGAAGGATTTCCTGGTGCACCTTTCT CATGCTGTAGCAA 3'	
TPCDK192	Site 2: GCACCTT (nucleotides 448 – 454)	5'GCAACACAGGTAAAAATGCACCTTTTA AAGCACTACGTTT 3'	
TPCDK193	Site 3: CCACCTT (nucleotides 2816 – 2822)	5'TTGGCTCACTCCAACCTCCACCTTCCA GGTTCAAGTGATT 3'	
negative control miScript target protector	#MTP0000002		

Mission siRNAs:			
	Catalogue number	**Sequence**	
NEDD9 human siRNA 1	#SASI_Hs01_00191226	GAUGGUGGCUGUGCUCGUU	Sigma–Aldrich, St Louis, MO
NEDD9 human siRNA 2	#SASI_Hs01_00191227	CCGGGUGAAGCUUCUGAUU	
CDK19 human siRNA 1	#SASI_Hs01_00108233	CAAUUCUCCUCUAAAGCCA	
CDK19 human siRNA 2	#SASI_Hs01_00108234	GAAGGUAUGGCUGCUGUUU	
negative control siRNA	#SIC001	-	

Table 3.7: Antibodies

Antibody	**Dilution**	**Supplier**
rabbit monoclonal anti-CDKN1A (12D1) #2947	1:1000 (for Western blot)	Cell Signaling Technology, Danvers, MA, USA
rabbit monoclonal anti-PTEN (D4.3) #9188	1:1000 (for Western blot)	Cell Signaling Technology, Danvers, MA, USA
rabbit monoclonal anti-BCL2L11 (C34C5) #2933	1:1000 (for Western blot)	Cell Signaling Technology, Danvers, MA, USA
mouse monoclonal anti-HEF1/NEDD9 (2G9) #4044	1:1000 (for Western blot)	Cell Signaling Technology, Danvers, MA, USA
Rabbit monoclonal anti-ACTB (ab8227)	1:5000 (for Western blot)	Abcam, Cambridge, MA, USA
Secondary horseradish peroxidase-conjugated goat anti-rabbit IgG	1:8000 (for Western blot secondary)	Immunopure, Thermo Scientific, Rockford, IL, USA
Secondary horseradish peroxidase-conjugated donkey anti-mouse IgG	1:8000 (for Western blot secondary)	Immunopure, Thermo Scientific, Rockford, IL, USA
Rabbit monoclonal anti- histone H3 (D2B12) XP # 4620	1:50 (for ChIP)	Cell Signaling Technology, Danvers, MA, USA
Rabbit anti-Normal rabbit IgG #2729	1:500 (for ChIP)	Cell Signaling Technology, Danvers, MA, USA
Rabbit polyclonal anti-acetyl-histone H3 (Lys 9/ Lys 14) #9677	1:50 (for ChIP)	Cell Signaling Technology, Danvers, MA, USA
Rabbit polyclonal anti-acetyl-histone H3 (Lys 27) #4353	1:25 (for ChIP)	Cell Signaling Technology, Danvers, MA, USA
Rabbit polyclonal anti-tri-methyl histone H3 (Lys 4) #9727	1:100 (for ChIP)	Cell Signaling Technology, Danvers, MA, USA

Table 3.8: Buffers and solutions

Buffer/ solution	Formula
10× PBS	For 1L: 8 g NaCl, 0.2 g KCl, 1.44 g Na_2HPO_4, 0.24 g KH_2PO_4 in 800 mL water. pH adjusted to 7.4 with HCl. water added to make 1L.
10× MOPS	For 400 mL: 16.74 g MOPS, 1.64 g NaOAC, 9 mL 0.5 M EDTA. pH adjusted to 7 with NaOH. Water added to make 400 mL.
Protein lysis buffer	6.7 M urea, 10 mM Tris/HCl pH 6.8, 10% glycerol, 1% SDS. For 1 L: 402.4 g urea, 1.21 g Tris/HCl, 100 mL glycerol, 1 g SDS, water to 1 L. pH adjusted using conc. HCl and 5 M NaCl.
SDS 4× Lower buffer	1.5 M Tris/HCl pH 8.8, 0.4% SDS. For 500 mL: 91 g Tris/HCl, 2 g SDS, water to 500 mL.
SDS 4× Upper buffer	0.5 M Tris/HCl pH 6.8, 0.4% SDS. For 500 mL: 30.4 g Tris/HCl, 2 g SDS, water to 500 mL.
5× SDS Running buffer	125 mM Tris Base, 1 M Glycine, 0.5% SDS. For 500 mL: 7.57 g Tris/HCl, 37.5 g Glycine, 25 mL of 10% SDS, water to 500 mL.
Western Transfer buffer	48 mM Tris Base, 19 mM Glycine, 0.37% SDS, 20% methanol. For 500 mL: 2.91 g Tris Base, 1.47 g Glycine, 0.19 g SDS, 100 mL methanol, water to 500 mL.
10× TBS	0.2 M Tris Base, 1.37 M NaCl. For 500 mL: 12.1 g Tris Base, 40 g NaCl, water to 500 mL. pH adjusted to 7.6 using conc. HCl.
1× TBS-T	1× TBS, 0.1% Tween-20 For 500 mL: 50 mL 10× TBS, 5 mL 10× Tween-20, water to 500 mL.
ChIP solutions for cross-linking, nuclei preparation, and nuclease digestion of chromatin	1) 10 mL 10× glycine 2) 200 mL 1× PBS 3) 10 mL 1× PBS + 100 µL PMSF 4) 10 mL 1× Buffer A (2.5 mL 4× Buffer A + 7.5 mL water) + 5 µL 1 M DTT + 50 µL 200× Protease Inhibitor Cocktail (PIC) + 100 µL PMSF 5) 11 mL 1× Buffer B (2.75 mL 4× Buffer B + 8.25 mL water) + 5.5 µL 1 M DTT 6) 1 mL 1× ChIP Buffer (100 µL 10× ChIP Buffer + 900 µL water) + 5 µL 200× PIC + 10 µL PMSF.
ChIP solutions for chromatin washing	1) Low salt wash: 3 mL 1× ChIP Buffer (300 µL 10× ChIP Buffer + 2.7 mL water) 2) High salt wash: 1 mL 1× ChIP Buffer (100 µL 10× ChIP Buffer + 900 µL water) + 70 µL 5 M NaCl.

Chapter 4. Butyrate alters microRNA expression in colorectal cancer cell lines

4.1 Introduction

4.1.1 Effect of butyrate on gene expression in colorectal cancer cells

The fermentation of fibre by intestinal microbiota results in the production of short-chain fatty acids such as butyrate. As outlined in Chapter 1, butyrate production is one of the main mechanisms by which fibre may protect against CRC development. Besides being a preferred energy source for colonic epithelium (Roediger 1982, Scheppach et al 1992, Young et al 2005), butyrate may play a chemo-protective role by affecting cell cycle regulation, apoptosis, proliferation, differentiation, inflammation, and DNA repair (Mariadason et al 2000, Iacomino et al 2001, Daly & Shirazi-Beechey 2006). A number of *in vitro* studies have investigated the effect of butyrate on CRC cells at the level of gene expression; however, prior to this study the effect of butyrate on miRNA expression in CRC cells had not previously been comprehensively characterised.

The effect of butyrate on gene expression has been studied in at least eleven DNA microarray analyses using human colorectal cell lines (Table 4.1). The HT29 human colorectal adenocarcinoma cell line was the most commonly used cell line in the microarray studies, while several studies also used primary colon tissue or non-malignant cell types. The studies treated cell lines with butyrate concentrations ranging from 2 mM to 10 mM, over time periods ranging from 2 to 72 h. The microarray studies generally used similar techniques, with the more recent studies benefiting from improved technology that allowed quantification of larger numbers of genes. While the microarray analyses allowed the parallel quantification of thousands of genes from multiple samples, there was inconsistency between the studies regarding which genes and sample types were examined, precluding direct comparisons between the studies. All studies used other methods such as real-time RT-PCR to confirm at least some of their results.

An early key study in the SW620 human colorectal adenocarcinoma cell line found that gene expression changes began as soon as 30 min after butyrate treatment, and continued to progress over time (Mariadason et al 2000). Over a 48 h period, 256 genes were up-regulated by butyrate and 333 were repressed (7% of total assayed) (Mariadason

et al 2000). Butyrate was shown to stimulate a $G_0 – G_1$ cell cycle arrest, induce differentiation, and trigger an apoptotic cascade. The study highlighted significantly modulated genes involved in signalling pathways and in regulation of cell cycle progression. It was noted that the large number of gene alterations suggests that each gene cannot be considered in isolation, and that the cell response to butyrate appears to be the result of interactions between large numbers of genes and their products (Mariadason et al 2000).

In another early study, Iacomino et al (2001) also observed in HT29 human colorectal adenocarcinoma cells that butyrate treatment increased the percentage of cells in G_1 phase and reduced the percentage of cells in S and G_2 – M phases. As markers of butyrate activity, Iacomino et al (2001) observed increases in alkaline phosphatase activity (a marker of differentiation), increased expression of the cyclin-dependent kinase inhibitor *CDKN1A* peaking at 48 – 72 h after butyrate addition, and down-regulation of the *C-MYC* oncogene 48 – 72 h after butyrate addition. As in the study by Mariadason et al (2000), the microarray results from this study showed multiple genes affected by butyrate, although this study was undertaken on a smaller scale. Genes involved in pathways for apoptosis, DNA synthesis, repair and recombination were the most affected by 72 h butyrate treatment in terms of gene up-regulation. Oncogenes, cell cycle control proteins, and transcription factors were also prominently modulated by butyrate, with these genes tending to be down-regulated (Iacomino et al 2001).

In single time-point studies such as Iacomino et al (2001), it is difficult to distinguish between primary responses to butyrate and downstream events (Williams et al 2003). Della Ragione et al (2001) attempted to address this issue by investigating the effects of butyrate treatment in the presence of cycloheximide, to inhibit *de novo* protein synthesis and observe transcriptional effects only. Using this method, Della Ragione et al (2001) identified a small number of genes regulated by butyrate. As a shorter treatment period of 5 h was used in this study it is difficult to compare results to that of Iacomino et al (2001); however, in a review analysis, Williams et al (2003) identified some overlap between the genes affected by butyrate in both studies.

The larger microarray studies support the earlier work by indicating that a substantial number of genes experience altered expression upon butyrate treatment. One study in a differentiated Caco2 colorectal adenocarcinoma cell line found that 7098 genes (24% of total on array) had a >2-fold variation above or below control levels upon treatment with various SCFAs, including butyrate (Alvaro et al 2008). Another large study in HT29

cells showed that 1984 genes (10.2%) had a >2-fold variation above or below control levels with 5 mM butyrate treatment for 24 h (Daly et al 2005, Daly & Shirazi-Beechey 2006). Of these, 796 genes were up-regulated (4.1%) and 1187 were down-regulated (6.1%). Daly and Shirazi-Beechey (2006) identified 221 butyrate-responsive genes (1.1%), including several transcription factors, as being specifically involved in the regulation of proliferation, differentiation, and apoptosis, and thus controlling colonic tissue homeostasis. Fifty-nine of these were up-regulated and 162 down-regulated. When Daly and Shirazi-Beechey (2006) compared these microarray data to public databases, they found that 78 potentially butyrate-responsive genes, associated with the regulation of colonic tissue homeostasis, had previously been shown to be deregulated in colon cancer tissue compared to normal healthy colonic mucosa. Of the 59 genes up-regulated with butyrate, 26 were associated with cell cycle regulation and arrest, such as *CDKN1A*, *CDX2*, *GADD45A*, *MAPK12* (p38), *FOS*, *PTEN*, and *TXNIP*, and a number of these genes had been shown to be down-regulated in colon cancer tissue compared to normal mucosa. Other genes up-regulated by butyrate were associated with transcriptional silencing through promoter regulation, induction of apoptosis, inhibition of β-catenin/TCF4 transcriptional activity, and inhibition of NF-κB signalling. Genes down-regulated by butyrate were associated with cell cycle progression, activation of NF-κB signalling, activation of β-catenin/TCF4 transcriptional activity, activation of PI3K-AKT/PKB signalling, activation of C-MYC, DNA replication, transcriptional silencing through promoter methylation, proliferation and metastasis, inhibition of apoptosis, and tumour markers (Daly & Shirazi-Beechey 2006).

In addition to the cell line studies, several studies have used microarray analyses to investigate butyrate-induced gene expression changes using an *in vivo* approach. Kameue et al (2006), for example, significantly increased butyrate production in rats through the ingestion of sodium gluconate, and performed a microarray on colonic RNA to show that six genes were up-regulated and four down-regulated with the sodium gluconate diet, compared with the control diet. Of the differentially expressed genes, the authors indicated that some were known for their roles in cell cycle and lipid metabolism and as hormone receptors and transporters (Kameue et al 2006). Another study by Vanhoutvin et al (2009) aimed to determine the effects of butyrate on the transcriptional regulation of human colonic mucosa *in vivo*. In a randomised cross-over trial with two experimental periods of two-weeks, human volunteers administered an enema containing 100 mM butyrate or a placebo once daily. At the end of each experimental period, biopsies were obtained, and a microarray analysis of RNA from the biopsies identified 501 genes to be

differentially expressed after the butyrate intervention compared to the placebo. Pathway analysis showed that the butyrate intervention mainly regulated genes associated with energy metabolism, fatty acid metabolism, and oxidative stress (Vanhoutvin et al 2009). Both these *in vivo* studies were performed in healthy subjects, which limits the applicability of the results to cancer cells, but indicates the ability of butyrate to maintain colonic homeostasis in healthy mucosa.

Multiple microarray studies have identified the capacity of butyrate to modulate gene expression in colorectal cells, *in vitro* and *in vivo*. As introduced in Chapter 1, one of the mechanisms by which butyrate is able to influence gene expression is an epigenetic mechanism, through its alteration of histone acetylation. It is however largely unknown whether these gene expression changes are solely a direct epigenetic response to butyrate, or whether some changes are mediated by altered miRNA expression. There is substantial evidence to indicate that miRNAs can act as tumour suppressors by targeting oncogenes, or can have oncogenic properties themselves by targeting tumour suppressor genes. It could be hypothesised that miRNA expression changes may mediate some of the changing gene expression patterns found in colorectal cells undergoing butyrate treatment.

Table 4.1: Microarray studies showing the effect of butyrate on gene expression using human colorectal cell lines.

Study	Cell type	Methods	Key results
Alvaro et al (2008)	Caco2/ TC-7 (human colorectal adenocarcinoma cell line)	- Cells grown at confluence for 21 days to cause differentiation. - 2 mM or 5 mM sodium butyrate for 24 h. Also 2 mM sodium acetate or sodium propionate for 24 h. - Microarray: Applied Biosystems Human Genome Survey Arrays with 29,098 human genes. - Differentially expressed genes classified using PANTHER. - Real-time RT-PCR to confirm changes.	**No. differentially expressed genes:** 7098 (24% of total on array) with >2-fold variation above or below control levels upon treatment with at least one SCFA (acetate, propionate, or butyrate). 5 mM butyrate had greater effect than 2 mM butyrate. **Genes/pathways affected:** Nine biological processes affected by butyrate (2 mM and 5 mM) ($P < 0.05$): Protein metabolism and modification; Nucleoside, nucleotide, and nucleic acid metabolism; Cell cycle; DNA metabolism; Lipid, fatty acid, and steroid metabolism; Carbohydrate metabolism; Amino acid metabolism; Intracellular protein traffic; Transport. Eleven metabolic pathways affected by butyrate (5 mM) ($P < 0.05$): GABA-B receptor II signalling; Endogenous cannabinoid signalling; Parkinson's disease; General transcription by RNA polymerase I; Glycolysis; 5HT1 type receptor-mediated signalling pathway; Heterotrimeric G-protein signalling pathway-rod outer segment phototransduction; Hedgehog signalling pathway; Metabotropic glutamate receptor group III pathway; Cholesterol biosynthesis; Androgen/estrogen/progesterone biosynthesis.
Blais et al (2007)	HIEC (undifferentiated non-transformed human crypt intestinal epithelial cell line)	- 5 mM sodium butyrate for 8 h. - Microarray: Affymetrix Human Genome U133 Plus 2.0 Array with 47,000 transcripts. - Gene classification according to biological processes using DAVID. - RT-PCR to confirm changes.	**No. differentially expressed genes:** 1464 genes with >2-fold variation above control levels ($P < 0.05$). 872 genes with >2-fold variation below control levels ($P < 0.05$). **Genes/pathways affected:** Biological processes: Apoptosis; Cell cycle; Chemotaxis; Cytokinesis; Cytoplasm organization and biogenesis; Defence response; Dephosphorylation; DNA packaging; G-protein coupled receptor protein; Signalling pathway; Inflammatory response; Intracellular transport; Ion transport; Nuclear organization and biogenesis; Phosphorylation; Protein biosynthesis; Protein catabolism; Protein kinase cascade; Protein transport; Regulation of cell proliferation; Regulation of transcription; Response to pest/pathogen/parasite; RNA processing; Small GTPase-mediated signal transduction; Ubiquitin cycle, WNT receptor signalling pathway.
Cai et al (2006)	HT29 (human colorectal adenocarcinoma cell line)	- 3 mM sodium butyrate for 48 h. - Array: Clontech Atlas human stress and toxicology array with 234	**No. differentially expressed genes:** NR **Genes/pathways affected:** Increased expression of several heat shock proteins including hsp70 family and hsp 27.

		genes. - Real-time RT-PCR to confirm changes.	
Daly et al (2005), Daly and Shirazi-Beechey (2006)	HT29 (human colorectal adenocarcinoma cell line)	- 5 mM sodium butyrate for 24 h. - Microarray: MWG Human 40K A array with 19,400 human genes. - Real-time RT-PCR to confirm changes.	**No. differentially expressed genes:** 1984 genes (10.2%) with >2-fold variation. 796 (4.1%) with up-regulation, 1187 (6.1%) with down-regulation. **Genes/pathways affected:** 221 genes (1.1%) associated with processes of apoptosis, proliferation and differentiation (59 (0.3%) up-regulated, 162 (0.8%) down-regulated including 13 known tumour markers) Also, 71 other transcription factors (39 up-regulated, 32 down-regulated). Up-regulated genes associated with: Cell cycle regulation; Transcriptional silencing through promoter regulation; Induction of apoptosis; inhibition of β-catenin/TCF4 transcriptional activity; Inhibition of NF-κB signalling. Down-regulated genes associated with: Cell cycle progression; Activation of NF-κB signalling; Activation of β-catenin/TCF4 transcriptional activity; Activation of PI3K-AKT/PKB signalling; Activation of C-MYC; DNA replication; Transcriptional silencing through promoter methylation; Inhibition of apoptosis; Proliferation/ metastasis; Tumour markers. Notable up-regulated genes: ALP1, CDKN1A, PTEN, GADD45A, DAPK1, AXIN2, HBP1, CDH1, CLU/APOJ, CASP8. Notable down-regulated genes: CCND1, BIRC5, PTGS2/COX2, PIK3CG, CFLAR, BCL-X_L, SPP1, RB1, CCT5, PCNA, MMP7, MECP2.
Della Ragione et al (2001)	HT29 (human colorectal adenocarcinoma cell line)	- 2 mM sodium butyrate for 5 h (or 0.3 μM TSA). Concomitant treatment with 36 μM cycloheximide. - Microarray: ATLAS cDNA expression assay with 588 transcripts for human genes. - RT PCR to confirm changes.	**No. differentially expressed genes:** 21 genes with >2-fold up-regulation by butyrate or TSA, 2 genes with >2-fold down-regulation. **Genes/pathways affected:** transcription factor, cell cycle regulators, chemokine receptor, transduction modulators, stress responses, detoxification, adhesion molecule.
Gaudier et al (2004)	HT29-C1.16E (clonal derivative of HT29 human adenocarcinoma cell line)	- Cells seeded at post-confluence (day 18) when differentiated, then further cultured for 8 days. - 2 mM sodium butyrate for 24 h.	**No. differentially expressed genes:** 9 genes with >2-fold variation. **Genes/pathways affected:** glycosylation related.

		- Microarray: MWG array with 252 human glycosylation related genes - Real-time RT-PCR to confirm changes.	
Iacomino et al (2001)	HT29 (human colorectal adenocarcinoma cell line)	- 4 mM sodium butyrate for 72 h. - Microarray: Atlas cDNA expression array with 588 human genes. - RT-PCR to confirm changes.	**No. differentially expressed genes:** 60 genes with >2-fold variation (39 up-regulated, 21 down-regulated) **Genes/pathways affected:** Apoptosis-related proteins, DNA synthesis, repair and recombination proteins; Oncogenes, tumour suppressors, and cell cycle control proteins; Ion channel, stress response proteins, transport proteins modulators/effectors/intracellular transducers; DNA binding/transcription/transcription factors; Cell receptors, interleukin/interferon receptors, hormone receptors, neurotransmitter receptors, cell surface antigens and adhesions; Extracellular cell signalling and communication proteins, interleukins and interferons, hormones.
Mariadason et al (2000)	SW620 (human colorectal adenocarcinoma cell lines)	- 5 mM sodium butyrate over 48 h time course. - Microarray: Array with 8,063 human gene sequences. - Real-time RT-PCR to confirm changes.	**No. differentially expressed genes:** Over a 48 h period, 256 gene sequences were up-regulated by butyrate, 333 were repressed (7% of total assayed). Of the 589 altered sequences, 345 represented named sequences, and the remainder was unnamed or expressed sequence tags. **Genes/pathways affected:** Signalling pathways; Regulation of cell cycle progression.
Ogawa et al (2003)	HIMEC (human intestinal microvascular endothelial cells)	- 5 mM sodium butyrate for 2 h followed by bacterial lipopolysaccharide stimulation. - Array: TranSignal NF-κB Target Gene Array with 110 genes. - Western blotting to confirm changes.	**No. differentially expressed genes:** NR **Genes/pathways affected:** ICAM-1 up-regulated, IL-6 and COX-2 gene expression attenuated.
Pool-Zobel et al (2005)	LT97 (human pre-malignant colon adenoma cell line); HT29 (human colorectal adenocarcinoma cell lines); Primary colon	- Primary 10 mM sodium butyrate for 12 h; LT97 1 mM or 2 mM for 72 h; HT29 4 mM for 48 h or 72 h. - Arrays: Superarray membrane; Affymetrix U133A gene expression arrays with probe sets	**No. differentially expressed genes:** NR **Genes/pathways affected:** p450 Family, Acetyltransferases, Glutathione S-transferases, Sulfotransferases, Miscellaneous, Metallothioneins, p-Glycoproteins.

	cells	recognizing 414 000 well-characterised human gene sequences. - Real-time RT-PCR to confirm changes.	
Sauer et al (2007)	Primary colon cells	- 10 mM sodium butyrate for 12 h. - Array: GEArray Q Series Human Stress &Toxicity Gene Array HS12 with 112 genes. - Real-time RT-PCR to confirm changes.	**No. differentially expressed genes:** NR **Genes/pathways affected:** Oxidative and metabolic stress associated (CAT, MT2A, GSR, COX-2, SOD-2).
Wilson et al (2010a)	30 colon cancer cell lines (Caco-2, Colo201, Colo205, Colo320, Dld-1, HCT116, HCT-15, HCT-8, HT29, LoVo, LS174T, RKO, SKCO-1, SW1116, SW403, SW48, SW480, SW620, SW837, SW948, T84, WiDr, HT29-Cl.16E, HT29-Cl.19A, LIM1215, LIM2405, HCC2998, KM12, RW2982, and RW7213).	- 5 mM sodium butyrate for 24 h - Array: 27,000 feature cDNA microarrays - Real-time RT-PCR and Western blotting to confirm changes.	**No. differentially expressed genes:** The overall number of genes changed in response to butyrate treatment ($P < 0.05$) and the range of transcriptional changes in terms of fold change was similar for butyrate-sensitive and butyrate-resistant cell lines **Genes/pathways affected:** 48 sequences were identified as significantly and preferentially induced by butyrate in sensitive cell lines: 7 of these 48 genes (Fos, Jun, Atf3, Arc, Nr4a1 (Nur77), Egr1, and Egr3) are immediate-early genes, and 7 genes have previously been classified as stress response genes (Gadd45b, Ndrg4, Mt1B, Mt1E, Mt1F, Mt1H, and MtlX). Forty-four genes preferentially repressed by butyrate in sensitive lines were also identified. These included several genes involved in organization of microtubules and the actin cytoskeleton (TRIP6, SRHML, PLXNB1, MAP7, LASP1, and LAD1), cell adhesion (OCLN, DSC2), transcriptional repression (NCoR2, SET), and apoptosis (FLIP, DAXX).

NR: not reported; PCR: polymerase chain reaction; SCFA: short chain fatty acid; RT: reverse transcription.

4.2 Aim

The aim of this Chapter was to determine whether butyrate treatment alters miRNA expression in CRC cell lines, through miRNA microarray analysis and subsequent real-time RT-PCR validation.

4.3 Methods overview

Experiments were conducted according to the general methods outlined in Chapter 3, with all experimental groups conducted in triplicate.

HT29 and HCT116 cell lines, which are two commonly used adherent epithelial colorectal carcinoma cell lines (ATCC, Manassas, VA, USA), were used to determine the effects of butyrate treatment on cell growth and on miRNA expression. Cells were treated with increasing doses of butyrate (0, 1, 5, 10, or 25 mM) for 48 h, and proliferation was measured in real-time using the xCELLigence RTCA DP instrument. In separate experiments, total RNA was extracted from treated cells using the TRIzol method, and initially a microarray analysis was used to assess miRNA expression in HT29 cells treated with 5 mM butyrate for 48 h, compared with untreated control. To validate the microarray, subsequent relative quantitation real-time RT-PCR analysis was performed on miRNAs shown to be differentially expressed. Butyrate treatment experiments were also conducted in parallel using HT29-BR and HCT116-BR cell lines, which have been shown previously to be partially resistant to the anti-proliferative and pro-apoptotic effects of butyrate (Fung et al 2009). Following the microarray results and real-time RT-PCR validation, the differentially expressed miRNAs were analysed using Ingenuity Pathway Analysis (IPA), to determine which potential pathways and target genes are associated with the miRNAs that are altered by butyrate.

4.4 Results

4.4.1 Proliferation of colorectal cancer cell lines with butyrate treatment

Treatment of HT29 and HCT116 CRC cells with increasing concentrations of butyrate led to decreased proliferation over a 48 h period. Proliferation measures using real-time cell growth analysis showed that at the physiological level of 5 mM butyrate, by 48 h proliferation was significantly reduced in HT29 cells compared with the untreated control cells ($P = 0.0005$) (Figure 4.1). Treatment of HCT116 cells revealed these to be

more susceptible than HT29 cells to the anti-proliferative effects of butyrate, with proliferation drastically reduced with 5 mM butyrate compared with the untreated control cells ($P < 0.0001$) (Figure 4.1).

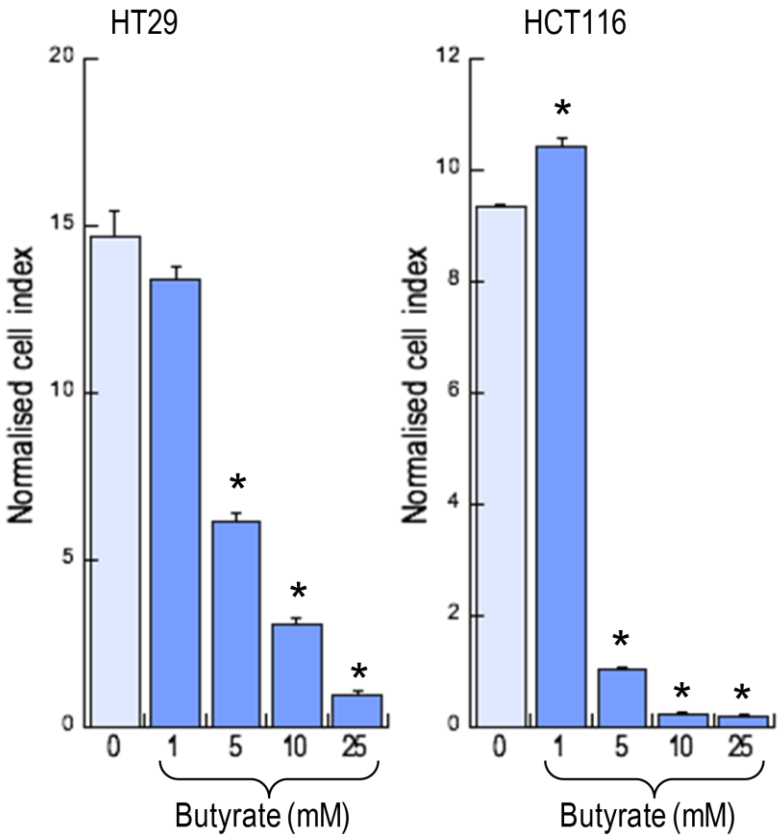

Figure 4.1: Proliferation of HT29 and HCT116 cells after 48 h of butyrate treatment.

Cell index measurements using the xCELLigence RTCA DP instrument in HT29 cells or HCT116 cells treated with increasing doses of butyrate, compared with cells in control medium (0) (* $P < 0.05$). The mean ± SEM of three cell culture replicates is shown.

4.4.2 microRNA microarray analysis of butyrate-treated colorectal cancer cell lines

Following 48 h exposure to the physiological level of 5 mM butyrate, proliferation was significantly reduced in both HT29 and HCT116 CRC cells compared with the respective untreated control cells, as shown in Section 4.4.1. A microarray analysis was then employed to assess miRNA expression in CRC cells treated with 5 mM butyrate for 48 h, compared with untreated controls. This microarray analysis was performed in the HT29 cell line, with findings subsequently validated in both HT29 and HCT116 cell lines, in order to compare response. The miRNA expression profiling was performed using the Exiqon v11 ready-to-spot probeset, using three replicate samples from each treatment group. The list of differentially expressed miRNAs is detailed in Table 4.2. miRNAs with a positive Bayesian log odds value were considered differentially expressed, with 33 human miRNAs up-regulated and 23 human miRNAs down-regulated in response to butyrate. These results are also displayed in a volcano plot in Figure 4.2. Human miRNAs which exhibited significant up-regulation in response to butyrate included hsa-miR-210, hsa-miR-1275, hsa-miR-584, hsa-miR-1290, hsa-miR-943, hsa-miR-33b, hsa-miR-874, hsa-miR-23a, hsa-miR-373*, hsa-miR-508-5p, hsa-miR-769-5p, and hsa-miR-23b. Human miRNAs which exhibited significant down-regulation in response to butyrate included hsa-miR-17*, hsa-miR-106a, hsa-miR-20a, hsa-miR-19b-1*, hsa-miR-20b, hsa-miR-20a*, hsa-miR-18b, hsa-miR-196b, hsa-miR-301a, hsa-miR-18a, hsa-miR-33a, hsa-miR-301b, hsa-miR-19b, hsa-miR-29b, hsa-miR-215, hsa-miR-192, hsa-miR-15b*, hsa-miR-92b, hsa-miR-17, hsa-miR-196a, and hsa-miR-136. A number of Exiqon proprietary miRNA sequences were also shown to be differentially expressed, with the majority of these up-regulated by butyrate.

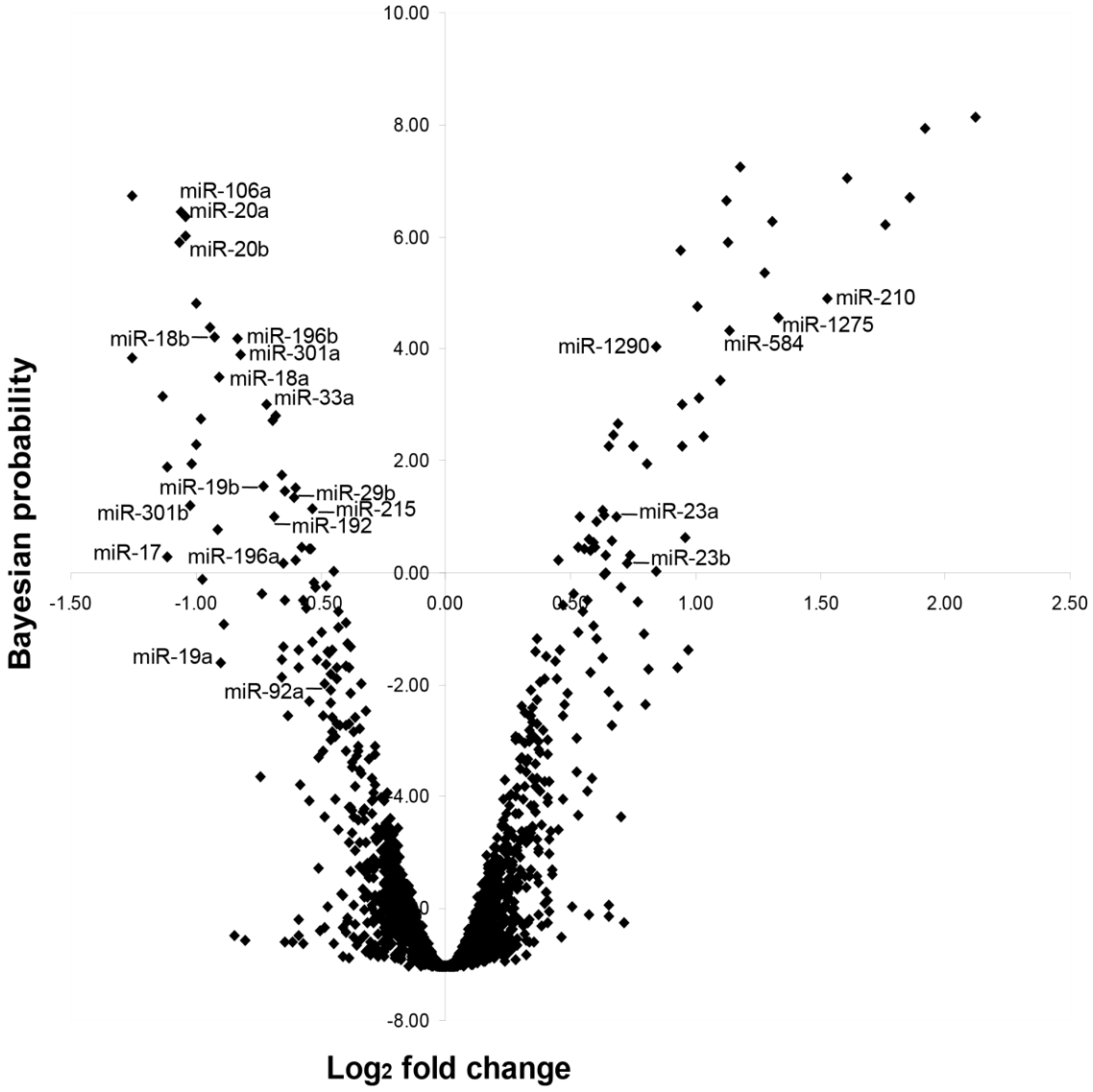

Figure 4.2: Microarray analysis of miRNA expression in HT29 cells after 48 h of butyrate treatment – volcano plot.

The x-axis of the volcano plot represents the differential expression (log_2 fold change) in HT29 cells with and without 5 mM butyrate treatment (n = 3 for each). The y-axis represents the empirical Bayesian log odds of differential expression, with a positive value considered significant. miRNAs that were significantly up-regulated or down-regulated, and were selected for subsequent real-time RT-PCR validation, are labelled.

Table 4.2: Microarray analysis of miRNA expression in HT29 cells after 48 h of butyrate treatment – list of differentially expressed miRNAs

miRNAs with a significant Bayesian log odds of differential expression (B > 0) and/or a significant adjusted *P* value ($P < 0.05$) are listed.

Name	Log fold change	Fold change	Regulation in butyrate	Average expression	Adjusted *P* value	B (Bayesian log odds)
hsa-miRPlus-E1028	2.12	4.35	up	9.11	0.00021	8.13
ebv-miR-BART6-3p	1.92	3.78	up	8.37	0.00021	7.95
hsa-miRPlus-E1033	1.61	3.05	up	12.07	0.000238	7.05
hsa-miR-17*	-1.25	2.38	down	9.82	0.000238	6.74
hsa-miRPlus-E1170	1.12	2.18	up	14.00	0.000238	6.66
hsa-miR-106a	-1.06	2.09	down	12.83	0.000239	6.45
hsa-miR-20a	-1.04	2.06	down	13.75	0.000239	6.37
hsa-miRPlus-E1117	1.31	2.48	up	12.62	0.000239	6.28
hsa-miR-19b-1*	-1.04	2.06	down	7.15	0.00026	6.02
hsa-miR-20b	-1.06	2.09	down	12.26	0.00026	5.90
hsa-miRPlus-E1108	0.94	1.92	up	13.89	0.00028	5.75
hsa-miRPlus-E1234	1.28	2.42	up	7.17	0.000394	5.35
hsa-miR-210	1.53	2.88	up	9.68	0.000586	4.90
hsa-miR-20a*	-1.00	2.00	down	7.84	0.000604	4.81
hsa-miRPlus-F1099	1.00	2.01	up	8.86	0.000609	4.74
hsa-miR-1275	1.33	2.52	up	9.48	0.000699	4.55
hsa-miR-584	1.14	2.20	up	8.57	0.000796	4.32
hsa-miR-18b	-0.93	1.90	down	11.24	0.000852	4.20
hsa-miR-196b	-0.84	1.79	down	8.86	0.000852	4.17
hsa-miR-1290	0.84	1.79	up	12.82	0.000926	4.04
hsa-miR-301a	-0.82	1.77	down	9.71	0.00104	3.88
hsa-miR-18a	-0.91	1.87	down	11.62	0.001398	3.50
hsa-miRPlus-E1067	1.10	2.15	up	9.39	0.001446	3.43
hsa-miR-33a	-0.72	1.65	down	10.76	0.001916	3.01
hsa-miRPlus-F1181	-0.68	1.61	down	9.97	0.002245	2.81
hsa-miRPlus-E1077	0.69	1.61	up	10.99	0.002357	2.67

hsa-miRPlus-E1141	0.67	1.59	up	12.87	0.002785	2.47
hsa-miRPlus-A1056	1.03	2.05	up	9.63	0.002827	2.43
hsa-miR-943	0.95	1.93	up	7.27	0.00301	2.27
hsa-miRPlus-E1045	0.75	1.69	up	11.60	0.00301	2.27
hsa-miRPlus-E1088	0.65	1.57	up	11.59	0.00301	2.26
hsa-miR-301b	-1.02	2.03	down	8.73	0.003894	1.95
hsa-miRPlus-D1116	0.81	1.75	up	9.65	0.003894	1.95
hsa-miR-19b	-0.73	1.66	down	12.38	0.005295	1.56
hsa-miR-29b	-0.61	1.52	down	13.78	0.006035	1.36
hsa-miR-215	-0.53	1.45	down	12.59	0.007053	1.15
hsa-miRPlus-E1035	0.63	1.55	up	10.57	0.007231	1.11
hsa-miR-33b	0.63	1.55	up	9.25	0.007543	1.02
hsa-miR-874	0.54	1.45	up	8.42	0.007543	1.01
hsa-miR-23a	0.68	1.61	up	12.45	0.007543	0.99
hsa-miR-192	-0.69	1.61	down	12.17	0.007543	0.99
hsa-miR-373*	0.60	1.52	up	6.69	0.008014	0.91
hsa-miR-508-5p	0.57	1.49	up	6.52	0.010092	0.61
hsa-miRPlus-F1042	0.59	1.51	up	7.53	0.010486	0.54
hsa-miR-15b*	-0.58	1.49	down	8.07	0.010586	0.46
hsa-miR-769-5p	0.53	1.45	up	8.86	0.010586	0.46
hsa-miRPlus-E1225	0.60	1.51	up	11.10	0.010586	0.44
hsa-miRPlus-E1205	-0.54	1.45	down	11.57	0.010586	0.44
hsa-miR-92b	-0.55	1.46	down	8.77	0.010586	0.44
hsa-miRPlus-F1170	0.58	1.50	up	12.56	0.010683	0.41
hsa-miRPlus-F1159	0.64	1.56	up	11.25	0.011437	0.32
hsa-miRPlus-D1036	0.74	1.67	up	10.28	0.011437	0.30
hsa-miR-17	-1.12	2.17	down	13.36	0.011437	0.29
hsa-miRPlus-E1153	0.45	1.37	up	12.61	0.011925	0.23
hsa-miR-23b	0.73	1.66	up	13.02	0.012237	0.17
hsa-miR-196a	-0.65	1.57	down	7.98	0.012237	0.17
hsa-miR-136	-0.45	1.37	down	8.57	0.013729	0.02

hsa-miRPlus-E1047	0.64	1.56	up	14.77	0.013903	-0.01
hsa-miRPlus-A1027	0.63	1.55	up	8.51	0.014076	-0.03
hsa-miR-451	-0.53	1.44	down	7.55	0.015648	-0.17
hsa-miRPlus-F1091	-0.48	1.39	down	10.65	0.016447	-0.24
hsa-let-7a*	-0.52	1.44	down	8.22	0.016447	-0.26
hsa-miRPlus-C1115	0.70	1.63	up	10.21	0.016447	-0.26
hsa-miRPlus-A1098	0.52	1.43	up	8.63	0.018074	-0.37
hsa-miR-19a*	-0.74	1.67	down	8.00	0.018074	-0.38
hsa-miR-18a*	-0.57	1.48	down	6.92	0.019558	-0.49
hsa-miR-142-3p	-0.64	1.56	down	8.99	0.019558	-0.50
hsa-miRPlus-F1037	0.77	1.70	up	11.18	0.019782	-0.52
hsa-miRPlus-E1065	0.47	1.39	up	13.96	0.020747	-0.59
hsa-miR-16-1*	-0.56	1.47	down	7.30	0.0214	-0.63
hsa-miR-135b	-0.43	1.35	down	10.61	0.022063	-0.68
hsa-let-7c*	0.55	1.46	up	7.01	0.022063	-0.68
hsa-miR-192*	-0.40	1.32	down	6.78	0.026479	-0.89
hsa-miR-194	-0.89	1.85	down	11.79	0.026955	-0.92
hsa-miRPlus-E1285	0.59	1.51	up	8.89	0.027181	-0.94
hsa-miR-452*	-0.43	1.34	down	8.09	0.028121	-0.98
hsa-miRPlus-F1080	0.53	1.44	up	7.33	0.030141	-1.06
hsa-miRPlus-E1139	-0.49	1.41	down	11.90	0.030222	-1.08
hsa-miRPlus-E1168	0.80	1.74	up	7.04	0.030451	-1.10
hsa-miR-16-2*	-0.39	1.31	down	7.60	0.034235	-1.26
hsa-miR-29a*	-0.65	1.57	down	8.92	0.035702	-1.32
hsa-miR-455-5p	-0.59	1.50	down	7.75	0.03671	-1.37
ebv-miR-BART8*	0.46	1.38	up	7.47	0.03671	-1.39
hsa-miRPlus-E1013	-0.46	1.37	down	11.87	0.03671	-1.39
hsa-miRPlus-E1082	-0.48	1.39	down	8.75	0.03671	-1.40
hsa-miR-659	0.36	1.29	up	8.67	0.036966	-1.41
hsa-miR-1246	0.40	1.32	up	14.59	0.03933	-1.50

hsa-miR-557	0.63	1.55	up	6.83	0.039965	-1.52
hsa-miR-106b	-0.65	1.57	down	12.36	0.040846	-1.56
hsa-miR-19a	-0.90	1.87	down	12.24	0.041654	-1.60
hsa-miR-30b*	-0.48	1.40	down	6.95	0.043105	-1.65
hsa-miR-652	-0.40	1.32	down	8.08	0.043318	-1.66
hsa-miRPlus-A1065	-0.44	1.35	down	9.85	0.043673	-1.70
hsa-miR-149	0.93	1.90	up	8.18	0.043673	-1.70
sv40-miR-S1-5p	0.58	1.50	up	10.18	0.046827	-1.79
hsa-miR-144	-0.46	1.38	down	8.13	0.04749	-1.81
hsa-miR-205	-0.65	1.57	down	8.81	0.04956	-1.87
hsa-miRPlus-F1024	0.39	1.31	up	12.25	0.050222	-1.89
hsa-miR-1274b	-0.43	1.35	down	7.68	0.050222	-1.90
hsa-miR-923	0.45	1.36	up	12.52	0.050222	-1.90
hsa-miR-296-3p	0.38	1.30	up	7.31	0.051891	-1.94
hsa-miR-92a	-0.49	1.40	down	9.01	0.053511	-1.99
hsa-miR-15b	-0.34	1.26	down	12.19	0.053511	-1.99
hsa-miR-7-1*	-0.46	1.38	down	7.10	0.05784	-2.09

4.4.3 Real-time RT-PCR validation of microRNAs with butyrate-induced expression changes in colorectal cancer cell lines

To validate the miRNA microarray data, differentially expressed miRNAs were selected for relative quantitation real-time RT-PCR analysis. HT29 and HCT116 CRC cell lines were treated for 48 h with 5 mM butyrate, or maintained in control medium. Among the miRNAs selected for validation were those shown to be up-regulated in the microarray, including miR-23a, miR-23b, miR-210, miR-584, miR-1275, and miR-1290. Other miRNAs selected for validation were those miRNAs shown in the microarray experiment to be potentially down-regulated, including miR-17, miR-18a, miR-19a, miR-20a, miR-19b, miR-92a, miR-18b, miR-20b, miR-106a, miR-29b, miR-33a, miR-192, miR-196a, miR-196b, miR-215, miR-301a, and miR-301b. The real-time RT-PCR miRNA expression data presented represent robust findings from multiple experiments; the experimental results shown in this Chapter replicate results from preliminary experiments (shown in Appendix 1).

The real-time RT-PCR results for miRNAs that were increased with butyrate treatment in the microarray experiment are shown in Figures 4.3 and 4.4. In both the HT29 and HCT116 cells, miRNAs that were shown to be significantly increased with butyrate

treatment included miR-23a ($P = 0.001$ in HT29 cells; $P = 0.04$ in HCT116 cells), miR-23b ($P = 0.0002$ in HT29 cells; $P < 0.0001$ in HCT116 cells), miR-210 ($P = 0.0002$ in HT29 cells; $P = 0.049$ in HCT116 cells), and miR-1290 ($P = 0.0003$ in HT29 cells; $P < 0.0001$ in HCT116 cells). miR-584 levels were unchanged with butyrate treatment in HT29 cells ($P = 0.26$), and decreased in HCT116 cells (P = 0.001). Similarly, miR-1275 levels were unchanged with butyrate treatment in the HT29 cells ($P = 0.26$), and were decreased in HCT116 cells ($P = 0.002$).

Figures 4.5 and 4.6 illustrate the real-time RT-PCR analysis of miRNAs that were decreased with butyrate in the microarray. Butyrate significantly decreased levels of miRNAs in the miR-17-92 cluster (miR-17, miR-18a miR-19a, miR-20a, miR-92a, miR-19b) and the miR-106a-363 paralog (miR-18b, miR-20b, miR-106a), in both HT29 and HCT116 cells (*P* values in Table 4.3). Other miRNAs that were significantly decreased with butyrate, in both cell lines, included miR-29b ($P = 0.03$ in HT29 cells; $P = 0.0007$ in HCT116 cells), miR-196a ($P = 0.01$ in HT29 cells; $P = 0.0001$ in HCT116 cells), miR-196b ($P = 0.01$ in HT29 cells; $P = 0.006$ in HCT116 cells), and miR-301a ($P = 0.009$ in HT29 cells; $P = 0.0007$ in HCT116 cells), with miR-301b significantly decreased in the HCT116 cell line only ($P = 0.0007$). miR-215 was significantly decreased in HT29 cells only ($P = 0.01$), and was significantly increased in HCT116 cells ($P = 0.0001$). Similarly, miR-192 appeared slightly decreased in HT29 cells only ($P = 0.06$), and was significantly increased in HCT116 cells ($P < 0.0001$).

Table 4.3: *P* values showing the significant decrease in miR-17-92 and miR-106a-363 cluster mature miRNA levels in standard HT29 and HCT116 treated with 5 mM butyrate for 48 h as detected by real-time RT-PCR.

P values represent significance relative to untreated control cells, for the mean of three cell culture replicates

miRNA	*P* value	miRNA	*P* value
Standard HT29 cells		**Standard HCT116 cells**	
miR-17	0.0005	miR-17	0.0002
miR-18a	0.0001	miR-18a	0.0001
miR-19a	0.0002	miR-19a	0.0002
miR-20a	0.0002	miR-20a	<0.0001
miR-19b	0.0002	miR-19b	<0.0001
miR-92a	0.0003	miR-92a	0.0003
miR-106a	0.001	miR-106a	0.0003
miR-18b	0.007	miR-18b	0.0008
miR-20b	0.0003	miR-20b	0.0006

Note: miR-19b-2 and miR-92a-2 in the miR-106a-363 cluster have the same sequence as miR-19b-1 and miR-92a-1 respectively in the miR-17-92 cluster, so the real-time RT-PCR results for these miRNAs do not distinguish between these. miR-363 was not examined as it showed no change in the microarray analysis.

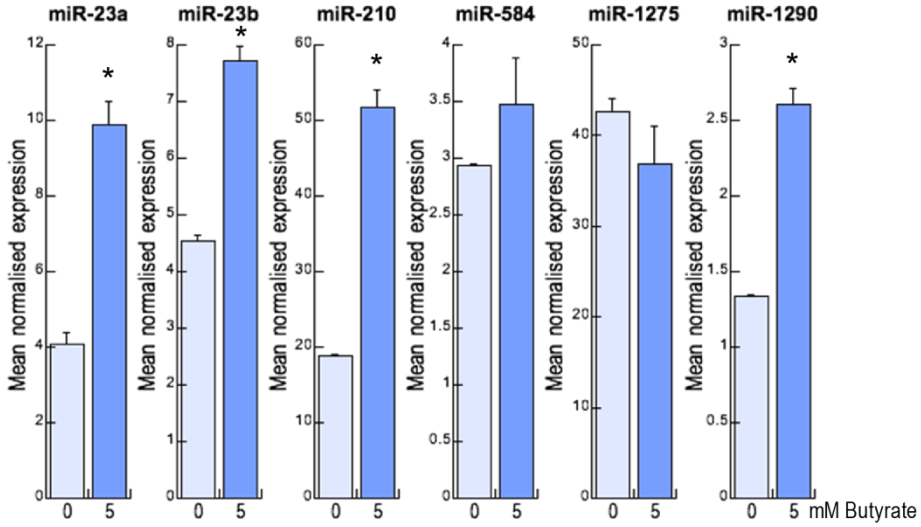

Figure 4.3: Real-time RT-PCR analysis of miRNA levels in HT29 cells for miRNAs identified by the microarray experiment as being up-regulated with 48 h butyrate treatment.

Cells treated with 5 mM butyrate, compared with cells in control medium (0) (* $P <$ 0.05). The mean ± SEM of three cell culture replicates is shown, and expression is normalised to RNU6B levels.

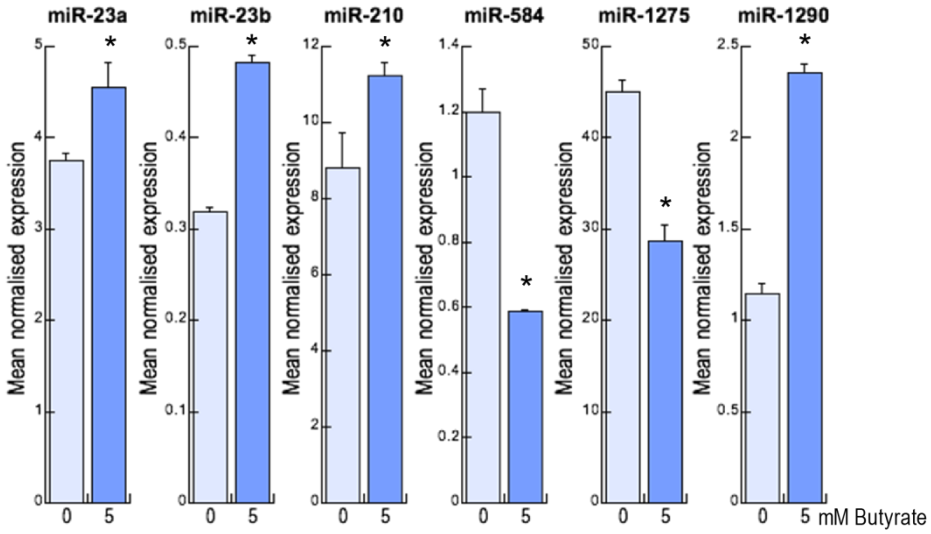

Figure 4.4: Real-time RT-PCR analysis of miRNA levels in HCT116 cells for miRNAs identified by the microarray experiment as being up-regulated with 48 h butyrate treatment.

Cells treated with 5 mM butyrate, compared with cells in control medium (0) (* $P <$ 0.05). The mean ± SEM of three cell culture replicates is shown, and expression is normalised to RNU6B levels.

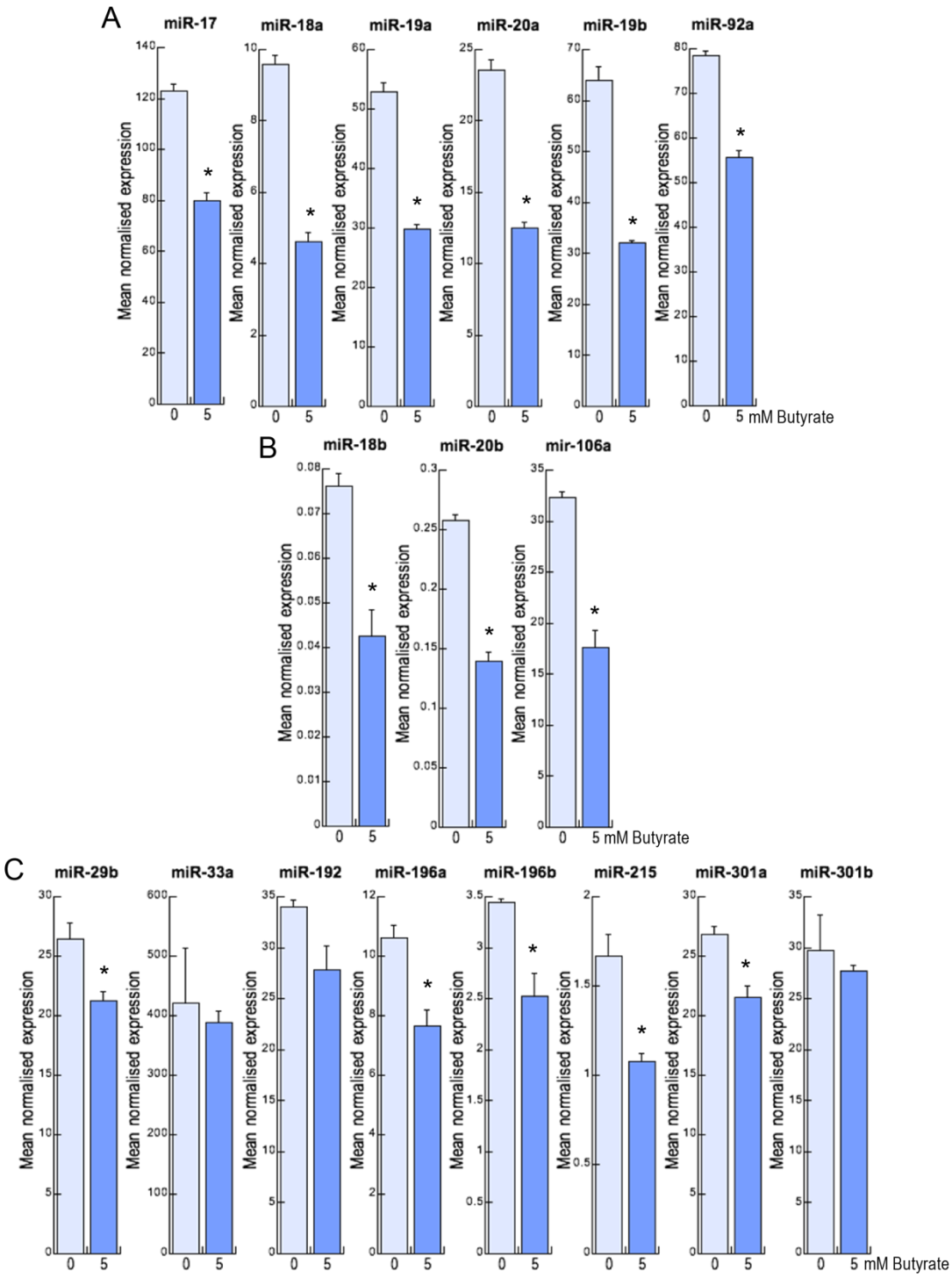

Figure 4.5: Real-time RT-PCR analysis of miRNA levels in HT29 cells for miRNAs identified by microarray as being down-regulated with 48 h butyrate treatment.

Cells treated with 5 mM butyrate, compared with cells in control medium (0) (* $P < 0.05$). The mean ± SEM of three cell culture replicates is shown, and expression is normalised to RNU6B levels. (A) miR-17-92 cluster of miRNAs. (B) miR-106a-363 cluster of miRNAs. (C) Other miRNAs.

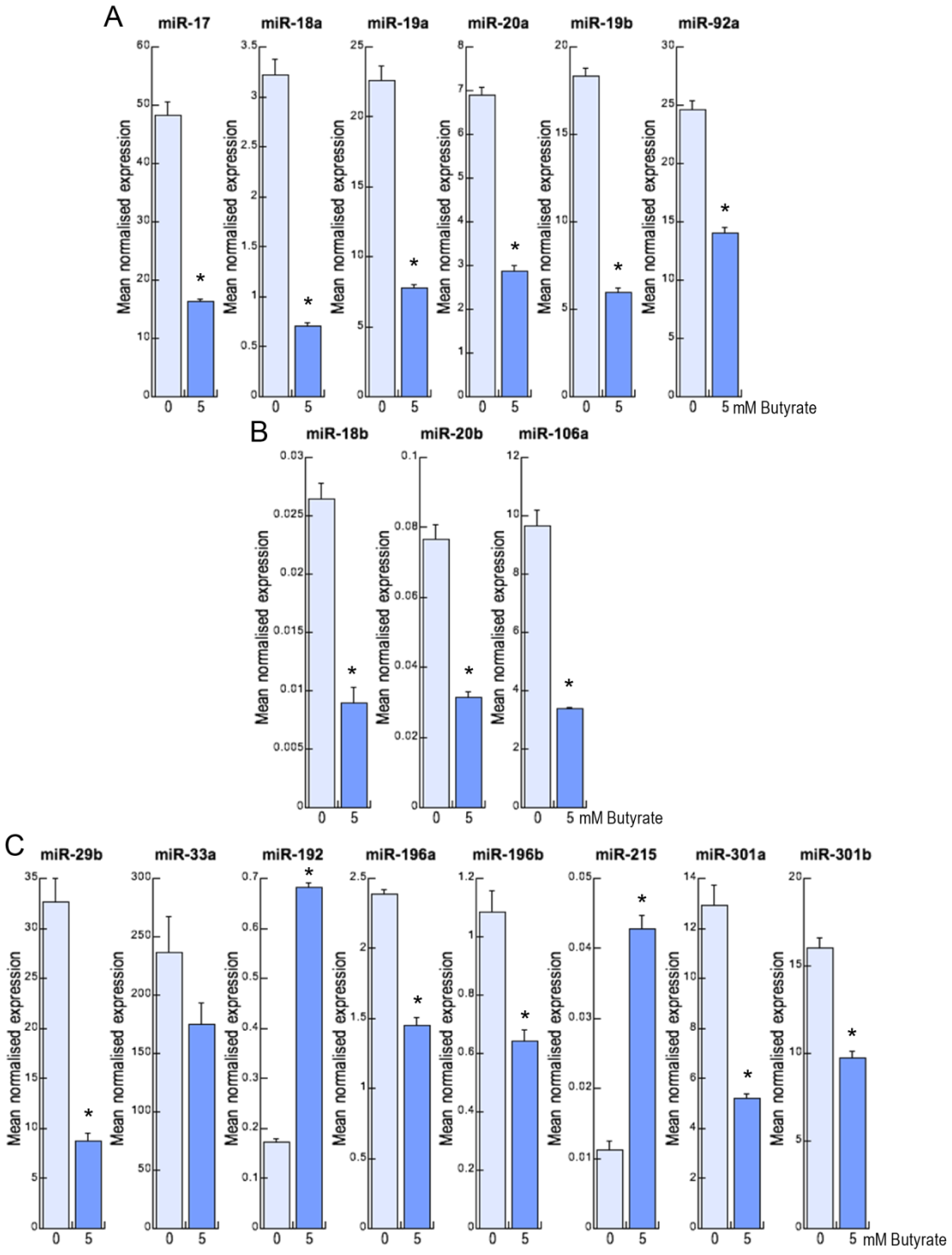

Figure 4.6: Real-time RT-PCR analysis of miRNA levels in HCT116 cells for miRNAs identified by microarray as being down-regulated with 48 h butyrate treatment.

Cells treated with 5 mM butyrate, compared with cells in control medium (0) (* $P < 0.05$). The mean ± SEM of three cell culture replicates is shown, and expression is normalised to RNU6B levels. (A) miR-17-92 cluster of miRNAs. (B) miR-106a-363 cluster of miRNAs. (C) Other miRNAs.

4.4.4 Butyrate-induced microRNA expression changes in butyrate-resistant versus standard colorectal cancer cell lines

The butyrate-resistant HT29 and HCT116 cell lines (HT29-BR and HCT116-BR) developed by Fung et al (2009) were used to determine any differences in the miRNA response to butyrate treatment, compared with the standard HT29 and HCT116 cell lines. The BR cells were maintained in 5 mM butyrate prior to use in any experiments, to retain their resistance (Fung et al 2009). The experiments in which standard HT29 and HCT116 CRC cell lines were treated for 48 h with butyrate, or maintained in control medium, were conducted simultaneously in the HT29-BR and HCT116-BR cell lines. These included the real-time cell growth, harvesting of RNA for miRNA expression analysis.

To test the levels of resistance in the BR cell lines, proliferation results for the standard and butyrate-resistant cell lines growing in increasing concentrations of butyrate were obtained (Figure 4.7). At lower butyrate concentrations (1 mM), proliferation was greater in the HT29-BR cell line compared with the standard HT29 cell line, but both cell lines had significantly decreased proliferation with 10 mM butyrate treatment, compared with the untreated control HT29 cells ($P < 0.05$). Similarly, while proliferation was greater in the HCT116-BR cell line compared with the standard HCT116 cell line at low butyrate concentrations, both cell lines were shown to have a significantly decreased proliferation with 5 mM butyrate treatment, compared with the untreated control HCT116 cells ($P < 0.05$).

miRNAs from the miR-17-92 cluster, which were all significantly reduced in butyrate-treated standard CRC cell lines, were also examined in the butyrate-resistant cell lines, to detect any expression differences between the strains (Figures 4.8 and 4.9). It could be hypothesised that in the butyrate-resistant cell lines, treatment with 5 mM butyrate would have little effect on miRNA expression, as these cells have been conditioned to growing at this level. In contrast, real-time RT-PCR analysis showed all of the selected miR-17-92 cluster miRNAs to be significantly down-regulated by 5 mM butyrate, in both standard HT29 and HT29-BR cells (*P* values in Table 4.3 and 4.4). Similarly, real-time RT-PCR analysis showed all of the selected miR-17-92 cluster miRNAs to be significantly down-regulated by 5 mM butyrate, in both standard HCT116 and HCT116-BR cells (*P* values in Table 4.3 and 4.4), with the exception of miR-17 in the HCT116-BR cell line. Expression was dose-dependent, with increasing butyrate concentration leading to decreasing levels of miR-17-92 cluster members, in both the standard and

butyrate-resistant cell lines. It was only at the low butyrate concentration of 1 mM that differences could be observed in butyrate-induced miRNA expression changes in the standard and butyrate-resistant cell lines.

Table 4.4 *P* values showing the significant decrease in miR-17-92 cluster mature miRNA levels in butyrate-resistant HT29 and HCT116 treated with 5 mM butyrate for 48 h as detected by real-time RT-PCR.

P values represent significance relative to untreated control cells, for the mean of three cell culture replicates

miRNA	*P* value	miRNA	*P* value
HT29-BR cells		**HCT116-BR cells**	
miR-17	0.0001	miR-17	0.07
miR-18a	0.001	miR-18a	0.003
miR-19a	0.002	miR-19a	0.02
miR-20a	<0.001	miR-20a	0.01
miR-19b	0.0001	miR-19b	0.01
miR-92a	0.003	miR-92a	0.04

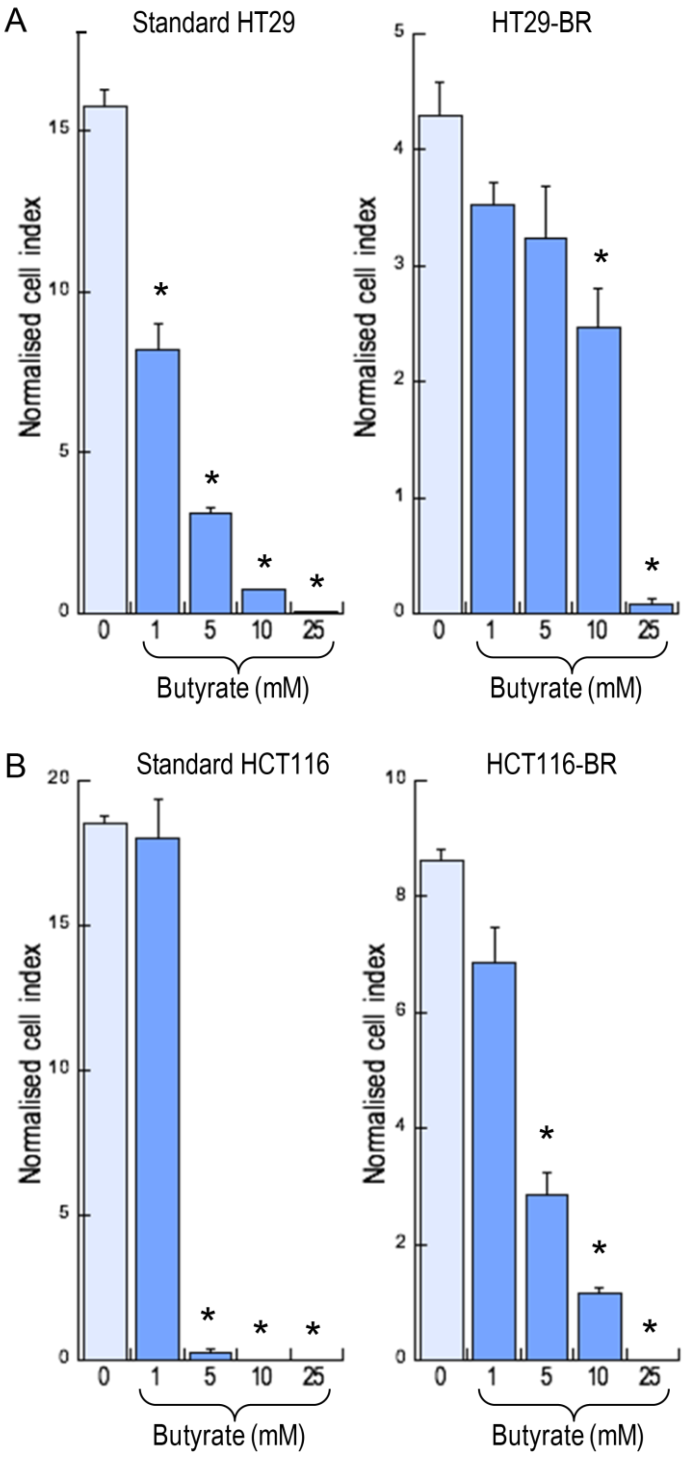

Figure 4.7: Proliferation of standard and butyrate-resistant HT29 and HCT116 cells after 48 h of butyrate treatment.

Cell index measurements using the xCELLigence RTCA DP instrument in HT29 standard or BR cells (A) or HCT116 standard or BR cells (B) treated with increasing doses of butyrate, compared with respective cells in control medium (0) (* $P < 0.05$). The mean ± SEM of three cell culture replicates is shown.

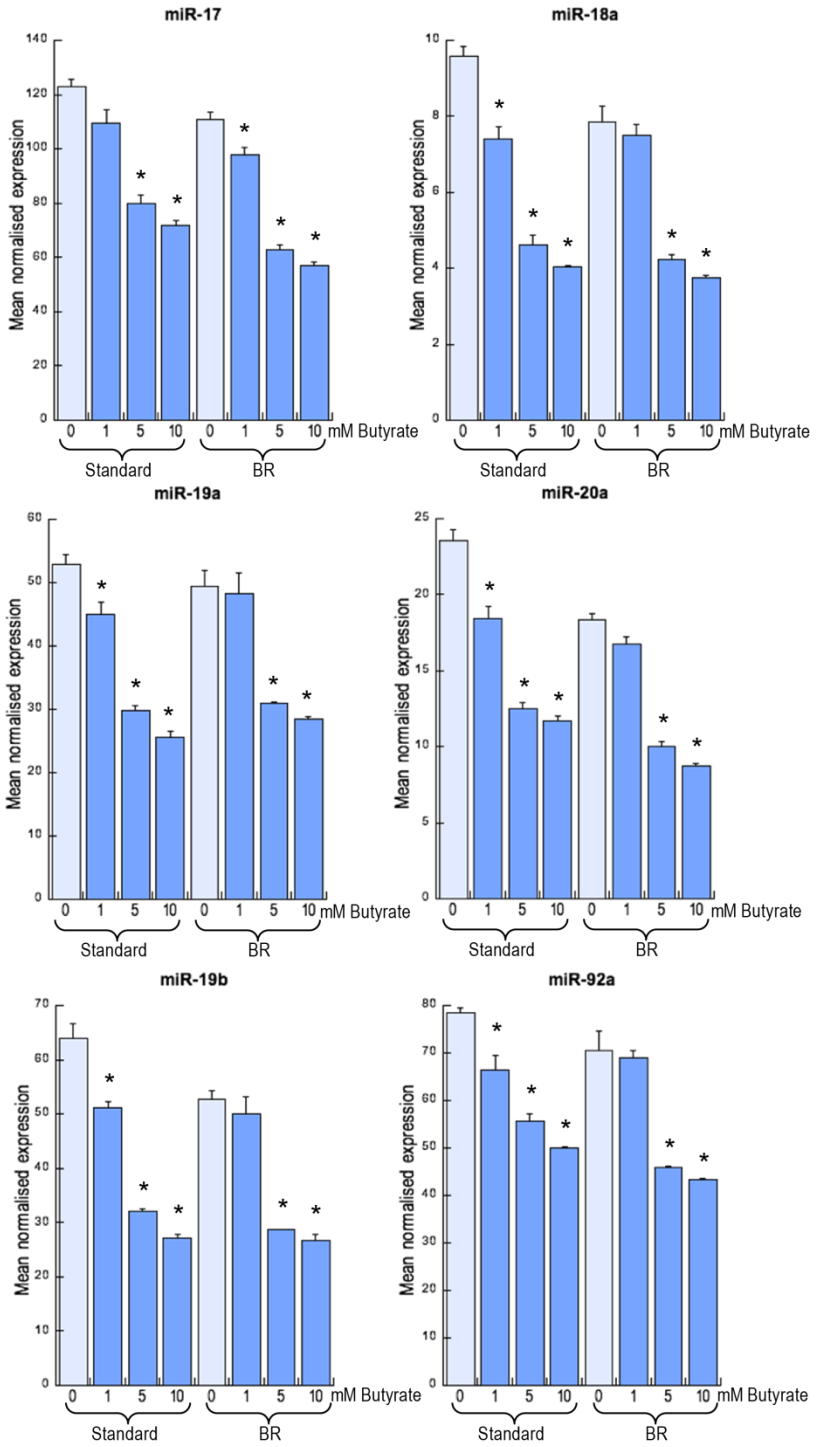

Figure 4.8: Real-time RT-PCR analysis of miRNAs levels for miRNAs identified by microarray as being down-regulated with 48 h butyrate treatment (miR-17-92 cluster) – comparison between standard HT29 and HT29-BR cells.

Cells treated with 5 mM butyrate, compared with cells in control medium (0) (* $P <$ 0.05). The mean ± SEM of three cell culture replicates is shown, and expression is normalised to RNU6B levels.

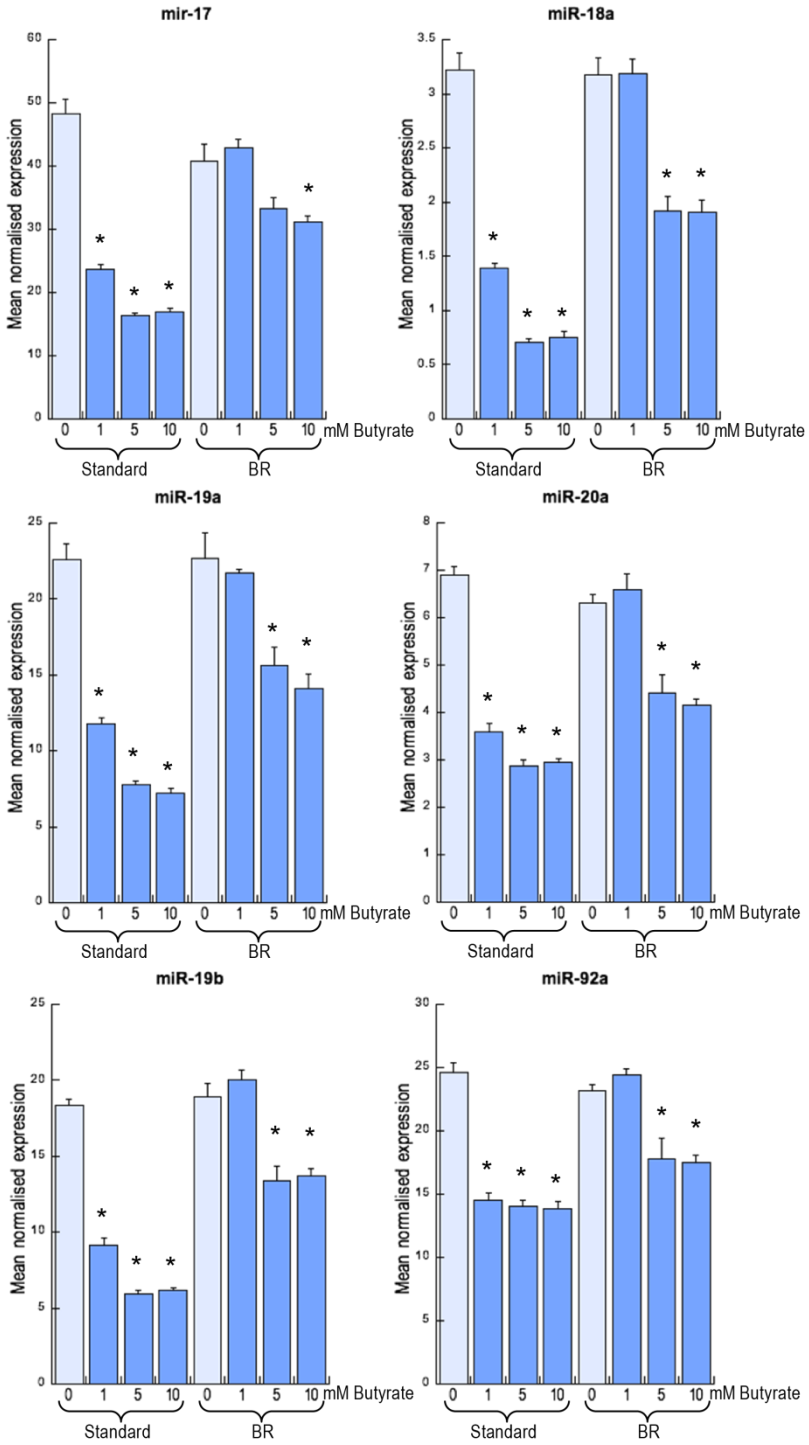

Figure 4.9: Real-time RT-PCR analysis of miRNAs levels for miRNAs identified by microarray as being down-regulated with 48 h butyrate treatment (miR-17-92 cluster) – comparison between standard HCT116 and HCT116-BR cells.

Cells treated with 5 mM butyrate, compared with cells in control medium (0) (* $P <$ 0.05). The mean ± SEM of three cell culture replicates is shown, and expression is normalised to RNU6B levels.

4.4.5 Ingenuity pathway analysis of microRNAs with butyrate-induced expression changes

Following the microarray analysis to assess miRNA expression in HT29 cells treated with 5 mM butyrate compared with untreated controls, an IPA analysis was performed. IPA software allows analysis of microarray and gene expression data to identify relevant pathways that contain these molecules. The analysis can provide insight into the potential causes of observed expression changes and into the predicted downstream biological effects of those changes.

The dataset analysed in the IPA consisted of miRNAs which were considered differentially expressed based on a positive Bayesian log odds value in the microarray analysis (Table 4.2). In the IPA analysis, both direct and indirect relationships were included, but results were filtered to consider only relationships which had been experimentally observed.

IPA analysis of the butyrate-regulated miRNAs showed subsets of these miRNAs to be involved in several relevant pathways (Tables 4.5 – 4.7). The top IPA networks associated with miRNAs that experienced butyrate-induced expression changes are listed in Table 4.5. The top two networks 'Connective Tissue Disorders, Genetic Disorder, Inflammatory Disease', and 'Cancer, Gastrointestinal Disease, Hepatic System Disease' are shown in Figures 4.10 and 4.11. The first network (Figure 4.10) is of note as it contains multiple differentially expressed miRNAs from the microarray analysis, including miR-17-92 cluster miRNAs, and contains genes important in CRC, such as the tumour suppressor TP53. Among the top IPA diseases and disorders associated with the miRNAs showing butyrate-induced expression changes (Table 4.6) are the relevant disorders of 'Cancer', 'Gastrointestinal Disease', and 'Genetic Disorder'. The top IPA molecular and cellular functions associated with the miRNAs with butyrate-induced expression changes (Table 4.7) included cell cycle, death, and proliferation, which are relevant in cancer development and progression.

Table 4.5: Top IPA networks associated with miRNAs showing butyrate-induced expression changes

Network number	Associated Network Functions	IPA Score
1	Connective Tissue Disorders, Genetic Disorder, Inflammatory Disease	34
2	Cancer, Gastrointestinal Disease, Hepatic System Disease	14
3	Unnamed network	3
4	Cell Cycle, Cancer, Cell-To-Cell Signaling and Interaction	3
5	Cellular Assembly and Organization, Genetic Disorder, Neurological Disease	3

Table 4.6: Top IPA diseases and disorders associated with miRNAs showing butyrate-induced expression changes

Name	*P* value	Number of molecules
Reproductive System Disease	8.71E-15 – 4.35E-02	13
Cancer	1.28E-12 – 3.43E-02	15
Gastrointestinal Disease	1.28E-12 – 4.87E-02	14
Genetic Disorder	1.28E-12 – 4.87E-02	15
Connective Tissue Disorders	5.20E-12 – 1.35E-02	8

Table 4.7: Top IPA molecular and cellular functions associated with miRNAs showing butyrate-induced expression changes

Name	*P* value	Number of molecules
Cellular Development	2.31E-09 – 2.57E-02	7
Cellular Growth and Proliferation	2.31E-09 – 3.72E-02	7
Cell Death	1.68E-04 – 3.30E-02	3
Cell Cycle	3.28E-04 – 1.72E-02	2
Cell-To-Cell Signaling and Interaction	1.08E-03 – 5.40E-03	2

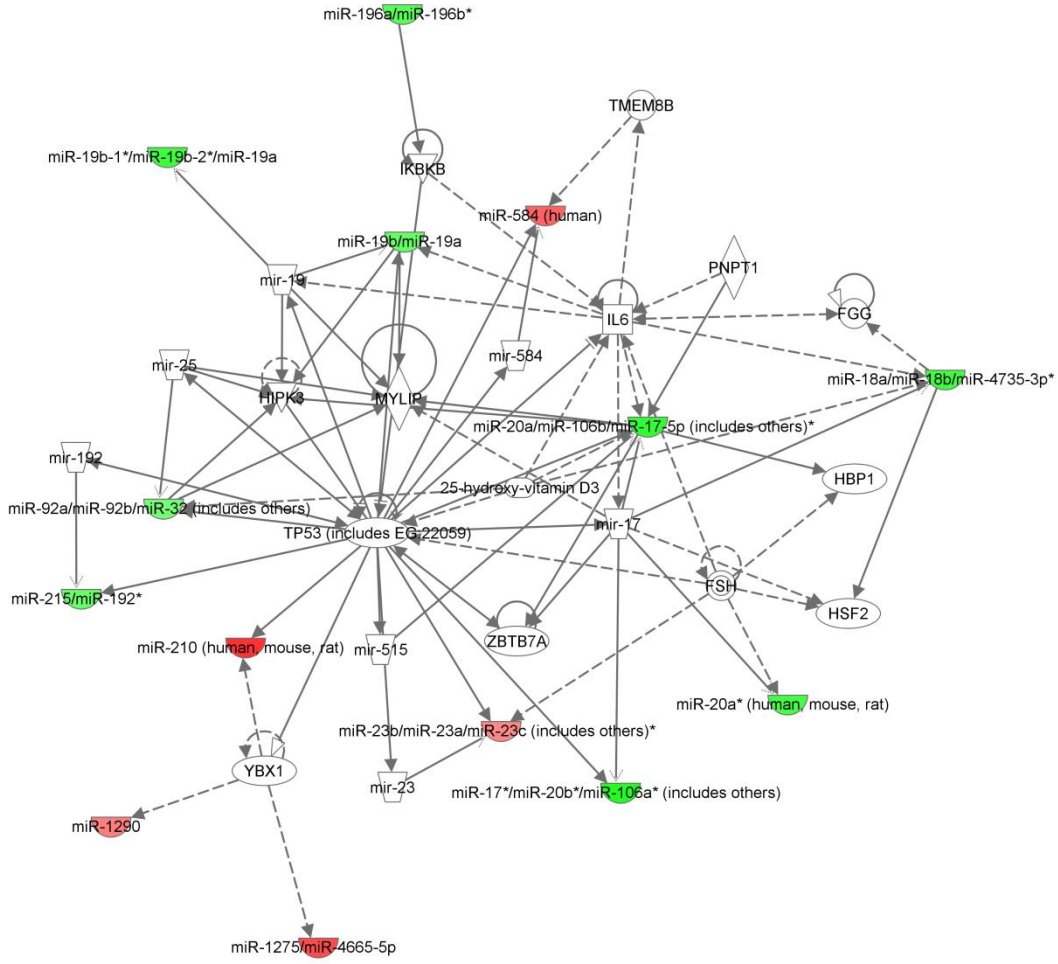

Figure 4.10: First top IPA network associated with miRNAs showing butyrate-induced expression changes, displaying predicted miRNA and gene interactions

miRNAs were associated with the IPA network of Connective Tissue Disorders, Genetic Disorder, Inflammatory Disease. Red indicates a miRNA that was increased with butyrate and green represents a miRNA that was decreased with butyrate.

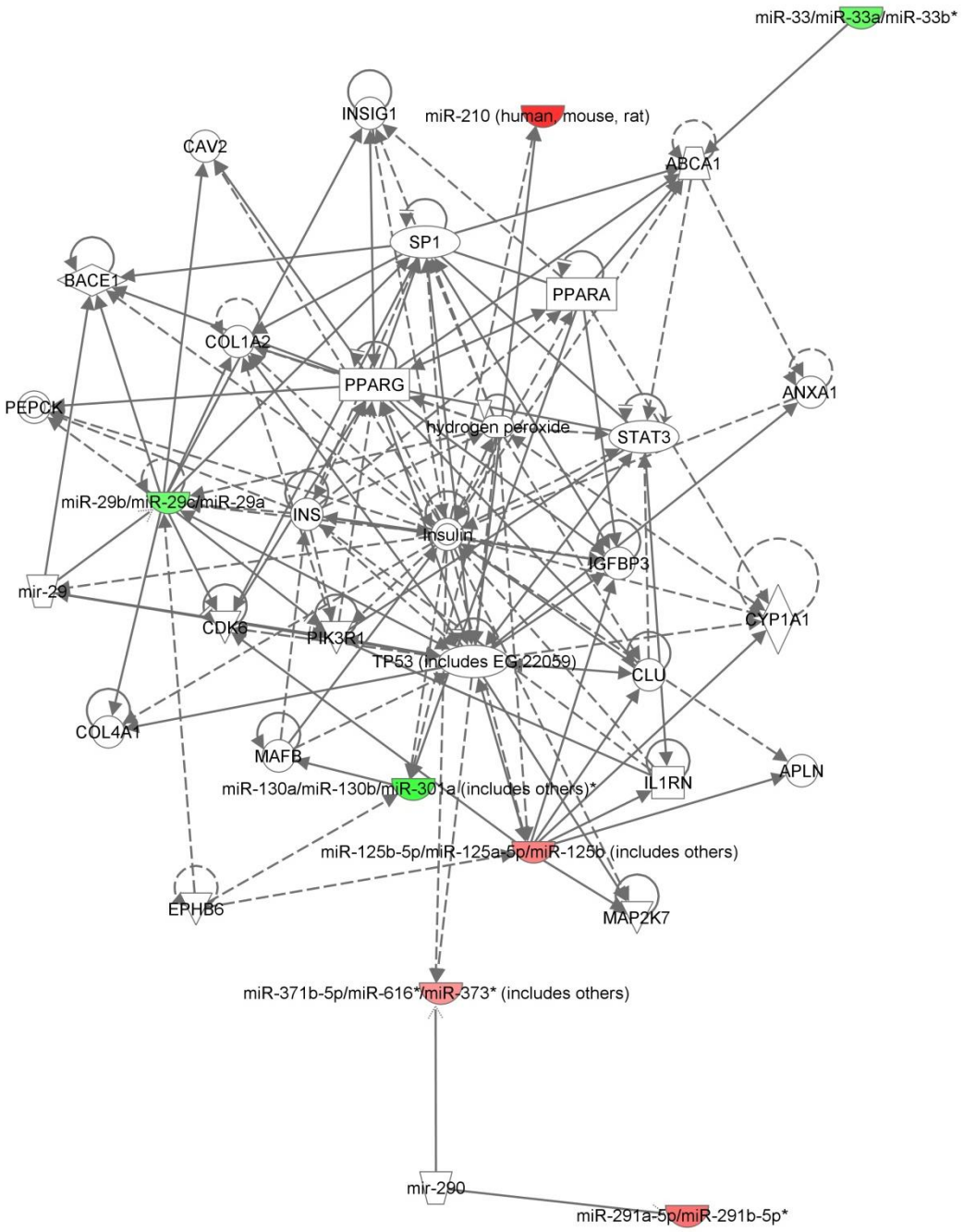

Figure 4.11: Second top IPA network associated with miRNAs showing butyrate-induced expression changes, displaying predicted miRNA and gene interactions

miRNAs were associated with the IPA network of Cancer, Gastrointestinal Disease, Hepatic System Disease. Red indicates a miRNA that was increased with butyrate and green represents a miRNA that was decreased with butyrate.

4.5 Discussion

This Chapter demonstrated the anti-proliferative effect of butyrate on HT29 and HCT116 CRC cell lines, with the HCT116 cell line showing greater susceptibility to the action of butyrate. Also in this Chapter, the effect of butyrate treatment on miRNA expression in CRC cell lines was displayed, through microarray analysis and real-time RT-PCR validation. In both the HT29 and HCT116 cell lines, butyrate was shown to alter the expression of miRNAs that have been found to be dysregulated in CRC. Expression profiles of miRNAs differ along the gastrointestinal tract (Slattery et al 2011) and are altered in CRC, with this dysregulation often contributing to tumour progression (Michael et al 2003, Lu et al 2005, Cummins et al 2006, Slaby et al 2007, Chen et al 2009).

The finding of decreased CRC cell growth with butyrate treatment was obtained using the xCELLigence RTCA DP instrument, which in this Chapter and subsequent Chapters was used to provide a cell index measure. A benefit of the xCELLigence system over traditional assays is that it allows continual real-time monitoring of cell growth over time. A limitation of the system, however, is that the cell index does not clearly distinguish between proliferation and other cellular events; for example, a reduced cell index could be due to reduced proliferation/cell cycle arrest, increased apoptosis or necrosis, morphological changes, or a combination. Additional measures of proliferation and apoptosis may have been of benefit; however, previous studies have already used assays to show that butyrate both reduces proliferation and increases apoptosis in CRC cells (Mariadason et al 2000, Iacomino et al 2001, Daly & Shirazi-Beechey 2006).

In this Chapter, treatment with 5 mM butyrate for 48 h led to down-regulation of all miR-17-92 cluster miRNAs, in both HT29 and HCT116 cells. miR-17-92 cluster members are derived from a single transcript which yields six mature miRNAs (miR-17, miR-18a, miR-19a, miR-20a, miR-19b-1, and miR-92a-1) (Tanzer & Stadler 2004), and thus are likely to be co-regulated. miR-17-92 over-expression has been observed in multiple tumour types, including CRC (Hayashita et al 2005, He et al 2005a, Cummins et al 2006, Chen et al 2009, Diosdado et al 2009). A recent study found a 2 to 5-fold increase in miR-17-92 cluster members in colorectal tumours compared with control epithelium (Diosdado et al 2009). The miR-17-92 cluster has oncogenic potential, and has been shown to promote proliferation and angiogenesis, inhibit differentiation, and sustain cell survival (Olive et al 2009). Mammals also possess miR-17-92 paralogs,

including the miR-106a-363 cluster on chromosome X, which is also over-expressed in CRC (Volinia et al 2006, Monzo et al 2008, Chen et al 2009, Luo et al 2012). miRNAs in the miR-106a-363 cluster, including miR-18b, miR-20b, and miR-106a, were also shown to be down-regulated with 5 mM butyrate treatment for 48 h.

Other miRNAs that experienced decreased expression in the colorectal cell lines with 5 mM butyrate treatment included miR-29b, miR-196a and miR-196b, and miR-301a and miR-301b. These miRNAs have all been shown to be up-regulated in CRC (Cummins et al 2006, Monzo et al 2008, Motoyama et al 2009). There is some evidence to suggest that high miR-196a levels promote the oncogenic phenotype of CRC cells (Schimanski et al 2009), and that a miR-196a polymorphism increases susceptibility to digestive system cancers (Guo et al 2012).

While multiple oncogenic miRNAs were decreased in colorectal cell lines in response to butyrate treatment, other miRNAs were shown to be increased with butyrate treatment. miR-23a and miR-23b have both been shown to be down-regulated in CRC (Cummins et al 2006, Chen et al 2009). There is evidence that miR-23b regulates a cohort of pro-metastatic targets, and thus aids in supressing tumour growth, invasion and angiogenesis (Zhang et al 2011). Treatment of HT29 and HCT116 cells with 5 mM butyrate resulted in increased expression of miR-23a and miR-23b. Another miRNA shown to be increased with butyrate treatment in both cell lines was miR-1290, which has also been shown to be decreased in CRC (Luo et al 2012). miR-210 was also increased with butyrate treatment in both cell lines. miR-210 can be induced by hypoxia (low oxygen), which is a common feature in tumourigenesis (Huang et al 2009). While miR-210 has been shown to have multiple functions, several studies have identified roles for miR-210 in repressing initiation of tumour growth, and inhibiting cancer cell survival and proliferation (Huang et al 2009, Tsuchiya et al 2011).

Also of note was the regulation of miR-215 by butyrate, which displayed cell line-specific action. In the microarray and subsequent real-time RT-PCR validation in HT29 cells, miR-215 was significantly decreased with butyrate treatment. In the HCT116 cell line, however, miR-215 was significantly increased with butyrate treatment, a finding also presented in a study by Hu et al (2011). miR-192 was also significantly increased with butyrate treatment in the HCT116 cell line only. Such variation in the butyrate response of the HT29 and HCT116 cell lines may provide insight into mechanisms for the increased sensitivity of the HCT116 cells to the pro-apoptotic effect of butyrate. For example, the over-expression of miR-192 and miR-215 has been shown to significantly

reduce cell proliferation in CRC cells by targeting cell cycle progression (Braun et al 2008, Boni et al 2010). These two miRNAs are often decreased in CRC (Braun et al 2008, Schetter et al 2008, Chen et al 2009, Earle et al 2010).

The real-time RT-PCR generally confirmed the initial findings from the microarray, with several exceptions. The microarray indicated, for example, that miR-33a was significantly decreased and miR-584 and miR-1275 were significantly increased in butyrate-treated HT29 cells, while subsequent real-time RT-PCR in the same cell line did not show significant changes for these miRNAs. Previous studies have similarly shown that while there is generally excellent correlation between microarray and real-time RT-PCR results, some miRNA levels do not correlate between the microarray and real-time RT-PCR measurements (Ach et al 2008, Git et al 2010). Microarrays are typically used as a screening tool, and it is important to confirm results with a more accurate detection method (van Rooij 2011). While a microarray screen followed by real-time RT-PCR validation is a common experimental workflow, alternative detection methods such as high-throughput sequencing are also emerging, and may have benefits in terms of sensitivity, measurement of absolute abundance, and novel miRNA discovery (Git et al 2010, van Rooij 2011). In this Chapter, while the microarray was only performed in one cell line, a strength of the work was that several CRC cell lines were used in the real-time RT-PCR analysis, to determine the generality of the findings.

This study made use of standard colorectal carcinoma cell lines, and variants developed by Fung et al (2009) which were less sensitive to the apoptotic effects of butyrate. Fung et al (2009) found that the apoptotic response to 48 h butyrate treatment was consistently lower in the HT29-BR cell line in comparison to the HT29 cells exposed to the same concentration of butyrate, but still identified a significant apoptotic response in both HT29 and HT29-BR cells at concentrations of 5 mM and greater ($P < 0.02$). The extent of differentiation, as measured by alkaline phosphatase activity, was less in the HT29-BR cell line compared with the HT29 cell line, but both cell lines were shown to have significantly increased alkaline phosphatase activity upon 5 mM butyrate treatment compared with the untreated control HT29 cells ($P < 0.005$). Fung et al (2009) identified a number of proteins that were differentially expressed between the HT29 and HT29-BR cell lines, and which potentially contributed to survival of cells insensitive to the tumour suppressing effects of butyrate, however, they also identified a large number of proteins which were similarly detected between the two cell lines. In this current study, the HT29-BR and HCT116-BR cell lines were shown to be slightly resistant to the anti-proliferative action of low butyrate concentrations compared to their standard

counterparts; however at higher butyrate concentrations (10 mM butyrate in the HT29-BR cells and 5 mM butyrate in the HCT116-BR cells), proliferation was still significantly reduced compared with the untreated controls. This was reflected in the miR-17-92 cluster expression results, where a 5 mM butyrate concentration significantly reduced miR-17-92 cluster miRNAs in both the standard and butyrate-resistant HT29 and HCT116 cell lines. It would appear that the butyrate-resistant cell lines are only insensitive to butyrate treatment at lower concentrations, such as 1 mM; thus these cell lines were not further utilised in subsequent Chapters.

Following the completion of this miRNA microarray study examining butyrate-modulated miRNA expression, a similar study was published by Hu et al (2011). Rather than using HT29 cells, Hu et al (2011) performed a miRNA microarray in the HCT116 human colorectal carcinoma cell line, using the miRCURY LNA microarray v.11.0 (Exiqon) that contained probes targeting all miRNAs for human, mouse, or rat registered in miRBase version 13 at the Sanger Institute. This present study also used the Exiqon v11 probeset, which offered an opportunity for comparison between the two studies. While the present study used a 5 mM butyrate treatment for 48 h, Hu et al (2011) used only 1 mM butyrate for 24 – 48 h; however as shown in this Chapter, HCT116 cells are more susceptible to butyrate than HT29 cells, which could account for the lower concentration used. The microarray performed by Hu et al (2011) identified 44 miRNAs that demonstrated significant changes in expression in response to butyrate treatment. miRNAs with decreased expression included miR-29b-1*, miR-18a, miR-92a, miR-20a*, miR-222*, miR-7, miR-18b, miR-29a*, let-7b*, miR-17, miR-196b, miR-20a, miR-20b, miR-19a, miR-34a, miR-106a, miR-221, miR-25, miR-106b, miR-19b, and miR-93, and miRNAs with increased expression included miR-96, miR-320b, miR-215, miR-194, miR-492, miR-184, miR-202, miR-381, miR-424, and miR-95. There was substantial overlap between the two studies for those miRNAs with decreased expression upon butyrate treatment. In particular, miRNAs from the miR-17-92 cluster and the paralogous cluster miR-106a-363, were significantly down-regulated in both studies. Both this study and the Hu et al (2011) study used real-time PCR to validate the microarray results. Hu et al (2011) also assessed expression levels of these miRNAs in six paired human sporadic colon cancers and surrounding normal appearing colon by microarray (mirVana miRNA Bioarrays v.2, Ambion). It was found that the miRNAs that decreased in butyrate-treated HCT116 cells were dramatically increased in tumour tissues compared with normal controls, including miR-17, miR-20a, miR-20b, miR-93, miR-106a, and miR-106b ($P < 0.05$) (Hu et al 2011).

This present study and that of Hu et al (2011) are the first to systematically identify changes in miRNA expression in response to butyrate in CRC cells. Also of interest, however, is an earlier somewhat related study by Bandres et al (2009), which treated CRC derived cell lines with 1 or 3 mM 4-phenylbutyric acid every 24 h for five days, in addition to treatment with a DNA methyltransferase inhibitor, 5-aza-2'deoxycytidine. Bandres et al (2009) looked specifically at five miRNAs included within 1000 base pairs of a CpG island, which were known to be down-regulated in CRC, and found that combined treatment with 4-phenylbutyric acid and the DNA methyltransferase inhibitor restored expression of three of these miRNAs (miR-9, miR-129, and miR-137). The changes in these miRNAs were not replicated in the microarray analyses by Hu et al (2011) and this present study; however, the study by Bandres et al (2009) is useful in displaying how both DNA methylation and histone modifications alter miRNA expression in CRC cells.

This Chapter identified multiple miRNAs that experienced altered expression with 5 mM butyrate treatment for 48 h. Some miRNAs that have oncogenic potential and are over-expressed in CRC, such as the miR-17-92 and miR-106a-363 clusters, were shown to be decreased with butyrate treatment. Others that are down-regulated in CRC and may play a protective role, such as miR-23a and miR-23b, were increased with butyrate treatment. Similar to the gene expression microarray studies, a limitation of this miRNA microarray was that it could not distinguish between miRNAs that had their transcription altered by direct butyrate action at the chromatin level, and miRNAs that experienced altered transcription due to butyrate-induced changes in regulator gene expression, including transcription factor activity. It was also unclear to what extent the butyrate-induced changes in miRNA expression mediated the anti-proliferative and pro-apoptotic effects of butyrate treatment. These issues will be addressed in later Chapters.

Chapter 5. HDI treatment reduces miR-17-92 cluster expression and increases expression of target genes

5.1 Introduction

Butyrate is a known HDI, which is one mechanism that allows the diet-derived substance to alter gene and miRNA expression in colorectal cells. Other HDIs, such as trichostatin A (TSA) and suberoylanilide hydroxamic acid (SAHA), have also been shown to similarly alter gene expression to reduce cell growth or induce apoptosis. The cellular pathways influenced by HDIs, such as cell cycle control and apoptosis, are also regulated by miRNAs. In Chapter 4, butyrate was shown to alter expression of multiple miRNAs, including those in the miR-17-92 cluster. The butyrate-induced decrease in miR-17-92 expression may mediate the anti-proliferative and pro-apoptotic effects of butyrate treatment. This Chapter explores this hypothesis, and examines the effect of different HDIs on miR-17-92 miRNA levels.

5.1.1 Histone deacetylase inhibitors

5.1.1.1 Classes of HDACs and HDAC inhibitors

Histones are an important component of chromatin structure, with the highly conserved core histone proteins H3, H4, H2A, and H2B acting with linker histones H1/H5 to package eukaryotic DNA into repeating units that are folded into higher-order chromatin (Strahl & Allis 2000). Various combinations of post-translational histone modifications allow regulation of gene expression, with such modifications including acetylation, methylation, phosphorylation, ubiquitination, and ADP-ribosylation (Strahl & Allis 2000, Kouzarides 2007). Such modifications mainly occur along the N-terminal tails, and to a lesser extent throughout other regions of the histone protein (Turner 1998, Strahl & Allis 2000). Enzymes that effect these modifications include, among others, HATs and HDACs, which are responsible for increasing and decreasing acetylation, respectively. Increased histone acetylation generally promotes a more relaxed chromatin structure, allowing transcriptional activation, while decreased acetylation can lead to transcriptional repression (Turner 1998, Strahl & Allis 2000).

HDACs catalyse the deacetylation of α-acetyl lysine that resides within the N-terminal tail of core histones, which can lead to decreased transcription (Thorne et al 1990, Strahl

& Allis 2000). Eighteen HDACs have been characterised in the human genome, and these are grouped into class I, class II, class III and class IV based on their sequence homology, their subcellular localization and their enzymatic activities (Thiagalingam et al 2003). Eleven classical HDACs have been described (class I, II and IV) (Table 5.1), as well as seven sirtuins (class III), with the classical HDACs and sirtuins differing in their catalytic mechanisms. Classical HDACs are Zn^{2+}-dependent enzymes, while sirtuins require NAD+ as a cofactor (de Ruijter et al 2003). Besides targeting histones, HDACs can also target non-histone proteins, including those that have regulatory roles in cell proliferation, migration, and apoptosis (Table 5.1). HDACs can either decrease or increase the function or stability of these non-histone proteins (Glozak et al 2005). Among the multiple non-histone proteins targeted by HDACs are DNA binding transcription factors such as p53 and the E2F family (Magnaghi-Jaulin et al 1998, Luo et al 2000, Robertson et al 2000, Ferreira et al 2001, Ito et al 2002). In addition to mediating transcriptional repression through altered histone acetylation and chromatin structure, by targeting non-histone proteins HDACs can also play other regulatory roles, including transcription-independent regulation. HDACs can often form subunits of multi-protein nuclear complexes that are important for gene repression (Huang et al 1999, Zhang et al 1999, Witt et al 2009).

Changes in normal patterns of histone modifications have been reported in various cancers (Ono et al 2002, Fraga et al 2005b, Enroth et al 2011), as have alterations in expression of different HDACs. In CRCs, over expression of HDAC1, HDAC2, and HDAC3 have been observed (Zhu et al 2004, Wilson et al 2006). Wilson et al (2006) found that HDAC3 and other class I HDAC proteins are up-regulated in colon tumours, may play a physiological role in maintaining cell proliferation and inhibiting maturation, and are involved in the repression of the cell cycle mediator *CDKN1A*. Zhu et al (2004) found increased HDAC2 expression in the majority of human colon cancers sampled compared with normal matched tissue, and also identified HDAC2 to play a role in inhibiting apoptosis in colon cancer cells. In contrast to the HDAC over-expression observed by Wilson et al (2006) and Zhu et al (2004), Ropero et al (2006) observed mutations in HDAC2 and loss of expression in a subset of MSI CRC cell lines and tumour samples. In addition to altered HDAC expression, in certain cancers the interaction between HDACs and oncogenic DNA-binding fusion proteins leads to aberrant recruitment of HDACs to promoters (Bolden et al 2006). These cancer-related changes in HDAC activity make them targets for anti-cancer therapy (Bolden et al 2006).

Inhibitors of HDACs include both natural and synthetic compounds, and can be divided into four chemical classes consisting of the SCFAs (aliphatic acids), hydroxamic acids, cyclic peptides, and benzamides (Table 5.2). The term 'HDAC inhibitor' is generally reserved for compounds that target the classical class I, II, and IV HDACs (Witt et al 2009), with HDIs acting by binding to the HDAC active site and blocking substrate-Zn chelation at the base of the site (Finnin et al 1999). Certain HDIs may preferentially inhibit certain HDACs (Xu et al 2007). One of the main anti-cancer effects of HDIs is cell cycle arrest (at G_1 or G_2 – M) (Mariadason et al 2000), which is associated with induction of cell cycle inhibitors such as *CDKN1A* (Archer et al 1998). HDIs can induce cell differentiation or cell death through various apoptotic pathways (Xu et al 2007), and can also inhibit angiogenesis (Deroanne et al 2002, Pellizzaro et al 2002, Gururaj et al 2003, Kim et al 2007b, Prasanna Kumar et al 2008) and metastasis (Liu et al 2003, Joseph et al 2004, Li et al 2004), and increase chemotherapy sensitivity (Noro et al 2010, Iwahashi et al 2011, Kretzner et al 2011).

While HDACs are distributed ubiquitously around chromatin, HDIs only alter expression of a select proportion of genes, usually between approximately 2% and 25% in *in vitro* experiments (Van Lint et al 1996, Gray et al 2004, Daly & Shirazi-Beechey 2006, Alvaro et al 2008). This selective effect on gene transcription may be due to altered acetylation of particular histone complexes and other proteins regulating gene expression (Dokmanovic et al 2007). Studies in CRC cells, as in other cancers, have shown that HDIs activate some genes but repress others, with at least as many genes down-regulated as up-regulated (Mariadason et al 2000, Daly & Shirazi-Beechey 2006). This complexity surrounding histone modifications and subsequent transcriptional activation or repression is discussed further in Chapter 7.

5.1.1.2 Butyrate, TSA, and SAHA

As summarised in Chapter 4, microarray studies in CRC cells have detected multiple genes modulated by the natural HDI butyrate, including genes associated with cell cycle regulation and arrest, differentiation and apoptosis (Mariadason et al 2000, Iacomino et al 2001, Daly & Shirazi-Beechey 2006). While butyrate's ability to epigenetically regulate gene expression is often attributed to its induction of histone hyperacetylation, it can also induce acetylation of non-histone proteins, alteration of DNA methylation, and selective regulation of histone methylation and phosphorylation (Boffa et al 1981, Boffa et al 1994, Daly & Shirazi-Beechey 2006). Use of a more specific and potent inhibitor of HDAC was deemed necessary to characterise the specific effects of HDIs, which led to

the development of TSA (Yoshida et al 1990). Originally reported as a fungistatic antibiotic by Tsuji et al (1976), TSA was then characterised as a HDI (Yoshida et al 1987, Yoshida & Beppu 1988, Yoshida et al 1990). At low (nanomolar) concentrations, TSA was shown to cause induction of Friend leukaemia cell differentiation, inhibition of the cell cycle of normal rat fibroblasts in both the G_1 and G_2 phases, accumulation of highly acetylated histones *in vivo*, and strong inhibition of HDAC activity *in vitro* (Yoshida et al 1987, Yoshida & Beppu 1988, Yoshida et al 1990). TSA was deemed to be an important tool in the analysis of the role of histone acetylation in regulation of chromatin structure, differentiation, and the cell cycle (Yoshida et al 1990).

Mariadason et al (2000) were among the first to comprehensively compare the response of colonic epithelial cells to butyrate and the selective HDAC inhibitor TSA, both of which induce cell cycle arrest and an apoptotic response, but are structurally unrelated. Microarray analysis was used to determine gene expression changes in SW620 human colorectal adenocarcinoma cell line, treated with 5 mM butyrate or 1 μM TSA for 0.5, 2, 12, 16, 24, and 48 h. Extensive alterations in gene expression were detected in response to butyrate. More limited changes were induced by TSA, although the profiles of gene expression induced by TSA and butyrate were similar. This was attributed to their shared mechanism of action as HDIs (Mariadason et al 2000). Della Ragione et al (2001) also compared the genes modulated by butyrate to those altered by TSA, in HT29 colorectal adenocarcinoma cells. Cells were treated with 2 mM butyrate or 0.3 μM TSA for 5 h, in the presence of cycloheximide to inhibit *de novo* protein synthesis and observe transcriptional effects only. Della Ragione et al (2001) identified a number of genes induced by both butyrate and TSA, including cell cycle regulators such as *CDKN1A*, transcription factors, chemokine receptors, transduction modulators, stress responses, detoxification genes, and adhesion molecules (Della Ragione et al 2001). In similar studies, Siavoshian et al (2000) and Chen et al (2004) also compared the molecular mechanisms of butyrate and TSA action on HT29 cells, and highlighted the ability of butyrate and TSA to stimulate expression of *CDKN1A*, at both the mRNA and protein level. Wu et al (2001) found early increases in *CDKN1A* mRNA levels with 5 mM butyrate or 0.3 μM TSA.

While there is overlap between the genes modulated by butyrate and TSA, there are also differences in the mechanisms of action of the two agents. Mariadason et al (2000) found that the kinetics of alteration of histone acetylation differed between the two agents. Butyrate induced a gradual increase in histone H4 acetylation that peaked at 16 h, while TSA produced a rapid and short-lived increase in H4 acetylation that peaked at

2 h (Mariadason et al 2000). Similarly, Siavoshian et al (2000) also found that exposure to butyrate or TSA induced histone H4 hyperacetylation, with histone H4 remaining hyperacetylated at 15 and 24 h with butyrate treatment, but returning to control levels in the presence of TSA. Siavoshian et al (2000) and Iacomino et al (2006) showed that butyrate treatment blocked cells mainly in the G_1 phase of the cell cycle, whereas TSA treatment blocked cells in both G_1 and G_2 phases. While both substances have HDI activity, butyrate and TSA appear to induce slightly different cell responses.

Aside from TSA, which was the first natural hydroxamic acid identified with HDI properties, substantial research has been conducted on a structurally similar HDI, SAHA (Vorinostat). SAHA is also a hydroxamic acid, and was the first of two HDIs to be approved by the US Food and Drug Administration (FDA) for the treatment of cutaneous T-cell lymphoma (Duvic et al 2007, Olsen et al 2007). This approval in 2006 followed the completion of a pivotal phase II single-arm open-label trial that enrolled 74 patients with cutaneous T-cell lymphoma who had failed two systemic therapies (Olsen et al 2007). Another phase II trial in 33 patients with cutaneous T-cell lymphoma also supported the approval (Duvic et al 2007). In both studies, the response rate (measured using the Severity-Weighted Assessment Tool or the Physician's Global Assessment Scale) to treatment with oral Vorinostat was approximately 30% (Duvic et al 2007, Olsen et al 2007), which was comparable to response rates obtained with other FDA-approved cutaneous T-cell lymphoma therapies (Mann et al 2007). The most common adverse events with the treatment were diarrhoea, fatigue, nausea, and anorexia (Duvic et al 2007, Olsen et al 2007). The other HDI to be FDA approved was Romidepsin (FK-228), also for cutaneous T-cell lymphoma (Piekarz et al 2009, Whittaker et al 2010). SAHA is also under investigation for use in other cancer types, with both phase I and phase II trials conducted in patients with solid tumours including CRC. Several small early phase II trials of SAHA in tumours including CRC were mainly concerned with safety and establishing appropriate dosage, and were unable to establish the efficacy of the treatment (Vansteenkiste et al 2008, Wilson et al 2010b). Other HDIs have also been examined mostly in hematopoietic malignancies, but have been used in mainly phase I trials in solid tumours including CRC (Table 5.2).

An *in vitro* microarray profiling study by LaBonte et al (2009) examined the response of CRC cells treated with the clinical hydroxamic acid HDI SAHA, and another hydroxamic acid explored in the clinical setting, LBH589. Using HCT116 and HT29 CRC cell lines, LaBonte et al (2009) found that treatment with 2 μM SAHA induced histone acetylation and cell cycle arrest, with increased H4 acetylation at 2 h (in HCT116

cells) or 4 h (in HT29 cells) post-treatment, and H3 acetylation as early as 0.5 h post-treatment in both cell lines. SAHA induced mainly G_2/M arrest in HCT116 cells, and mainly G_1 arrest in HT29 cells. In the HCT116 cells, 3566 genes (7% of total gene set analysed) were modulated by either LBH589 or SAHA, with 3100 differentially expressed with SAHA. In the HT29 cells, 2645 genes (5% of total gene set analysed) were modulated by either LBH589 or SAHA, with 2448 differentially expressed with SAHA. An IPA analysis identified five networks to be altered by the HDIs, based on these networks possessing significantly more of the identified differentially expressed genes than would be expected by random chance. These networks were cell cycle, DNA replication, recombination and repair, apoptosis, gene expression, and cell growth and proliferation (LaBonte et al 2009).

Other studies have also examined the effect of SAHA treatment on various CRC cell lines *in vitro*. Portanova et al (2008) showed that in HT29 cells, SAHA caused apoptosis, and induced an accumulation of cells in the G_2/M phase of the cell cycle at 4 – 8 h, and a progressive increase in the percentage of cells confined to the sub-G_0/G_1 phase with longer treatment. Another study in 320 HSR colon cancer cells also found SAHA to induce apoptosis and sub-G_1 arrest, and reduce anti-apoptosis proteins (Sun et al 2010). Wilson et al (2010a) examined the effect of HDIs in multiple CRC cell lines including HCT116 and HT29, and within a particular cell line the apoptotic response was comparable with 2.5 μM SAHA, 1 μM TSA, or 5 mM butyrate. Bressan et al (2010) found that chronic exposure to SAHA induced a less aggressive phenotype in human colon carcinoma HCT116 cells, while Lobjois et al (2009) used multicellular tumour spheroids of HCT116 cells to mimic an *in vivo* tumour situation and show that SAHA effects such as cell cycle arrest and apoptosis are dependent on the position of the cells within the spheroid. Combination treatment with SAHA and other chemotherapeutic agents has also been investigated in CRC cell lines, with SAHA shown to act in synergy with other agents, including 5-fluorouracil, Bortezomib, and Selumetinib, to decrease proliferation and increase apoptosis (Fazzone et al 2009, Pitts et al 2009, Morelli et al 2012). Fazzone et al (2009) also showed that SAHA may assist in overcoming resistance to 5-fluorouracil by repressing thymidylate synthase (TS), which when over-expressed promotes 5-fluorouracil resistance.

CDKN1A (p21) is one of the most commonly reported genes to be induced in cells treated with butyrate, TSA, SAHA and other HDIs, and is important in mediating the cell cycle arrest observed in response to HDI treatment (Janson et al 1997, Nakano et al 1997, Siavoshian et al 1997, Archer et al 1998, Siavoshian et al 2000, Kobayashi et al

2003, Orchel et al 2003, Daly & Shirazi-Beechey 2006, Wilson et al 2006). Altered *CDKN1A* expression can be observed within a few hours of HDI treatment (Archer et al 1998). Current literature presents conflicting evidence, with some studies showing the HDI-induced increase in *CDKN1A* expression to be p53 independent (Archer et al 1998, Kobayashi et al 2003), and others showing it to be influenced by p53 (Zhao et al 2006, Habold et al 2008). The increase in *CDKN1A* expression may be associated with modifications in acetylation and methylation patterns in histones H3 and H4 associated with the *CDKN1A* promoter region. In a multiple myeloma cell line, Gui et al (2004) found HDI treatment to induce a specific increase in acetylation of histone H3 lysine 9 and 14, acetylation of histone H4 lysine 5, 8, 12, and methylation of histone H3 lysine 4. This was associated with more open chromatin, increased DNase I sensitivity and restriction enzyme accessibility in the *CDKN1A* promoter (Gui et al 2004). Increased H3 and H4 acetylation at the *CDKN1A* promoter region has also been demonstrated in CRC cells treated with HDIs (Chen et al 2004, Fang et al 2004). HDIs can also induce alterations in components of *CDKN1A*-associated proteins, leading to activation of *CDKN1A* expression. Alterations included a decrease in HDAC1 and MYC bound to the *CDKN1A* promoter and an increase in RNA polymerase II associated with the promoter bound proteins (Gui et al 2004). Changes in other promoter-associated proteins such as SP1 and SP3 may also lead to *CDKN1A* induction (Xiao et al 2000, Davie 2003, Hammill et al 2005). CDKN1A is known to induce G_1 cell cycle arrest, and to affect downstream regulators such as cyclin B (Archer et al 2005). Multiple mechanisms appear to regulate CDKN1A levels, and it has been suggested that direct modification of histone acetylation alone is insufficient to induce *CDKN1A* expression by butyrate (Kobayashi et al 2003, Kobayashi et al 2004). Changes in specific miRNA levels may also play a regulatory role.

Table 5.1: Classical histone deacetylases (HDACs)

Class	Name	Location	Selected protein targets/ substrates
Class I	HDAC1	N	p53 (Luo et al 2000, Ito et al 2002)
			MYOD (Mal et al 2001)
			E2F1 (Magnaghi-Jaulin et al 1998, Robertson et al 2000, Ferreira et al 2001)
			STAT3 (Yuan et al 2005, Ray et al 2008)
			Androgen receptor (Gaughan et al 2005)
			SHP (Gobinet et al 2005)
			YY-1 (Yang et al 1996, Yao et al 2001)
			GCMa (Chuang et al 2006)
			SMAD7 (Simonsson et al 2005)
	HDAC2	N	BCL-6 (Bereshchenko et al 2002)
			STAT3 (Yuan et al 2005, Pang et al 2011)
			Glucocorticoid receptor (Ito et al 2006)
			YY-1 (Yang et al 1996, Yao et al 2001)
	HDAC3	N	GATA-1 (Watamoto et al 2003)
			GATA-2 (Ozawa et al 2001)
			GCMa (Chuang et al 2006)
			RelA (Chen et al 2001)
			MEF2D (Gregoire et al 2007)
			YY-1 (Yang et al 1996, Yao et al 2001, Sankar et al 2008)
			SHP (Gobinet et al 2005)
			SMAD7 (Simonsson et al 2005)
	HDAC8	N	-
Class IIa	HDAC4	N/C	GCMa (Chuang et al 2006)
			GATA-1 (Watamoto et al 2003)
			HP-1 (Zhang et al 2002)
	HDAC5	N/C	SMAD7 (Simonsson et al 2005)
			HP-1 (Zhang et al 2002)
			GCMa (Chuang et al 2006)
			GATA-1 (Watamoto et al 2003)
	HDAC7	N/C	PLAG1 and PLAGL2 (Zheng & Yang 2005)
	HDAC9	N/C	-
Class IIb	HDAC6	C	α-Tubulin (Hubbert et al 2002)
			HSP90 (Bali et al 2005)
			SHP (Gobinet et al 2005)
			SMAD7 (Simonsson et al 2005)
			β-catenin (Li et al 2008)
	HDAC10	C	HSP90 (Park et al 2008)
Class IV	HDAC11	N/C	-

C: cytoplasm; N: nucleus; -: none identified.

Table 5.2: Known histone deacetylase (HDAC) inhibitors

Chemical class	Selected compounds	HDAC target	Potency	Clinical trials in solid tumours, including CRC
Short-chain fatty acids/ aliphatic acids	Sodium butyrate	Class I and IIa	mM	-
	Phenylbutyrate	Class I and IIa	mM	Phase I: (Gilbert et al 2001, Camacho et al 2007, Sung & Waxman 2007, Lin et al 2009)
	Valproate	Class I and IIa	mM	Phase I: (Atmaca et al 2007, Munster et al 2007); Phase I-II: (Munster et al 2009a)
	AN-9 (Pivanex)	-	µM	Phase I: (Patnaik et al 2002)
Hydroxamic acids	TSA	Class I and II	nM	-
	SAHA (Vorinostat)	Class I and II	µM	Phase I: (Fakih et al 2009, Munster et al 2009b, Fakih et al 2010, Ramalingam et al 2010, Ree et al 2010, Dickson et al 2011, Stathis et al 2011); Phase I-II: Wilson et al (2010b); Early Phase II: Vansteenkiste et al (2008)
	LAQ-824 (Dacinostat)	Class I and II	nM	Phase I: (de Bono et al 2008)
	PDX-101 (Belinostat)	Class I and II	µM	Phase I: (Steele et al 2008, Lassen et al 2010)
	LBH-589 (Panobinostat)	Class I and II	nM	Phase I: (Jones et al 2011, Morita et al 2011, Fukutomi et al 2012)
	CBHA	-	µM	-
	ITF2357	Class I and II	nM	-
	PCI-24781	Class I and II	NR	-
Cyclic peptides	FK-228 (Romidepsin)	Class I	nM	Phase II: (Whitehead et al 2009)
Benzamides	MS-275 (Entinostat)	HDAC1, HDAC2, HDAC3	µM	Phase I: (Gore et al 2008, Pili et al 2012)
	MGCD-0103 (Mocetinostat)	Class I	µM	Phase I: (Siu et al 2008)

NR: not reported; -: none identified.

5.1.2 The miR-17-92 cluster

In addition to its effects on gene expression, the HDI butyrate was shown in Chapter 4 to decrease expression of multiple miRNAs, including those in the polycistronic miR-17-92 cluster and its paralog cluster, miR-106a-363. The human miR-17-92 host gene is located at 13q31.3, a chromosomal region amplified in several hematopoietic malignancies and solid tumours (Ota et al 2004). Over-expression of miR-17-92 has been observed in lymphomas and multiple solid tumours including colon, breast, lung, pancreas, prostate, and stomach tumours (Ota et al 2004, Hayashita et al 2005, He et al 2005a, Cummins et al 2006, Volinia et al 2006, Petrocca et al 2008, Chen et al 2009, Diosdado et al 2009). He et al (2005a) were the first to show that besides the over-expression of miRNAs from this cluster in tumours and tumour cell lines, miR-17-92 could modulate tumour formation and act as an oncogene *in vivo*. The miR-17-92 cluster was therefore designated oncomir-1 due to its oncogenic properties (He et al 2005a).

The host gene of miR-17-92 is known as C13 open reading frame 25 (*C13ORF25*), or more recently as *MIR17HG* (Figure 5.1), with the miR-17-92 cluster located in the third intron of the ~ 7 kb primary transcript (Ota et al 2004). The transcript of the miR-17-92 cluster contains six stem-loop hairpins that are processed to yield six mature miRNAs: miR-17, miR-18a, miR-19a, miR-20a, miR-19b-1, and miR-92a-1 (Tanzer & Stadler 2004). Complementary star form miRNAs (*) are also derived from the miR-17-92 pre-miRNAs. As shown in Figure 5.1, the six mature miR-17-92 miRNAs can be categorised into four miRNA families based on their seed sequences, which are the regions considered most important for target selection: the miR-17 family (miR-17, miR-20a), the miR-18 family (miR-18a), the miR-19 family (miR-19a, miR-19b-1), and the miR-92 family (miR-92a-1) (Mendell 2008). Gene duplication events have also resulted in two miR-17-92 paralog clusters in mammals. The host gene of one paralog cluster, miR-106b-25, is *MCM7* on Chromosome 7, and the primary transcript of another paralogous cluster, miR-106a-363 on Chromosome X, has not been well characterised (Tanzer & Stadler 2004, Poliseno et al 2010). Each paralog contains homologous miRNAs to a subset of miR-17-92 components (Figure 5.1).

The miR-17-92 cluster host gene has several known regulators (Figure 5.2). He et al (2005a) provided some of the first evidence of the oncogenic activity of the miR-17-92 cluster, and also demonstrated the interaction between miR-17-92 and C-MYC. Over-expression of the miR-17–92 cluster accelerated c-Myc-induced lymphomagenesis in mice, and tumours resulting from combined c-Myc and miR-17-92 expression also

showed increased tumour invasion and reduced apoptosis (He et al 2005a). A study by Tagawa et al (2007) also indicated that miR-17-92 is stably up-regulated in the presence of constitutive expression of *MYC*, and that the deregulation of the miR-17-92 cluster and *MYC* synergistically contributes to aggressive cancer development by repressing tumour suppressor genes (Tagawa et al 2007). O'Donnell et al (2005) determined that miR-17-92 host gene transcription is directly activated by C-MYC binding, while Schulte et al (2008) showed that N-MYC also activates miR-17-92 host gene transcription. In addition to regulation by C-MYC, the E2F family of transcription factors also regulate miR-17-92, with E2F1 and E2F3 in particular known to bind to the miR-17-92 promoter region and activate transcription (Sylvestre et al 2007, Woods et al 2007, Pickering et al 2009). E2F family members are essential for cell cycle progression, can drive progression from G_1 to S phase, and can also induce apoptosis at high levels in response to DNA damage (Lin et al 2001). Cycling cells are likely to have elevated miR-17-92 due to increased E2F activity during S phase (Olive et al 2010). There also exists a potential homeostatic feedback loop between E2F factors and miR-17-92 cluster miRNAs; miR-20 has been shown to target *E2F1*, and miR-17 has been shown to target *E2F3* (O'Donnell et al 2005). Another feedback loop has also been suggested where C-MYC and E2F members can transcriptionally activate each other (O'Donnell et al 2005). It has been postulated that the feedback between E2F factors and miR-17-92 acts to dampen the apoptotic potential of E2F1, and assists the miR-17-92 cluster in exerting its anti-apoptotic effect (O'Donnell et al 2005, Olive et al 2010). Figure 5.2 displays the key regulators of the miR-17-92 cluster, and also selected key target genes.

The miR-17-92 cluster of miRNAs has been shown to target genes that are important in cell cycle control (Figure 5.2). Studies in mainly lymphoma models have shown that the cell cycle inhibitor *CDKN1A* (p21) and the pro-apoptotic genes *PTEN* and *BCL2L11* (Bim) are regulated by miR-17-92 (Ventura et al 2008, Inomata et al 2009, Mu et al 2009, Olive et al 2009, Wong et al 2010). The anti-apoptotic effect of miR-17-92 could be mediated by the targeting of *PTEN* and *BCL2L11* (Koralov et al 2008, Ventura et al 2008, Xiao et al 2008), while the proliferative effect of miR-17-92 could be partially attributed to its ability to repress *CDKN1A* translation (Cloonan et al 2008, Fontana et al 2008). In studies in CRC cells, HDIs including butyrate, TSA and SAHA also regulated *CDKN1A* and *PTEN* (Siavoshian et al 2000, Chen et al 2004, Daly & Shirazi-Beechey 2006). It could be hypothesised that the butyrate-induced decrease in miR-17-92 cluster expression shown in Chapter 4 may mediate the anti-proliferative and pro-

apoptotic effects of butyrate treatment. Other HDIs may have similar effects on miR-17-92 cluster genes and their targets, and are investigated in this Chapter.

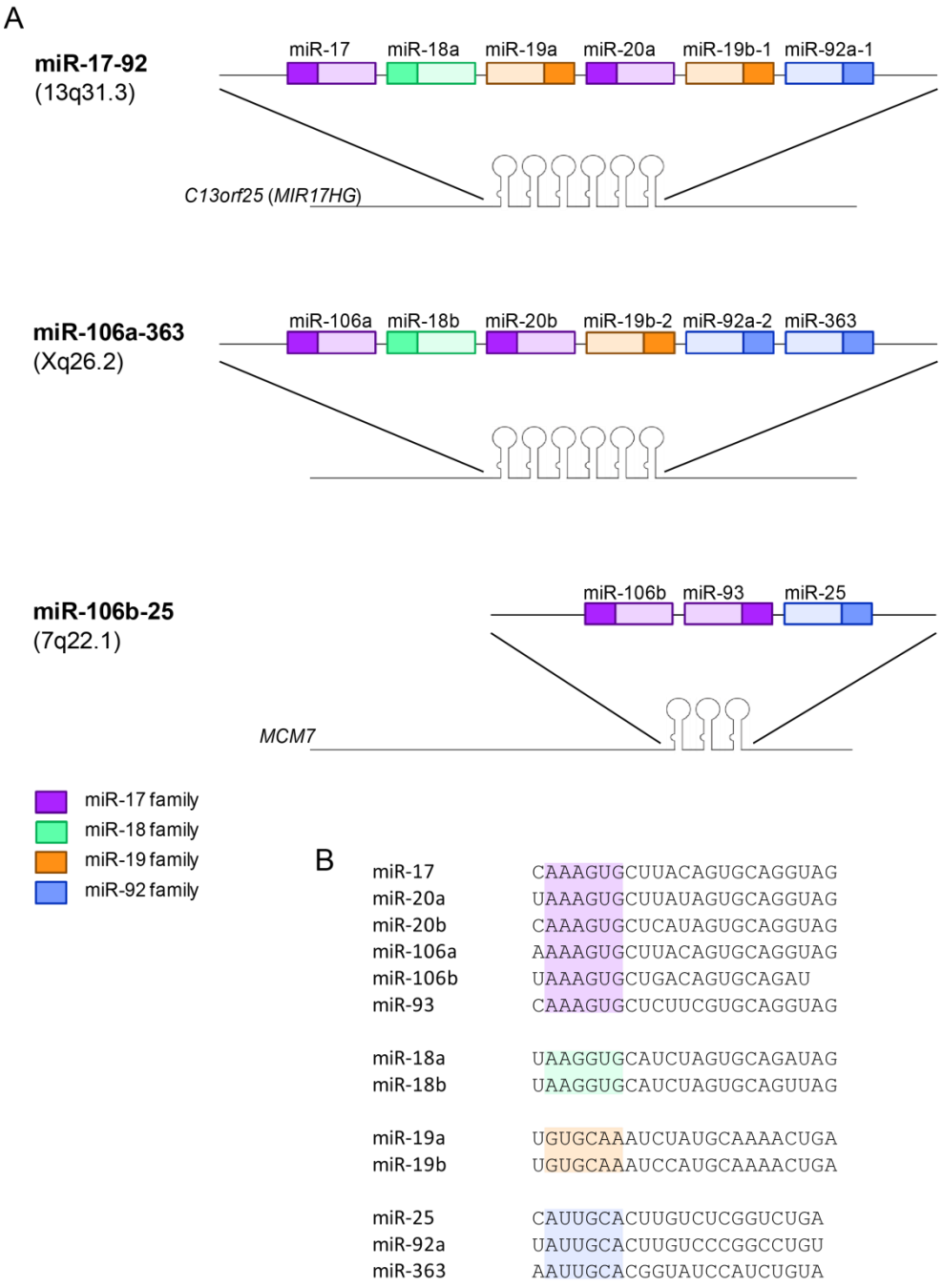

Figure 5.1: Structure of the human miR-17-92 cluster and its paralogs, miR-106a-363 and miR-106b-25.

(A) Primary transcript organisation of the human miR-17-92 cluster and its paralogs, miR-106a-363 and miR-106b-25. The host gene of miR-17-92 is *MIR17HG* (*C13ORF25*) on Chromosome 13, and the host gene of miR-106b-25 is *MCM7* on Chromosome 7. The miR-106a-363 transcript on Chromosome X has not been characterised. miRNAs from the clusters can be categorised into separate miRNA families based on their seed sequences (the miR-17 family, miR-18 family, miR-19 family, and miR-92 family). (B) Mature miRNA sequences of the miR-17-92 cluster and its paralogs, with the seed sequences shaded.

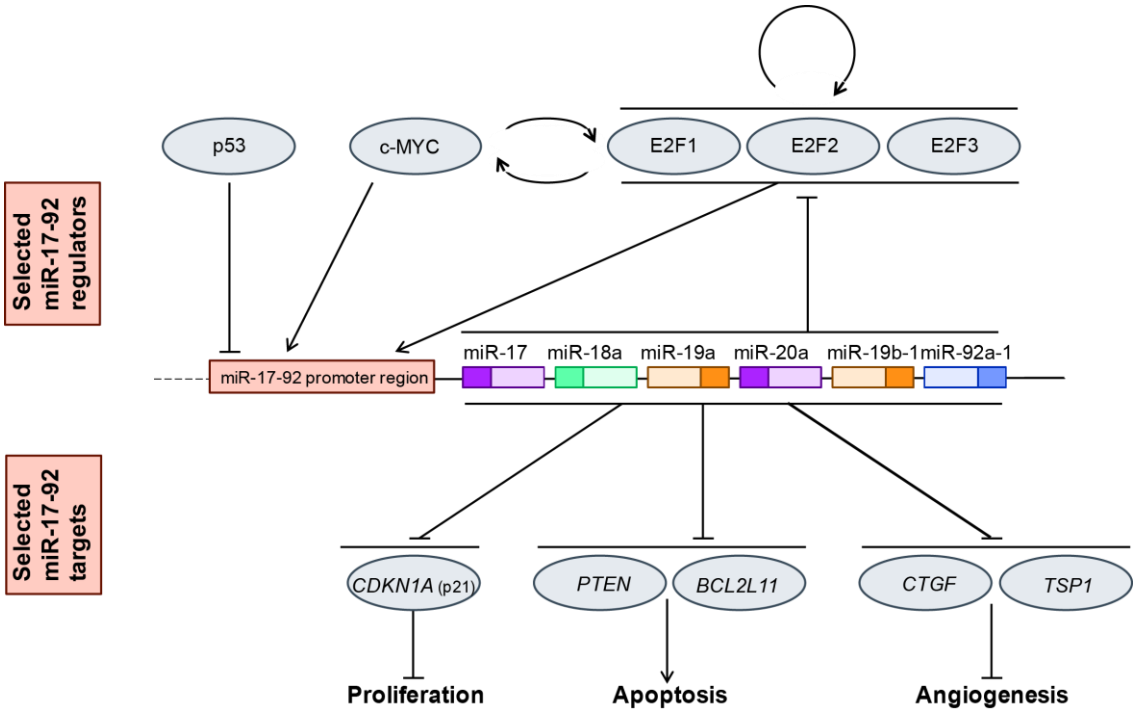

Figure 5.2: Transcriptional regulation and target mRNAs of the miR-17-92 cluster

The miR-17-92 cluster is a transcriptional target of C-MYC and the E2F family of transcription factors. miRNAs in the miR-17-92 cluster have multiple target genes. Well-validated targets include the cell cycle inhibitor *CDKN1A* (p21) (target of miRs 17 and 20a) and the pro-apoptotic genes *PTEN* (target of miRs 17, 19a, 19b, and 20a) and *BCL2L11* (Bim) (target of miRs 17, 18a, 19a, 20a, 19b and 92a).

5.2 Aims

The aims of this Chapter were to compare the effect of butyrate and other HDIs on miR-17-92 expression in CRC cells, and to confirm the effect of HDIs on miR-17-92 target gene expression.

5.3 Methods overview

Experiments were conducted according to the general methods outlined in Chapter 3, with all experimental groups conducted in triplicate.

HT29 and HCT116 cell lines were used to determine the effects of different HDIs on cell growth, miRNA expression, and expression of miR-17-92 target genes. Cells were treated with increasing doses of butyrate (0, 1, 5, 10, or 25 mM) or SAHA (0, 1, 2 or 3 μM) for 48 h, and proliferation was measured in real-time using the xCELLigence RTCA DP instrument. In separate experiments, cells were treated for 48 h with 1, 5 or 10 mM butyrate, 2 μM SAHA or 0.3, 0.5, or 0.7 μM TSA, or maintained in control medium, and total RNA was extracted from treated cells using the TRIzol method. Relative quantitation real-time RT-PCR analysis was performed on miR-17-92 miRNAs. To confirm the effect of HDIs on miR-17-92 target genes, relative quantitation real-time RT-PCR analysis was used to determine mRNA levels of target genes in 5 mM butyrate-treated cells and cells in control medium. Western blots were used to determine protein levels of miR-17-92 target genes in 5 mM butyrate-treated cells and cells in control medium. The miR-17-92 target genes examined were *CDKN1A*, *PTEN*, and *BCL2L11*. mRNA levels of miR-17-92 regulators, including *C-MYC* and *E2F1*, were also examined in 5 mM butyrate-treated cells and cells in control medium, using relative quantitation real-time RT-PCR analysis. Real-time RT-PCR analysis was also used to compare levels of miR-17-92 cluster miRNAs and target gene transcripts in the butyrate-treated and control medium CRC cell lines, with levels in normal human rectal mucosa. This mucosa was previously utilised by Michael et al (2003).

5.4 Results

5.4.1 Proliferation of colorectal cancer cell lines with HDI treatment

As shown in Chapter 4, treatment of HT29 and HCT116 CRC cells with increasing concentrations of butyrate led to decreased proliferation over a 48 h period, when measured with real-time cell growth analysis. In this Chapter, the anti-proliferative effect

of butyrate was compared to that of a structurally unrelated HDI, SAHA (Figure 5.3A). By 48 h, treatment with 5 mM butyrate significantly reduced proliferation in HT29 cells compared with the untreated control cells ($P = 0.0005$), and in HCT116 cells compared with the untreated control cells ($P < 0.0001$). The HCT116 cells were more susceptible to the anti-proliferative effect of 5 mM butyrate. At 48 h, SAHA treatment at 2 μM had an equivalent effect on proliferation in HT29 cells as 5 mM butyrate ($P = 0.007$ compared with untreated controls), although the growth kinetics appeared to differ between treatments (Figure 5.3B). Treatment of HCT116 cells with 2 μM SAHA also reduced proliferation compared with untreated controls ($P = 0.002$).

5.4.2 Real-time RT-PCR of miR-17-92 changes in colorectal cancer cells treated with butyrate and other HDIs

HT29 and HCT116 CRC cell lines were treated for 48 h with 1, 5 or 10 mM butyrate, 2 μM SAHA or 0.3, 0.5, or 0.7 μM TSA, or maintained in control medium, to compare the effect of these HDIs on expression of miR-17-92 cluster miRNAs and the miR-106a-363 paralog miRNAs. Following 5 mM butyrate treatment, all of the miR-17-92 cluster miRNAs exhibited significant differential expression in the microarray analysis (Bayesian log odds value > 0) in the previous Chapter, with the exception of miR-19a and miR-92; however, these miRNA also showed potential down-regulation and were examined further. As shown in Chapter 4, real-time RT-PCR analysis showed all of the selected miR-17-92 and miR-106a-363 cluster miRNAs to be significantly down-regulated by 5 mM butyrate, in both HT29 and HCT116 cells ($P < 0.05$). In this Chapter, the effects of various butyrate doses were compared to the effects of HDIs from a different class, the hydroxamic acids TSA and SAHA, on miR-17-92 and miR-106a-363 cluster miRNA levels. Expression was dose-dependent, with increasing butyrate concentration generally leading to decreasing levels of miR-17-92 cluster members in both the HT29 and HCT116 cells (Figure 5.4 and Figure 5.5). Similar results were achieved with SAHA and TSA, with all of the miR-17-92 cluster miRNAs significantly down-regulated by 2 μM SAHA or 0.5 μM TSA, in both HT29 and HCT116 cells ($P < 0.05$) (Figure 5.4 and Figure 5.5). As with butyrate, an increasing TSA dose led to decreasing levels of miR-17-92 miRNAs. With 5 mM butyrate, 2 μM SAHA or 0.5 μM TSA treatment, miRNAs from the miR-106a-363 cluster were reduced to a similar extent to miRNAs from the miR-17-92 cluster (Table 5.3). The fold-decrease in miR-17-92 and miR-106a-363 cluster miRNAs levels in response to HDI treatment was greater in the HCT116 cell line compared with the HT29 cell line (Table 5.3).

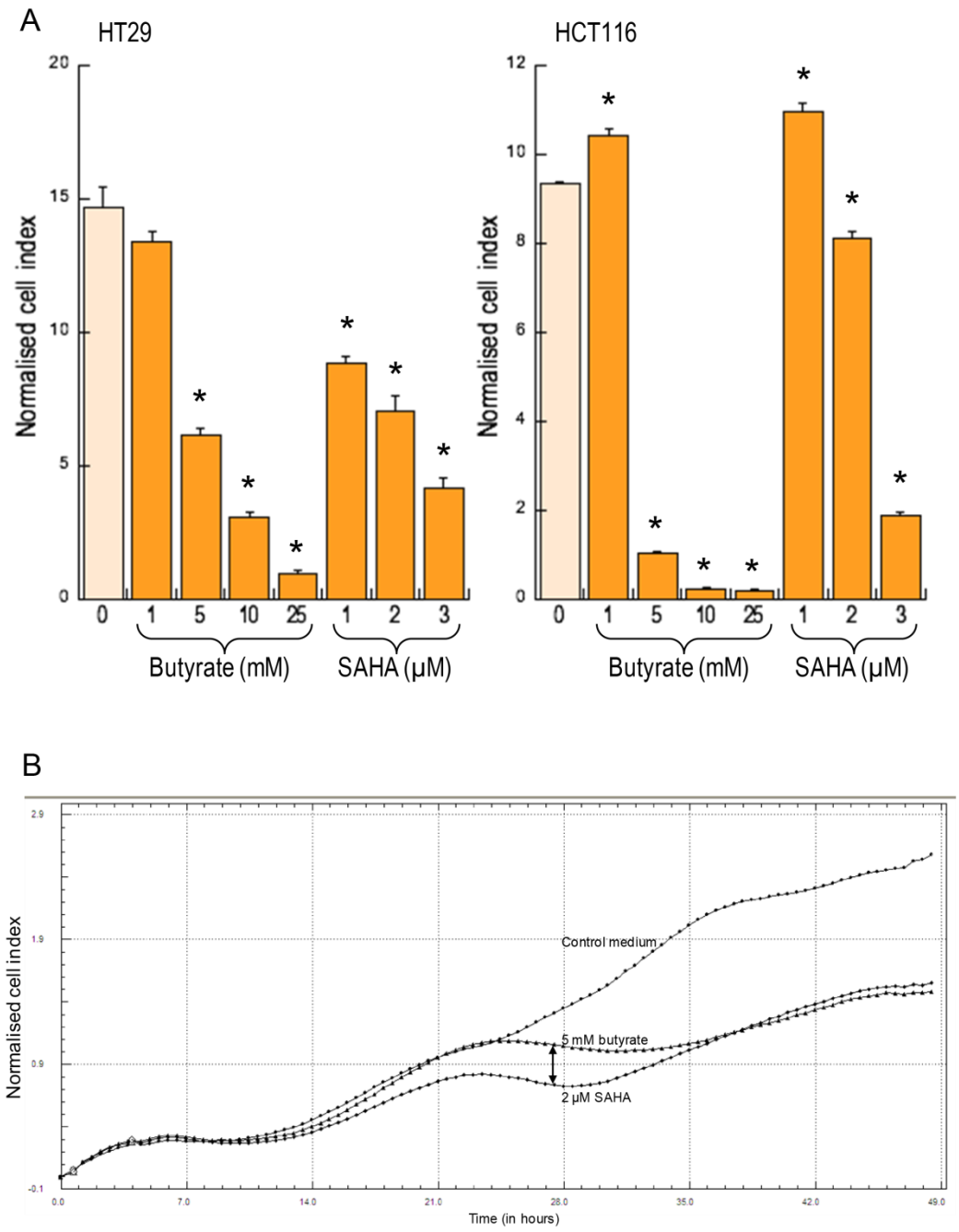

Figure 5.3: Proliferation of HT29 and HCT116 cells after 48 h of butyrate or SAHA treatment.

(A) Cell index measurements at 48 h using the xCELLigence RTCA DP instrument in HT29 cells or HCT116 cells treated with increasing doses of butyrate or SAHA, compared with cells in control medium (0) (* $P < 0.05$). (B) xCELLigence real-time proliferation graph demonstrating differences in growth kinetics between 5 mM butyrate and 2 μM SAHA treatments in HT29 cells. The mean ± SEM of three cell culture replicates is shown.

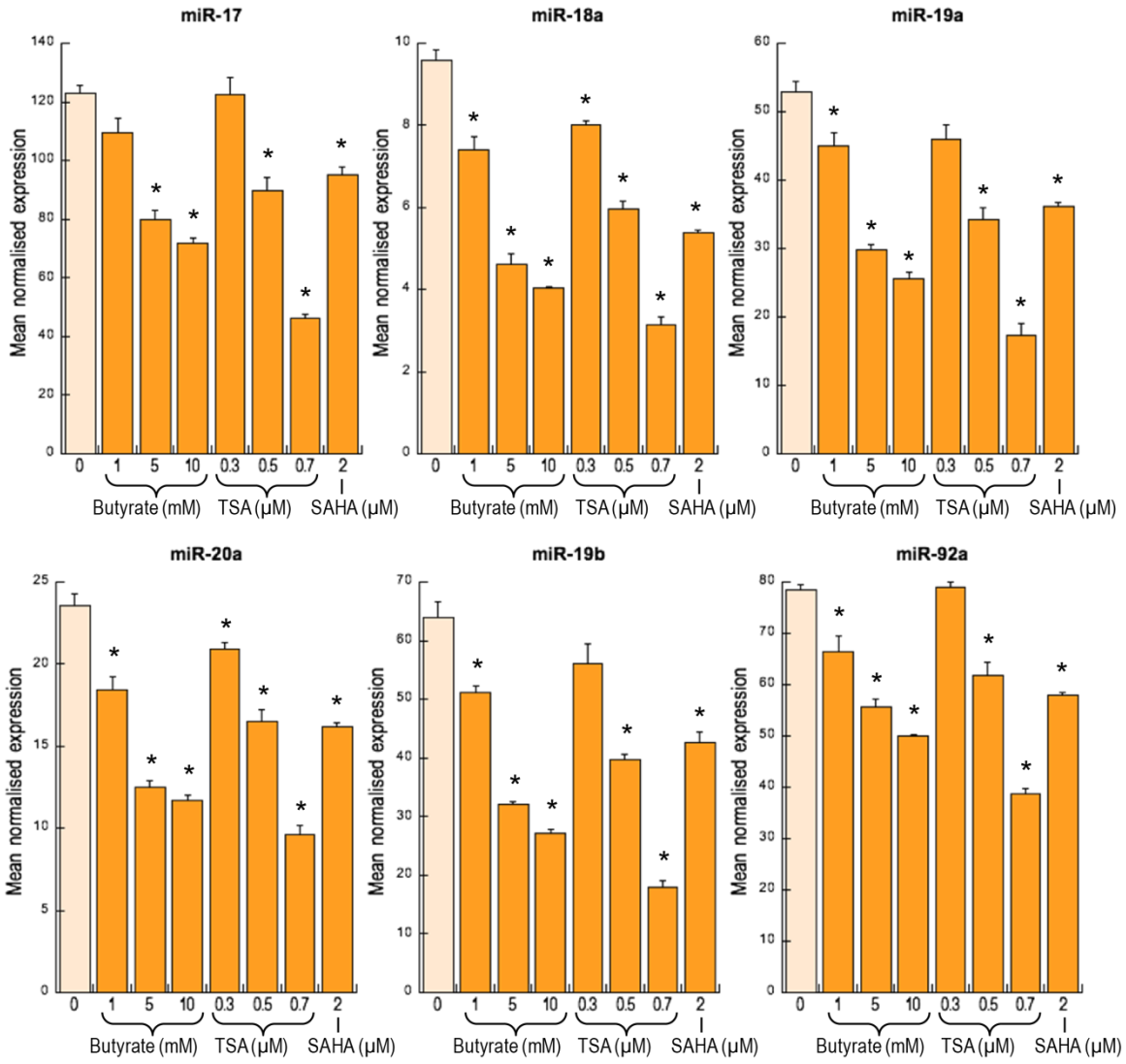

Figure 5.4: Real-time RT-PCR validation of miR-17-92 cluster changes in HT29 cells after 48 h of butyrate, TSA or SAHA treatment

miR-17-92 cluster miRNA levels in cells treated with increasing doses of butyrate or TSA, or with SAHA, compared with cells in control medium (0) (* $P < 0.05$). The mean ± SEM of three cell culture replicates is shown, and expression is normalised to RNU6B levels.

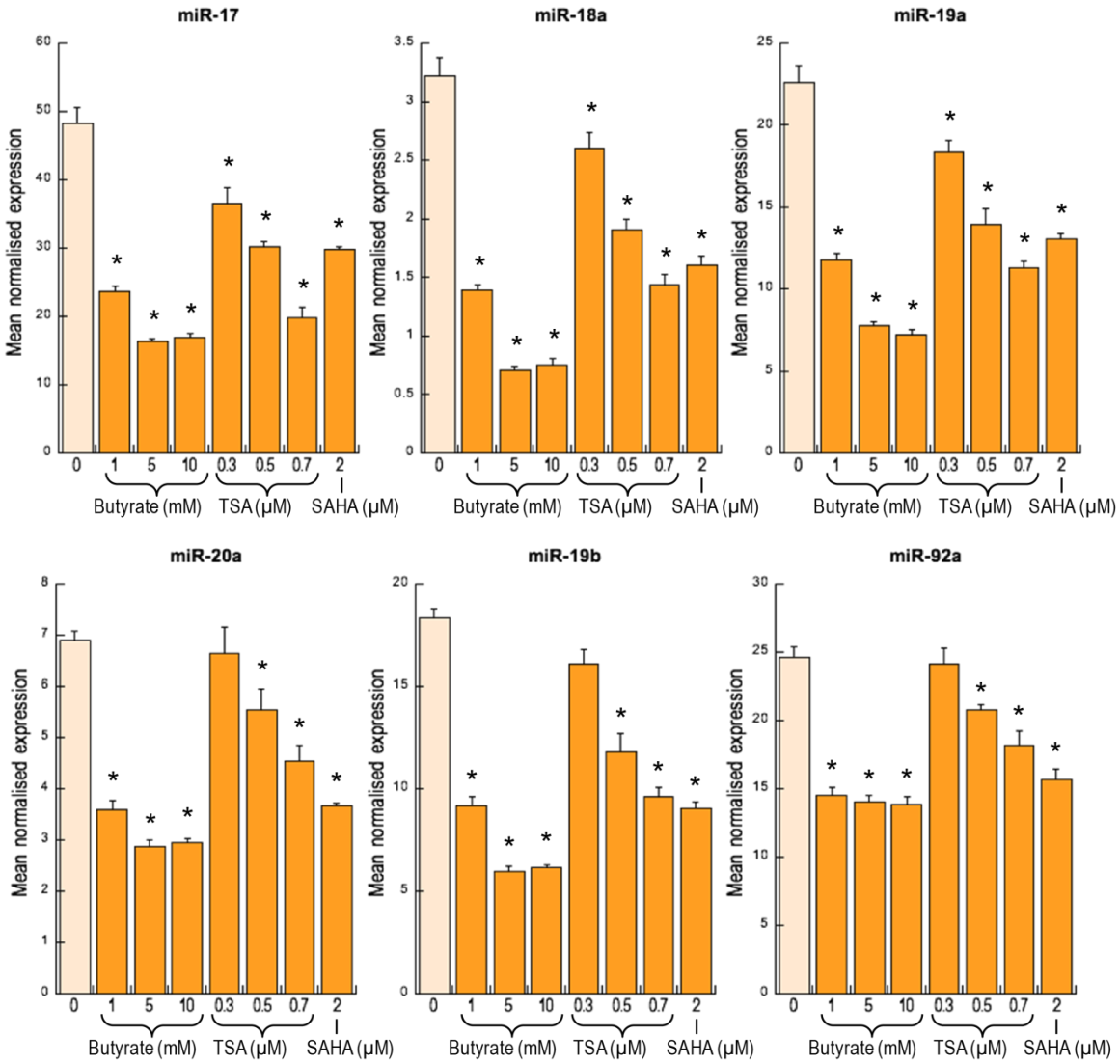

Figure 5.5: Real-time RT-PCR validation of miR-17-92 cluster changes in HCT116 cells after 48 h of butyrate, TSA or SAHA treatment

miR-17-92 cluster miRNA levels in cells treated with increasing doses of butyrate or TSA, or with SAHA, compared with cells in control medium (0) (* $P < 0.05$). The mean ± SEM of three cell culture replicates is shown, and expression is normalised to RNU6B levels.

Table 5.3: **Changes in miR-17-92 and miR-106a-363 cluster mature miRNA levels in HT29 and HCT116 cells treated with butyrate, TSA or SAHA for 48 h as detected by real-time RT-PCR.**

Values represent fold changes (and *P* values) relative to untreated control cells. Expression is normalised to RNU6B levels and the mean of three cell culture replicates is shown.

	Butyrate			**TSA**			**SAHA**
	1 mM	5 mM	10 mM	0.3 µM	0.5 µM	0.7 µM	2 µM
miR-17-92 cluster							
HT29 cells							
miR-17	-1.13	-1.54	-1.71	-1.00	-1.37	-2.66	-1.29
	(0.07)	(0.0005)	(<0.0001)	(0.96)	(0.003)	(<0.0001)	(0.001)
miR-18a	-1.30	-2.07	-2.37	-1.20	-1.61	-3.05	-1.78
	(0.006)	(0.0001)	(<0.0001)	(0.004)	(0.0004)	(<0.0001)	(0.001)
miR-19a	-1.18	-1.78	-2.06	-1.15	-1.54	-3.07	-1.47
	(0.04)	(0.0002)	(0.0001)	(0.05)	(0.001)	(0.0001)	(<0.0001)
miR-20a	-1.28	-1.89	-2.01	-1.13	-1.43	-2.44	-1.45
	(0.008)	(0.0002)	(<0.0001)	(0.03)	(0.002)	(<0.0001)	(0.0002)
miR-19b	-1.25	-2.00	-2.37	-1.14	-1.61	-3.56	-1.50
	(0.009)	(0.0002)	(0.0001)	(0.14)	(0.0008)	(<0.0001)	(0.002)
miR-92a	-1.18	-1.41	-1.57	+1.01	-1.27	-2.03	-1.36
	(0.02)	(0.0003)	(<0.0001)	(0.75)	(0.003)	(<0.0001)	(0.0005)
HCT116 cells							
miR-17	-2.04	-2.97	-2.85	-1.32	-1.60	-2.44	-1.62
	(0.0005)	(0.0002)	(0.0002)	(0.02)	(0.002)	(0.0006)	(<0.0001)
miR-18a	-2.32	-4.57	-4.27	-1.24	-1.69	-2.23	-2.00
	(0.0003)	(<0.0001)	(0.0001)	(0.04)	(0.002)	(0.0006)	(0.001)
miR-19a	-1.91	-2.91	-3.14	-1.23	-1.62	-2.00	-1.73
	(0.0007)	(0.0002)	(0.0002)	(0.03)	(0.004)	(0.0006)	(<0.0001)
miR-20a	-1.92	-2.40	-2.34	-1.04	-1.24	-1.52	-1.88
	(0.0002)	(<0.0001)	(<0.0001)	(0.67)	(0.04)	(0.003)	(<0.0001)
miR-19b	-2.00	-3.08	-2.98	-1.14	-1.56	-1.90	-2.03
	(0.0001)	(<0.0001)	(<0.0001)	(0.06)	(0.003)	(0.0001)	(0.0007)
miR-92a	-1.69	-1.76	-1.78	-1.02	-1.19	-1.36	-1.58
	(0.0004)	(0.0003)	(0.0003)	(0.73)	(0.01)	(0.009)	(0.008)
miR-106a-363 cluster[a]							
HT29 cells							
miR-106a	-1.23	-1.82	-1.98	-1.01	-1.35	-2.27	-1.51
	(0.02)	(0.001)	(<0.001)	(0.70)	(0.002)	(<0.001)	(<0.0001)
miR-18b	-1.52	-1.78	-2.17	-1.14	-1.55	-2.30	-1.30
	(0.004)	(0.007)	(0.0002)	(0.31)	(0.002)	(0.0004)	(0.06)
miR-20b	-1.22	-1.85	-2.01	+1.02	-1.40	-2.51	-1.51
	(0.03)	(0.0003)	(<0.0001)	(0.73)	(0.0004)	(<0.0001)	(0.001)
HCT116 cells							
miR-106a	-2.13	-2.86	-2.85	-1.17	-1.42	-1.72	-1.89
	(0.0007)	(0.0003)	(0.0003)	(0.11)	(0.01)	(0.003)	(<0.0001)
miR-18b	-1.68	-2.96	-3.48	-1.08	-1.44	-1.30	-1.95
	(0.006)	(0.0008)	(0.0002)	(0.35)	(0.01)	(0.02)	(<0.0001)
miR-20b	-1.83	-2.44	-2.36	-1.08	-1.33	-1.72	-1.85
	(0.002)	(0.0006)	(0.0006)	(0.40)	(0.04)	(0.006)	(0.0002)

[a] miR-19b-2 and miR-92a-2 in the miR-106a-363 cluster have the same sequence as miR-19b-1 and miR-92a-1 respectively in the miR-17-92 cluster, so the fold change results for these miRNAs do not distinguish between these. miR-363 was not examined as it showed no change in the microarray analysis.

5.4.3 Expression of miR-17-92 validated target genes and regulators in colorectal cancer cells treated with butyrate

Elevated expression of the miR-17-92 cluster promotes proliferation and suppresses apoptosis in cancer cells (Mu et al 2009, Olive et al 2009). To understand how the butyrate-induced decrease in miR-17-92 miRNAs affected proliferation and apoptosis, the influence of these miRNAs on target genes was studied. Experimentally validated targets whose expression was modulated by miR-17-92 miRNAs in other, mainly lymphoma, cell models were examined first, including *CDKN1A* (target of miRs 17 and 20a), *PTEN* (target of miRs 17, 19a, 19b and 20a), and *BCL2L11* (target of miRs 17, 18a, 19a, 20a, 19b and 92a) (Ventura et al 2008, Inomata et al 2009, Mu et al 2009, Olive et al 2009, Wong et al 2010) (Figure 5.2). Real-time RT-PCR was used to determine mRNA levels of these target genes in HT29 and HCT116 cells with and without 5 mM butyrate treatment for 48 h. The decrease in miR-17-92 levels in response to butyrate correlated with an increase in transcript levels of *CDKN1A* ($P = 0.02$ in HT29 cells; $P = 0.004$ in HCT116 cells), *PTEN* ($P = 0.001$ in HT29 cells; $P = 0.02$ in HCT116 cells), and *BCL2L11* ($P = 0.001$ in HT29 cells; $P = 0.0001$ in HCT116 cells) (Figure 5.6). To investigate the effect of butyrate on translation of these genes, Western blot analysis was used to display changes in protein levels in target genes. Again, the decrease in miR-17-92 in response to butyrate correlated with an increase in CDKN1A ($P = 0.006$ in HT29 cells; $P = 0.01$ in HCT116 cells), PTEN ($P = 0.001$ in HT29 cells; $P = 0.001$ in HCT116 cells), and BCL2L11 ($P = 0.002$ in HT29 cells; $P < 0.0001$ in HCT116 cells) proteins (Figure 5.7 and Figure 5.8).

The transcription factors E2F1, E2F2, and E2F3 and C-MYC and are known regulators of the *MIR17HG*, the host gene of the miR-17-92 cluster of miRNAs (O'Donnell et al 2005, Woods et al 2007). Real-time RT-PCR was used to investigate mRNA levels of these transcription factors in HT29 and HCT116 cells with and without 5 mM butyrate treatment for 48 h, to determine whether altered transcription of these genes may be responsible for the decrease in miR-17-92 miRNAs observed with butyrate treatment. At the mRNA level, *E2F1* decreased in response to butyrate treatment ($P = 0.0002$ in HT29 cells; $P < 0.0001$ in HCT116 cells), whereas *C-MYC* was not significantly changed in HT29 cells ($P = 0.77$), but was significantly increased in HCT116 cells ($P = 0.0008$) (Figure 5.9).

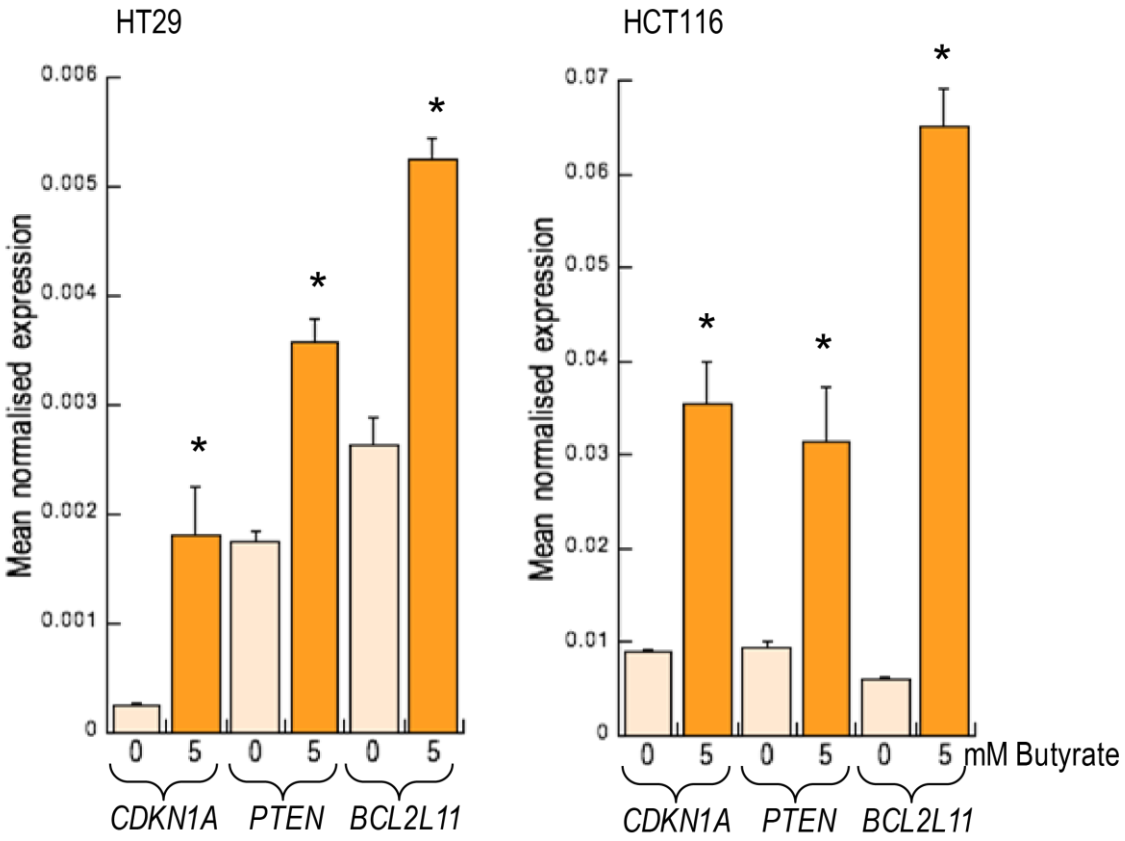

Figure 5.6: Changes in miR-17-92 cluster target gene mRNA levels in HT29 and HCT116 cells after 48 h of butyrate treatment: Real-time RT-PCR.

CDKN1A, *PTEN* and *BCL2L11* mRNA levels in cells treated with butyrate (5 mM), compared with cells in control medium (0) (* $P < 0.05$). The mean ± SEM of three cell culture replicates is shown and expression normalised to *ACTB* levels.

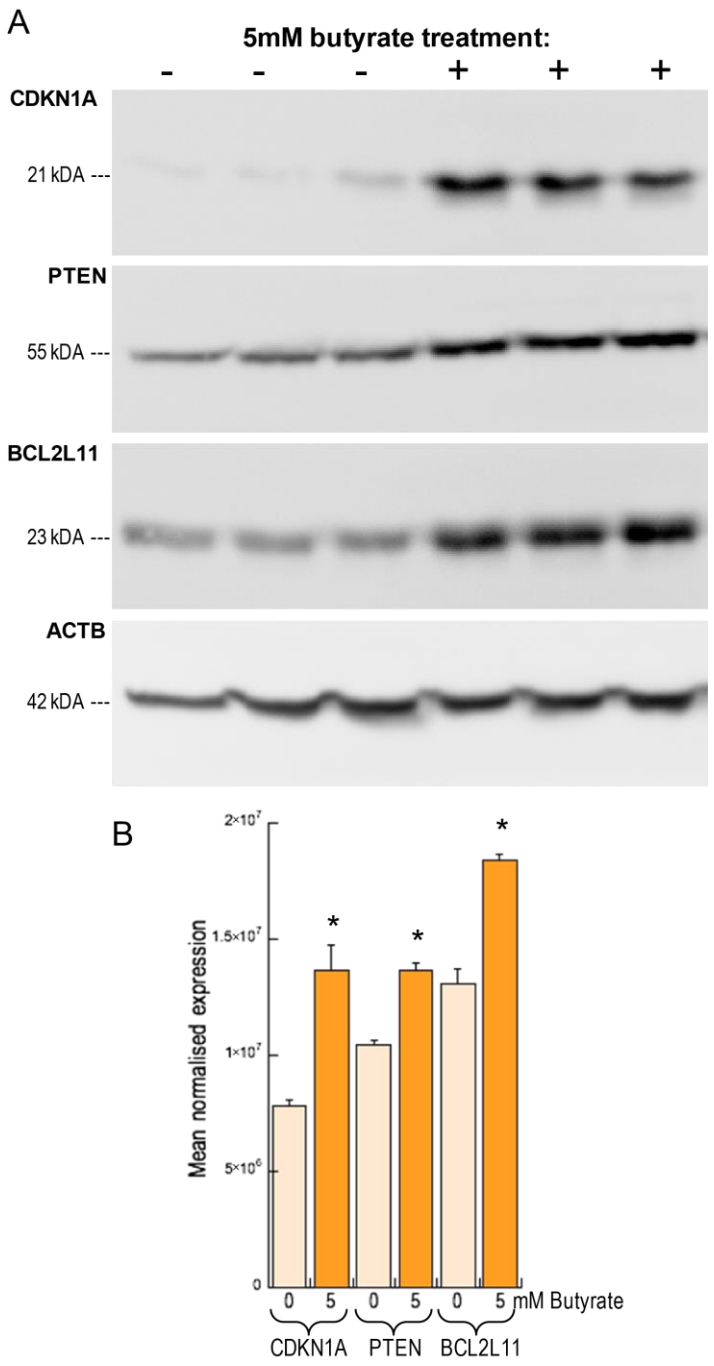

Figure 5.7: Changes in miR-17-92 cluster target gene protein levels in HT29 cells after 48 h of butyrate treatment: Western blot.

(A) CDKN1A, PTEN and BCL2L11 protein levels in cells treated with 5 mM butyrate (+) compared with cells in control medium (-), as measured by Western blot analysis using three cell culture replicates. (B) Densitometry results were normalised to ACTB levels, and cells treated with butyrate (5 mM) were compared with cells in control medium (0) (* $P < 0.05$). The mean ± SEM of three cell culture replicates is shown.

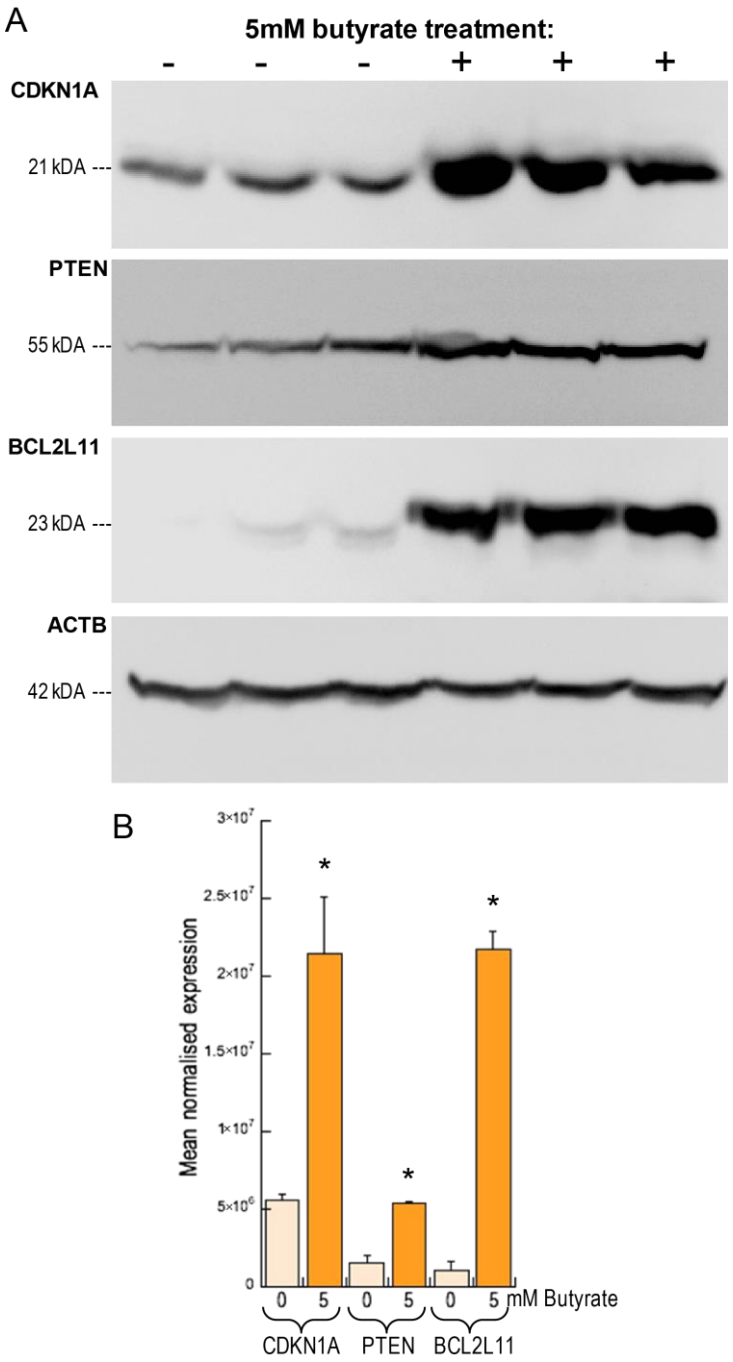

Figure 5.8: Changes in miR-17-92 cluster target gene protein levels in HCT116 cells after 48 h of butyrate treatment: Western blot.

(A) CDKN1A, PTEN and BCL2L11 protein levels in cells treated with 5 mM butyrate (+) compared with cells in control medium (-), as measured by Western blot analysis using three cell culture replicates. (B) Densitometry results were normalised to ACTB levels, and cells treated with butyrate (5 mM) were compared with cells in control medium (0) (* $P < 0.05$). The mean ± SEM of three cell culture replicates is shown.

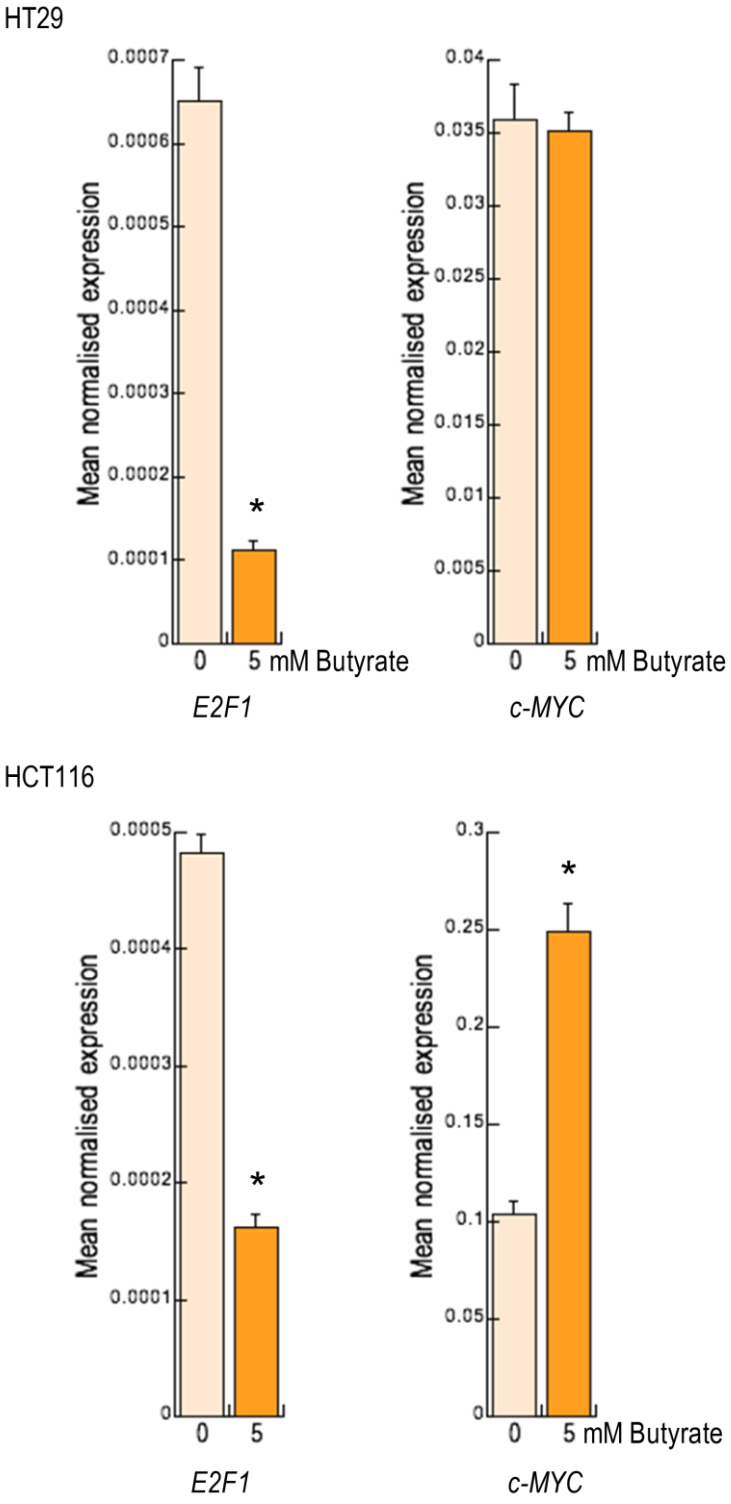

Figure 5.9: Changes in mRNA levels of transcription factors that regulate *MIR17HG* (the miR-17-92 host gene) in HT29 and HCT116 cells after 48 h of butyrate treatment: Real-time RT-PCR.

mRNA levels of the miR-17-92 cluster regulators *E2F1* and *C-MYC* in cells treated with butyrate (5 mM), compared with cells in control medium (0) (* $P < 0.05$). The mean ± SEM of three cell culture replicates is shown and expression normalised to *ACTB* levels.

5.4.4 miR-17-92 microRNAs and target genes in colorectal cancer cells and normal human rectal mucosa

To determine whether butyrate treatment was able to restore miR-17-92 expression to a more normal level, a comparison of miR-17-92 miRNA levels in untreated control HT29 and HCT116 cells, 5 mM butyrate-treated cells HT29 and HCT116 cells, and normal human rectal mucosa was performed (Figure 5.10). In the HCT116 cells, 5 mM butyrate treatment allowed miR-17-92 levels to fall to a level similar to that in normal human rectal mucosa. In the HT29 cells, miR-17-92 levels also fell with 5 mM butyrate treatment, but did not reach the low levels found in normal human rectal mucosa.

A similar comparison was performed for miR-17-92 target gene mRNA levels in untreated control and 5 mM butyrate-treated HT29 and HCT116 cells, and normal human rectal mucosa, again to determine whether butyrate treatment restored target gene expression to a more normal level (Figure 5.11). Expression of the target genes *CDKN1A*, *PTEN*, and *BCL2L11* were increased in the context of a butyrate-induced reduction in miR-17-92 levels. Particularly in the HCT116 cells, *CDKN1A*, *PTEN*, and *BCL2L11* mRNA levels in the butyrate-treated cells were restored to levels similar or greater than those detected in normal human rectal mucosa. In the HT29 cells, *CDKN1A*, *PTEN*, and *BCL2L11* mRNA levels also increased with butyrate treatment, but did not reach the levels found in normal human rectal mucosa.

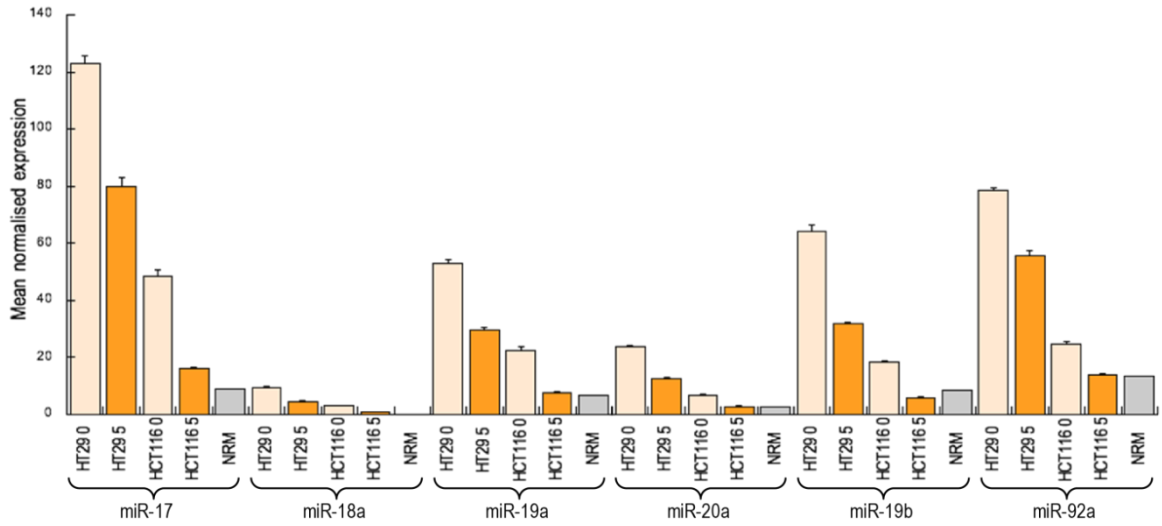

Figure 5.10: Comparison of miR-17-92 miRNA levels in untreated control CRC cells, 5 mM butyrate-treated CRC cells and normal human rectal mucosa

miR-17-92 cluster miRNA levels in cells in control medium, 5 mM butyrate-treated cells, or normal rectal mucosa. The mean ± SEM of three cell culture replicates is shown and expression is normalised to RNU6B levels.

HCT116 0: untreated control HCT116 cells; HCT116 5: 5 mM butyrate-treated HCT116 cells; HT29 0: untreated control HT29 cells; HT29 5: 5 mM butyrate-treated HT29 cells; NRM: normal human rectal mucosa.

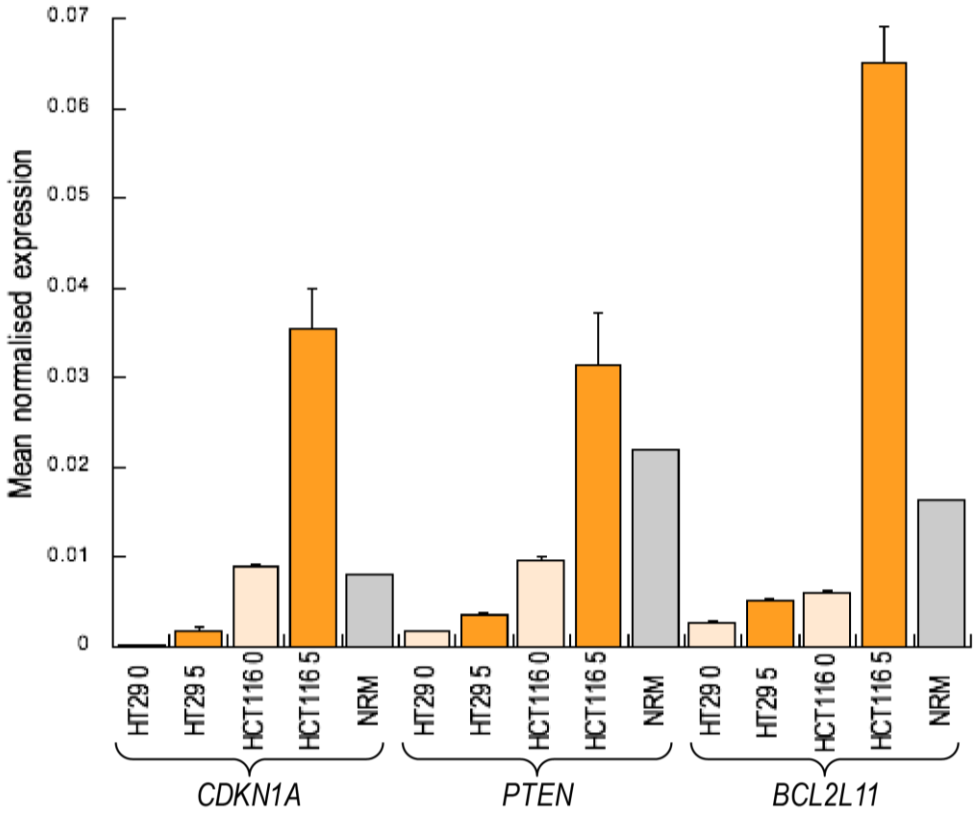

Figure 5.11: Comparison of *CDKN1A*, *PTEN*, and *BCL2L11* mRNA levels in untreated control CRC cells, 5 mM butyrate-treated CRC cells and normal human rectal mucosa

CDKN1A, *PTEN* and *BCL2L11* mRNA levels in cells in control medium, 5 mM butyrate-treated cells, or normal rectal mucosa. The mean ± SEM of three cell culture replicates is shown, with each sample assayed in triplicate and expression normalised to *ACTB*.

HCT116 0: untreated control HCT116 cells; HCT116 5: 5 mM butyrate-treated HCT116 cells; HT29 0: untreated control HT29 cells; HT29 5: 5 mM butyrate-treated HT29 cells; NRM: normal human rectal mucosa.

5.5 Discussion

In this Chapter, the effects of the natural HDI butyrate were compared with those of other HDIs, in particular the hydroxamic acids TSA and SAHA. At the concentrations used, these three HDIs were all shown to decrease expression of the miR-17-92 cluster of miRNAs in CRC cell lines. As in the previous Chapter, the HCT116 cell line showed greater susceptibility than the HT29 cell line to the anti-proliferative effects of HDIs, and the decrease in miR-17-92 cluster expression in response to HDI treatment was also greater in the HCT116 cell line. The decrease in miR-17-92 cluster miRNA levels corresponded with an increase in expression of genes targeted by the cluster, including *CDKN1A*, *PTEN* and *BCL2L11*.

The miR-17-92 cluster has been shown to have oncogenic properties and is increased in CRC; thus the reduction of these miRNAs with butyrate and other HDIs is potentially protective against CRC. As previously discussed in Chapter 4, multiple studies have found miR-17-92 cluster miRNAs to be up-regulated in CRC (Cummins et al 2006, Chen et al 2009). Compared to some previous studies, a recent study by Diosdado et al (2009) isolated pure epithelial cells rather than whole normal mucosa biopsies, in order to more accurately compare differences in expression of miR-17-92 cluster miRNAs between control and CRC samples. The study found a 2 to 5-fold increase in miR-17-92 cluster members in colorectal tumours compared with control epithelium, and also higher expression in adenocarcinomas than in adenomas, indicating a role in tumour progression (Diosdado et al 2009). Of the six members of the cluster, all except miR-18a showed significantly increased expression in colorectal tumours with miR-17-92 locus gain compared with tumours without miR-17-92 locus gain (Diosdado et al 2009). The finding by this current study that 5 mM butyrate, 2 μM SAHA or 0.5 μM TSA decreased levels of miR-17-92 cluster miRNAs approximately 2-fold in CRC cells implies that these compounds restore miR-17-92 expression to a more normal level. This was particularly true in the HCT116 cells, where 5 mM butyrate treatment allowed miR-17-92 levels to fall to a level similar to that in normal human rectal mucosa. It should be noted that in this Chapter, *in vitro* examination of the effect of butyrate was limited to cancer cell lines; a comparison of the effect of butyrate treatment in primary non-cancerous colorectal epithelial cells would also be useful, particularly in light of *in vivo* findings described later in Chapter 8.

This Chapter demonstrated that butyrate and other HDIs had similar effects on miR-17-92 expression. No other studies have previously compared the effects of multiple

HDIs on miRNA expression in CRC; however several other recent studies in CRC cells show the effects of individual HDIs on miRNA expression. As discussed in Chapter 4, one other study has examined the effect of butyrate on miRNA levels in HCT116 CRC cells, and found miRNAs from the miR-17-92 cluster and the paralogous cluster miR-106a-363 to be significantly down-regulated (Hu et al 2011). Another study by Bandres et al (2009) examined the modulation of several miRNAs in CRC cell lines with 4-phenylbutyric acid treatment, but did not examine miR-17-92 expression changes. There has also been one study which examined the effect of SAHA on miRNA expression in CRC cells (Shin et al 2009b). Shin et al (2009b) identified miRNA expression profiles induced by SAHA in the HCT116 colorectal carcinoma cell line, which contains wild-type p53, and a null-p53 derivative HCT116 cell line. Cell lines were treated for 24 h with 0 or 1.5 μM SAHA, and a miRNA microarray was performed using a human miRNA microarray kit (version 2, Agilent Technologies) to examine 723 human miRNAs. Of the miRNAs studied, 144 showed >2-fold change in the presence of SAHA or p53. In the wild-type p53 HCT116 cells, treatment with SAHA resulted in altered expression of 51 miRNAs, and in the null-p53 HCT116 cells, SAHA treatment altered expression of 123 miRNAs; 31 of these miRNAs were common between cell types. In the wild-type p53 HCT116 cells 32 miRNAs were up-regulated and 19 were down-regulated, while in the null-p53 HCT116 cells 29 were up-regulated and 94 were down-regulated. This difference in SAHA-induced down-regulation of miRNAs in the two HCT116 cell lines implies that p53 is responsible for some regulation of miRNA expression. When the wild-type p53 HCT116 cells and null-p53 HCT116 cells were compared in the absence of SAHA, 40 miRNAs showed different expression levels due to p53 status alone. There was substantial overlap in the miRNAs that changed with p53 status and those that changed with SAHA treatment (Shin et al 2009b). In terms of the specific miRNAs altered by SAHA or p53 status, the authors only presented the miRNAs that changed >5-fold between groups, and not all the miRNAs that changed >2-fold. miRNAs in the miR-17-92 cluster were not present in the list of miRNAs that changed >5-fold, but it is unclear whether any smaller changes in their expression were observed with SAHA treatment in the study by Shin et al (2009b). In this current study, for instance, the reduction in miR-17-92 cluster miRNAs in response to SAHA in HCT116 cells was approximately 2-fold.

The effects of HDIs on miRNA expression in CRC cells have only been examined in this present study and in the two above mentioned studies; however, some additional studies have looked at the interaction between HDI treatment and miRNA expression

in other cancer types, including lymphoma, lung, pancreas, and breast cancer cells, and in cultured primary hepatocytes (Zhang et al 2008, Lee et al 2009, Bolleyn et al 2011, Kretzner et al 2011, Rhodes et al 2012). Several of these studies identified miRNAs from the miR-17-92 cluster to be among those down-regulated by HDIs, in lymphoma, lung and pancreatic cancer cells (Zhang et al 2008, Lee et al 2009, Kretzner et al 2011).

There are several potential mechanisms that explain why butyrate and other HDIs alter the expression of the miR-17-92 cluster in cancer cells. HDIs can epigenetically regulate gene expression through induction of histone hyperacetylation and also through acetylation of non-histone proteins. In addition, butyrate has been shown affect DNA methylation and histone methylation and phosphorylation (Boffa et al 1981, Boffa et al 1994, Daly & Shirazi-Beechey 2006, Mathew et al 2010, Huang et al 2011, Marinova et al 2011). This study and other recent studies have confirmed that butyrate and other HDIs such as SAHA (Bandres et al 2009, Shin et al 2009b, Hu et al 2011) can alter miRNA expression in colorectal cells, with this Chapter showing the different HDIs to have similar effects on expression of miR-17-92 cluster miRNAs. Generally, increased histone acetylation caused by HDIs is associated with increased gene transcription (Mariadason et al 2000), and by this method epigenetically silenced antineoplastic genes, or in this case miRNAs, can be reactivated (Rada-Iglesias et al 2007). For miRNAs such as the miR-17-92 cluster that decreased following HDI treatment, histone modification may still be involved, as butyrate action appears to be region-specific. Hinnebusch et al (2003) observed localised changes in a butyrate-treated CRC cell line, with histone acetylation increasing in some regions while remaining the same in others. Rada-Iglesias et al (2007) showed that butyrate may actually reduce histone H3 and H4 acetylation close to some transcription start sites, and by this mechanism may decrease transcription.

While histone modification may account for the altered miR-17-92 host gene transcription in response to HDIs, additional mechanisms may assist. Transcription of *MIR17HG*, the miR-17-92 cluster host gene, is directly activated by C-MYC and by E2F1 and E2F3 (O'Donnell et al 2005, Woods et al 2007). In CRC samples, *C-MYC* and miR-17-92 expression levels have been shown to be significantly correlated, illustrating this transcriptional regulation by C-MYC on the miR-17-92 cluster (Diosdado et al 2009). In some studies HDIs reduced *C-MYC* expression in CRC cells (Daly & Shirazi-Beechey 2006, Daroqui & Augenlicht 2010), while in others HDI treatment had no effect (Fang et al 2004). Jiang et al (2007) have suggested that cancer cells with deregulated *MYC* might be more sensitive to treatment with HDIs. In this

study no significant *C-MYC* decrease was observed at the mRNA level in butyrate-treated HT29 cells, whereas in HCT116 cells there was an increase. In contrast, in this study *E2F1* expression was significantly reduced with butyrate in both cell lines, which is in keeping with other studies that have shown a decrease in E2F in response to HDIs (Boutillier et al 2003, Abramova et al 2006, Abramova et al 2010, Noro et al 2010). This decrease in *E2F1* could play a role in the observed decrease in miR-17-92 levels.

The miR-17-92 host gene is also a target for p53 mediated gene repression (Yan et al 2009). Several transcription factors, including p53, are regulated by acetylation events, and their expression can be influenced by HDI treatment (Palmer et al 1997, Murphy et al 1999, Zhao et al 2006, Roy & Tenniswood 2007). p53 is normally present in cells at low levels, and is activated in response to DNA damage or cellular stress to regulate cell cycle arrest, DNA repair or apoptosis (Baker et al 1990a, Kastan et al 1991, Fritsche et al 1993). This activation is by post-translational modification, which leads to protein stabilisation and increased half-life (Kastan et al 1991). Mutation of the p53 gene is a common late stage event in CRC development, which can promote oncogenic transformation (Baker et al 1990b). Multiple studies have investigated the role of butyrate and other HDIs in modulating p53 expression, with most demonstrating a decrease in p53 in response to HDI treatment in CRC and pre-malignant colonic adenoma cells (Gope & Gope 1993, Heruth et al 1993, Janson et al 1997, Palmer et al 1997, Coradini et al 2000, Emenaker et al 2001, Taniguchi et al 2012). Despite this observed decrease in overall p53 levels in cancer cells with HDI treatment, it has been hypothesised that low-levels of wild type p53 protein may retain the ability to be activated, and that p53 levels are not directly proportional to activity (Williams et al 1999). It is even possible that HDI treatment could increase p53 stability and activity by inhibiting HDAC targeting of p53 (Luo et al 2000, Roy & Tenniswood 2007). HDAC1, for example, has been shown to regulate the transcription factor activity of p53, with deacetylation by HDAC1 reducing p53 stability, repressing its interaction with DNA, and its transactivation activity, and in turn modulating p53-mediated cell growth arrest and apoptosis (Gu & Roeder 1997, Luo et al 2000, Roy & Tenniswood 2007). Acetylated p53 has been shown to have a longer half-life (Zhao et al 2006), which again illustrates the complexity of p53 regulation by HDIs.

Various alterations in p53 expression and activity by HDIs may in turn alter miRNA expression (Shin et al 2009b). Shin et al (2009b) found both p53 and the HDI SAHA had effects on miRNA expression. While their study attempted to address the role of p53 by using cancer cells differing in the presence or absence of the p53 gene, there is

added complexity in cancer cells that have accumulated various genetic mutations in the p53 gene. This current study used HT29 cells which have mutated p53, and HCT116 cells which have wild-type p53 (ATCC). In this study the HCT116 cells appeared to respond to HDI treatment to a greater extent than the HT29 cells. This is consistent with earlier findings by Williams et al (1993), Palmer et al (1997), and Emenaker et al (2001) showing that mutations in p53 reduced response to butyrate. This is also in keeping with the study by LaBonte et al (2009) which highlighted the difference between HT29 and HCT116 cell lines in a number of key genes reported to determine response to chemotherapeutics, including the presence of mutant p53 in HT29 cells and activating *KRAS* and β-catenin mutations in HCT116 cells. When measuring HDI-induced reductions in proliferation, the study found that the HCT116 cells demonstrated a 1.5-fold increase in sensitivity to Vorinostat ($P = 0.027$) over the HT29 cells (LaBonte et al 2009). The HCT116 cells were also significantly more sensitive to onset of HDI-induced apoptosis (LaBonte et al 2009). This was confirmed by Wilson et al (2010a) when 30 different CRC cell lines were treated with butyrate; the HCT116 cell line was among the five CRC cell lines with the highest sensitivity and apoptotic response to low-dose butyrate treatment, the HT29 cell line was in the middle of the panel, and five other cell lines had the greatest resistance and lowest apoptotic response to high-dose butyrate treatment. Colony formation was significantly reduced in sensitive compared with resistant lines ($P = 0.01$), and cell lines sensitive and resistant to butyrate-induced apoptosis were likewise differentially sensitive to other HDIs tested, including TSA and SAHA (Wilson et al 2010a).

Further study is required to elucidate the precise mechanism of miR-17-92 regulation by HDIs, but it would appear that down-regulation of miR-17-92 mediated by a decrease in regulator proteins such as E2F1 may be possible. This Chapter was limited to examining changes in several regulators of the miR-17-92 cluster at the mRNA level; however, further investigation of E2F1 changes at the protein level may be beneficial, as would exploration of potential changes in other regulators such as p53. In addition, the possibility of a direct transcriptional response via histone modification cannot be discounted. This possible direct regulation of miR-17-92 expression is examined further in Chapter 7.

The miR-17-92 cluster functions during normal development and malignant transformation to promote proliferation and angiogenesis, inhibit differentiation, and sustain cell survival (Dews et al 2006, Olive et al 2009). The cell cycle inhibitor *CDKN1A* and the pro-apoptotic genes *PTEN* and *BCL2L11* are regulated by miR-17-

92 (Ventura et al 2008, Inomata et al 2009, Mu et al 2009, Olive et al 2009, Mavrakis et al 2010, Wong et al 2010), and butyrate can also regulate *CDKN1A* and *PTEN* expression (Daly & Shirazi-Beechey 2006). Expression of these genes is decreased in CRC, but in the context of a butyrate-induced reduction in miR-17-92 levels both *CDKN1A* and *PTEN* mRNA and protein levels were increased and, particularly in the HCT116 cells, were restored to levels similar or greater than those detected in normal human rectal mucosa.

The findings in this Chapter demonstrate the high degree of complexity surrounding epigenetic regulation of cancer cells by HDIs. The multiple genes modulated by HDIs play distinct but complementary roles to facilitate the decreased proliferation and increased apoptosis observed in HDI-treated CRC cell lines. For example, one gene that has increased expression with HDIs such as butyrate is *CDKN1A*, which can induce growth arrest, but can also inhibit apoptosis and differentiation when over-expressed (Izawa et al 2005, Sun et al 2010). However, other butyrate-induced genes such as *PTEN* and *BCL2L11* promote apoptosis. As indicated by Mariadason et al (2000), cell response to butyrate appears to be the result of interactions between large numbers of genes. This Chapter has displayed an additional layer of complexity whereby the butyrate response is also mediated by miRNA interactions with regulator and target genes. Butyrate was shown to decrease miR-17-92 cluster miRNAs and increase target gene expression. It remains to be confirmed in the subsequent Chapter whether the effect of butyrate on target genes is, at least in part, directly mediated by the miR-17-92 cluster miRNAs.

Chapter 6. Treatment with HDIs reveals competing roles for miR-17-92 cluster members

6.1 Introduction

Treatment of CRC cell lines with HDIs such as butyrate was shown in previous Chapters to decrease proliferation, decrease levels of miR-17-92 cluster miRNAs and increase expression of the miR-17-92 target genes *CDKN1A*, *PTEN* and *BCL2L11*. The effect of butyrate on overall cell proliferation, and on cell cycle inhibitors and pro-apoptotic genes, could be mediated in part by the observed decrease in miR-17-92 cluster miRNAs. This hypothesis is addressed in this Chapter. miR-17-92 miRNAs may also regulate other predicted target genes to mediate changes in proliferation.

6.1.1 microRNA mimics

In this Chapter, levels of individual miR-17-92 cluster miRNAs were manipulated to determine their role in influencing the response of CRC cell lines to HDIs. The use of miRNA mimics to reverse the butyrate-induced reduction in miR-17-92 miRNA levels assisted in determining the effect of miR-17-92 cluster miRNAs on proliferation and gene expression. miRNA mimics are small, chemically-synthetic and optimised nucleic acids designed to mimic endogenous mature miRNA molecules in cells. They can directly enter the miRNA processing pathway and undergo the same incorporation into RISC as endogenous miRNAs within the cell (Wang 2011).

The development of miRNA mimics emerged from earlier RNA interference (RNAi) techniques. Double stranded RNA (dsRNA) was first used for RNAi experiments, where dsRNAs could induce the degradation of corresponding target mRNAs (Fire et al 1998, Svoboda et al 2000, Wianny & Zernicka-Goetz 2000); however, introducing long dsRNA was found to be less than ideal in most mammalian cells because it had non-specific inhibitory effects including induction of the antiviral interferon response which led to cell death (Stark et al 1998, Dorsett & Tuschl 2004). Investigations of the mechanisms guiding RNAi in different organisms revealed that one important feature of using long dsRNA for RNAi was its processing by Dicer and other proteins into 21 – 23 nucleotide small interfering RNAs (siRNAs) of defined structure (Zamore et al 2000). These siRNAs are integrated into the RISC, where they can bind and inhibit

complementary mRNAs. siRNAs could be used to silence genes in mammalian tissue culture without triggering the interferon response (Bernstein et al 2001, Caplen et al 2001, Elbashir et al 2001). Subsequently, short hairpin RNAs (shRNA) have been developed to evoke a specific RNAi-type response, and to induce sequence-specific gene silencing in mammalian cells (McManus et al 2002, Paddison et al 2002). These shRNAs are similar in structure to precursor miRNAs, and when transfected into cells were shown to be processed to smaller 21 – 23 nucleotide size RNAs, consistent with cleavages in the loop sequence (McManus et al 2002). They have been shown to successfully target the 3'UTR of target gene mRNAs (McManus et al 2002). The early studies by McManus et al (2002) and others (Brummelkamp et al 2002, Lee et al 2002, Paddison et al 2002, Paul et al 2002, Sui et al 2002, Yu et al 2002) indicated that shRNAs can be effective silencers, and are likely to be processed in a similar fashion to precursor miRNAs that occur naturally in cells, through cleavage by Dicer and incorporation into RISCs. Synthesised hairpins may be transfected into cells for transient target gene silencing, or transcribed from plasmid vectors for longer-term or stable silencing (Brummelkamp et al 2002, Lee et al 2002, McManus et al 2002, Paddison et al 2002, Paul et al 2002). shRNA-expressing transgenic mice have also been created, to generate widespread and sustained expression of an shRNA with a structure that mimics a human miRNA (Xia et al 2006).

A number of commercial sources of synthetic precursor miRNAs that mimic miRNA activity are now available (Ford 2006). These miRNA mimics can be used to control specific miRNA cellular levels, and enable up-regulation of miRNA activity for miRNA functional analysis. They can be used to screen for miRNAs that regulate expression of a gene or affect a cellular process, and can assist in miRNA target site identification and validation. Several studies have made use of miRNA mimics for the miR-17-92 cluster of miRNAs (Fontana et al 2008, Carraro et al 2009, Lakner et al 2012, Tao et al 2012). Besides the transfection of miRNA mimics, stable genetic models of miRNA over or under-expression can also be created. These genetic models have also been used to explore functions of the miR-17-92 cluster (Ventura et al 2008, Mu et al 2009, Olive et al 2009). Another common miRNA manipulation technique is the use of miRNA inhibitors such as antagomirs to silence miRNAs and inhibit their regulation of complementary mRNAs (Krutzfeldt et al 2005).

6.1.2 Validation of microRNA targets

miRNAs are known to regulate gene expression by cleaving complementary mRNA or more frequently, where there is imperfect complementarity, by acting through translational inhibition and transcript destabilization (Hutvagner & Zamore 2002, Filipowicz et al 2008, Guo et al 2010). Each miRNA may have hundreds of evolutionarily conserved targets and even more non-conserved targets (Bentwich et al 2005). Multiple methods are available for identifying miRNA target genes and confirming their biological efficacy (Kuhn et al 2008). This Chapter describes an examination of miR-17-92 targets that were previously validated in other cell types, and also the validation of novel targets of the miR-17-92 cluster member, miR-18a.

Commonly the first step in identifying miRNA targets is bioinformatic prediction. Different bioinformatics algorithms use distinct parameters to predict the probability of a functional miRNA binding site within a given mRNA target, thus each algorithm varies in sensitivity and specificity of target prediction and may predict distinct miRNA binding sites (Kuhn et al 2008). Commonly used bioinformatics algorithms that predict miRNA target sites include miRanda (John et al 2004), TargetScan (Lewis et al 2003, Lewis et al 2005), PicTar (Krek et al 2005), and DIANA-microT (Kiriakidou et al 2004). All of these algorithms allow the investigation of a specific gene by predicting miRNA target sites within that gene, mainly within the 3'UTR mRNA sequence. The algorithms also allow the determination of all the putative mRNA targets of a given miRNA. It is generally recommended that more than one algorithm should predict the same miRNA binding site before additional validation experiments are conducted (Kuhn et al 2008). Interfaces such as miRGen and miRWalk provide access to the unions and intersections of several widely used target prediction programs, and experimentally supported targets from TarBase (Megraw et al 2007). These interfaces can be used to compare and combine algorithms, allowing the user to focus on genes common to two or more prediction programs (Megraw et al 2007). In addition to bioinformatics prediction, further *in silico* analysis may be performed to predict accessibility of miRNA binding sites (Kuhn et al 2008).

Predicting candidate genes with computational algorithms can lead to a large number of false positive predictions (Nicolas 2011). Following bioinformatics prediction, experimental validation of the miRNA/mRNA interaction is required. It has been proposed that multiple criteria should be met to confirm a miRNA target (Kuhn et al 2008), which typically could comprise:

- Confirmation of miRNA and target mRNA co-expression, which can be simply demonstrated using quantitative real-time PCR using total RNA isolated from the cell type of interest and primers specific for the given miRNA and mRNA target. Alternatively, *in situ* hybridisation can be used to demonstrate co-expression.
- Determination of a miRNA effect on target mRNA and protein, which can be demonstrated by transient over-expression of a given miRNA mimic in a cell type known to express the target gene. The effect of the miRNA mimic on the target mRNA can be assayed, although as miRNAs can modulate gene expression by translational repression rather than mRNA cleavage, a decrease in mRNA levels may not always be detected (Hutvagner & Zamore 2002, Filipowicz et al 2008, Guo et al 2010). Examining whether a miRNA mimic decreases the target gene protein levels is therefore also of importance, and can be assessed using Western blot analysis. In addition to mimic experiments, an antisense miRNA inhibitor for the specific endogenous mature miRNA of interest can also be used to determine whether there is an increase in target gene expression.
- Validation of a direct rather than indirect miRNA/mRNA interaction, as discussed further below.
- Demonstration that the miRNA-mediated regulation of target gene expression equates to altered biological function. Depending on the target protein of interest, biological functions to be measured could include cell proliferation, differentiation, apoptosis, migration, or signalling (Kuhn et al 2008).

Experimental approaches based on expression profiles can predict indirect targets, in addition to the real direct targets for each miRNA (Nicolas 2011). Such preliminary expression experiments require subsequent confirmation of direct miRNA/mRNA interaction. A commonly used method to validate a sequence as a direct miRNA target is a reporter based system where the 3'UTR of the candidate target gene is inserted into a reporter plasmid downstream of a luciferase or green fluorescent protein sequence. The plasmid can then be transiently transfected into a host cell line, along with the miRNA of interest, if not endogenously expressed. Subsequent fluorescence or luciferase activity can be assayed, with this activity predicted to decrease if the miRNA binds to the target gene of interest, compared with the appropriate controls such as a negative control with a mutated binding sequence (Kuhn et al 2008, Nicolas 2011).

While such a reporter plasmid system is a useful screening tool to assess the ability of a miRNA to repress translation of reporter genes, it remains a surrogate for examining the effects of a miRNA on an endogenous target gene transcript (Kuhn et al 2008). One experimental method that allows more direct testing is the Argonaute immunoprecipitation (AgoIP) method. The Argonaute family of proteins associate with miRNAs and bind to complementary sequences in the 3'UTR of target mRNAs. Using specific antibodies, Argonaute proteins can be co-immunoprecipitated with the bound mRNAs, and the mRNAs can be identified. This approach allows the identification of functional miRNA targets (Beitzinger et al 2007, Easow et al 2007), but doesn't easily allow the specific examination of a selected miRNA/mRNA interaction.

Target protector experiments are a relatively recent alternative technique to allow the determination of direct miRNA/mRNA interaction. Target protectors are single-stranded, modified RNAs that specifically interfere in the interaction between a miRNA and a single target, while leaving the regulation of other targets of the same miRNA unaffected (Qiagen). Target protectors complementary to miRNA binding sites in target mRNAs were first developed by Choi et al (2007), to disrupt the interaction of specific miRNA-mRNA pairs and to determine the function of a particular miRNA. Additional studies have since used target protectors both *in vitro* and *in vivo* to explore how a particular miRNA directly interacts with a specific target mRNA (Gehrke et al 2010, Goljanek-Whysall et al 2011, Long & Lahiri 2011, Staton & Giraldez 2011).

Commercially synthesised target protectors are now available, and can be custom designed for each putative miRNA binding site in the target gene 3'UTRs, to elucidate the precise silencing role of a miRNA on this target (Qiagen). When transfected into host cells, the target protector binds to the miRNA-binding site, blocking miRNA access to the site and preventing gene down-regulation by the specific miRNA/RISC complex. Increased target gene expression after transfection of a target protector provides evidence that the miRNA is directly targeting the mRNA in question. Experiments can purely consist of target protector transfection if the miRNA under study is endogenously expressed in the cell type; alternatively the target protector can be co-transfected with a miRNA mimic if the miRNA is expressed at low levels or not endogenously expressed. Routine controls should also be designed, including the use of a negative control target protector which has no homology to any known mammalian gene (Qiagen). In contrast to the reporter plasmid system with luciferase or fluorescence assay, this approach investigates regulation of the endogenous transcripts rather than introduced reporter constructs, and is therefore of greater biological relevance.

6.2 Aims

The aims of this Chapter were to examine the roles of members of the miR-17-92 cluster in the context of the anti-proliferative effects of HDIs, and to determine the specific roles of these miRNAs in modulating target gene expression.

6.3 Methods overview

Experiments were conducted according to the general methods outlined in Chapter 3. All experimental groups were conducted in triplicate, with the exception of the real-time proliferation measures of transfected cells, where each experimental group had six replicates.

HT29 and HCT116 cell lines were used to determine the specific roles of miR-17-92 cluster members. Transfections were performed using Lipofectamine 2000. Cells were reverse transfected with miRNA mimics of the miR-17 family (miR-17 and miR-20a), miR-18 family (miR-18a), miR-19 family (miR-19a and miR-19b), miR-92 family (miR-92a), entire miR-17-92 cluster, miR-17-92 cluster minus miR-18a, or mimic negative control (NC), and then treated with 5 mM butyrate, 2 μM SAHA, or control medium for 48 h, and proliferation was measured in real-time using the xCELLigence RTCA DP instrument. In separate experiments, cells were transfected with mimics, and then treated for 48 h with 5 mM butyrate or maintained in control medium, and either total RNA or protein was harvested from treated cells. Relative quantitation real-time RT-PCR analysis was used to determine mRNA levels of miR-17-92 targets in 5 mM butyrate-treated cells and cells in control medium, upon transfection with different mimics. Western blots were used to determine protein levels of miR-17-92 target genes in 5 mM butyrate-treated cells and cells in control medium, upon transfection with miRNA mimics. The miR-17-92 target genes examined were *CDKN1A*, *PTEN*, and *BCL2L11*. Novel predicted targets of miR-18a were also investigated, following target prediction using multiple algorithms through miRGen (Megraw et al 2007).

Additional experiments were performed in the HT29 and HCT116 cells to confirm miR-18a predicted targets. Cells were reverse co-transfected with miR-18a mimics and also with miScript target protectors designed for miR-18a predicted target genes *NEDD9* and *CDK19*, or with a negative control miScript target protector. Cells were then treated with 5 mM butyrate or control medium and grown for 48 h, and RNA harvested. Relative quantitation real-time RT-PCR analysis was used to determine mRNA levels of *NEDD9* and *CDK19* following the various manipulations. In separate

experiments, two pre-designed siRNAs for *NEDD9* or for *CDK19* or a negative control siRNA were reverse transfected, cells were also treated with 5 mM butyrate or control medium, and proliferation was recorded for 48 h using the xCELLigence RTCA DP instrument.

6.4 Results

6.4.1 Proliferation of colorectal cancer cell lines following manipulation of mir-17-92 cluster members during HDI treatment

In Chapter 5, it was shown that HDIs reduced CRC cell proliferation, and also decreased miR-17-92 miRNA levels. In this Chapter, levels of miR-17-92 cluster miRNAs were raised using synthetic miRNA mimics, to determine how they influence the response of HT29 and HCT116 CRC cells to the HDIs butyrate or SAHA. In an initial screen, HT29 cells were transfected with mimics of the individual miRNA families (categorised according to their similar sequences into the miR-17 family (miR-17, miR-20a), the miR-18 family (miR-18a), the miR-19 family (miR-19a, miR-19b), and the miR-92 family (miR-92a)), with the entire cluster, or with a mimic negative control (NC) sequence that does not represent a human miRNA (sham transfection), in order to dissect how different cluster members influence the cells' proliferative capacity. When examining cell proliferation at 48 h, transfection with miR-19 family mimics increased proliferation compared with the NC transfection, particularly in the 5 mM butyrate-treated cells ($P = 0.0003$) (Figure 6.1). The miR-19 family transfection in the 5 mM butyrate-treated cells was shown to reverse the HDIs' anti-proliferative effect, and restored growth closer to that of the control medium NC-transfected cells. In contrast, transfection with miR-18a mimics decreased proliferation compared with the NC transfection, in the 5 mM butyrate-treated cells ($P = 0.04$) (Figure 6.1). Transfection with the entire miR-17-92 cluster did not increase proliferation to the same extent as miR-19 family transfection alone, and there was no significant difference compared with the NC transfection, in the 5 mM butyrate-treated cells ($P > 0.05$) (Figure 6.1).

A subsequent experiment was designed to further investigate the specific roles of miR-19 (a and b) and miR-18a in the context of decreased proliferation induced by HDIs. HT29 and HCT116 cells were transfected with mimics of miR-19 (a and b), miR-18a, the entire miR-17-92 cluster, the miR-17-92 cluster minus miR-18a, or a mimic NC. In the HT29 cells, transfection with miR-19 (a and b) or with miR-17-92 (minus miR-18a)

significantly increased growth compared with the NC transfection at 48 h, in cells treated with 5 mM butyrate (miR-19 family: $P = 0.01$; miR-17-92 (minus miR-18a): $P = 0.049$), 2 μM SAHA (miR-19 family: $P = 0.02$; miR-17-92 (minus miR-18a): $P = 0.046$), or with control medium (miR-19 family: $P = 0.007$; miR-17-92 (minus miR-18a): $P = 0.007$) (Figure 6.2). Similarly to the initial screen experiment, in the HDI-treated cells, this transfection with miR-19 (a and b) or miR-17-92 (minus miR-18a) reversed the HDIs' anti-proliferative effect and restored growth closer to that of the control medium NC-transfected cells. Transfection with miR-18a significantly decreased growth compared with the NC transfection at 48 h, in cells treated with 5 mM butyrate ($P = 0.01$) or control medium ($P = 0.02$) (Figure 6.2). Transfection with miR-17-92, including miR-18a, led to proliferation levels similar to those of NC-transfected cells for each of the control medium and HDI treatments ($P > 0.05$) (Figure 6.2). A similar effect was observed in the HCT116 cells, with miR-19 (a and b) or with miR-17-92 (minus miR-18a) significantly increasing growth compared with the NC transfection at 48 h, in both HDI-treated and untreated control ($P < 0.05$) (Figure 6.2). Also in the HCT116 cells, miR-18a or miR-17-92 (including miR-18a) significantly decreased growth compared with the NC transfection, in both HDI-treated and untreated control cells ($P < 0.05$) (Figure 6.2).

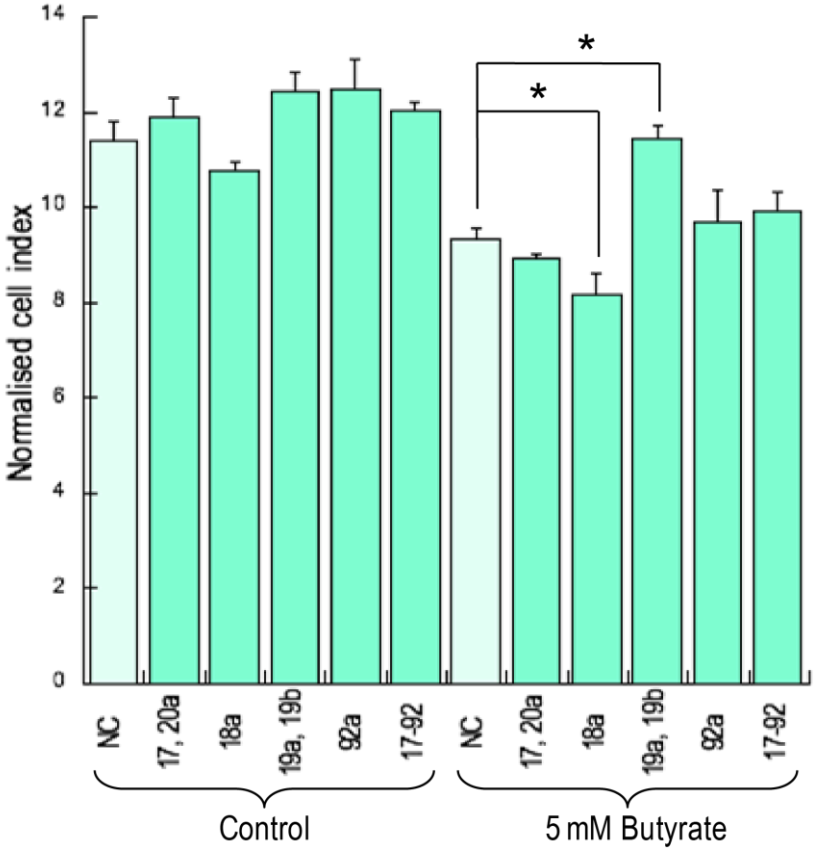

Figure 6.1: Proliferation of HT29 cells after transfection with miR-17-92 miRNAs and treatment with butyrate or control medium for 48 h

Cell index measurements using the xCELLigence RTCA DP instrument showing the different effects of miR-17-92 cluster members on proliferation, in the control medium and 5 mM butyrate-treated HT29 cells. The mean ± SEM of six cell culture replicates is shown.

NC: mimic negative control transfection; 17-92: entire miR-17-92 cluster transfection.

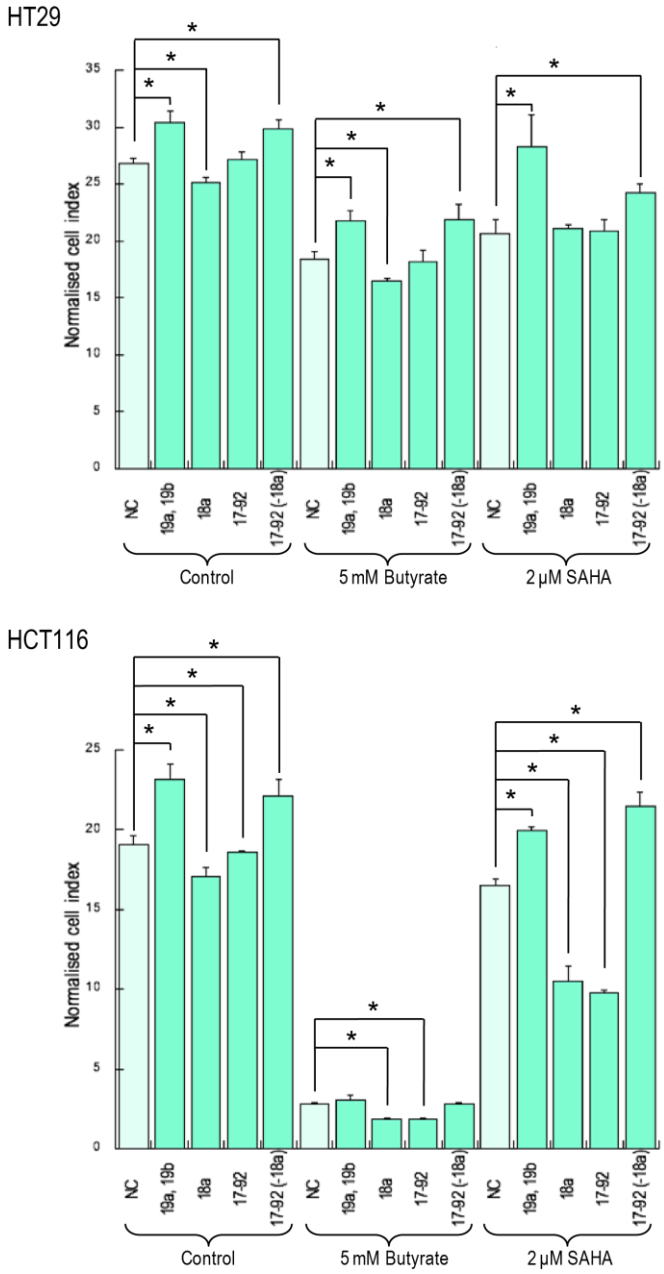

Figure 6.2: Proliferation of HT29 and HCT116 cells after transfection with miR-19 (a and b), miR-18a, miR-17-92 (minus miR-18a), or all miR-17-92 miRNAs and treatment with butyrate, SAHA or control medium for 48 h

Cell index measurements using the xCELLigence RTCA DP instrument in the 5 mM butyrate, 2 µM SAHA or control medium HT29 or HCT116 cells showing increased growth in cells transfected with miR-19 (a and b) or the entire miR-17-92 cluster (minus miR-18a), and decreased growth in cells transfected with miR-18a, compared with the NC transfection (* $P < 0.05$). The mean ± SEM of six cell culture replicates is shown. NC: mimic negative control transfection; 17-92: entire miR-17-92 cluster transfection; 17-92 (-18a): miR-17-92 cluster (minus miR-18a) transfection.

6.4.2 Expression of miR-17-92 validated target genes in colorectal cancer cells following transfection with miR-19 (a and b), 17, 20a, and 92a during HDI treatment

Following transfection with miR-17-92 cluster mimics in the presence or absence of 5 mM butyrate, mRNA levels of predicted target genes were quantified using real-time RT-PCR to confirm that individual miR-17-92 components contribute to their regulation. The decreased miR-17-92 expression in response to butyrate was already shown in Chapter 5 to correlate with increased transcript levels of miR-17-92 validated targets *CDKN1A*, *PTEN*, and *BCL2L11* (Figure 5.6). In the 5 mM butyrate-treated HT29 cells, transfection with the predicted regulator miR-19 (a and b) ($P = 0.02$) or with miR-92a ($P = 0.0002$) significantly down-regulated *PTEN* mRNA levels compared with the mimic NC transfection at 48 h, while transfection with miR-17 and miR-20a did not significantly change levels (Figure 6.3). Also in the 5 mM butyrate-treated cells, transfection with miR-17 and miR-20a ($P = 0.007$) or with miR-92a ($P = 0.008$) but not miR-19 (a and b) significantly down-regulated *CDKN1A* mRNA levels, and transfection with miR-19 (a and b) ($P = 0.006$) or with miR-92a ($P = 0.0004$) but not miR-17 and miR-20a significantly down-regulated *BCL2L11* mRNA levels (Figure 6.3). The same patterns of significant down-regulation were replicated in the HCT116 cells ($P < 0.05$) (Figure 6.4), with the exception of miR-92a transfection, which did not have a significant effect on *CDKN1A* or *PTEN* mRNA levels in this cell line ($P > 0.05$). Interestingly, miR-18a transfection was shown to increase *CDKN1A* mRNA levels in both cell lines treated with 5 mM butyrate ($P = 0.04$ in HT29 cells; $P = 0.01$ in HCT116 cells), with the magnitude of this change greater in the HT29 cells (Figure 6.3 and 6.4).

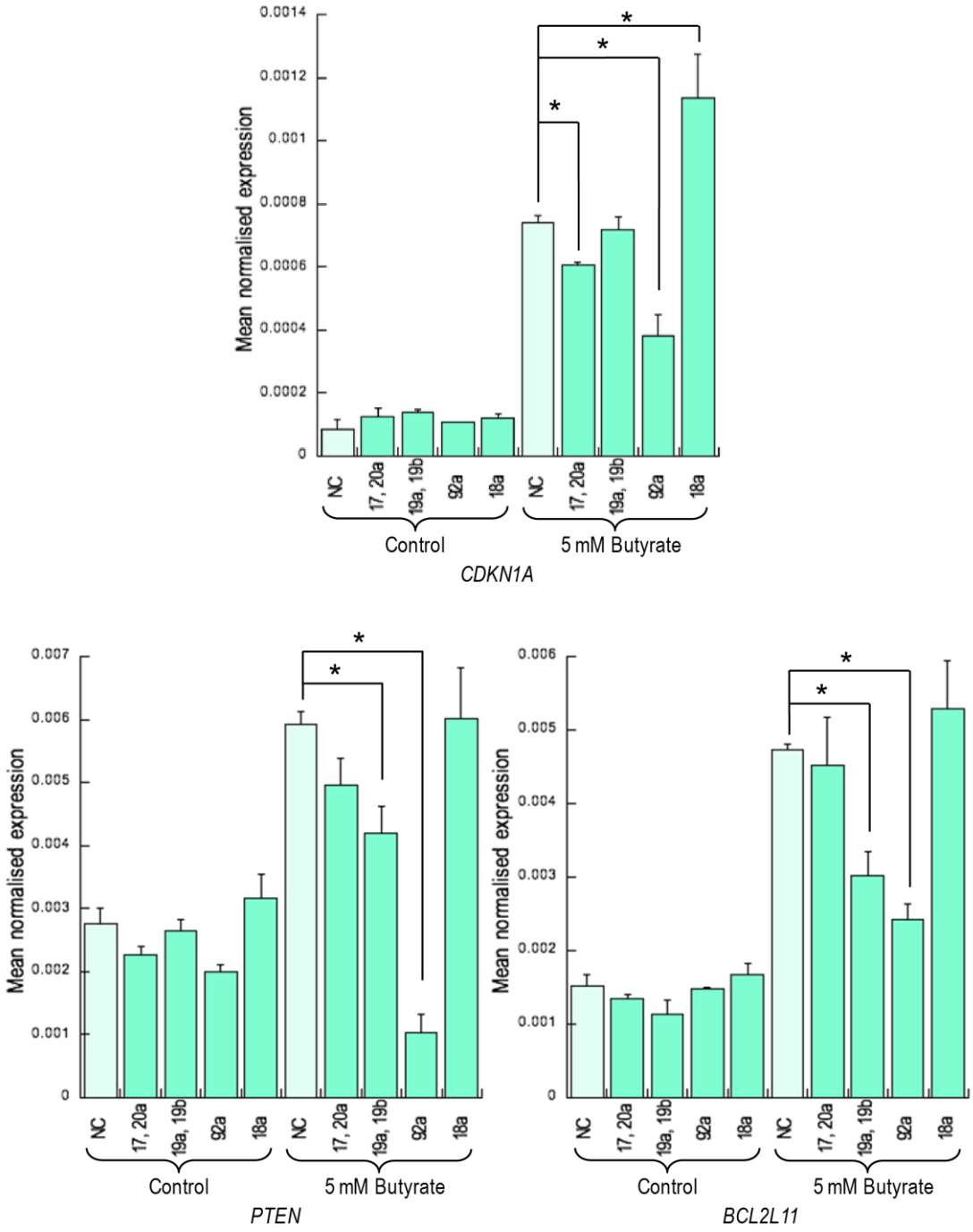

Figure 6.3: Target gene expression in HT29 cells after transfection with miR-17-92 miRNAs and treatment with butyrate or control medium

CDKN1A, *PTEN* and *BCL2L11* mRNA levels in HT29 cells transfected with individual miR-17-92 cluster members or NC, and treated with butyrate (5 mM) or control medium for 48 h (* $P < 0.05$). The mean ± SEM of three cell culture replicates is shown and expression normalised to *ACTB* levels. NC: mimic negative control transfection

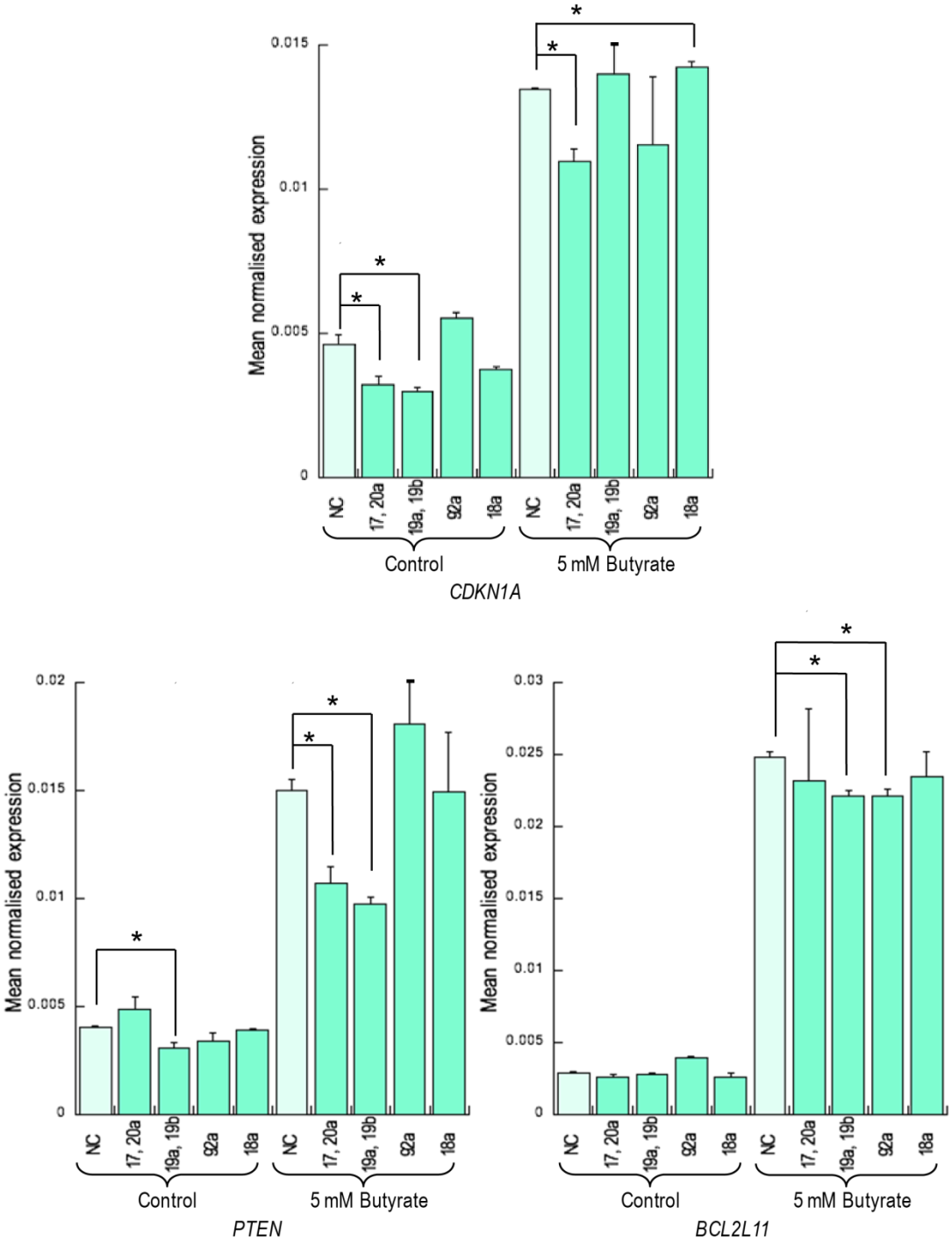

Figure 6.4: Target gene expression in HCT116 cells after transfection with miR-17-92 miRNAs and treatment with butyrate or control medium

CDKN1A, *PTEN* and *BCL2L11* mRNA levels in HCT116 cells transfected with individual miR-17-92 cluster members or NC, and treated with butyrate (5 mM) or control medium for 48 h (* $P < 0.05$). The mean ± SEM of three cell culture replicates is shown and expression normalised to *ACTB* levels. NC: mimic negative control transfection.

6.4.3 Expression of miR-18a predicted target genes in colorectal cancer cells following transfection with miR-18a during HDI treatment

While transfection with miR-19 (a and b), miR-17, miR-20a, and miR-92a mimics confirmed several cell cycle inhibitor and pro-apoptotic genes as validated targets, few validated target genes for miR-18a had been described in the literature. Potential miR-18a targets were identified using miRGen (Megraw et al 2007). Focusing on the intersection of genes common to two or more prediction programs led to the identification of 91 potential target genes. Ingenuity Pathway Analysis (IPA) detected genes involved in proliferation and cell cycle control, and expressed in colorectal cells. Details of the IPA analysis of potential miR-18a target genes are presented in Appendix 2. Such predicted target genes of miR-18a involved in cell cycle and proliferation pathways and expressed in colorectal cells included *CCDC88A* (coiled-coil domain containing 88A), *CDK19* (cyclin-dependent kinase 19), *GAB1* and *2* (GRB2-associated binding protein 1 and 2), *LIN28A* (lin-28 homolog A), and *NEDD9* (neural precursor cell expressed, developmentally down-regulated 9). Transfection with miR-18a mimics confirmed two of these genes, *NEDD9* and *CDK19*, to be likely targets. In the 5 mM butyrate-treated HT29 and HCT116 cells, transfection with miR-18a significantly down-regulated *NEDD9* ($P = 0.01$ in HT29 cells; $P = 0.03$ in HCT116 cells) and *CDK19* ($P = 0.02$ in HT29 cells; $P = 0.01$ in HCT116 cells) mRNA levels compared with the NC transfection at 48 h (Figure 6.5), and also decreased NEDD9 protein levels ($P = 0.04$ in HT29; $P = 0.03$ in HCT116) (Figure 6.6 and 6.7). A suitable antibody to detect CDK19 protein levels could not be obtained. Transfection with miR-18a did not significantly alter transcript levels of *CCDC88A*, *GAB1* and *2*, or *LIN28A* ($P > 0.05$), and these potential targets were not studied further.

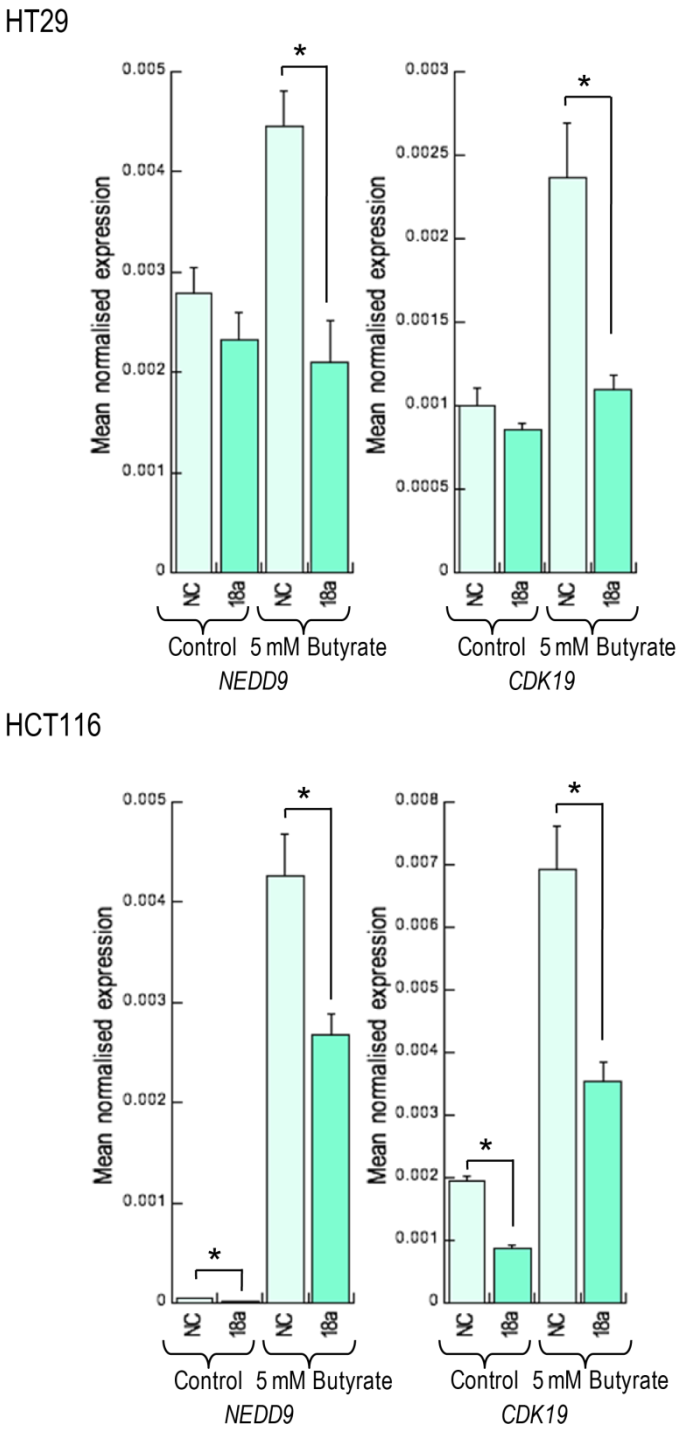

Figure 6.5: Target gene mRNA levels in HT29 and HCT116 cells after transfection with miR-18a and treatment with butyrate or control medium

mRNA levels of miR-18a predicted targets genes *NEDD9* and *CDK19* in cells transfected with miR-18a or NC mimics, and treated with butyrate (5 mM) or control medium for 48 h (* $P < 0.05$). The mean ± SEM of three cell culture replicates is shown and expression normalised to *ACTB* levels. NC: mimic negative control transfection.

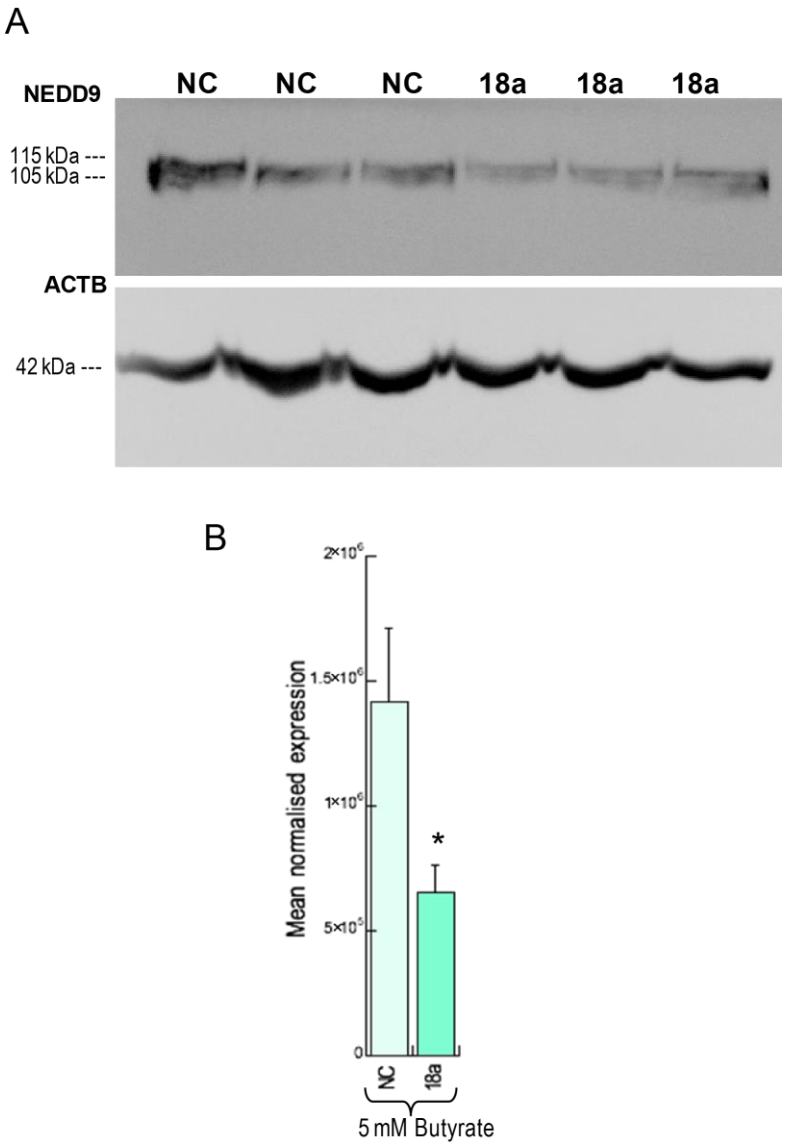

Figure 6.6: Target gene protein levels in HT29 cells after transfection with miR-18a and treatment with butyrate

NEDD9 protein levels in cells transfected with miR-18a or NC mimics, in the presence of 5 mM butyrate for 72 h, as measured by Western blot analysis using three cell culture replicates. Densitometry results were normalised to ACTB levels, and cells transfected with miR-18a were compared with NC cells (* $P < 0.05$). The mean ± SEM of three cell culture replicates is shown. NC: mimic negative control transfection.

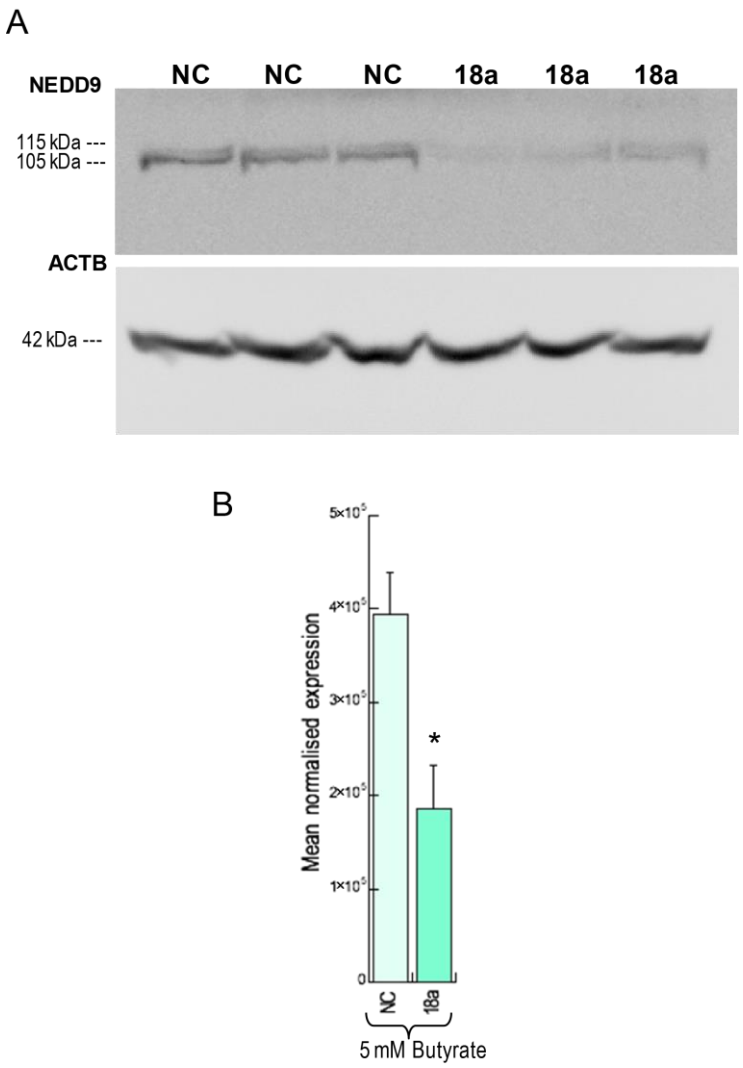

Figure 6.7: Target gene protein levels in HCT116 cells after transfection with miR-18a and treatment with butyrate

NEDD9 protein levels in cells transfected with miR-18a or NC mimics, in the presence of 5 mM butyrate for 72 h, as measured by Western blot analysis using three cell culture replicates. Densitometry results were normalised to ACTB levels, and cells transfected with miR-18a were compared with NC cells (* $P < 0.05$). The mean ± SEM of three cell culture replicates is shown. NC: mimic negative control transfection.

6.4.4 Validation of *NEDD9* and *CDK19* as miR-18a targets

Based on multiple target prediction algorithms, including TargetScan (Lewis et al 2003, Lewis et al 2005) and miRanda (John et al 2004), the 3'UTR of *NEDD9* contains four potential binding sites for miR-18a, while the 3'UTR of *CDK19* contains three (Figure 6.8 and 6.9).

To confirm that *NEDD9* and *CDK19* are directly targeted by miR-18a, miScript target protectors were employed. These single-stranded, modified RNAs specifically interfere with the interaction of a miRNA with a single endogenous target, while leaving the regulation of other targets of the same miRNA unaffected. Target protectors were designed for the four putative miR-18a binding sites on the *NEDD9* 3'UTR and three binding sites on the *CDK19* 3'UTR (Figures 6.8 and 6.9, Table 3.6), and a co-transfection experiment was performed to elucidate the precise functional role of miR-18a on these targets. A Negative Control miScript Target Protector was also used with no homology to any known mammalian gene. In HT29 and HCT116 cultures treated with 5 mM butyrate, transfection with the miR-18a mimic significantly down-regulated *NEDD9* ($P = 0.04$ in HT29 cells; $P = 0.001$ in HCT116 cells) and *CDK19* ($P = 0.02$ in HT29 cells; $P = 0.03$ in HCT116 cells) mRNA levels compared with the mimic NC transfection at 48 h (Figure 6.10). Addition of gene-specific target protectors shielded *NEDD9* and *CDK19* transcripts from miR-18a binding and regulation, and resulted in increased mRNA levels which were not significantly different from the NC transfection for both *NEDD9* ($P = 0.42$ in HT29 cells) and *CDK19* (P = 0.73 in HT29 cells, P = 0.22 in HCT116 cells), or were only slightly decreased compared with the NC transfection (*NEDD9* in HCT116 butyrate-treated cells; $P = 0.01$) (Figure 6.10). In the butyrate-treated cells, *NEDD9* transcripts were significantly decreased in the miR-18a transfected cells compared with the miR-18a plus *NEDD9* target protector co-transfected cells ($P = 0.03$ in HT29 cells; $P = 0.007$ in HCT116 cells), and *CDK19* transcripts were significantly decreased in the miR-18a transfected cells compared with the miR-18a plus *CDK19* target protector co-transfected cells ($P = 0.008$ in HT29 cells; $P = 0.01$ in HCT116 cells). Introduction of a negative control target protector did not protect *NEDD9* and *CDK19* from miR-18a binding and regulation (Figure 6.10). This supports the finding that *NEDD9* and *CDK19* transcripts are direct targets of miR-18a-mediated repression.

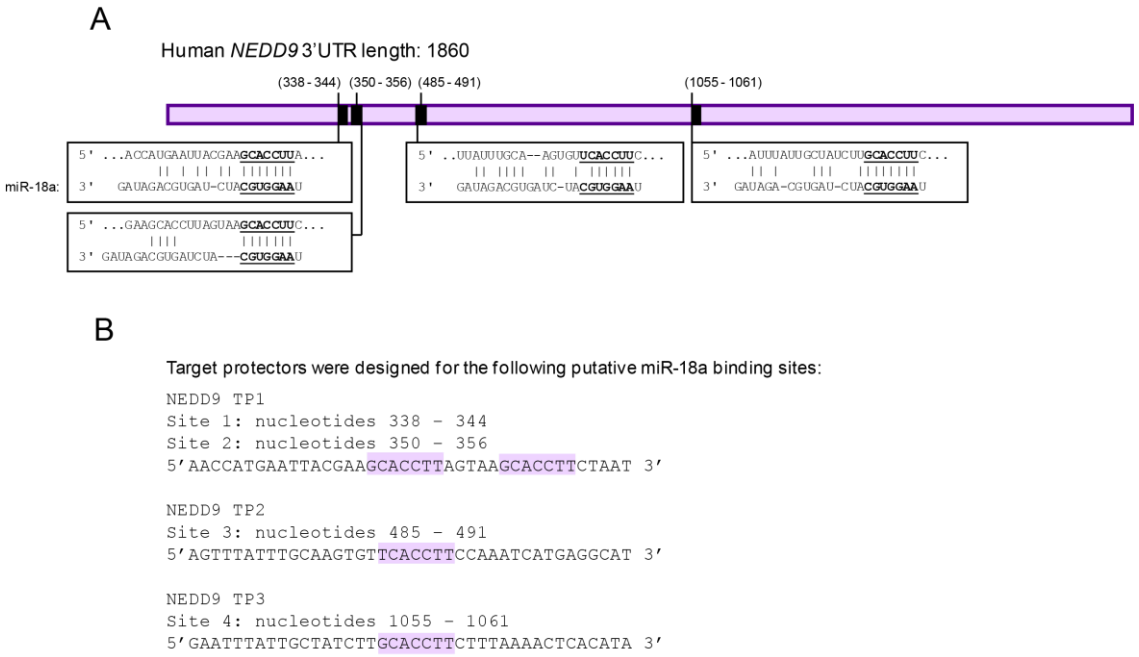

Figure 6.8: Schematic of the miR-18a seed region that targets the *NEDD9* 3'UTR at four sites, with designed target protector details

(A) Predicted miR-18a binding sites in the *NEDD9* 3'UTR. Underlined sequences represent the miRNA seed sequence. (B) Target protectors were designed to inhibit miR-18a binding to four predicted binding sites.

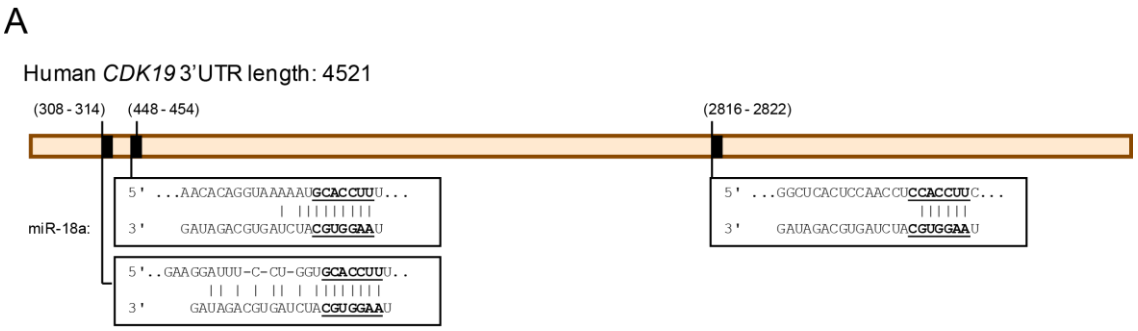

B

Target protectors were designed for the following putative miR-18a binding sites:

CDK19 TP1
Site 1: nucleotides 308 - 314
5'TTGAAGGATTTCCTGGTGCACCTTTCTCATGCTGTAGCAA 3'

CDK19 TP2
Site 2: nucleotides 448 - 454
5'GCAACACAGGTAAAAATGCACCTTTTAAAGCACTACGTTT 3'

CDK19 TP3
Site 3: nucleotides 2816 - 2822
5'TTGGCTCACTCCAACCTCCACCTTCCAGGTTCAAGTGATT 3'

Figure 6.9: Schematic of the miR-18a seed region that targets the *CDK19* 3'UTR at three sites, with designed target protector details

(A) Predicted miR-18a binding sites in the *CDK19* 3'UTR. Underlined sequences represent the miRNA seed sequence. (B) Target protectors were designed to inhibit miR-18a binding to four predicted binding sites.

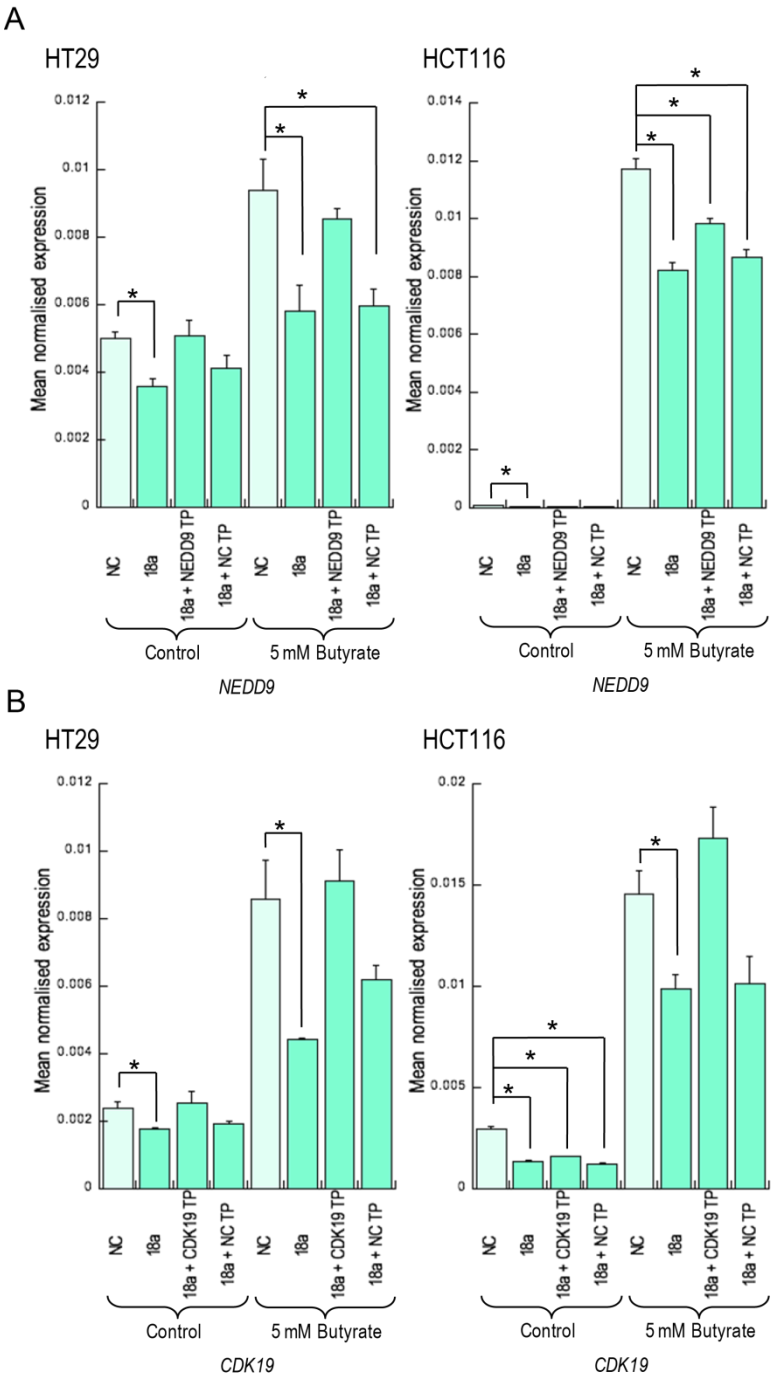

Figure 6.10: *NEDD9* and *CDK19* expression in butyrate-treated HT29 and HCT116 cells after co-transfection with miR-18a and specific target protectors.

mRNA levels of miR-18a target genes *NEDD9* (A) and *CDK19* (B) in cells co-transfected with miR-18a or NC mimics and with NCTP, NEDD9TP or CDK19TP target protectors, and treated with butyrate (5 mM) or control medium for 48 h (* $P < 0.05$). The mean ± SEM of three cell culture replicates is shown. CDK19TP: combined *CDK19* target protectors; NC: mimic negative control; NEDD9TP: combined *NEDD9* target protectors; NCTP: negative control target protector.

6.4.5 Confirmation of *NEDD9* and *CDK19* as genes that influence proliferation

To confirm that the miR-18a target genes could affect biological function in CRC cells, the roles of *NEDD9* and *CDK19* in altering proliferation of HT29 and HCT116 cells were examined. An RNA interference approach was used to knock-out the activity of these genes and determine the resultant effect in cell behaviour. Transfection with siRNAs targeting *NEDD9* significantly decreased growth compared with a negative control siRNA transfection at 48 h post-transfection, in cells treated with 5 mM butyrate ($P = 0.004$ in HT29; $P < 0.0001$ in HCT116) or control medium ($P = 0.002$ in HT29; $P = 0.02$ in HCT116) (Figure 6.11). Similarly, transfection with siRNAs targeting *CDK19* significantly decreased growth compared with a negative control siRNA transfection, in cells treated with 5 mM butyrate ($P = 0.0002$ in HT29; $P < 0.0001$ in HCT116) or control medium ($P = 0.006$ in HT29; $P = 0.02$ in HCT116) (Figure 6.11). As interference with these genes decreased proliferation, this indicates that *NEDD9* and *CDK19* contribute to proliferation in these cell lines.

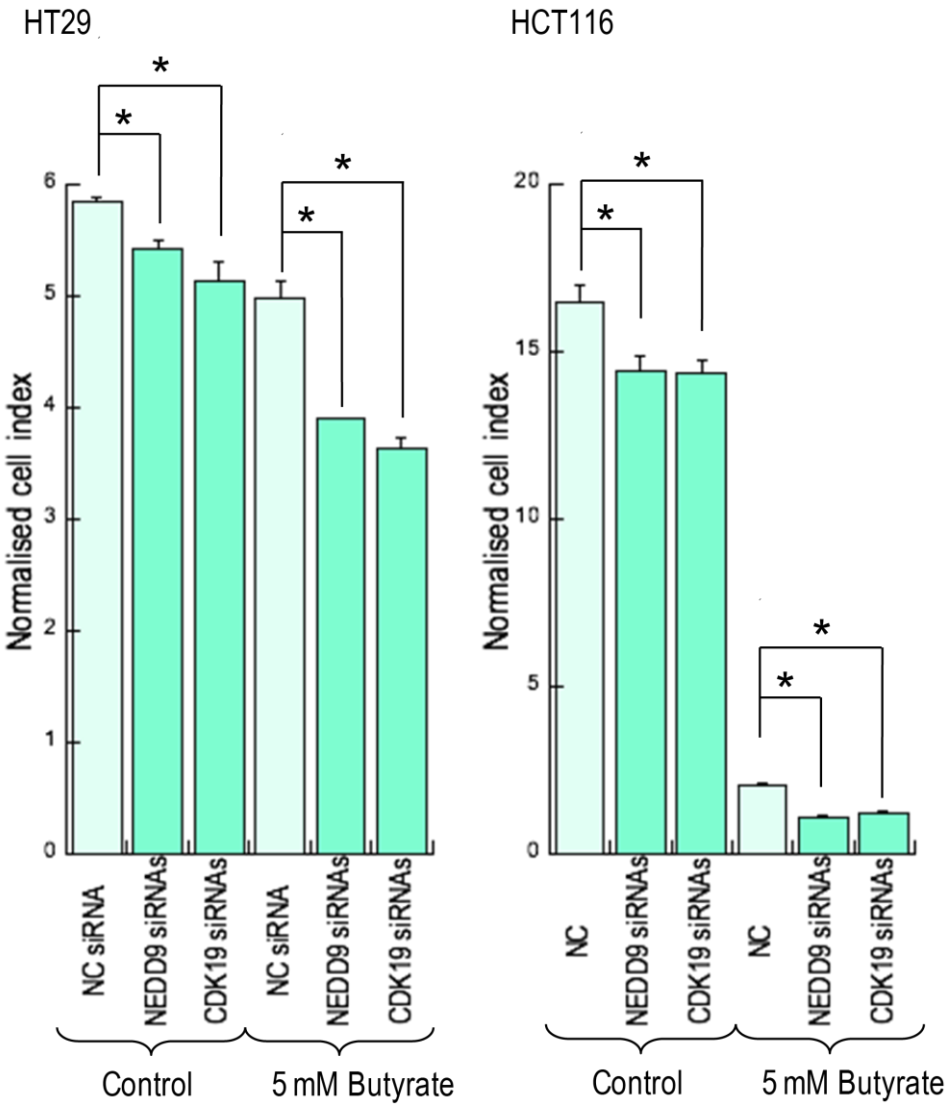

Figure 6.11: Effect of *NEDD9* and *CDK19* RNA interference on proliferation of HT29 and HCT116 cells

Cell index measurements at 48 h using the xCELLigence RTCA DP instrument in control medium or 5 mM butyrate cells showing decreased growth in cells transfected with siRNAs for *NEDD9* or *CDK19*, compared with the NC siRNA transfection (* $P < 0.05$). The mean ± SEM of four cell culture replicates is shown. NC siRNA: siRNA negative control

6.5 Discussion

This Chapter provided evidence to support the concept that miRNAs can mediate the effects of HDIs on gene expression. Decreased miR-17-92 expression may be partly responsible for the anti-proliferative effects of HDIs, as transfection with miR-17-92 miRNAs reversed this effect. As shown in the previous Chapter, in the context of a butyrate-induced reduction in miR-17-92 levels, *CDKN1A*, *PTEN*, and *BCL2L11* mRNA and protein levels were increased. In this Chapter, reversal of this butyrate effect through transfection with miR-19 (a and b), 17, 20a or 92a mimics decreased transcript levels of *CDKN1A*, *PTEN*, and *BCL2L11*, with various cluster members targeting different genes. The down-regulation of miR-17-92 and subsequent target gene de-repression is a plausible mechanism to explain some of the anti-proliferative and pro-apoptotic effects of HDIs, which may be additional to direct chromatin-mediated regulation of gene expression. This Chapter also identified competing roles of miR-17-92 cluster members in CRC cells. miR-19 (a and b) were primarily responsible for promoting proliferation, while miR-18a acted against the other miR-17-92 cluster members to decrease proliferation. Two targets for miR-18a were confirmed, *NEDD9* and *CDK19*. *NEDD9* and *CDK19* were shown in this Chapter to promote cellular proliferation, with repression of these genes by RNA interference reducing proliferation.

The effects of miR-17-92 have been examined in multiple development and disease models and various cancer types (Ventura et al 2008, Mu et al 2009, Olive et al 2009). A close link exists between deregulation of developmental programs and tumourigenesis, and studies have identified miR-17-92 as both a potential oncogene, and a crucial component of normal vertebrate development (Ventura et al 2008). While specific functions of miR-17-92 cluster miRNAs may be dependent on cell type and developmental context, this miRNA cluster has generally been shown to function during both normal development and oncogenic transformation to promote proliferation and angiogenesis, and inhibit differentiation and apoptosis (Olive et al 2010).

Ventura et al (2008) assisted in establishing a link between the oncogenic properties of miR-17-92 and its functions during normal development, in particular B lymphopoiesis and lung development. Their study found that deletion of miR-17-92 in mice led to neonatal lethality, and specific defects in the development of lungs (lung hypoplasia), heart (ventricular septal defect) and B-cells (inhibited B-cell development at the pro-B to pre-B transition). Absence of miR-17-92 also led to increased levels of the pro-apoptotic protein BCL2L11; *BCL2L11* was identified as a direct miR-17-92 target, and this

targeting was suggested to be a potential mechanism through which deletion or over-expression of miR-17-92 affected B-cell development and lymphomagenesis (Ventura et al 2008). Additional evidence for the role of miR-17-92 in normal development was provided by a study by de Pontual et al (2011), which identified hemizygous deletions of the miR-17-92 host gene in a group of human subjects with microcephaly, short stature and digital abnormalities. These features were replicated in a mouse model with targeted deletions in the miR-17-92 cluster, with mice hemizygous for miR-17-92 smaller than their wild-type littermates and harbouring digital abnormalities. Homozygous deletion of the miR-17-92 cluster host gene led to perinatal lethality, and examination of mouse embryos with this deletion revealed severe growth and skeletal defects. The study presented the first example of a miRNA gene, in this case the miR-17-92 host gene *MIR17HG*, being responsible for a syndromic developmental disorder in humans (de Pontual et al 2011). In various tissues, miR-17-92 levels have been found to be higher in early stages of development, then progressively decreased during later development (Lu et al 2007, Monzo et al 2008, Carraro et al 2009, Jevnaker et al 2011). These findings are consistent with the concept that the miR-17-92 cluster is fundamental to normal embryonic development (Jevnaker et al 2011). They are also consistent with the observation that dysregulation of miR-17-92 cluster miRNAs promotes abnormal growth and oncogenic transformation in mature cells. The role of miR-17-92 in normal lung and B-cell development can be linked with findings by He et al (2005a) in lymphoma and Hayashita et al (2005) in lung cancer. He et al (2005a) were among the first to describe oncogenic potential of miR-17-92 cluster, by finding that the mir-17-92 cluster acted with c-myc to accelerate tumour development in a mouse B-cell lymphoma model. Hayashita et al (2005) found that miR-17-92 over-expression also enhanced lung cancer cell growth. The pro-proliferative capacity of the cluster has since been shown in multiple cancers, including CRC. Monzo et al (2008), for example, found that the miR-17-92 cluster exhibited a similar pattern of high expression in human colon development and colonic carcinogenesis, increasing cell proliferation in both cases. Conversely, when differentiation of the epithelium occurred, expression of miR-17-92 miRNAs decreased. By regulating proliferation, the miR-17-92 cluster plays a particular role in both embryonic development and neoplastic transformation of the colonic epithelium (Monzo et al 2008).

The six mature miRNAs that form the miR-17-92 cluster likely act independently yet co-ordinately once cleaved from primary transcript, and different mRNAs may be targeted by a combination of miR-17-92 components varying in the degree of binding affinity

(Olive et al 2010). miR-17-92 cluster members may perform specific yet overlapping functions, and are unlikely to contribute equally to all the biological functions of the cluster (Ventura et al 2008). This current study was the first to show that individual miR-17-92 cluster members have opposing effects on proliferation in CRC cells. The HDI-mediated decrease in miR-17-92 levels was associated with decreased proliferation, while transfection with miR-19 (a and b) restored growth to a level closer to that of untreated cells in control medium. The study by Hu et al (2011) demonstrated that miR-106b can also inhibit butyrate's anti-proliferative effects, and can inhibit butyrate-induced *CDKN1A* expression. In this present study, the proliferation increase was similar in the HDI-treated cells transfected with miR-19 (a and b) or with the entire miR-17-92 cluster (minus miR-18a). miR-17, miR-20a, and miR-92a had little additional effect. When the entire miR-17-92 cluster (including miR-18a) was transfected, in the presence of a HDI, growth was still inhibited and similar to the respective NC-transfected cells, or even reduced (in the HCT116 cell experiment). miR-18a appears responsible for subduing the cluster's proliferative effect, and transfection with miR-18a alone reduced proliferation to levels lower than the NC-transfected cells. In the cells in control medium without HDI treatment, similar trends of increased proliferation with miR-19 (a and b) and decreased proliferation with miR-18a were apparent; however, this reached significance in some but not all experiments. If experiments are performed in cells with high endogenous miRNA levels, the effects of miRNA mimic over-expression on the target gene may not be detectable (Kuhn et al 2008); thus in these non-HDI-treated cells the effect of the mimics may have been masked by the existing high endogenous levels of miR-17-92 miRNAs. This was overcome with the HDI treatment which lowered endogenous miR-17-92 levels, and the different effects of the various miRNA mimics could be more clearly observed. The use of HDI treatment as a surrogate measure for knockdown of miR-17-92 miRNAs is a limitation of the study. Cell lines with low endogenous miR-18a levels could have been useful for the mimic experiments, and complete knockdown of individual miRNAs in the cluster using miRNA inhibitors may have provided further insight into their roles in proliferation.

Several other studies have dissected the functional roles of individual miR-17-92 cluster members in various cancer models (Takakura et al 2008, Mu et al 2009, Olive et al 2009, Mavrakis et al 2010). In lymphoma cells, miR-19 (a and b) have been shown to be primarily responsible for promoting growth and suppressing apoptosis (Mu et al 2009, Olive et al 2009). In thyroid cancer cells, inhibition of miR-17-3p, miR-17-5p, miR-19a, miR-19b, and miR-20a significantly reduced cell growth, whereas suppression of miR-

18a only moderately reduced cell growth, which the authors suggested may have been due to the miR-18a inhibitor binding weakly to miR-17-5p or miR-20a (Takakura et al 2008). Tsuchida et al (2011) found that miR-92a inhibition induced apoptosis of colon cancer-derived cell lines, while Bonauer et al (2009) presented a differing theory that miR-92a may repress pro-angiogenic genes in endothelial cells and ischaemic tissue. Despite these somewhat conflicting theories regarding the roles of miR-17-92 cluster members, miR-19 is consistently described as an oncogenic growth-promoting miRNA, which is in line with the findings in this Chapter.

Several studies are in agreement that among the six miR-17-92 cluster miRNAs, miR-19 (a and b) are the primary oncogenic determinants, and are required and largely sufficient for promoting the oncogenic properties of the cluster in lymphoma models (Mu et al 2009, Olive et al 2009). In vivo, miR-19 was required for promoting lymphomagenesis in an Eμ-myc mouse B-cell lymphoma model (Mu et al 2009, Olive et al 2009). miR-19 over-expression led to highly malignant early-onset B lymphomas, whereas disabling miR-19 biogenesis resulted in delayed tumour onset, incomplete penetrance, and extended life span (Olive et al 2009). Following miR-17-92 deletion in lymphoma cells, reintroduction of miR-19 alone restored growth and suppressed apoptosis (Mu et al 2009). Over-expression of miR-19b (but not miR-17, miR-18a, or miR-20a) *in vitro* significantly down-regulated PTEN mRNA and protein levels in mouse fibroblasts and primary B-cells (Olive et al 2009). Mavrakis et al (2010) presented a similar finding in acute lymphoblastic leukaemia cells, where miR-19b was sufficient to promote leukaemogenesis, and was shown to target *PTEN*, *BCL2L11*, and other tumour suppressors. This current study showed that the butyrate-induced decrease in miR-19 (a and b) corresponded with increased expression of the tumour suppressor genes, *PTEN* and *BCL2L11*, in CRC cells, while miR-19 (a and b) transfection partially reversed this increase.

While several studies have highlighted a key oncogenic role for miR-19 (a and b), there has been little research to date on the role of miR-18a in cancer. One study has identified the alternate product of the same precursor miRNA, miR-18a*, as a potential tumour suppressor in CRC cells (Tsang & Kwok 2009). Another study has indicated that miR-18a may potentially target genes associated with angiogenesis, including connective tissue growth factor (*CTGF*) which depending on cellular context can either promote or inhibit angiogenesis (Dews et al 2006). Since the completion of research for this Chapter, another study in a bladder cancer cell line has also used miRNA mimics to show that miR-18a suppressed cell proliferation (Tao et al 2012). miR-18a was also

shown to target Dicer in bladder cancer cells, which could indicate a potential feedback loop where the regulation of Dicer by miR-18a controls miRNA output and prevents over-expression. Knockdown of Dicer expression by siRNA mimicked the cell growth suppression induced by miR-18a over-expression in the bladder cancer cells (Tao et al 2012).

miR-18a may have a homeostatic function in helping to contain the oncogenic effect of the entire miR-17-92 cluster. While miR-19 subdued tumour suppressor gene expression, thus promoting proliferation, miR-18a was predicted to target and decrease expression of pro-proliferative genes, with this study identifying *NEDD9* as one such target. The NEDD9 protein (neural precursor cell expressed, developmentally down-regulated 9) (also known as human enhancer of filamentation 1 (HEF1) or CAS-L), is a member of the CAS family of scaffolding proteins (Law et al 1996, Minegishi et al 1996, O'Neill et al 2007). NEDD9 is a multi-domain scaffolding protein and an important integrin signalling adaptor, allowing integrin-dependent cell adhesion, migration, and invasion, and also modulation of proliferation and apoptosis (van Seventer et al 2001, Natarajan et al 2006). Genomic amplification and/or transcriptional up-regulation of *NEDD9* have been observed during cancer progression, and NEDD9 is abundant in epithelial derived tumour cells, lymphoma cells, and glioblastomas (Astier et al 1997, Natarajan et al 2006). Elevated *NEDD9* expression has been reported in CRC cell lines and primary tumours, with NEDD9 levels in human CRC found to increase with tumour grade (Li et al 2011b). Li et al (2011b) established NEDD9 as a mediator of the canonical WNT/β-catenin signalling pathway. Two studies in CRC cell lines have shown that *NEDD9* down-regulation reduced proliferation and in one study also inhibited xenograft tumour growth, while *NEDD9* over-expression increased proliferation and migration (Xia et al 2010, Li et al 2011b). *NEDD9* has previously been reported to be a putative target of miR-145 and miR-125b, both of which have potential tumour suppressor functions (Tran et al 2008). This Chapter has identified miR-18a as a novel regulator of *NEDD9*, and shown *NEDD9* to be pro-proliferative, with siRNA knockout of its transcript decreasing proliferation in CRC cells. This finding is consistent with current literature. Cell cycle control has been investigated more extensively in another CAS protein, BCAR1, with this protein shown to act as a scaffold for proteins necessary to support transition through G_1 phase and cell proliferation (Hakak & Martin 1999). NEDD9, as another CAS protein, is also likely to mediate growth factor-induced signals (Izumchenko et al 2009) and, as demonstrated by Li et al (2011b), Xia et al (2010) and this current Chapter, is able to promote proliferation.

The other identified miR-18a target, *CDK19* (also known as *CDC2L6*), has been less characterised, although it is a paralog of *CDK8* with sequence homology and functional similarities (Malumbres et al 2009). *CDK8* has been identified as a CRC oncogene that modulates β-catenin activity and promotes CRC cell proliferation (Firestein et al 2008). The kinase activity of CDK8 has been found to be necessary to regulate β-catenin dependent transcription and transformation (Firestein et al 2008). Like *NEDD9*, *CDK19* was also shown in this Chapter to be pro-proliferative, with siRNA knockout of its transcript decreasing proliferation in CRC cells.

Knockdown of *NEDD9* and *CDK19* induced growth arrest, suggesting a pro-proliferative role for these genes. Interestingly, in the butyrate treated cells which exhibit decreased growth, *NEDD9* and *CDK19* levels were actually increased, possibly due to the reduction in miR-18a levels in these treated cells. This discrepancy requires further investigation, but is likely to simply reflect the complexity of miRNA/mRNA interactions, where multiple miRNAs are modulated by butyrate, and in turn regulate many different target genes. In this situation, while a decrease in miR-18a may allow an increase in several pro-proliferative genes, this may be outweighed by a decrease in other miRNAs (such as the other miRNAs in the miR-17-92 cluster) that target anti-proliferative and pro-apoptotic genes.

Besides targeting pro-proliferative genes, the mimic transfection experiments revealed that miR-18a also appears to increase expression of the cell cycle inhibitor *CDKN1A*. It is possible that this is an indirect effect, and that miR-18a is targeting proteins which regulate *CDKN1A* transcription or expression. It could even be hypothesised that the miR-18a-induced decrease in NEDD9 could assist in this process; it has been suggested that NEDD9 possibly plays a role in the transcriptional repression of *CDKN1A* (Cabodi et al 2010).

This study confirmed *NEDD9* and *CDK19* as direct targets of miR-18a, and fulfilled the four criteria proposed by Kuhn et al (2008) for target validation. The miRNA/mRNA target pairs miR-18a and *NEDD9* and miR-18a and *CDK19* were validated by: verifying miRNA/mRNA target interaction using miRNA mimics and target protectors; ensuring predicted miRNA and mRNA target gene were co-expressed; determining that the miRNA decreased target mRNA and protein expression; and showing that the miRNA-mediated regulation of target gene expression equated to altered biological function, in this case proliferation. A limitation of the study was that while validated *NEDD9* and

CDK19 siRNAs were utilised, their knockdown efficiency was not specifically determined.

An additional limitation of this study was that similar amounts of each mimic were introduced by transfection, which may not reflect the relative stoichiometry of endogenous miRNA levels in colorectal cells. Several studies have noted differences in levels of expression of members of the miR-17-92 cluster (Venturini et al 2007, Diosdado et al 2009, Chaulk et al 2011, Jevnaker et al 2011). Jevnaker et al (2011) found that in a variety of cell types, miR-18a levels were lower than levels of some other members of the miR-17-92 cluster. In previous Chapters, miR-18a levels also appeared to be lower than levels of the other miR-17-92 cluster miRNAs in CRC cell lines (Figure 5.10); however as relative rather than absolute quantitation of the different amplicons was used in this real-time RT-PCR analysis, this can only be taken as a rough comparison of different miRNAs. In CRC cells, Diosdado et al (2009) described that DNA copy number gain of the miR-17-92 locus was associated with increased expression of all components of the miR-17-92 cluster except miR-18a. In chronic myeloid leukaemia cells transfected with a miR-17-19b construct (a variant of the miR-17-92 polycistron lacking miR-92a) to induce miRNA over-expression, expression of miR-17-5p, miR-17-3p, miR-19a, miR-20a, and miR-19b was increased by 2 to 5-fold, while miR-18a expression was not changed compared with the control cells (Venturini et al 2007). Monzo et al (2008) listed miR-17, miR-19, miR-20, and miR-92, but not miR-18a, among the miRNAs differentially expressed in CRC versus normal tissue, and also characteristic of early embryonic development in the colon. It is possible that tumour progression is associated with selection against the expression of miR-18a (Diosdado et al 2009), combined with selection for the other miRNAs in the cluster; thus in normal cells miR-18a may play a homeostatic role, while in cancer cells the elevation of other members of the miR-17-92 cluster may lead to increased oncogenic potential.

Specific processing of individual miRNAs within the polycistronic miR-17-92 cluster can lead to complex variations in miRNA expression and function in different cell types and contexts (Guil & Caceres 2007, Suarez et al 2008). Besides regulation of the miR-17-92 cluster by a network of transcriptional machineries, it is also further processed and regulated by post-transcriptional mechanisms (Guil & Caceres 2007). Following transcription of the pri-miRNA transcript, the first major processing step in miRNA biogenesis involves Drosha, as part of the microprocessor complex, releasing miRNA containing hairpins from the pri-miRNA (Gregory et al 2004). These pre-miRNAs are

then exported from the nucleus to the cytoplasm where the next major processing step involves Dicer cleavage to form the mature miRNA, which is incorporated into RISC (Hutvagner & Zamore 2002). Thomson et al (2006) were among the first to show that a large fraction of miRNA genes are regulated post-transcriptionally, and that expression levels of a primary transcript do not always correlate with levels of the mature miRNA. While many transcripts incorporate a single pre-miRNA stem-loop that is processed into a pre-miRNA and then a mature miRNA, the polycistronic miR-17-92 cluster represents an additional layer of complexity where miRNAs that are part of the same primary transcript are differentially processed (Chakraborty et al 2012). Thomson et al (2006) postulated that the widespread down-regulation of miRNAs observed in cancer may be due to a failure at the Drosha processing step; however this finding is of less relevance to the miR-17-92 cluster which, unlike many other miRNAs, is increased in cancer (Cummins et al 2006, Diosdado et al 2009). It is known that accessory proteins in addition to the microprocessor complex are sometimes required for processing of a primary transcript; such accessory proteins may provide a mechanism for the differential processing of the miR-17-92 cluster miRNAs (Guil & Caceres 2007, Chakraborty et al 2012).

Guil and Caceres (2007) suggested that an additional accessory protein is required specifically for processing of miR-18a from the primary transcript. A variety of RNA-binding proteins, collectively known as hnRNP proteins, have been shown to associate with transcribed mRNA and assist in the post-transcriptional control of gene expression. Among these is hnRNPA1 (heterogeneous nuclear ribonucleoprotein A1), which is involved in RNA transport and metabolism. When examining direct hnRNPA1 targets using cross-linking and immunoprecipitation, Guil and Caceres (2007) found a single miRNA, miR-18a, to be among these targets. hnRNPA1 was shown to bind specifically to human pri-miR-18a, the stem loop of miR-18a on the primary miR-17-92 transcript, and to facilitate its processing by Drosha. When hnRNPA1 was depleted using RNA interference, the production of pre-miR-18a was nearly totally suppressed, while processing of the other pre-miRNAs in the miR-17-92 cluster was not dependent on hnRNPA1 levels and still occurred when hnRNPA1 was depleted. The decrease in pre-miR-18a was concomitant with an accumulation of pri-miR-18a. As an assay for miR-18a activity, a luciferase-based reporter with a miR-18a target site was used where miR-18a expression decreased luciferase activity. This assay showed that depletion of hnRNPA1 resulted in de-repression of the luciferase mRNA and increased luciferase activity, indicating that hnRNPA1 was required for miR-18a repression of a functional

target. The authors hypothesised that binding of hnRNPA1 to the pri-miR-18a stem-loop structure could ensure the maintenance of an optimal secondary structure for DGCR8 (a subunit of the microprocessor complex) and Drosha recognition, or could also prevent the binding of an unknown inhibitory factor. They identified that hnRNPA1 was required for miR-18a binding only in a context dependent manner, where the pri-miRNA sequences on the miR-17-92 transcript surrounding pri-miR-18a were important in the requirement for hnRNPA1. It was proposed that the sequences and structure of the entire miR-17-92 primary transcript may create a suboptimal recognition site for DGCR8 and Drosha, and may make the processing of pri-miR-18a to pre-miR-18a dependent on hnRNPA1 (Guil & Caceres 2007). This was further examined by Michlewski et al (2008) who identified two hnRNPA1 binding regions: a primary site corresponding to the terminal loop of pri-miR-18a, and a secondary site corresponding to the bottom of the stem. Binding of hnRNPA1 to the stem structure in pri-miR-18a likely acted to unwind or rearrange the structure, creating a more favourable Drosha cleavage site. Binding to the terminal loop was also shown to be important for effective processing (Michlewski et al 2008).

Conflicting evidence exists for the role of hnRNPA1 in cancer. Several studies have shown hnRNPA1 to be increased in various cancer types, including CRC (Zerbe et al 2004, Ushigome et al 2005, David et al 2010); alternatively a recent study has shown that progression to breast cancer is associated with decreased hnRNPA1 (Pelisch et al 2012). Likewise, some studies have indicated a role for hnRNPA1 in increasing cell proliferation, decreasing apoptosis, and ensuring cell viability in response to stress (Patry et al 2003, He et al 2005b, Guil et al 2006), while another study has shown hnRNPA1 to have a suppressive effect on cell growth in prostate cancer (Yang et al 2007). Further study is required to determine hnRNPA1 activity in CRC, and the extent to which this protein impacts on miR-18a concentrations relative to other miR-17-92 cluster miRNAs in cancer.

Examination of the structure of the miR-17-92 primary transcript may offer additional mechanisms for the differential processing efficiencies of individual miR-17-92 cluster miRNAs despite their co-transcription (Chakraborty et al 2012). All six miRNAs contain the canonical secondary structure features for Drosha processing, and hairpins have similar levels of conservation. Thus tertiary structure could provide an explanation for the differential processing of individual miRNAs within the cluster (Chaulk et al 2011). While Guil and Caceres (2007) and Michlewski et al (2008) alluded to a role of the miR-17-92 transcript structure in the differential processing of miR-18a, the folding of the

pri-miR-17-92 transcript into a tertiary structure was further explored by Chakraborty et al (2012) and Chaulk et al (2011). Chakraborty et al (2012) hypothesised that the primary miRNA cluster transcript may self-orchestrate the binding of accessory proteins associated with processing different miRNA domains, allowing their differential regulation. The study used various biochemical and biophysical methods coupled with mutational studies, to show that pri-miR-17-92 adopts a defined higher-order tertiary structure. Folding of the RNA transcript into its tertiary structure may be facilitated by the conserved terminal loop sequences in miRNA domains (especially miR-19a and miR-18a), and also by intervening regions between the distinct pri-miRNA domains. Shuffling of the discrete pri-miRNA domains led to perturbed tertiary structure, and altered the relative abundance of the processed pre-miRNAs. The tertiary structure of pri-miR-17-92 poses a kinetic barrier to its own processing, with suboptimal display of recognition sites for the microprocessor complex. This may provide the opportunity for different proteins to bind and remodel the structure, and mediate an alternative processing fate for the primary miRNAs. For example, for the examined pri-miR-18a region, the authors found that this hairpin loop, including hnRNPA1 binding sites, is buried in the course of pri-miR-17-92a adopting its tertiary structure; specific protein binding to the tertiary structure may be required to unmask the hnRNPA1 binding sites and allow further remodelling (Chakraborty et al 2012).

Chaulk et al (2011) also reported that pri-miR-17-92 adopts a higher order compact structure, where the 5' region of the cluster folds on a 3' core domain. The miR-19b and miR-92a domains were within the protected 3' core, and the miR-18a domain was also protected inside the structure, while the other miRNA domains were more exposed. Internalised miRNA hairpins were processed less efficiently than those on the surface of the structure. Chaulk et al (2011) discussed the tertiary structure in relation to miR-17-92 cluster roles specifically in angiogenesis, where miR-92a has the opposite biological function to other miR-17-92 miRNAs, through a miR-92a mediated repression of some pro-angiogenic mRNAs. It is plausible that the suppressed expression of miR-92a through its sequestration within the cluster tertiary structure facilitates the overall pro-angiogenic effects of expression of miR-17-92 (Chaulk et al 2011). These inferences could similarly apply to miR-18a in the context of proliferation in cancer cells, where tertiary structure and specific protein binding results in miR-18a being processed less efficiently, and facilitates the pro-proliferative effects of the other miR-17-92 cluster members.

This Chapter identified competing roles of miR-17-92 cluster members in CRC cells, with miR-18a acting in opposition to other members of the oncogenic miR-17-92 cluster to suppress proliferation. miR-18a may play a potentially homeostatic role in containing the oncogenic effects of the entire cluster, but may be selectively decreased in CRC compared with other miR-17-92 cluster members. This imbalance is likely to promote the increased proliferation that is characteristic of cancer cells, and provides potential therapeutic opportunities.

Chapter 7. Butyrate alters miR-17-92 cluster transcription via specific histone modifications

7.1 Introduction

In previous Chapters, miR-17-92 cluster miRNA levels were shown to decrease in HT29 and HCT116 CRC cells when treated with the HDI butyrate. Also shown in Chapter 5 was one potential mechanism for this regulation, via HDI-induced decreases in regulatory proteins such as the transcription factor E2F1. It is also possible that HDIs like butyrate have a direct regulatory effect on transcription of the miR-17-92 host gene, via the epigenetic mechanism of histone modification.

7.1.1 Histone modifications and chromatin remodelling

Histone modifications influence chromatin remodelling, which regulates accessibility of the genetic sequence (Strahl & Allis 2000). The fundamental unit of chromatin consists of genomic DNA wrapped around histone proteins to form nucleosomes. Each nucleosome consists of approximately 147 base pairs of DNA, wrapped around a core histone octamer composed of two copies of each core histone protein (H2A, H2B, H3, and H4) (Luger et al 1997, Davey et al 2002). Consecutive nucleosomes are joined by a linker histone (H1), which protects the inter-nucleosomal linker DNA and contributes to chromatin structure (Bednar et al 1998). The N-terminal domains, and in some cases the C-terminal domains, of core histones protrude from the chromatin unit. These tails are rich in basic residues and are subject to multiple post-translational modifications (Luger et al 1997, Campos & Reinberg 2009). They can contact adjacent nucleosomes in higher chromatin order structure, and through various modifications can alter chromatin structure (Luger et al 1997, Strahl & Allis 2000, Hake et al 2004). There are two broad forms of chromatin; these are heterochromatin which is tightly compacted and associated with transcriptionally silent genomic regions, and euchromatin which has a more open conformation that is accessible to factors that bind DNA, allowing transcription. While euchromatin is less condensed, it still remains relatively nucleosome dense, and nucleosome remodelling and displacement is required for full access to the DNA (Ioshikhes et al 2006, Segal et al 2006, Workman 2006). Multiple levels of chromatin remodelling occur, and include DNA modification, histone modification,

exchange of core histones with variant histones, and disruption of basic nucleosome structure and histone DNA contacts (Hake et al 2004).

7.1.1.1 DNA modification

The predominant form of DNA modification is methylation, which is a covalent modification involving the addition of a methyl group to cytosine residues at adjacent cytosine and guanine nucleotides (CpG di-nucleotides). The transfer of a methyl group is catalysed by DNA methyltransferase enzymes, including DNMT1 which maintains existing DNA methylation patterns, and DNMT3A and DNMT3B which mainly target previously unmethylated areas (Bird 2002, Rodriguez-Paredes & Esteller 2011). CpG di-nucleotides, which are the usual targets of DNA methylation, are scattered in low concentration throughout the genome, but occur in high concentration in certain areas. These areas of approximately 1000 base pairs are referred to as CpG islands. CpG islands are often found at the 5' promoter region of genes, and around 60% of genes have a CpG island at their promoter (Bird 2002). DNA methylation of a CpG island at a gene promoter can lead to silencing of this gene, by directly inhibiting binding of transcription factors and by recruiting methyl-binding domain proteins, which are present in transcription co-repressor complexes (Boyes & Bird 1991, Cross et al 1997, Nan et al 1997, Nan et al 1998). These complexes can cause chromatin reconfiguration and gene silencing (Nan et al 1998). DNA methylation patterns are relatively stable in adult cells, with methylation used in normal cells for gene silencing, in such cases as silencing of large repetitive sequences (endogenous repeats, centromeres, and retrotransposon elements), inactivation of an X chromosome in women, or tissue-specific repression of germ cell-specific genes (Bird 2002, Rodriguez-Paredes & Esteller 2011). In cancer, DNA methylation is an alternative mechanism to genetic mutations for the silencing of tumour suppressor genes, and is likely an early event in tumourigenesis (Toyota et al 1999, Esteller et al 2001). In CRC, promoter-specific hypermethylation can be more frequent than genetic changes (Schuebel et al 2007). Examples of aberrant methylation in CRC and other cancers have been observed for genes with tumour suppressor function, such as cyclin-dependent kinase inhibitor 2A (*CDKN2A*), the DNA mismatch repair protein MutL homolog 1 (*MLH1*), and the DNA repair protein O-6-methylguanine-DNA methyltransferase (*MGMT*) (Toyota et al 1999, Shen et al 2005). A subset of CRCs display a CpG island methylator phenotype (CIMP), and includes the majority of sporadic CRCs with MSI related to *MLH1* methylation and silencing (Toyota et al 1999, Hawkins et al 2002, Weisenberger et al 2006). In contrast to the high levels of gene promoter methylation present in many tumours, global DNA

hypomethylation has also been observed in various cancers, including CRC, which may predispose to genomic instability and disruption of normal gene expression patterns (Matsuzaki et al 2005, Rodriguez et al 2006), and has also been linked to poorer prognosis in CRC (Ogino et al 2008). Regional DNA hypermethylation and global hypomethylation are associated with altered chromatin conformation and also with altered histone acetylation in CRC (Deng et al 2006).

7.1.1.2 Histone modifications and variants

Histone modification occurs largely at the tail domains that protrude from the chromatin unit. Covalent modification of tail domains of histones can include acetylation of lysine residues, methylation of lysine and arginine residues (mono-, di-, or tri-methylation of lysine and mono- or di-methylation of arginine), phosphorylation of serine and threonine residues, ADP-ribosylation, ubiquitination, sumolation, and others (Figure 7.1) (Hake et al 2004). Numerous enzymes are involved in histone modifications (Allis et al 2007, Kouzarides 2007). Levels of histone methylation, for example, are controlled by HMTs and HDMs. Levels of histone acetylation are controlled by opposing activities of HATs and HDACs (Chapter 5 presents a more detailed HDAC description). Acetylation of lysine residues directly relieves positive charges on histone N-terminal domains (Campos & Reinberg 2009). Generally, decreased acetylation (hypoacetylation) of histone N-terminals is a characteristic of more condensed heterochromatin, while increased acetylation (hyperacetylation) is found in more relaxed euchromatin (Strahl & Allis 2000). Additional layers of complexity exist, however, with distinct patterns of specific histone modifications shown to play particular roles in gene activation or silencing.

This complexity gave rise to the 'histone code' hypothesis, which was initially proposed by Strahl and Allis (2000). The basis of this epigenetic marking system is that one modification or combination of histone modifications can determine a particular functional output (Strahl & Allis 2000, Jenuwein & Allis 2001). The pattern of histone modifications in a given cellular and developmental context is regulated by histone-modifying enzymes that can carry out 'writing' or 'erasing' events (Chi et al 2010). An enzyme that catalyses a chemical modification of histones in a residue-specific manner, such as a HMT or HAT, can be referred to as a writer, while an enzyme that removes a chemical modification from histones, such as a HDM or HDAC can be referred to as an eraser (Strahl & Allis 2000, Jenuwein & Allis 2001, Chi et al 2010).

The subsequent effects of histone modifications can then be categorised as effector-mediated, intrinsic or extrinsic (Campos & Reinberg 2009). In the histone code hypothesis, histone modifications can be 'read', which is an effector-mediated event where effector proteins specifically bind to one or a combination of histone modifications (Chi et al 2010). This binding can lead to altered intra- and inter-nucleosomal dynamics and chromatin structure. There are numerous examples of effector proteins that recognise specific histone modifications, for example, effectors with chromodomains and PHD domains recognise methylated residues, and effectors with bromodomains recognise acetylated residues (Campos & Reinberg 2009). The Polycomb group (PcG) protein complex is an example of a well-studied effector, with a chromodomain that can 'read' methyl marks; this protein complex also contains domains that can modify histone marks (Fischle et al 2003, Cao & Zhang 2004, Flanagan et al 2005). PcG protein complexes and their marks are classically associated with repressed transcriptional states, while Trithorax Group (TrxG) proteins counteract the function of PcG proteins and thereby activate genes (Schuettengruber et al 2007, Hublitz et al 2009). In addition to effector-mediated events, histone modification can also directly modulate chromatin structure or alter intra-nucleosomal and inter-nucleosomal contacts through steric or charge interaction (Chi et al 2010). Modifications, or other intra-nucleosomal component variations, that directly alter physical nucleosome properties such as DNA contacts and motility, size and confirmation, or stability are intrinsic effects, while modifications that directly alter inter-nucleosomal contacts and chromatin structures are extrinsic effects (Campos & Reinberg 2009). A simple example of direct modulation is the aforementioned neutralization of the positive charges of histone N-terminal domains by lysine acetylation, leading to perturbation of histone-DNA contacts (Strahl & Allis 2000, Jenuwein & Allis 2001).

The outcomes of histone modifications can be to initiate transcriptional activation, silencing or other cellular responses (Strahl & Allis 2000, Jenuwein & Allis 2001). Initiation of transcription is clearly affected by chromatin remodelling that promotes accessibility to underlying DNA, and nucleosome placement can be predictive of transcription (Ioshikhes et al 2006, Segal et al 2006, Ozsolak et al 2007, Schones et al 2008). The open reading frames of genes are nucleosome dense, but in actively transcribed genes a short area flanking the transcription start site (TSS) may be partly histone-depleted compared to non-expressed genes (Koch et al 2007, Ozsolak et al 2007, Schones et al 2008). The same may apply to miRNA genes (Ozsolak et al 2008).

TSSs of active genes have been shown to have a characteristic signature of histone modification that is highly distinct from inactive genes, for example H3K4me3 and H3ac near the TSS (Koch et al 2007). It is generally agreed that correlations exist between several histone post-translational modifications and the transcriptional state of chromatin (Strahl & Allis 2000). Studies have observed that gene activation is correlated with tri-methylation of lysines 4, 36 or 79 on H3 (H3K4me3, H3K36me3 and H3K79me3), mono-methylation of lysines 20 on H4 and 5 on H2B (H4K20me and H2BK5me), and acetylation of lysines 9, 14, and 27 on H3 (H3K9ac, H3K14ac and H9K27ac), as well as other modifications; these may be referred to as activating histone marks. Conversely, gene repression is associated with di- or tri-methylation of lysine 9 on H3 (H3K9me2 and H3K9me3) and tri-methylation of lysine 27 on H3 and 20 on H4 (H3K27me3 and H4K20me3), as well as other modifications; these may be referred to as silencing histone marks (Strahl & Allis 2000, Jenuwein & Allis 2001, Barski et al 2007, Bhaumik et al 2007, Mikkelsen et al 2007, Rodriguez-Paredes & Esteller 2011).

In recent years there has been acknowledgement that the histone code hypothesis requires refinement (Berger 2007, Campos & Reinberg 2009). The outcome of a certain histone mark may to some extent be dependent on the biological context. The numerous combinations of histone modifications and complexity of the chromatin structure will also impact on the outcome. An example of this complexity is the existence of histone variants, which can contribute to the intrinsic and extrinsic properties of chromatin structure. While histones H4 and H2B are largely invariant, H3 and H2A variants have been shown to affect nucleosome stability and chromatin folding (Suto et al 2000, Hake et al 2004). Variants of linker histones can also be present. Another example of the complexity surrounding the outcome of histone modifications is the presence of cross-talk mechanisms between histone acetylation and histone methylation networks (Huang et al 2011), and links between DNA methylation and histone modification mechanisms (Nan et al 1998).

Controlled regulation of histone modifications determines cell fate during embryogenesis and development, and in adult cells allows fine-tuning of gene transcriptional output at gene loci during DNA damage repair or other cellular functions (Mikkelsen et al 2007, Chi et al 2010). In tumourigenesis, alteration in the homeostasis between activating versus silencing chromatin states leads to inappropriate expression or silencing of genes and altered cellular outcomes, for example, proliferation rather than senescence or differentiation (Chi et al 2010). In addition to DNA methylation changes, certain disruptions to normal patterns of histone modifications are also characteristic of

cancer development. An example observed in many primary tumours is global reduction of H4K20me3 and H4K16ac (Fraga et al 2005b). In CRC, changes in expression of active genes positive for H3K4me4, and repressed genes positive for H3K27me3 have been observed (Enroth et al 2011). There are also many instances of alterations in 'writer' and 'eraser' enzymes, and dysregulation of effector proteins. In CRC, for example, HAT and HDAC mutations and expression changes have been observed, with HDAC changes in CRC explored in Chapter 5. Changes in expression or activity of HMTs and HDMs may also occur. A HMT subunit of the PcG protein complex, for example, has been found to be over-expressed in a variety of different tumours, including CRC (Mimori et al 2005, Richly et al 2011). The 3D organisation of chromatin has also been shown to be important in the formation of chromosomal alterations and in cancer development. Distant genomic loci that are brought spatially close by 3D chromatin architecture during interphase are more likely to undergo structural alterations and become end points for amplifications or deletions observed in cancer (Fudenberg et al 2011).

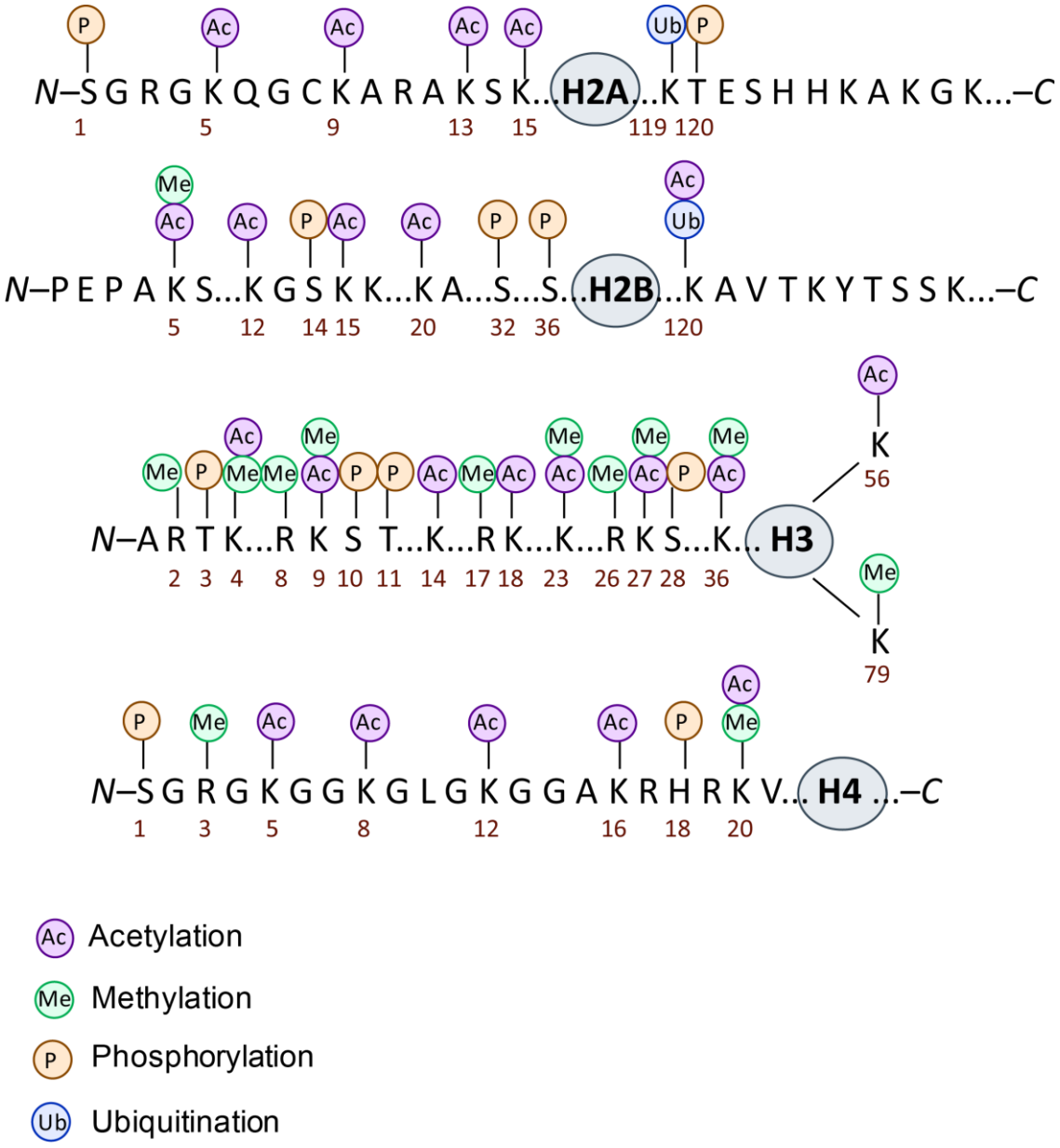

Figure 7.1: Possible post-translational histone modifications on N-terminal and C-terminal regions of the four core histones.

Possible acetylation, methylation, phosphorylation and ubiquitination of residues on core histones H2A, H2B, H3, and H4. K: lysine; R: arginine; S: serine; T: threonine.

7.1.2 Detection of histone modifications at the *MIR17HG* gene locus

Several studies have shown a role for epigenetics and chromatin modifications in miRNA expression in cancer cells (Saito et al 2006, Lujambio et al 2008, Toyota et al 2008, Bandres et al 2009, Choudhry & Catto 2011, Suzuki et al 2011). These studies have largely focused on DNA methylation patterns. Histone modifications may also play a role in the dysregulated expression of the miR-17-92 cluster in cancer cells. HDIs such as butyrate may have a direct effect on the transcription of the miR-17-92 host gene in cancer cells, via alteration of histone modification patterns. As a HDI, butyrate is known to alter acetylation, but also has other effects including acetylation of non-histone proteins, selective regulation of histone methylation and phosphorylation, and alteration of DNA methylation (Boffa et al 1981, Boffa et al 1994, Daly & Shirazi-Beechey 2006, Mathew et al 2010, Huang et al 2011, Marinova et al 2011).

The host gene of miR-17-92, *MIR17HG*, contains the miR-17-92 cluster in the third intron of the ~ 7 kb primary transcript (Ota et al 2004). A CpG island (CG content ~80%) exists less than 2 kb from the miR-17-92 pre-miRNA coding region, specifically within the region spanning 1.2 to 3.3 kb upstream of the first nucleotide of the pre-miR-17 sequence (O'Donnell et al 2005, Pospisil et al 2011, Suzuki et al 2011). This CpG island is located at the putative promoter region of *MIR17HG*, near the TSS (Suzuki et al 2011). Histone modifications at the promoter region and TSS may influence *MIR17HG* transcription.

Chromatin immunoprecipitation (ChIP) was used to investigate the possibility of a direct effect of butyrate on *MIR17HG* transcription through specific histone modifications. First developed in the 1980s (Gilmour & Lis 1984, Gilmour & Lis 1985, Gilmour & Lis 1986, Solomon et al 1988), ChIP is commonly used to study interactions between specific proteins or modified proteins and a genomic DNA region. This could include determining whether a transcription factor interacts with a candidate target gene, or whether histones with a specific post-translational modification are present at specific genomic locations (Carey et al 2009). Several variations on ChIP have been used in the literature, and specific ChIP kits are also supplied by several manufacturers. In addition to the examination of a specific genome region, variations of ChIP can also be used to study protein-DNA interactions at a genome-wide scale, via ChIP-chip and, more recently, ChIP-sequencing (ChIP-Seq) assays (Carey et al 2009). The experimental flow for a ChIP protocol to identify the presence of specific histone modifications at a DNA region of interest is shown in Figure 7.2. Briefly, this ChIP protocol consisted of cross-

linking of DNA and protein and subsequent digestion, detection of specific histone modifications using antibodies, precipitation using agarose beads, isolation of DNA, and quantitation using real-time qPCR. In this Chapter, a validated ChIP assay (Cell Signaling) was used to investigate the effect of butyrate treatment on the levels of histone acetylation and methylation. This used Micrococcal Nuclease for optimal chromatin digestion. ChIP relies on appropriate antibodies for detection (Haring et al 2007), and in this Chapter, antibodies that had been validated for ChIP were used. Real-time qPCR rather than standard PCR is recognised as best practice to analyse precipitated material (Haring et al 2007), and was used here. There is no consensus in the literature on how best to normalise and analyse ChIP-qPCR data; however a method referred to as the percent input method has been proposed as best practice (Haring et al 2007).

7.2 Aims

The aims of this Chapter were to determine the effect of butyrate on miR-17-92 host gene transcription, and specifically to investigate the effect of butyrate treatment on the levels of acetylation and methylation at DNA-bound histones surrounding *MIR17HG*, the miR-17-92 host gene.

7.3 Methods overview

Experiments were conducted according to the general methods outlined in Chapter 3.

7.3.1 Cycloheximide treatment

HT29 and HCT116 cell lines were used to determine the effects of butyrate treatment on miRNA expression, in the presence and absence of cycloheximide treatment to block *de novo* protein synthesis. All experimental groups were conducted in triplicate. For the cycloheximide treatment, cells were cultured with 5 μg/mL cycloheximide, which was added 3 h prior to other treatments, and again when cells were treated with butyrate or maintained in control medium. Both cycloheximide-treated and untreated cells were cultured with 5 mM butyrate or control medium for 48 h, total RNA was extracted from treated cells using the TRIzol method, and relative quantitation real-time qPCR analysis was performed on miR-17-92 cluster miRNAs.

7.3.2 ChIP analysis of activating histone methylation and acetylation marks

HT29 cells were also used for ChIP, to observe the effect of butyrate treatment on activating histone methylation and acetylation marks around the miR-17-92 cluster host gene, *MIR17HG*. The experimental flow for the ChIP experiment is shown in Figure 7.2. Cells were treated with 5 mM butyrate or control medium for 48 h, followed by cross-linking of proteins and associated chromatin using formaldehyde. Nuclei were isolated, and Micrococcal Nuclease was used to digest chromatin. An optimisation experiment was performed to determine the appropriate amount of Micrococcal Nuclease stock. The digested chromatin was clarified and viewed using agarose gel electrophoresis to determine optimal digestion. The digested chromatin was then diluted, and a 2% input sample removed for later real-time qPCR analysis. Subsequently, the diluted chromatin was incubated overnight with the positive control rabbit monoclonal Histone H3 (D2B12) XP (ChIP Formulated) and the negative control Normal Rabbit IgG, as well as the antibodies of interest including rabbit polyclonal anti-acetyl-histone H3 (Lys 9/ Lys 14), rabbit polyclonal anti-acetyl-histone H3 (Lys 27), and rabbit polyclonal anti-tri-methyl histone H3 (Lys 4). The antibody-bound chromatin fragments were then captured with agarose beads, and this immunoprecipitated chromatin washed and eluted, and cross-links reversed. DNA was purified using a column method, and real-time qPCR carried out to quantify the purified DNA for each immunoprecipitation sample. For the real-time qPCR, twelve primer pairs were designed to target intron and exon regions of the *MIR17HG* gene, as well as to target up to 4 kB upstream of the TSS. A control primer provided by the manufacturer for human ribosomal protein L30 (*RPL30*) Exon 3 was also used. PCR reactions were performed for each primer pair, for the histone samples of interest, the positive control Histone H3 sample, the negative control Normal Rabbit IgG sample, a tube with no DNA to control for contamination, and a serial dilution of the 2% input chromatin DNA (undiluted, 1:5, 1:25, 1:125).

Real-time qPCR data were normalised and analysed using the percent input method. With this method, signals obtained from each immunoprecipitation were expressed as a percent of the total input chromatin. In addition, an alternative method of analysis was used to compare outcomes, with expression levels normalised to the 2% starting input fraction using Qgene, which took into account the efficiency of amplification using a serial dilution standard curve.

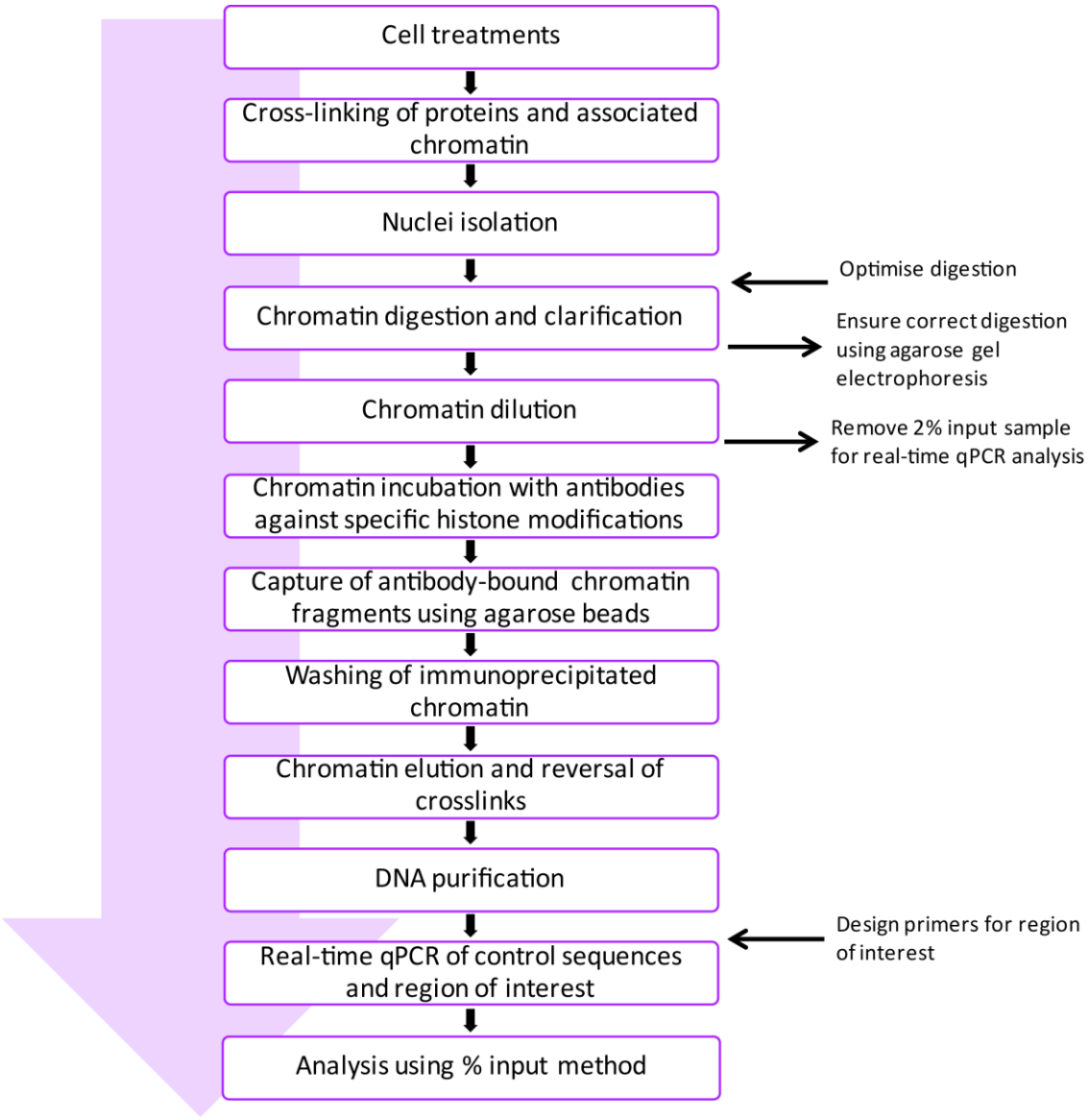

Figure 7.2: Experimental outline of the chromatin immunoprecipitation (ChIP) procedure used to analyse histone acetylation and methylation patterns at the *MIR17HG* locus.

7.4 Results

7.4.1 Real-time RT-PCR of miR-17-92 changes in colorectal cancer cells treated with butyrate, in the presence or absence of cycloheximide

Experiments in which HT29 and HCT116 CRC cell lines were treated for 48 h with butyrate, or maintained in control medium, were conducted simultaneously in cells that had been treated with 5 μg/mL cycloheximide 3 h prior to other treatments. Cycloheximide interferes with the translocation step in protein synthesis and blocks translational elongation (Schneider-Poetsch et al 2010). This concentration of cycloheximide has been shown in previous experiments in HT29 CRC cells to block *de novo* protein synthesis (Della Ragione et al 2001, Andoh et al 2002). It can be used to distinguish between primary responses to butyrate and downstream events, as the inhibition of *de novo* protein synthesis allows the observation of transcriptional effects only (Della Ragione et al 2001, Williams et al 2003). It could be hypothesised that if the decrease in miR-17-92 levels in response to butyrate is mediated by other regulator proteins and is reliant on new factors, then treatment with 5 mM butyrate would have less effect on miRNA expression in the cycloheximide treated cells where *de novo* protein synthesis is inhibited. The alternative hypothesis is that if the decrease in miR-17-92 levels is a primary transcriptional response to butyrate, this response will be similar in the cell lines with and without cycloheximide treatment.

Cells treated with cycloheximide had different morphology to the standard cells after 48 h, with fewer visible membrane protrusions (filopodia). Real-time RT-PCR analysis showed all of the miR-17-92 cluster miRNAs to be significantly down-regulated by 5 mM butyrate treatment for 48 h, in both standard HT29 and cycloheximide-treated HT29 cells (standard HT29: miR-17: $P = 0.0005$; miR-18a: $P = 0.0001$; miR-19a: $P = 0.0002$; miR-20a: $P = 0.0002$; miR-19b: $P = 0.0002$; miR-92a: $P = 0.0003$; cycloheximide treated HT29: miR-17: $P = 0.47$; miR-18a: $P = 0.002$; miR-19a: $P = 0.006$; miR-20a: $P = 0.0009$; miR-19b: $P = 0.002$; miR-92a; $P = 0.0009$) (Figure 7.3). The exception to this was miR-17, which was not significantly decreased in the cells treated with butyrate in the presence of cycloheximide. Real-time RT-PCR analysis also showed all of the selected miR-17-92 cluster miRNAs to be significantly down-regulated by 5 mM butyrate in both standard HCT116 and cycloheximide-treated HCT116 cells (standard HCT116: miR-17: $P = 0.0002$; miR-18a: $P < 0.0001$; miR-19a: $P = 0.0002$; miR-20a: $P < 0.0001$; miR-19b: $P < 0.0001$; miR-92a: $P = 0.0003$; cycloheximide treated HCT116:

miR-17: $P = 0.008$; miR-18a: $P = 0.002$; miR-19a: $P = 0.005$; miR-20a: $P < 0.0001$; miR-19b: $P = 0.001$; miR-92a: $P = 0.0007$) (Figure 7.4). Differences could be observed, however, between the butyrate-induced miRNA expression changes in the standard and cycloheximide-treated cells, with the decrease in miR-17-92 expression greater in the cells that were not treated with cycloheximide, for both cell lines (Figures 7.3 and 7.4).

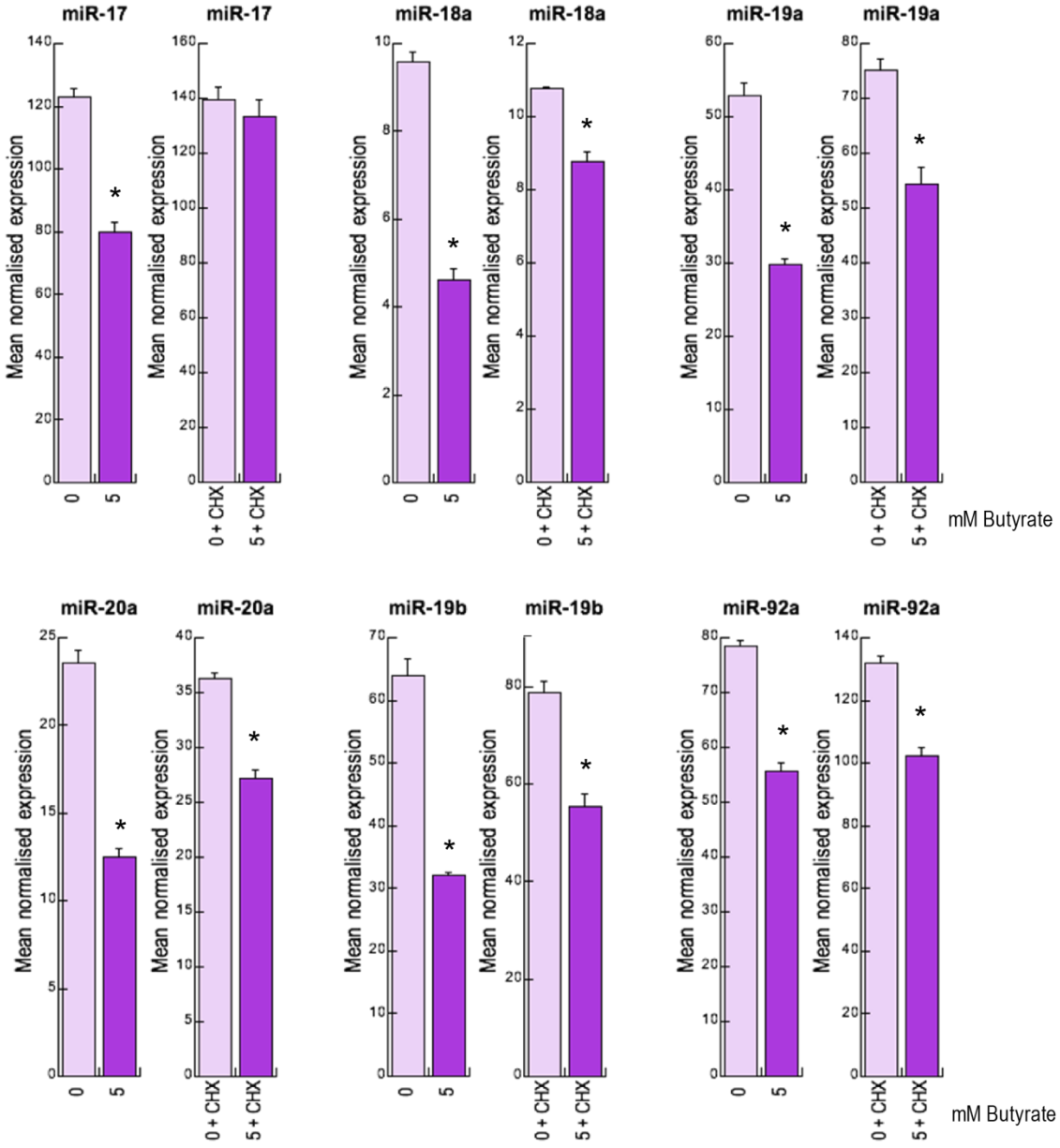

Figure 7.3: Real-time RT-PCR validation of miR-17-92 cluster changes in HT29 cells after 48 h of butyrate treatment, in the absence or presence of cycloheximide

miR-17-92 cluster miRNA levels in cells treated with butyrate (5 mM) compared with cells in control medium (0), in the absence or presence of 5 μg/mL cycloheximide (CHX) (* $P < 0.05$). The mean ± SEM of three cell culture replicates is shown, and expression is normalised to RNU6B levels.

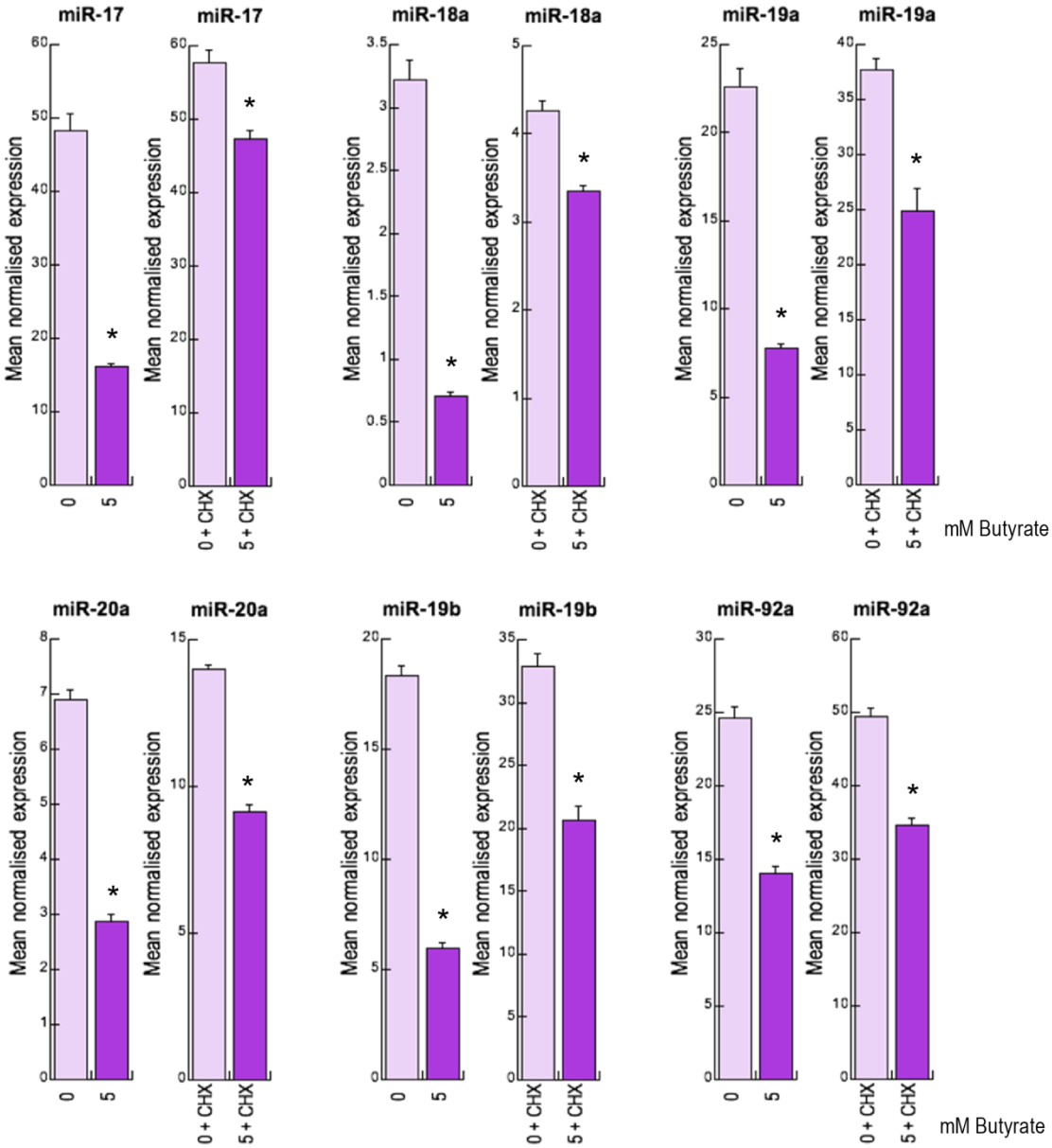

Figure 7.4: Real-time RT-PCR validation of miR-17-92 cluster changes in HCT116 cells after 48 h of butyrate treatment, in the absence or presence of cycloheximide

miR-17-92 cluster miRNA levels in cells treated with butyrate (5 mM) compared with cells in control medium (0), in the absence or presence of 5 μg/mL cycloheximide (CHX) (* $P < 0.05$). The mean ± SEM of three cell culture replicates is shown, and expression is normalised to RNU6B levels.

7.4.2 ChIP analysis of butyrate-induced H3 histone modifications – preparatory experiment (*MIR17HG* primer design)

Following the cycloheximide experiments, which indicated that the butyrate-induced decrease in miR-17-92 miRNAs in CRC cell lines may, in part, be due to direct transcriptional regulation, the epigenetic effect of butyrate on miR-17-92 host gene transcription was examined further using ChIP. Specifically, histone acetylation and methylation patterns were examined at the miR-17-92 host gene, *MIR17HG*, including the activating histone acetylation marks H3K9ac, H3K14ac, and H3K27ac, and the activating histone methylation mark H3K4me3. The final analysis of a ChIP experiment can be performed using real-time qPCR, which is the preferred method over conventional PCR to analyse the precipitated material (Haring et al 2007). Before performing the ChIP experiment, primers for real-time qPCR were designed to span the regions of interest. The forward and reverse primers were designed to amplify a representation of each intron and exon region of the *MIR17HG* gene, and also up to 4 kb upstream of the gene, to cover the potential promoter region and TSS (Suzuki et al 2011). Where possible, *MIR17HG* gene primer pairs that had been designed and validated in previous studies were used (Table 3.6) (O'Donnell et al 2005, Pospisil et al 2011); in addition, to cover all regions of the gene and the upstream region, several new primer pairs were designed using Primer Express Software, with adherence to the criteria outlined in Section 3.1.11.8. Dissociation curve analysis for each primer pair confirmed that each reaction produced a single specific product as indicated by a single dissociation curve peak. The PCR amplification efficiency of each primer pair was determined from a standard curve, using serial dilutions of the 2% input sample from the subsequent ChIP experiment. Efficiency should be as close to 2 (100%) as possible. Eight primer pairs had an ideal efficiency of 1.9 – 2.0, two primer pairs had efficiency of 1.8 (3 and 5), and two primer pairs (7 and 9) had efficiency of 2.1 – 2.2. The location of the primer pairs can be seen in Figure 7.5, with the primers spanning the upstream regions, potential promoter region and TSS, and introns and exons of *MIR17HG*.

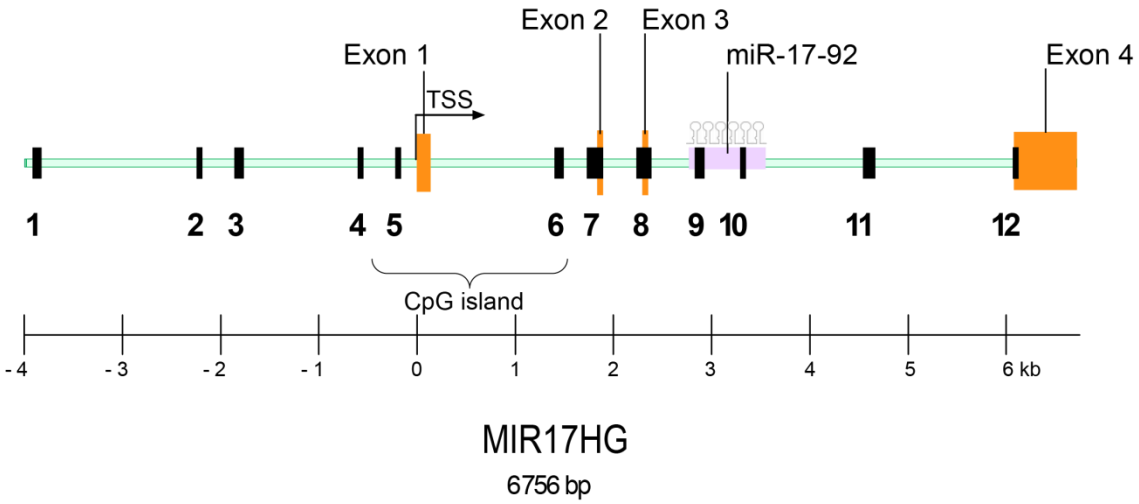

Figure 7.5: Location of primer pairs for amplification of the *MIR17HG* gene and upstream region, including the proximal promoter region and TSS.

Black bands indicate the positions of primers utilised for amplification of DNA fragments spanning the region 4 kb upstream of the *MIR17HG* TSS, and the region within *MIR17HG*, including introns and exons. The miR-17-92 cluster sequence is located in the third intron of *MIR17HG* (purple box). A CpG island is located at the putative promoter region of *MIR17HG*, near the TSS (1.2 to 3.3 kb upstream of the first nucleotide of the pre-miR-17 sequence) (Pospisil et al 2011, Suzuki et al 2011). TSS: transcription start site.

7.4.3 ChIP analysis of butyrate-induced H3 histone modifications – preparatory experiment (micrococcal nuclease optimisation)

In ChIP experiments, the cross-linked chromatin can be sheared by sonication or digested by nucleases (Haring et al 2007). For this ChIP protocol, the SimpleChIP Enzymatic Chromatin IP kit (Cell Signaling) used Micrococcal Nuclease stock (2000 gel units/μL) to digest the chromatin. Before performing ChIP on the butyrate-treated and control HT29 cells, optimal conditions for digestion of cross-linked DNA to 150 – 900 base pairs in length were determined according to the manufacturer's instructions. For the optimisation, cross-linked nuclei from 4×10^7 HT29 cells was obtained, and digested using 0 μL, 2.5 μL, 5 μL, 7.5 μL or 10 μL of diluted Micrococcal Nuclease (1:5 dilution from stock of 2000 gel units/μL). Following subsequent sonication to break nuclear membranes, DNA fragment size was determined by agarose gel electrophoresis. The manufacturer advised that chromatin DNA should be sheared into mono-, di-, tri-, tetra- and penta-nucleosome units of 150 – 900 base pairs in length (Cell Signaling). From the agarose gel shown in Figure 7.6, the enzyme volume which produced DNA in the desired range of 150 – 900 base pairs was determined to be the 2.5 μL volume of diluted Micrococcal Nuclease. This is equivalent to the volume of Micrococcal Nuclease stock required to be added to the to 4×10^7 cells in the subsequent experimental chromatin digestion; thus 2.5 μL Micrococcal Nuclease stock (2000 gel units/μL) was used for the subsequent ChIP experiment.

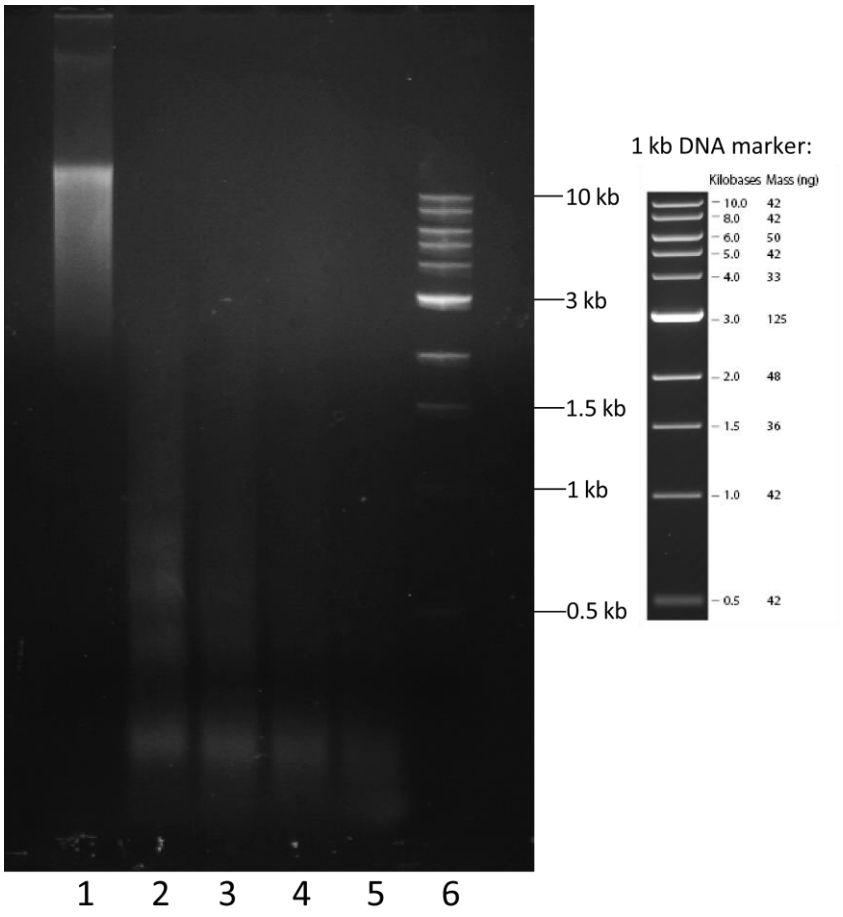

Figure 7.6: Agarose gel electrophoresis analysis of HT29 chromatin digestion optimisation using increasing concentrations of Micrococcal Nuclease

Chromatin was digested using 0 μL, 2.5 μL, 5 μL, 7.5 μL or 10 μL of diluted Micrococcal Nuclease (1:5 dilution from stock of 2000 gel units/μL). DNA was purified and separated by electrophoresis on a 1% agarose gel and stained with ethidium bromide. Lane 1 has the undigested chromatin (0 μL), lane 2 – 5 has increasingly digested chromatin (2.5 μL, 5 μL, 7.5 μL, 10 μL Micrococcal Nuclease), and lane 6 has the 1 kb DNA marker. Lane 2 shows that the majority of chromatin was ideally digested to 1 to 5 nucleosomes in length (150 – 900 bp) using 2.5 μL Micrococcal Nuclease. bp: base pairs; kb: kilobases.

7.4.4 ChIP analysis of butyrate-induced H3 histone modifications at the *MIR17HG* locus

ChIP was used to determine the effect of 5 mM butyrate treatment for 48 h on the levels of acetylation and methylation at DNA-bound histone H3 at the locus of *MIR17HG*, the miR-17-92 host gene, in the HT29 CRC cell line. Specifically, the activating histone marks H3K9ac, H3K14ac, H3K27ac, and H3K4me3 were examined.

Cross-linking, nuclei preparation and nuclease digestion of chromatin were performed for 4×10^7 cells grown in control medium or 5 mM butyrate for 48 h. Agarose gel electrophoresis was used to assess the chromatin digestion, prior to performing immunoprecipitations. The manufacturer provided an example agarose gel showing ideal chromatin appearance on a 1% agarose gel stained with ethidium bromide (Figure 7.7A), with chromatin DNA sheared into mono-, di-, tri-, tetra- and penta-nucleosome units of 150 – 900 base pairs in length (Cell Signaling). For this nuclease digestion of chromatin from control and butyrate-treated cells, the agarose gel also shows that optimal DNA digestion was achieved using 2.5 μL Micrococcal Nuclease (2000 gel units/μL), with fragment lengths of 150 – 900 base pairs in length (Figure 7.7B). According to the manufacturer, the digested chromatin DNA concentration is typically at 125 – 250 μg/mL with various cell types, and for this experiment was in this concentration range.

ChIP was performed on the digested chromatin samples, and immunoprecipitation samples were further processed and purified for real-time qPCR. The manufacturer advised that PCR results will vary based on PCR primer sets and antibodies used. Experiments were designed with appropriate positive and negative control antibodies and also primers, to ensure that the PCR reaction is properly amplifying and the signal obtained is real, as per the Cell Signaling protocol. In addition to the antibodies of interest including rabbit polyclonal anti-acetyl-histone H3 (Lys 9/ Lys 14), rabbit polyclonal anti-acetyl-histone H3 (Lys 27), and rabbit polyclonal anti-tri-methyl histone H3 (Lys 4), the positive control rabbit monoclonal Histone H3 (D2B12) XP (ChIP Formulated) and the negative control Normal Rabbit IgG was also used. For the real-time qPCR, in addition to primers for *MIR17HG*, a control primer provided by the manufacturer for human ribosomal protein L30 (*RPL30*) Exon 3 was also used. Results were analysed using the percent input method which is the most accepted method (Haring et al 2007), and are presented in this Chapter. An alternative analysis method using Q gene, which takes into account amplification, showed nearly identical findings.

Positive ChIP enrichments can range from as little as 0.5% total input chromatin to as high as 40 – 50% total input chromatin, depending on the protein examined. When the Human *RPL30* Exon 3 control primer is used, the manufacturer advised that for the positive control rabbit monoclonal Histone H3 (D2B12) XP (ChIP Formulated) enrichment of the *RPL30* promoter should be between 2 to 4% of the total input chromatin. In this experiment, for the positive control Histone H3, enrichment of the *RPL30* promoter was 2.2% and 2.4% for the control medium and butyrate treatments respectively, which is in the appropriate range (Figure 7.8). When the Human *RPL30* Exon 3 control primer is used, background enrichment with the negative control Normal Rabbit IgG should be less than 0.1% of the total input chromatin. In this experiment, for the negative control Normal Rabbit IgG, enrichment of the *RPL30* promoter was 0.1% and 0.1% for the control medium and butyrate treatments respectively, which is in the appropriate range (Figure 7.8).

ChIP detected histone acetylation and methylation patterns at the *MIR17HG* locus for control and butyrate-treated HT29 cells, using 12 *MIR17HG* primer pairs (Figure 7.9). In the butyrate-treated cells, there was decreased acetylation of H3K9/H3K14 and H3K27, specifically centred around the proximal promoter and TSS of *MIR17HG*, compared with the cells in control medium (Figure 7.9A and B). Regions for primers 4 to 6 showed decreased H3K9/14ac, corresponding to the region -0.5 to +1.5 kb from the TSS; regions for primers 4 to 7 showed decreased H3K27ac, corresponding to the region -0.5 to +1.8 kb from the TSS. Further upstream and downstream of this promoter and TSS region, in butyrate-treated cells there was increased H3K9ac/H3K14ac and H3K27ac, compared with the cells in control medium. Also in the butyrate-treated cells, there was decreased tri-methylation of H3K4, again centred around the proximal promoter and TSS of *MIR17HG*, compared with the cells in control medium (Figure 7.9 C). Regions for primers 2 and 4 to 7 showed decreased H3K4me3, corresponding to the region -2.2 to +1.8 kb from the TSS. Further upstream and downstream of this promoter and TSS region, H3K4me3 was similar in the butyrate-treated cells and cells in control medium. These results are summarised in Figure 7.10, as percent change in histone acetylation and methylation patterns with butyrate treatment relative to control. This clearly demonstrates that compared to control, butyrate treatment led to a specific decrease in H3K9ac/H3K14ac, H3K27ac and H3K4me3 purely around the promoter and TSS region of *MIR17HG*, but tended to increase these histone modification marks at other regions. These modifications are

activating histone marks, and their decrease can correspond to direct transcriptional repression.

The ChIP results obtained with the positive control Histone H3 antibody were also used to examine whether butyrate treatment affected distribution of total histone H3. There was little change in the total histone H3 levels in the butyrate-treated HT29 cells compared with the cells in control medium, at any region of the *MIR17HG* locus examined (Figure 7.11).

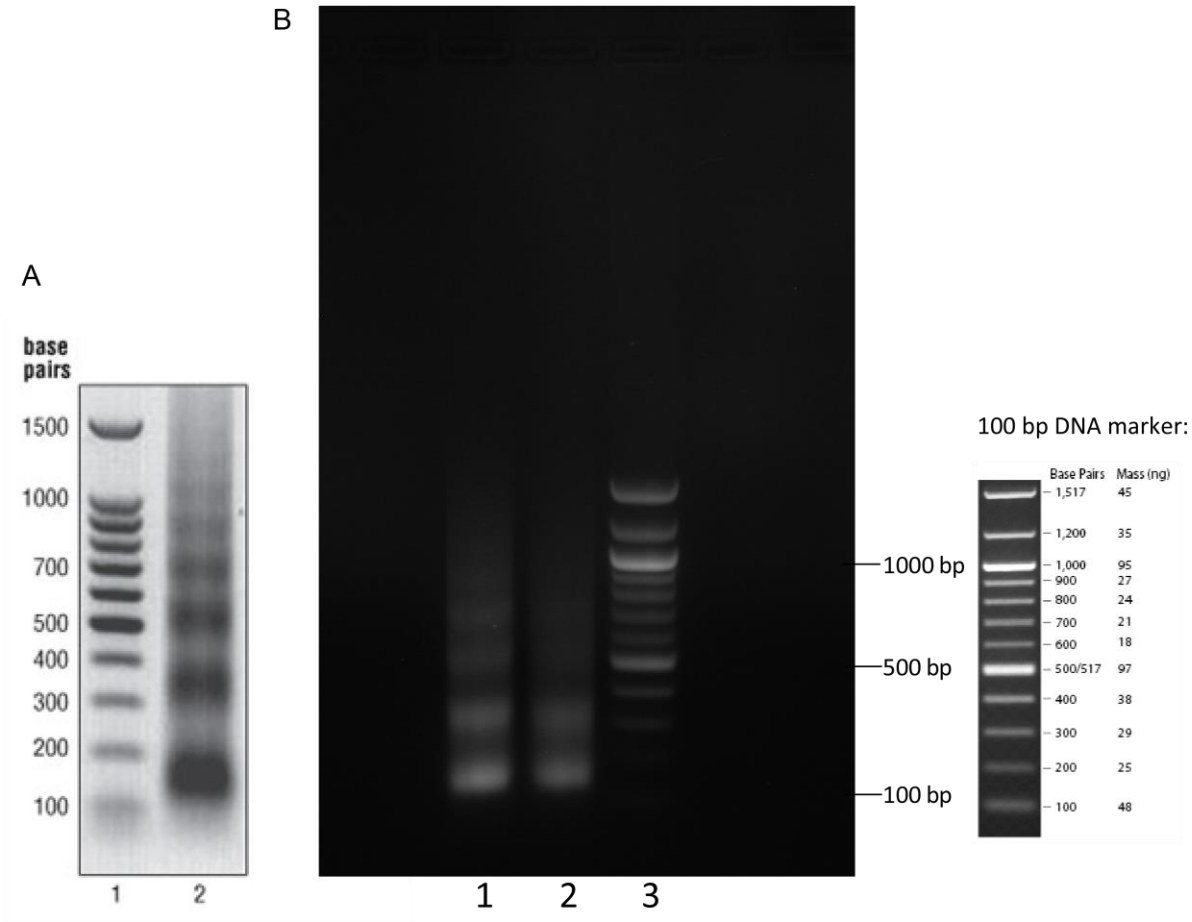

Figure 7.7: Agarose gel electrophoresis analysis of chromatin digestion of control and butyrate-treated HT29 cells, using optimised concentration of Micrococcal Nuclease

(A) Manufacturer example of a gel analysis illustrating optimal chromatin digestion in Lane 2 (Cell Signaling). (B) Chromatin was digested using 2.5 μL of Micrococcal Nuclease stock (2000 gel units/μL), purified, separated by electrophoresis on a 1% agarose gel and stained with ethidium bromide. Lane 1 has the digested chromatin from cells in control medium, lane 2 has the digested chromatin from 5 mM butyrate-treated cells, and lane 3 has the 100 bp DNA marker. For both samples, the majority of chromatin was ideally digested to 1 to 5 nucleosomes in length (150 – 900 bp). bp: base pairs.

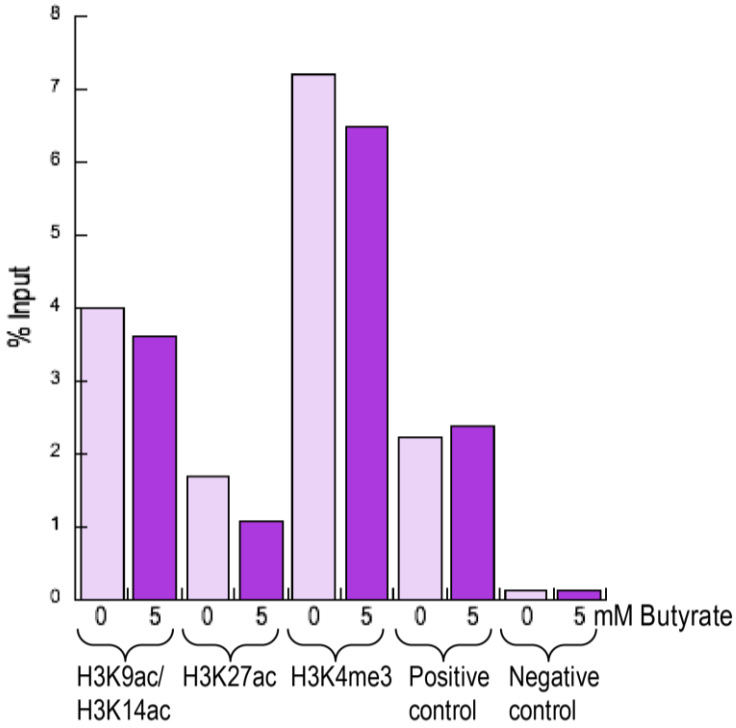

Figure 7.8: Real-time qPCR analysis of chromatin immunoprecipitation using Human *RPL30* Exon 3 control primer set, for control and butyrate-treated HT29 cells

Chromatin immunoprecipitations were performed using digested chromatin from control and butyrate-treated cells and rabbit polyclonal antibodies for histone modification of interest (H3K9ac/H3K14ac, H3K27ac, H4K4me3), positive control rabbit monoclonal Histone H3 (D2B12) XP (ChIP Formulated) and negative control Normal Rabbit IgG. Results analysed using the percent input method, where the amount of immunoprecipitated DNA in each sample is represented as signal relative to the total amount of input chromatin. Analysis from pooled cell culture replicates (4×10^7 cells from n = 8 plates) for control and butyrate-treated cells.

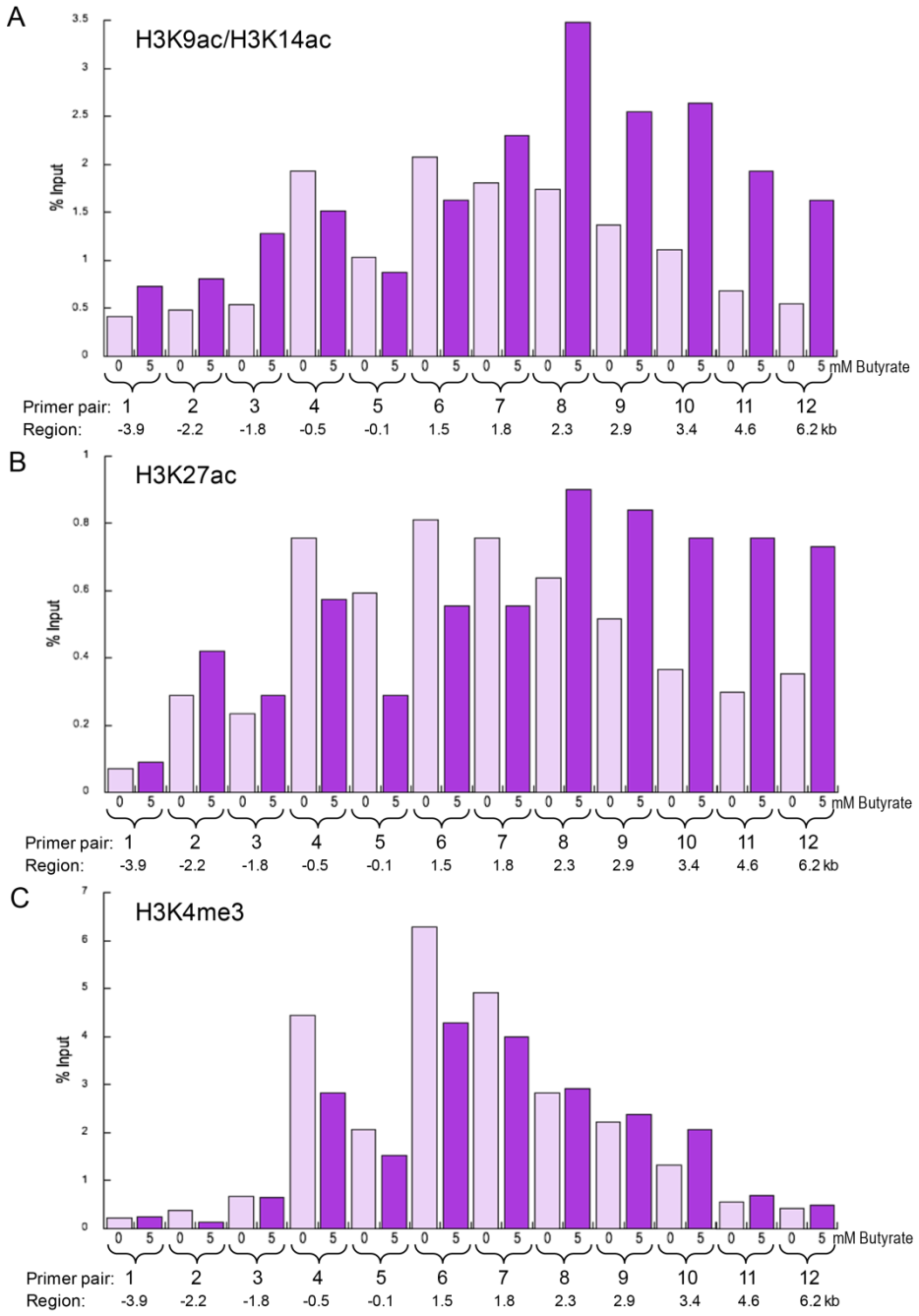

Figure 7.9: Real-time qPCR analysis of chromatin immunoprecipitation to detect histone acetylation and methylation levels at *MIR17HG* locus for control and butyrate-treated HT29 cells

Chromatin immunoprecipitations were performed using digested chromatin from control and 5 mM butyrate-treated cells and rabbit polyclonal antibodies for H3K9ac/H3K14ac (A), H3K27ac (B), and H4K4me3 (C). Results analysed using the percent input method, where the amount of immunoprecipitated DNA in each sample is represented as signal relative to the total amount of input chromatin. Analysis of pooled cell culture replicates (4×10^7 cells from n = 8 plates) for control and butyrate-treated cells. Kb: kilobases.

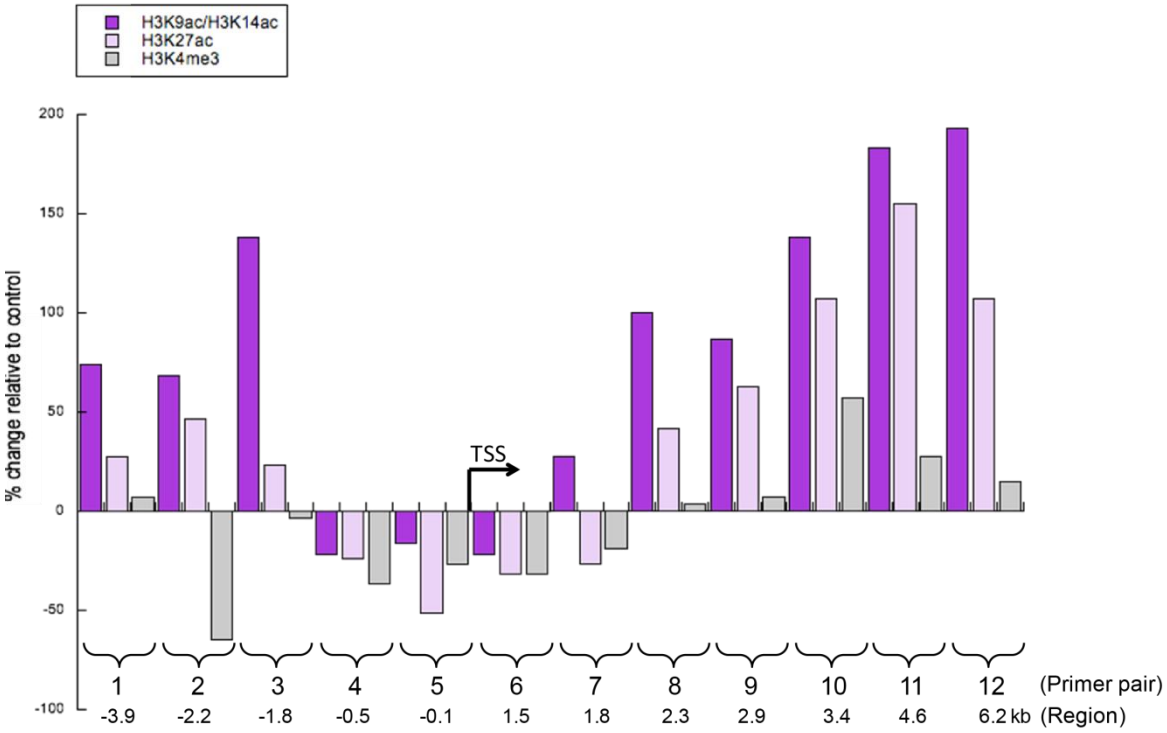

Figure 7.10: Summary of changes in histone acetylation and methylation distribution surrounding *MIR17HG* in butyrate-treated HT29 cells compared with control cells

Chromatin immunoprecipitations were performed using digested chromatin from control and 5 mM butyrate-treated cells and rabbit polyclonal antibodies for histone modifications of interest (H3K9ac/H3K14ac, H3K27ac, and H4K4me3). Results analysed using the percent input method, and levels in butyrate cells presented as percent change from control cells. Analysis from pooled cell culture replicates (4×10^7 cells) for control and butyrate-treated cells. Kb: kilobases, TSS: transcription start site.

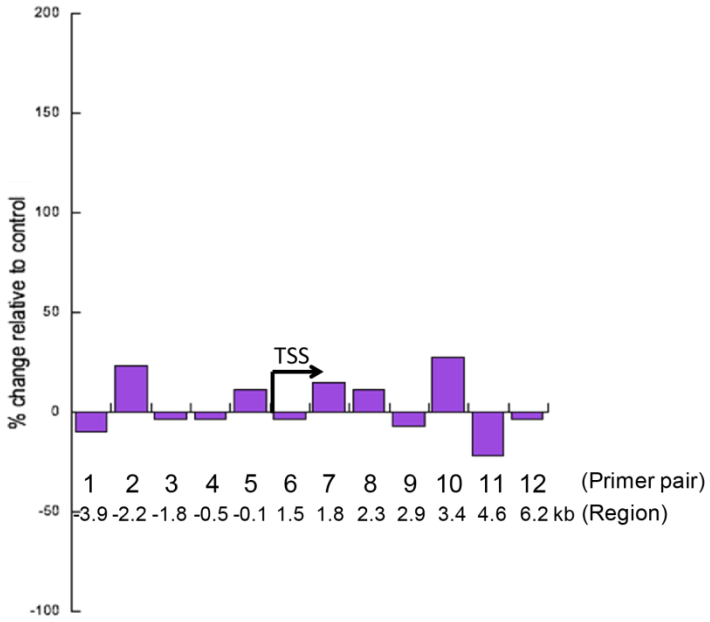

Figure 7.11: Summary of changes in total histone H3 distribution surrounding *MIR17HG* in butyrate-treated HT29 cells compared with control cells

Chromatin immunoprecipitations were performed using digested chromatin from control and 5 mM butyrate-treated cells and rabbit monoclonal antibody for histone H3. Results analysed using the percent input method, and levels in butyrate cells presented as percent change from control cells. Analysis from pooled cell culture replicates (4×10^7 cells) for control and butyrate-treated cells. Kb = kilobases, TSS = transcription start site. Figure to same y-axis scale as Figure 7.10.

7.5 Discussion

This Chapter further explored the mechanisms by which a HDI such as butyrate can alter levels of miR-17-92 cluster miRNAs. An initial experiment used cycloheximide to investigate the effect of butyrate on miR-17-92 cluster miRNA levels, when *de novo* protein synthesis was blocked. The cycloheximide experiment indicated that the butyrate-induced decrease in miR-17-92 miRNAs may be a combination of a primary transcriptional response, and an indirect response mediated by changes in regulatory proteins. The levels of all of the miR-17-92 cluster miRNAs were significantly down-regulated by 5 mM butyrate, in both the standard and cycloheximide-treated HT29 and HCT116 cells; however, the decrease in miR-17-92 expression was greater in the cell lines that were not treated with cycloheximide. The smaller butyrate-induced decrease in miR-17-92 levels in cycloheximide-treated cells compared with standard cells indicated that while the inhibition of *de novo* protein synthesis impacted on miR-17-92 regulation, alternative regulation of miR-17-92 host gene transcription was also possible. One possible mechanism for the butyrate response was discussed in Chapter 5, where the butyrate-induced decrease in miR-17-92 regulators like E2F1 could lead to decreased *MIR17HG* transcription. Another possible mechanism for a direct butyrate response brought about by histone modification was examined in this Chapter with ChIP analysis.

ChIP was used to determine how butyrate-induced histone modifications at the miR-17-92 cluster host gene, *MIR17HG*, may lead to altered transcription. While the MIR17HG promoter region needs to be defined further, several studies provide evidence to support the putative MIR17HG promoter as the regulatory region for the miR-17-92 cluster. Harada et al (2012), for example, investigated the action of dexamethasone, a glucocorticoid found to decrease miR-17-92 levels in leukemic cells. To determine whether this was a direct response, ChIP was used to analyse glucocorticoid receptor binding to the MIR17HG promoter region (defined as 800 bases upstream from the TSS), the locus surrounding exon 1, and the locus within exon 1. Dexamethasone treatment resulted in increased glucocorticoid receptor binding specifically at the upstream promoter region of MIR17HG, with this increase comparable to or greater than binding to a known glucocorticoid receptor target positive control region (the MYC promoter) (Harada et al 2012). In another study, Pospisil et al (2011) examined miR-17-92 cluster repression by an EGR2/JARID1B-mediated H3K4 demethylation mechanism. ChIP was used to identify that EGR2 specifically bound to the CpG island upstream of the miR-17-92 gene and mediated H3K4 demethylation of this region. The

promoter region identified by Harada et al (2012) (defined as the region 800 bases upstream from the TSS) and also by Pospisil et al (2011) (defined as the CpG island region) is the same region spanned by primers 4 and 5 in this current ChIP experiment, and is the area which showed specific changes in histone acetylation and methylation in response to butyrate treatment.

The ChIP results presented in this Chapter represent preliminary findings; while multiple biological replicates were used during cell culture, for the ChIP analysis these replicates were pooled, and technical replicates were used for the real-time qPCR. Despite this limitation, the preliminary ChIP results appeared to show that the butyrate-treated cells had decreased acetylation of H3K9/H3K14 and H3K27, centred around the proximal promoter and TSS of *MIR17HG*. This was in contrast to increased acetylation of these lysine residues further upstream and downstream of the TSS, in the butyrate-treated cells. Also in the butyrate-treated cells, there appeared to be decreased tri-methylation at H3K4, again centred around the proximal promoter and TSS of *MIR17HG*. This observed pattern of histone acetylation and methylation changes does not appear to simply be the result of redistribution of total histone H3 with butyrate treatment, as the ChIP results showed that total histone H3 levels remained similar in butyrate-treated cells relative to control cells, across all examined regions of the *MIR17HG* locus. The ChIP findings thus imply specific histone modification rather than general redistribution. As H3K9ac, H3K14ac, H3K27ac, and H3K4me3 are generally accepted as activating histone marks (Strahl & Allis 2000, Jenuwein & Allis 2001, Barski et al 2007, Mikkelsen et al 2007, Rodriguez-Paredes & Esteller 2011), their decrease suggests a direct epigenetic mechanism for decreased *MIR17HG* transcription in response to butyrate. Use of appropriate antibody and primer controls for the ChIP experiment confirmed that these ChIP findings are valid. These findings indicate that both indirect and direct epigenetic mechanisms play a role in miRNA regulation by butyrate in CRC cells.

In cancer progression, multiple epigenetic effects can alter expression of genes, and also alter transcription of miRNAs. Human miRNA genes are frequently located at fragile sites and genomic regions involved in cancers (Calin et al 2004b), and miRNAs are often decreased in tumour tissues compared with corresponding normal tissues (Michael et al 2003, Thomson et al 2006, Suzuki et al 2011). Multiple mechanisms involved in regulating miRNA levels are affected in cancer, many of which are not yet fully understood. Regulatory mechanisms include specific transcriptional regulation, epigenetic mechanisms including DNA methylation and histone modifications, and

genetic mutations in miRNA regions, or in regions encoding proteins involved in the processing, maturation and stability of miRNAs (as discussed in Chapter 6) (Thomson et al 2006, Melo et al 2009, Melo et al 2010, Melo et al 2011). Epigenetic silencing due to promoter CpG island hypermethylation is one of the more common mechanisms by which tumour suppressor genes are inactivated during tumourigenesis (Toyota et al 1999, Schuebel et al 2007). Likewise, miRNA genes are also targets of epigenetic silencing. Current research on epigenetic regulation of miRNA genes in cancer has largely focused on DNA methylation, especially at CpG islands, with only preliminary evidence for epigenetic regulation via histone modifications. In addition, the focus has mainly been on miRNAs that are silenced in cancer, rather than those that are increased in cancer such as the miR-17-92 cluster of miRNAs.

Saito et al (2006) provided some of the first evidence for the involvement of DNA methylation in the regulation of miRNA expression in cancer cells. Pharmacologic or genetic disruption of DNA methylation in cancer cell lines induces up-regulation of substantial numbers of miRNAs, and Saito et al (2006) showed that treatment with an inhibitor of DNA methyltransferase, 5-aza-2'deoxycytidine, led to up-regulation of 17 miRNAs in bladder cancer cells. There is also evidence in CRC cells for epigenetic silencing of miRNAs through CpG island methylation, particularly in miRNAs that play tumour suppressor roles such as miR-34b and miR-34c, two components of the p53 network (Toyota et al 2008). A miRNA hypermethylation profile may also contribute to human cancer metastasis, with cancer-specific CpG island hypermethylation leading to silencing of miR-148a, miR-34b/c, and miR-9, which are miRNAs shown to inhibit metastasis (Lujambio et al 2008). Bandres et al (2009) also explored DNA methylation-induced silencing of miRNAs in CRC cells, and in addition superficially examined histone modification-associated miRNA silencing. Bandres et al (2009) examined five miRNAs that were within 1000 base pairs of a CpG island, and had previously been identified as being down-regulated in primary CRC: miR-9, miR-124, miR-129, miR-137, and miR-149. Expression of miR-9 and miR-137 were increased after treatment with the demethylating agent 5-aza-2'deoxycytidine or with the HDI 4-phenylbutyric acid, but was more pronounced with combined treatment. miR-129 expression was also up-regulated with combined treatment with the demethylating agent and the HDI. Bandres et al (2009) observed hypermethylation of miR-9, miR-129 and miR-137 CpG island promoter regions in some CRC cell lines, which was partially reversed with 5-aza-2'deoxycytidine treatment, and also in primary CRC tissues compared with normal tissues. Levels of H3 acetylation were also investigated as a broad mark of

transcriptionally active chromatin, with 4-phenylbutyric acid found to induce an increase in H3ac in miR-9 and miR-127. Thus, some miRNAs could be regulated by aberrant DNA methylation and also histone modification in CRC.

Examining promoter CpG island hypermethylation led to identification of candidate tumour-suppressive miRNAs whose silencing was associated with CpG methylation. Kunej et al (2011) integrated data from 45 publications that reported identification of epigenetically regulated miRNAs in cancer, through aberrant hypermethylation of CpG islands or by histone modifications. From these existing studies, it was found that approximately 20% of epigenetically regulated miRNAs had a CpG island within the range of 5 kb upstream, and among them 14% of miRNAs resided within the CpG island (Kunej et al 2011). Similarly, Choudhry and Catto (2011) analysed the latest draft of the human genome and miRBase and found that 13% and 28% of human miRNA genes were located within 3 and 10 kb of CpG islands, respectively. These miRNAs are susceptible to silencing by adherent DNA hypermethylation (Choudhry & Catto 2011).

In addition to the role of DNA methylation, epigenetic regulation of miRNA genes is also tightly linked to chromatin signatures, with transcriptionally active miRNA genes characterised by activating histone marks, such as H3K4me3 (Suzuki et al 2011). Suzuki et al (2011) screened for epigenetically silenced miRNAs in CRC cell lines, and found that the demethylating agent 5-aza-2'deoxycytidine up-regulated expression of a large number of miRNAs, while combination treatment with 5-aza-2'deoxycytidine and the HDI 4-phenylbutyric acid induced even greater numbers of miRNAs in CRC cells. Many of these miRNAs had growth suppressive effects. ChIP analysis was then performed to examine chromatin signatures of active and silenced miRNA genes, using H3K4me3 as an active mark, H3K79me2 which is associated with transcriptional elongation, and H3K27me3 as a repressive mark. Enrichment of H3K4me3 was identified around the proximal upstream CpG island regions of two abundantly expressed miRNA clusters, miR-17-92 and miR-200b. Gene bodies were marked with H3K79me2, indicating active transcriptional elongation, and almost completely lacked the repressive H3K27me3 mark. In contrast, miRNAs whose silencing was associated with promoter CpG island hypermethylation, such as miR-34b/c, miR-124, and miR-9, lacked both the active histone marks. Suzuki et al (2011) also attempted to identify putative miRNA promoter regions in CRC cells, using H3K4me3 as a marker for identifying active miRNA gene promoters. By this method, putative promoters of 166 intragenic miRNAs were identified, with the majority of H3K4me3 marks observed at the TSS of the host gene, some more than 20 kb upstream of the pre-miRNA coding

region. Twenty-two miRNAs were also identified that had their own promoters and were transcribed independently of the host gene, with intragenic H3K4me3 marks. Putative promoters of 66 intergenic miRNAs were also identified, the majority of which were less than 2 kb upstream of the pre-miRNA coding region. For the miR-17-92 cluster, H3K4me3 marks were found to overlap with the known TSS (Suzuki et al 2011). In this Chapter, butyrate was shown to decrease H3K4me3 marks around the *MIR17HG* TSS.

The previous studies that have looked at epigenetic regulation of miRNA genes in cancer have particularly focused on silenced miRNAs. Some used 4-phenylbutyric acid, which is the same class of HDI as butyrate, but usually only to observe its combined action with the demethylating agent 5-aza-2'deoxycytidine, and to examine DNA methylation or histone methylation changes (Bandres et al 2009, Suzuki et al 2011). This Chapter examined further how HDIs like butyrate alter the dysregulated expression of miRNA genes observed in cancer, and examined both the histone acetylation and methylation patterns resulting from butyrate treatment, for *MIR17HG*. While HDIs such as butyrate can increase global histone acetylation in cancer cells by blocking HDAC activity, which should theoretically reactivate epigenetically silenced genes, numerous studies have shown that a similar number or even more genes are down-regulated than up-regulated with butyrate treatment (as reported in Chapter 4 and 5) (Daly & Shirazi-Beechey 2006). A number of studies have explored how butyrate-induced histone modifications can activate gene expression in various cell types; Shin et al (2012), for example, demonstrated that butyrate induced acetylation of H3K9 and H3K27 in bovine cells, while Huang et al (2011) showed that butyrate induced H3K4me in prostate cancer cells. In contrast, research by Rada-Iglesias et al (2007) and Daroqui and Augenlicht (2010) provided a mechanism for how butyrate-induced histone modifications can silence gene expression.

Rada-Iglesias et al (2007) characterised the acetylation status of DNA-bound histones H3 and H4 after treating hepatocarcinoma HepG2 cells with butyrate. After first observing increases in global histone H3 and H4 acetylation after 12 h of butyrate treatment, ChIP-chip was used to further characterise acetylation levels at DNA-bound histones H3 and H4 for regions in the ENCODE array (around 400 genes, or approximately 1% of the human genome). In the untreated cells, enrichment of H3ac and H4ac at TSSs was observed; conversely, after a 12 h incubation with butyrate, signal at 116 regions for H3ac and 124 regions for H4ac was significantly decreased or lost, while 181 regions for H3ac and 119 regions for H4ac remained unchanged. In

particular, many genomic regions close to TSSs were deacetylated after the butyrate exposure. For the regions with decreased acetylation, a total of 102/116 regions for H3ac and 47/124 regions for H4ac were within 5 kb of the TSS of known genes, while 80/181 and 42/119 of the unchanged regions for H3ac and H4ac, respectively, were in such locations. Thus, after butyrate treatment, deacetylation at H3 and H4 occurred in around 25% and 12% of genes in the ENCODE regions, respectively. Among these genes, significantly over-represented categories included cell cycle and proliferation related genes, and genes involved in protein biosynthesis, including translation elongation factors and ribosomal proteins. Rada-Iglesias et al (2007) also showed that the global increase in acetylated histones was mainly localised at the nuclear periphery, possibly affecting heterochromatin or free histones, and indicating that it might not be associated with euchromatin. Rada-Iglesias et al (2007) further examined ten selected regions with butyrate-mediated deacetylation, and found that the butyrate response was time dependent, with a slight initial increase after 15 min at some of the targets, before deacetylation was detected after 2 h and reaching maximum levels by 6 h. The butyrate-induced deacetylation of promoters was accompanied by decreased gene expression; however, deacetylation was shown to be reversible upon withdrawal of butyrate treatment. Deacetylation of promoters was also seen after treatment with TSA and thus may be a general effect of HDIs. In addition, similar histone deacetylation events were specifically observed in the HT29 CRC cell line; when these cells were treated with butyrate, there was clear deacetylation of H3 and H4 at investigated regions (Rada-Iglesias et al 2007).

Daroqui and Augenlicht (2010) also observed butyrate-induced changes in acetylation and methylation in CRC cells, at specific promoter sites for certain genes associated with tumourigenesis. Butyrate induced transcriptional attenuation at the cyclin D1 (*CCND1*) and *C-MYC* genes in two human CRC cell lines, at approximately 100 nucleotides downstream of the TSS, with concomitant decrease of RNA polymerase II occupancy at the 5' end of each gene. In addition, ChIP analysis showed butyrate to induce modest decreases in H3K4me3 and H3K36me3 along the *CCND1* and *C-MYC* genes, with a similar effect on acetylated H3, and a moderate increase in H3me3K27. Transcriptome analysis using novel microarrays demonstrated that butyrate-induced attenuation is widespread throughout the genome, with 42 loci identified as being potentially paused by butyrate (Daroqui & Augenlicht 2010).

Such studies by Rada-Iglesias et al (2007) and Daroqui and Augenlicht (2010) provide some explanations for the observation that while some genes have increased expression

with butyrate treatment, there is also frequent repression of many genes during HDI treatment. In Chapter 4, a similar phenomenon was observed for miRNAs, with similar numbers of miRNAs increased and decreased in CRC cells with butyrate treatment. Rada-Iglesias et al (2007) found that regions close to TSSs were deacetylated after butyrate treatment. In this Chapter, butyrate treatment selectively decreased acetylation of H3K9/H3K14 and H3K27, particularly around the promoter and TSS for *MIR17HG*. Rada-Iglesias et al (2007) found that CpG islands were significantly more common in regions that were deacetylated with butyrate, especially regarding H3ac; this is in keeping with the current finding of deacetylation around the *MIR17HG* TSS, which also has a nearby CpG island (Suzuki et al 2011). In the Rada-Iglesias et al (2007) study, H3K4me3 levels did not change upon butyrate treatment for the particular regions investigated, while Daroqui and Augenlicht (2010) reported a modest decrease in H3K4me3 for the genes investigated. In this Chapter, butyrate decreased H3K4me3 around the promoter and TSS of *MIR17HG*. These differences between the studies for H3K4me3 may be simply due to the different regions examined, or may be due to the longer butyrate treatment time used in this Chapter.

Whilst most miRNA studies focus on DNA methylation around miRNA promoter regions, this Chapter highlights the significance of histone modifications in miRNA regulation, with use of ChIP to identify changes in activating histone marks. While ChIP can provide valuable data on histone modifications, it also has limitations. Known difficulties with a ChIP assay can include low signals and low signal-to background ratios, and problems with antibodies cross-reacting with other nuclear proteins. More relevant to this experiment is the limitation that while ChIP can show that certain histone modifications exist at specific genome locations, it cannot demonstrate the precise functional significance of this association (Carey et al 2009). While the preliminary ChIP data showed that the reduction in miR-17-92 cluster miRNAs observed with butyrate treatment correlated with a reduction in H3K9ac/H3K14ac, H3K27ac and H3K4me3 around the *MIR17HG* promoter and TSS, this does not explicitly imply causation. As these are known activating marks, however, it is very possible their decrease could be playing a role in reduced *MIR17HG* transcription, and subsequent reduced levels of miR-17-92 miRNAs. It should be noted that while these findings provide a mechanism for miR-17-92 reduction by butyrate through histone modifications, further ChIP experiments are required to confirm and expand these results. It may be useful to investigate whether the butyrate treatment results can be replicated with a different HDI such as SAHA.

Chapter 8. Red meat and resistant starch alter microRNA expression in rectal tissue of healthy human volunteers

8.1 Introduction

The majority of cancers involve accumulated genetic and epigenetic changes, which may be influenced by internal and environmental factors. Food and nutrition are important environmental factors in cancer development, and epithelial cells of the colon and rectum in particular are directly exposed to dietary compounds (WCRF 2007). A single dietary component can modify numerous processes in normal cells and cancer cells (Milner 2004), and may directly affect the genome (nutrigenomics) or epigenetically alter gene expression without altering the DNA sequence (nutritional epigenomics) (WCRF 2007). As highlighted in previous Chapters, the diet-derived compound butyrate can alter both gene expression and miRNA levels in CRC cells *in vitro*, through epigenetic mechanisms such as histone modification. Butyrate may have a similar effect on miRNA expression in colorectal cells *in vivo*, but this has not previously been investigated. Other dietary components such as red meat (RM) have been shown to impact on CRC development at high intake levels, and may also modify miRNA expression in colorectal cells *in vivo*.

8.1.1 Dietary fibre and resistant starch

Butyrate has already been shown to alter gene expression, decrease proliferation, and increase apoptosis in CRC cells *in vitro*, as discussed in Chapter 4. The influence of butyrate on CRC development has also been indirectly investigated *in vivo*, via epidemiological studies looking at effects of dietary fibre intake, and interventional studies supplementing diets with substances designed to raise colonic luminal butyrate levels. A link between dietary fibre and CRC was proposed several decades ago, with Burkitt (1971) noting that a main difference between the diet of the Western world where CRC is most prevalent, and that of less-developed communities where it has its lowest incidence, is the proportion of unabsorbable fibre and refined carbohydrate in the ingested food. Western diets are characteristically lower in fibre and higher in refined carbohydrates, with this change altering colonic activity, intestinal transit time,

stool bulk and consistency, and bacterial flora, and potentially accounting for the higher incidence of CRC in economically developed countries (Burkitt 1971). Possible mechanisms for a protective effect of dietary fibre include the dilution of faecal contents, increased stool weight and decreased transit time, binding of carcinogens and bile salts, increased colonic microbiota and altered species balance, and production of fermentation products, in particular the SCFA butyrate (Young et al 2005, WCRF 2007).

Several comprehensive systematic reviews have been performed on the role of fibre in CRC risk (Asano & McLeod 2002, WCRF 2007). The World Cancer Research Fund (2007) determined that foods containing dietary fibre probably protect against CRC. A clear dose-response relationship was apparent from generally consistent cohort studies, supported by evidence for plausible mechanisms, but residual confounding could not be excluded (WCRF 2007). Sixteen cohort studies and 91 case-control studies investigated dietary fibre and CRC; most showed decreased risk with increased intake. Meta-analysis was possible on eight studies (Heilbrun et al 1989, Bostick et al 1993, Fuchs et al 1999, Colbert et al 2001, Terry et al 2001, Konings et al 2002, Higginbotham et al 2004, Norat et al 2005), giving a summary effect estimate (relative risk) of 0.90 (95% confidence interval (CI) 0.84 – 0.97) per 10 g/day increment with moderate heterogeneity (10% decreased risk of CRC per 10 g fibre/day intake) (WCRF 2007).

This association between fibre and CRC is present in many, but not all, human cohort studies. One of the largest cohort studies, in 519,978 individuals taking part in the European Prospective Investigation into Cancer and Nutrition (EPIC) study, found that dietary fibre in foods was inversely related to incidence of CRC, with an adjusted relative risk for the highest versus lowest quintile of fibre from food intake of 0.58 (95% CI 0.41 – 0.85) (Bingham et al 2003). In contrast, another prospective study in two large cohorts, the Nurses' Health Study (76,947 women) and the Health Professionals Follow-up Study (47,279 men), found less association between fibre intake and incidence of CRC, with a hazard ratio for a 5 g/day increase in fibre intake of 0.91 (95% CI 0.87 – 0.95) after adjusting for covariates used in the EPIC study (Michels et al 2005). Differences in fibre sources may account for some of the variability in the cohort studies. One study found that in a cohort of 291,988 men and 197,623 women, fibre from grains was associated with a lower risk of CRC (multivariate relative risk for the highest compared with the lowest intake quintile: 0.86; 95% CI: 0.76, 0.98; *P* for trend = 0.01) (Schatzkin et al 2007).

While meta-analyses of cohort studies show fibre to have an overall protective effect (WCRF 2007), several interventional studies have failed to reproduce this effect. A Cochrane review of five randomised studies (McKeown-Eyssen et al 1994, MacLennan et al 1995, Alberts et al 2000, Bonithon-Kopp et al 2000, Schatzkin et al 2000) concluded that increasing fibre in a Western diet for two to four years did not lower the risk of CRC (Asano & McLeod 2002). Combined study data revealed no difference between intervention and control groups for the number of subjects with at least one adenoma (relative risk 1.04 (95% CI 0.95 – 1.13). It was noted that longer-term trials and higher dietary fibre levels may be needed to reproduce the effect of dietary fibre shown in the observational studies, while the source of the dietary fibre may also influence its effect (Asano & McLeod 2002, Young et al 2005, Schatzkin et al 2007).

The definition of fibre traditionally encompassed soluble and insoluble non-starch polysaccharides (NSP) that resist digestion. Some starch and starch degradation products have also been observed to resist small intestinal digestion and enter the large bowel in normal humans (Anderson et al 1981, Stephen et al 1983, Englyst et al 1992, Topping & Clifton 2001). Starch may resist digestion due to physical inaccessibility and entrapment within a food, the structure of the starch granules, or retrogradation or chemical modification during food processing (Cummings et al 1996, Topping & Clifton 2001). The definition of dietary fibre has now been expanded to encompass these resistant starches and other food materials that are resistant to digestion. Dietary fibre can be defined as the fraction of the edible parts of plants or their extracts, or synthetic analogues, that are resistant to digestion and absorption in the small intestine, usually with complete or partial fermentation in the large intestine (FSANZ 2012). This includes polysaccharides, oligosaccharides (degree of polymerisation >2) and lignins, that promote one or more of the following beneficial physiological effects: laxation, reduction in blood cholesterol, or modulation of blood glucose (FSANZ 2012).

Resistant starch (RS) has received recent attention as a component of total dietary fibre that, in addition to non-starch polysaccharides, alters colonic microbiota and stimulates SCFA production in the colon, promotes colonic function and potentially reduces CRC risk (Cummings et al 1996, Topping & Clifton 2001). In an early study in humans, addition of various RS instead of NSP to the diet led to a significant increase in stool weight and increase in mean total faecal SCFA concentrations (Cummings et al 1996). While the faecal bulking action of RS has since been shown to be variable (Topping & Clifton 2001), RS has more consistently been shown to increase SCFA levels through bacterial fermentation, in animal and human studies (Ferguson et al 2000, Le Leu et al

2003, McOrist et al 2011). In humans, faecal butyrate levels vary widely, but are generally increased by a diet high in RS. A randomised cross-over trial showed that butyrate, acetate and total SCFA concentrations were higher with RS supplemented in addition to NSP, compared with a habitual (entry) diet ($P < 0.01$) and NSP diet without RS ($P < 0.01$) (McOrist et al 2011).

RS can be modified to increase its health benefits. High amylose maize starch, a type of RS, has been used as a base to manufacture starches acetylated with various SCFAs. The RS acts as a vehicle for the sustained delivery of the specific SCFA to the colon with the undigested starch (Annison et al 2003, Bajka et al 2006). The SCFA is then released by bacterial enzymes and is available for absorption and utilisation by the colonocytes or gut microbiota (Clarke et al 2007). Acetylating starches allows the delivery of a specific SCFA, in addition to the SCFAs obtained through the fermentation of the RS component, leading to a greater elevation of the SCFA of interest (Clarke et al 2007). In rats, feeding butyrylated high amylose maize starch led to higher caecal butyrate levels than the unmodified high amylose maize ($P < 0.001$) (Bajka et al 2006). Butyrylated high amylose maize starch has been shown to effectively deliver esterified butyrate to the human colon, leading to increased faecal butyrate levels compared with the standard high amylose maize starch ($P < 0.0001$) (Clarke et al 2011b). One human trial showed that significant fractions (over 70%) of esterified butyrate survived digestion in the small intestine (Clarke et al 2007). Another found that approximately 60% of the ingested esterified butyrate was released in the colon (Clarke et al 2011b).

A number of *in vivo* intervention studies have used dietary RS to modify CRC risk. Several studies in rats have tested the hypothesis that feeding RS as high amylose maize starch would protect against azoxymethane-induced colon carcinogenesis and favourably influence the colonic luminal environment (Le Leu et al 2007a, Le Leu et al 2007b, Le Leu et al 2009). The RS diets significantly increased butyrate and total SCFA and reduced pH in the caecal content and faeces (Le Leu et al 2007a, Le Leu et al 2007b, Le Leu et al 2009), with certain forms of RS producing higher butyrate levels along the length of the colon (Le Leu et al 2009). In rats with short-term azoxymethane treatment (four weeks), RS prevented the colonic atrophy which was observed with the control diet, and reduced epithelial cell proliferation (Le Leu et al 2009). In rats treated with long-term azoxymethane (25 weeks), feeding RS significantly reduced the incidence ($P < 0.01$) and multiplicity ($P < 0.05$) of adenocarcinomas in the colon compared to the control diet, and also reduced cell proliferation in the distal colon, and increased apoptosis. The latter could be a regulatory mechanism to remove damaged cells,

maintain colonic homeostasis and protect against cancer development (Le Leu et al 2007a). Another study examined the effect of a butyrylated form of high amylose maize starch in rats treated with azoxymethane for 6 h. The butyrylated high amylose maize starch produced higher butyrate concentrations in large bowel digesta and hepatic portal venous plasma than the standard high amylose maize starch, and was associated with increased rates of apoptotic deletion of DNA-damaged colonocytes in the distal colonic epithelium, compared with standard high amylose maize starch ($P < 0.05$) or a low RS diet ($P < 0.01$) (Clarke et al 2012).

While rodent studies with carcinogen administration show a clear protective effect of RS supplementation, several human studies which supplemented diets with RS have been less conclusive to date. One trial in healthy human volunteers showed no differences in epithelial kinetics with RS supplementation (Worthley et al 2009), while another trial in CRC patients presented some evidence that RS supplementation may reduce cell proliferation in the upper part of colonic crypts and alter expression of several cell cycle regulatory genes (Dronamraju et al 2009). In patients with the hereditary conditions of FAP or HNPCC (Lynch syndrome), long-term RS supplementation did not alter the incidence of colorectal adenoma or carcinoma (Burn et al 2008, Burn et al 2011).

8.1.2 Red meat and processed meat

As opposed to dietary fibre and RS, high intake of red or processed meats may increase CRC risk. It has even been suggested that the lower incidence of CRC in developing countries may be more associated with low animal product consumption, rather than high fibre intake (O'Keefe et al 1999). Based on systematic review evidence, the World Cancer Research Fund (2007) found RM to be a convincing cause of CRC, and that intake of more than approximately 500 g of cooked meat per week is associated with significantly increased risk of CRC. A substantial amount of data from cohort and case-control studies showed a dose-response relationship, supported by evidence for plausible mechanisms operating in humans (WCRF 2007). Sixteen cohort studies and 71 case-control studies investigated RM (beef, pork, lamb, and goat) and CRC; nearly all showed increased risk with higher intake. Meta-analysis was possible on seven studies that measured intake in times per week (Willett et al 1990, Bostick et al 1994, Giovannucci et al 1994, Chen et al 1998, Singh & Fraser 1998, Tiemersma et al 2002, English et al 2004), giving a summary effect estimate (relative risk) of 1.43 (95% CI 1.05 – 1.94) per times/week with moderate heterogeneity , and three studies that measured grams per day (Pietinen et al 1999, Larsson et al 2005, Norat et al 2005), giving a

summary estimate (relative risk) of 1.29 (95% CI 1.04 – 1.60) per 100 g/day with low heterogeneity (43% increased risk per time consumed/week, or a 15% increased risk per 50 g/day).

Processed meat in particular has been independently investigated as a convincing cause of CRC. Another systematic review by the World Cancer Research Fund (2007) indicated there is a substantial amount of evidence, with a dose-response relationship apparent from cohort studies, and strong evidence for plausible mechanisms operating in humans (WCRF 2007). Fourteen cohort studies and 44 case-control studies investigated processed meat (meats (usually RMs) preserved by smoking, curing, or salting, or by the addition of preservatives) and CRC; nearly all showed increased risk with higher intake. Meta-analysis was possible on five studies (Goldbohm et al 1994, Pietinen et al 1999, Chao et al 2005, Larsson et al 2005, Norat et al 2005), giving a summary effect estimate (relative risk) of 1.21 (95% CI 1.04 – 1.42) per 50 g/day increment with low heterogeneity (21% increased risk per 50 g/day).

Other systematic reviews investigating the effect of RM or processed meats on CRC risk are in agreement with the WCRF (2007) reviews, with meta-analysis of prospective studies supporting the hypothesis that high consumption of RM or processed meat is associated with increased CRC risk (Larsson & Wolk 2006, Chan et al 2011). Another systematic review showed weaker associations between RM consumption and CRC risk, and noted difficulty in isolating the independent effects of RM due to potential confounding from other dietary and lifestyle factors (Alexander & Cushing 2011). The authors also identified problems in combining studies with different definitions of RM (Alexander & Cushing 2011). The individual larger human cohort studies also provide examples of the potential association between high red or processed meat intake and increased risk of CRC. The EPIC study, for example, used data from 478,040 individuals to identify that CRC risk was positively associated with intake of red and processed meat, with a hazard ratio for the highest (>160 g/day) versus lowest (<20 g/day) intake level of 1.35 (95% CI 0.96 – 1.88; *P* trend = 0 .03), and a hazard ratio per 100 g increase in intake of red and processed meat of 1.55 (95% CI 1.19 – 2.02, *P* trend = 0 .001) after calibration (Norat et al 2005). Other large observational studies presented similar findings (Chao et al 2005, Larsson et al 2005).

There are several possible mechanisms for increased CRC risk with RM or processed meat consumption, and its associated degradation and fermentation in the colon. RM has been shown to increase DNA damage and induce DNA strand breaks (Toden et al

2006, Toden et al 2007). The generation of potentially carcinogenic N-nitroso compounds through RM consumption can increase DNA alkylation in the colon and enhance formation of DNA adducts such as O6-methyl-2-deoxyguanosine (O6MeG), a known mutagenic lesion (Lewin et al 2006). The production of heterocyclic amines and polycyclic aromatic hydrocarbons when RM is cooked at high temperature can also induce DNA damage (Rohrmann et al 2009), and in addition, RM also contains haem iron and free iron that can lead to the production of free radicals and reactive oxygen species (Glei et al 2006). High RM intake also increases bacterial fermentation of the protein in the colon, which can alter biomarkers associated with CRC formation (Hughes et al 2000). Processed meat contains high levels of salt and nitrate which may also be detrimental to bowel health (WCRF 2007).

8.1.3 Resistant starch may attenuate red-meat induced damage

Resistant starch may protect against damage to the colon caused by high consumption of RM. An early study suggested that RS can reduce the accumulation of toxic by-products of microbial protein fermentation in the human colon (Birkett et al 1996). Interventional evidence in rodent models has shown that RS supplementation to a high RM diet can increase colonic butyrate levels, and can attenuate RM-induced DNA damage, including the reduction of strand breaks and adduct formation (Toden et al 2006, Toden et al 2007, Winter et al 2011). In a recent mouse study by Winter et al (2011), for example, where pro-mutagenic DNA adducts (O6MeG) in the colon and p-cresol concentrations in the faeces were significantly higher with RM than with another protein source (casein) ($P < 0.018$), RS supplementation opposed the mutagenic effects of dietary RM. RS supplementation to the diet lowered faecal pH, ammonia, and phenol concentrations ($P < 0.05$) and increased all faecal SCFAs, including butyrate ($P < 0.0001$). DNA adducts ($P < 0.01$) were lower in the mice fed resistant starch, as was apoptosis ($P < 0.001$). RS may potentially have other benefits such as attenuating the colonocyte telomere shortening which may occur with high dietary RM intake (O'Callaghan et al 2012). Supplementation with RS may also be beneficial in dietary situations other than very high RM intake; for example, it has also been shown to protect against colonic DNA damage and alter microbiota and gene expression in rats fed a Western diet moderate in fat (19%) and protein (20%) (Conlon & Bird 2009). In the context of a high-protein diet in rats, butyrylated high amylose maize starch has been shown to be twice as effective as standard amylose maize starch in lowering genetic damage as measured by the comet assay (Bajka et al 2008).

One human trial has suggested inconclusively that fibre may play a role in modifying DNA adduct formation in the context of high RM consumption (Lewin et al 2006). In 13 volunteers who were fed a high fibre and RM diet, a high RM diet, and a vegetarian diet in a cross-over design, O6-carboxymethylguanine (O6CMG) adducts in exfoliated colon cells were lower in the vegetarian diet compared with the high RM diet ($P < 0.0001$), and levels were intermediate on the high-fibre RM diet ($P = 0.054$ compared with the RM diet). Despite promising evidence from rodent models, to date no other trials have attempted to examine the effect of RM and RS in humans. This led to the overall aim of the trial described in this Chapter, which was to determine if consumption of a high RM diet by humans increases toxic fermentation products that could damage DNA, and if supplementation of the diet with RS (in the form of butyrylated high amylose maize starch) can ameliorate these effects. In addition, no *in vivo* trials have investigated the effect of RM and RS on miRNA expression in colorectal cells. It was hypothesised that regulation of miRNA expression may explain some of the chemoprotective effects of RS and possibly carcinogenic potential of high RM intake, with this mechanism explored in this Chapter.

8.2 Aim

The aim of this Chapter was to investigate the effect of high red meat intake and resistant starch supplementation on miRNA expression in the rectal mucosa cells of healthy human volunteers.

8.3 Methods overview

A randomised cross-over trial was conducted according to the methods outlined in Chapter 3, comparing the effects of a control diet, high red meat (RM) diet, and high red meat diet supplemented with resistant starch (RM + RS) on markers of CRC risk in healthy volunteers aged 50 – 75 years. Specifically, the effect of the dietary interventions on miRNA expression patterns in rectal biopsy tissue was examined in this Chapter. Recruitment details and participant inclusion and exclusion criteria are detailed in Chapter 3. Participants were monitored throughout the study by a dietitian (Karen Humphreys). The study consisted of two intervention periods of four weeks each, proceeded by a four-week run-in (control diet) period and separated by a four-week washout period (Figure 8.1). Participants were randomised to a RM diet or RM + RS diet for the first intervention, and for the second intervention received the alternative diet. For the RM diet, participants were required to consume 300 g (raw weight) of lean

RM per day for four weeks. For the RM + RS diet, participants were required to consume 300 g (raw weight) of lean RM per day for four weeks, with the addition of 40 g of RS per day in the form of StarPlus™, a butyrylated high amylose maize starch. A recent study has shown that ingestion of 40 g of this butyrylated high amylose maize starch released 50.2 ± 2.4 mmol esterified butyrate per day in the gastrointestinal tract (79.0 ± 3.1% of total ingested esterified butyrate). Accounting for absorption in the small intestine and losses in faeces, around 33.1 mmol of this butyrate was released in the large bowel (Clarke et al 2011b). Blood samples, rectal pinch biopsy, mucosal swabs, faecal & urine specimens, and three-day weighed records of food intake were obtained at the end of each four-week dietary period, with a total of four sample collection visits, at the end of the run-in control diet, first intervention diet, washout diet, and second intervention diet. While various outcomes were examined by other trial researchers (as specified in Chapter 3), this Chapter focused specifically on outcomes relevant to the aim of determining how the dietary interventions influence miRNA expression in rectal tissue. Outcomes measured were the effect of high RM and RS on dietary nutrient intake, faecal SFCA levels (specifically butyrate) and rectal mucosa responses (specifically miRNA expression profiles and target gene mRNA levels). Analysis of dietary intake was performed by a dietitian (KH), and quantitation of miRNA expression profiles in the rectal biopsy samples was also performed by KH, using relative quantitation real-time RT-PCR as detailed in Chapter 3. Real-time RT-PCR was performed for the miR-17-92 cluster miRNAs, miR-21 (another miRNA with known oncogenic properties) (Meng et al 2007, Zhu et al 2007, Asangani et al 2008, Schetter et al 2008), and miR-16 (a miRNA generally abundantly and ubiquitously expressed in normal tissue) (Chang et al 2010). Real-time RT-PCR was also performed by KH to examine changes in specific miRNA target genes, at the mRNA level, as detailed in Chapter 3. Faecal samples were analysed for SCFA levels by trial researchers at CSIRO. As detailed in Chapter 3, the cross-over study design with two intervention periods provided two statistical analysis options; pooling of participant outcome measures by treatment regardless of intervention period, or separate analysis of participant measures based on intervention period. If no significant carry-over effect could be detected, the pooling of participants was deemed valid.

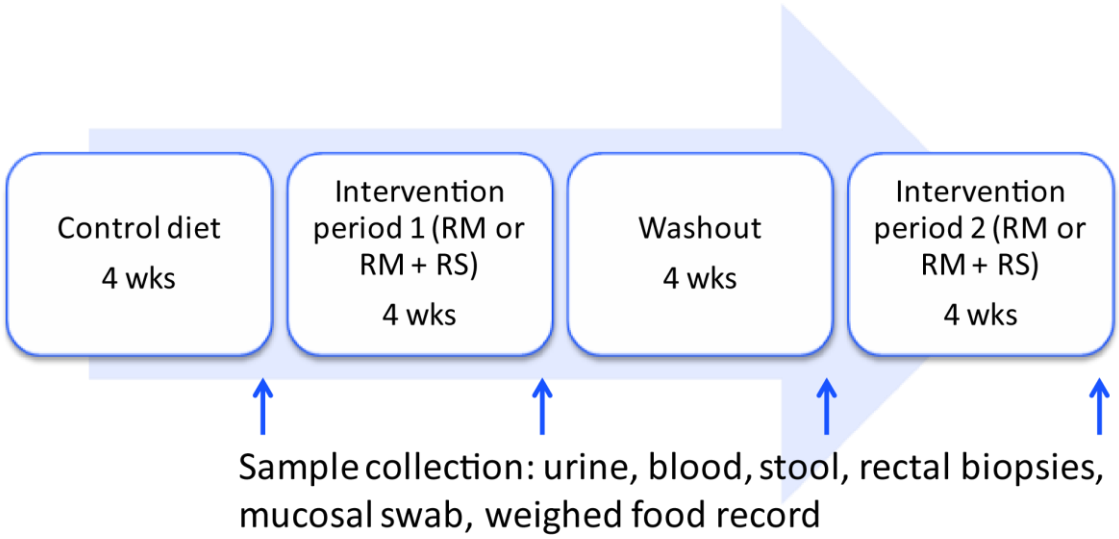

Figure 8.1: High red meat and resistant starch cross-over trial intervention and data collection flow diagram

RM: red meat; RM + RS: red meat + resistant starch.

8.4 Results

8.4.1 Trial description and participant demographics

Recruitment of participants for the randomised cross-over trial commenced in July 2009, with each participant followed-up for the four month duration of the dietary intervention periods. Data collection was completed by September 2010. As shown in the CONSORT diagram (Schulz et al 2010) (Figure 8.2), 25 participants were randomly assigned, with 12 allocated to the RM dietary intervention first, and 13 allocated to the RM + RS dietary intervention first. Two participants who were allocated to the RM dietary intervention first withdrew following randomisation but prior to commencement of intervention diets. One of these withdrawals was due to other unrelated medical problems, while the other participant was unable to tolerate the first rectal biopsy procedure. At study completion, 23 participants had received both the intended intervention diets, and data from these 23 participants were analysed.

Recruited participants were aged 50 – 75 years of age, with no active bowel disease or previous bowel surgery (excluding polypectomy). At study commencement (after four weeks on control diet), mean body weight was 80.4 ± SD 15.3 kg, with this to be maintained throughout the study. A food frequency questionnaire was completed as each participant commenced the study, to initially determine normal dietary intake

patterns (Table 8.1); more precise intake data was obtained throughout the study using weighed food diaries.

There were no major complications during the study. All volunteers tolerated sample collection, with the exception of the one volunteer who had to withdraw due to heightened sensitivity to the rectal biopsy procedure. All volunteers tolerated the dietary interventions, with the exception of one volunteer who usually had a predominantly vegetarian diet and was unable to tolerate 300 g RM per day. For this volunteer, the intervention was modified to 200 g RM per day. Approximately one third of volunteers reported increase in flatulence on trial diets; it was unclear whether this could be linked to increased RM intake, or intake of RS.

Table 8.1: **Usual dietary intake of study participants in the high red meat and resistant starch trial, based on food frequency questionnaire data (Cancer Council Victoria 2005)**

Nutrient	Mean intake/ day
Energy (kJ)	9060.0 ± 3244.2
Protein (g)	114.2 ± 54.3
Fat (g)	95.6 ± 42.6
Saturated fat (g)	36.9 ± 17.8
Carbohydrate (g)	214.0 ± 81.2
Sugar (g)	94.4 ± 39.7
Starch (g)	118.5 ± 45.0
Fibre (g)	24.5 ± 8.7
Alcohol (g)	20.9 ± 26.8

Note: energy, protein, and carbohydrate analysis only from food, not alcohol.

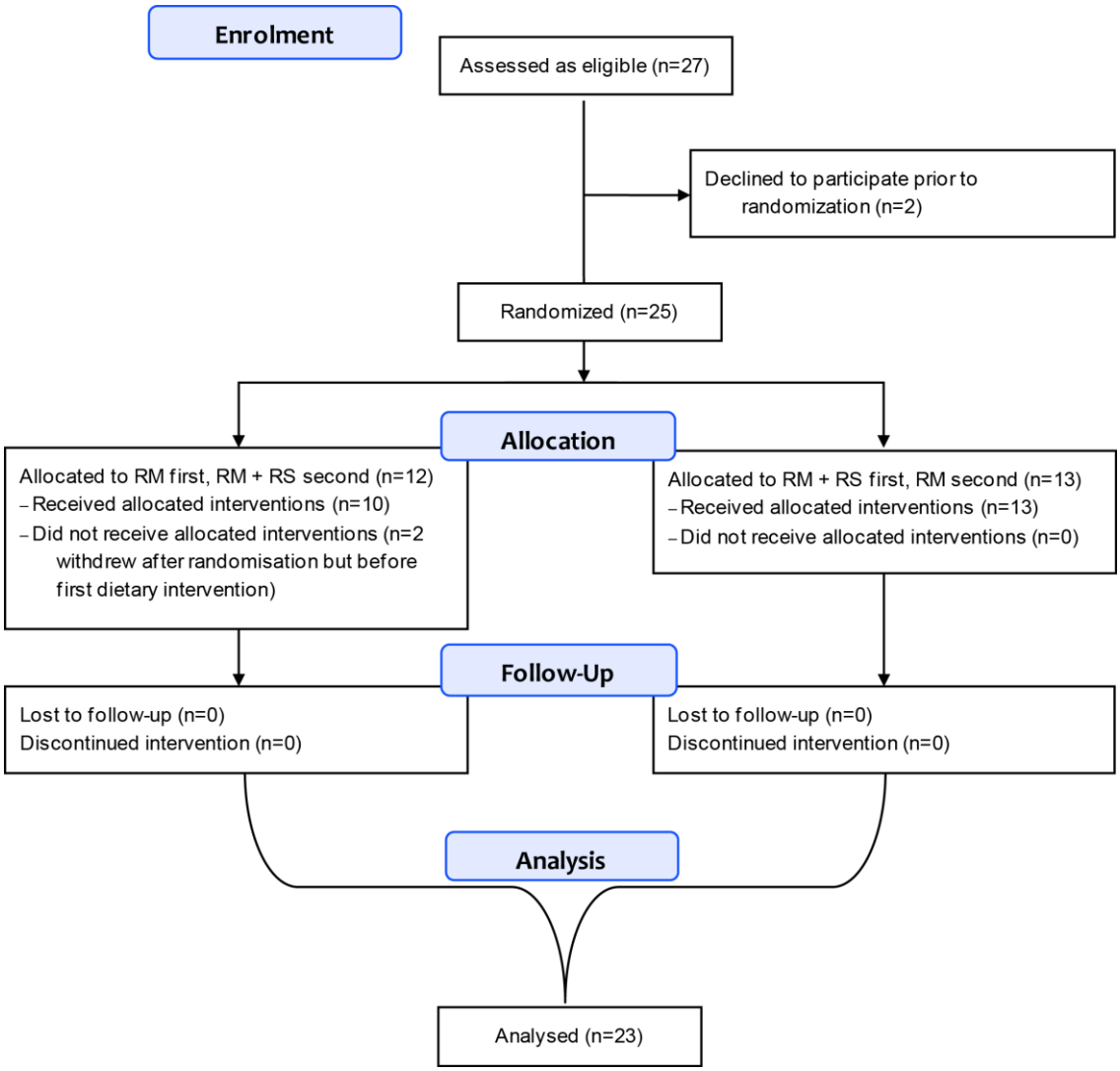

Figure 8.2: CONSORT diagram of participant flow for the high red meat and resistant starch trial

RM: red meat; RM + RS: red meat + resistant starch.

8.4.2 Body weight and dietary intake assessed using three-day weighed food records

Participants maintained consistent body weight over the course of the study, with mean body weight at 80.4 ± 15.3 kg after the run-in control diet, at 80.5 ± 15.2 kg after the RM diet, at 80.3 ± 15.4 kg after the washout phase, and at 80.5 ± 15.1 kg after the RM + RS diet ($P > 0.05$).

The dietary intake of participants during each dietary period was assessed using a three-day weighed food diary, completed for the last three days of each dietary period (Table 8.2). When energy and macronutrient intakes were analysed, there was no statistically significant difference between the diet periods for intake of energy, fat, sugar, or alcohol ($P > 0.05$). Compared with the control diet, protein intake was significantly increased in the high RM diet period ($P < 0.0001$) and also in the high RM + RS diet period ($P = 0.0004$), and was similar in the high RM and high RM + RS dietary periods ($P = 0.18$). This increased protein intake during the two intervention periods serves as an indirect measure of compliance. Fibre intake was decreased in the high RM diet compared with the control diet ($P < 0.001$) and high RM + RS diet ($P < 0.001$). Starch intake also appeared to be slightly decreased in the high RM diet compared with the control diet ($P = 0.005$) and high RM + RS diet ($P = 0.008$). Saturated fat intake was slightly higher in the high RM diet compared with the control diet ($P = 0.02$).

Table 8.2: Dietary intake of study participants in the high red meat and resistant starch trial during each diet period, based on three-day weighed food records

	Control	RM	Washout	RM + RS
Energy (kJ)	8835.0 ± 1858.4	9167.0 ± 1864.6	8780.6 ± 1842.3	9116.1 ± 1877.8
Protein (g)	93.3 ± 25.2	124.3 ± 20.0	90.7 ± 23.8	119.4 ± 23.7
Fat (g)	72.5 ± 24.0	76.7 ± 25.2	77.4 ± 23.9	68.4 ± 25.9
Saturated fat (g)	27.1 ± 12.5	31.9 ± 12.3	28.3 ± 8.8	30.4 ± 12.3
Carbohydrate (g)	233.9 ± 72.4	217.7 ± 58.9	222.2 ± 67.9	241.3 ± 58.3
Sugar (g)	116.6 ± 45.2	121.8 ± 35.8	106.4 ± 42.5	122.8 ± 35.9
Starch (g)	116.1 ± 40.1	93.3 ± 45.8	114.4 ± 46.1	115.8 ± 32.5
Fibre (g)	26.3 ± 8.6	20.0 ± 8.9	25.2 ± 10.3	26.3 ± 10.1
Alcohol (g)	15.4 ± 14.8	14.3 ± 19.1	15.9 ± 22.9	13.9 ± 16.5

RM: red meat, RM + RS: red meat + resistant starch.

8.4.3 SCFA levels in faecal samples

The faecal samples provided by participants during the last 24 h of each dietary period were analysed by study investigators at CSIRO for acetate, propionate, butyrate, and total SCFA levels. Acetate, propionate, butyrate, and total SCFA faecal levels all increased in the RM + RS dietary period, compared with the other dietary periods (Figure 8.3), which could serve as an indirect measure of compliance with the RS supplementation.

Participant measures for RM and RM + RS intervention diets were analysed based on intervention period for treatment effect, period effect and carry-over effect. Butyrate, the SCFA of most relevance to the study aims, was analysed by this method, which showed that faecal butyrate levels were significantly increased in the RM + RS diet compared with the RM diet (Table 8.3). There was no significant carry-over effect for butyrate levels (Table 8.3). There was also no significant period effect for butyrate levels (Table 8.3); however, the groups-by-periods plot shows that the mean faecal butyrate levels for RM + RS group appeared increased in the 2nd period (Appendix 3, Figure A3.1). No such period changes were found in the RM group.

As the carry-over effect was not significant, the data from the two periods could be combined and analysed; thus, findings from a pooled analysis are also valid for this outcome variable (Figure 8.3). When participant measures were pooled by treatment regardless of intervention period, there was a statistically significant increase in acetate ($P = 0.0007$), propionate ($P = 0.0002$), butyrate ($P = 0.001$), and total SCFA ($P = 0.0002$) for the RM + RS diet period, compared with the control diet period. Similarly, there was a statistically significant increase in propionate ($P = 0.005$), butyrate ($P = 0.013$), and total SCFA ($P = 0.047$) for the RM + RS diet period, compared with the RM diet period; this increase was not significant for acetate ($P = 0.23$). There was no significant difference between the control and RM diet periods for any of the SCFAs measured ($P = 0.09$ for acetate; $P = 0.16$ for propionate; $P = 0.46$ for butyrate; $P = 0.17$ for total SCFAs). There was also no significant difference between the control and washout diet periods for any of the SCFAs measured ($P = 0.18$ for acetate; $P = 0.10$ for propionate; $P = 0.56$ for butyrate; $P = 0.19$ for total SCFAs), which is another indication that there is likely to be no carry-over effect.

Table 8.3: Faecal butyrate levels for high red meat and high red meat + resistant starch intervention diets, with analysis of variance for treatment effect, period effect and carry-over effect

Outcome	RM (Mean ± SD)	RM + RS (Mean ± SD)	Treatment effect (*P* value)	Carry-over effect (*P* value)	Period effect (*P* value)
Faecal butyrate levels (µmol/g)	14.2 ± 8.0	21.2 ± 12.8	$P < 0.01$	$P = 0.09$	$P = 0.09$

RM: red meat, RM + RS: red meat + resistant starch.

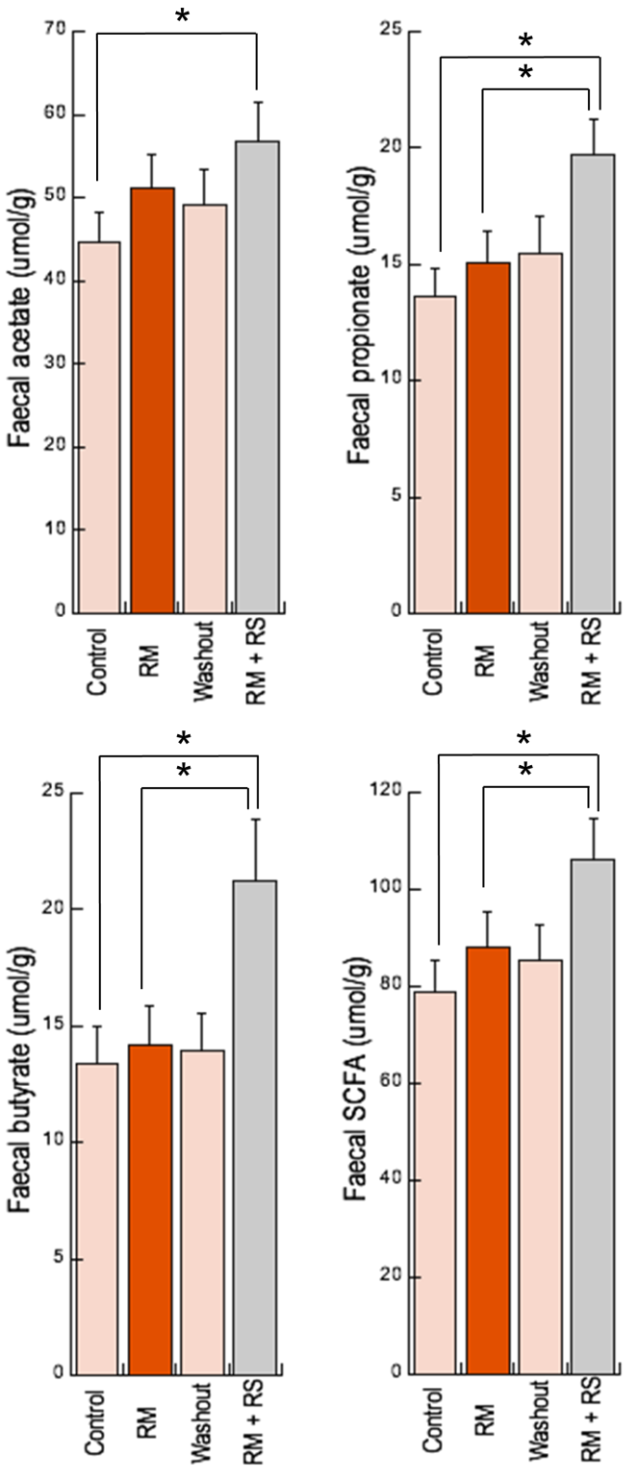

Figure 8.3: Faecal butyrate, acetate, propionate, and total SCFA levels of participants in the high red meat and resistant starch trial

Faecal samples collected at the end of each four-week diet (* $P < 0.05$). The mean ± SEM of the 23 participants is shown for each diet. Control: control diet; RM: red meat diet; RM + RS: red meat + resistant starch diet.

8.4.4 Real-time RT-PCR analysis of microRNA levels in rectal biopsy samples

The rectal biopsy samples collected from participants at the end of each dietary period were processed to obtain total RNA, and analysed using relative quantitative real-time RT-PCR for changes in miRNA levels. The miR-17-92 cluster miRNAs were examined, as these were shown in previous Chapters to be altered with butyrate treatment, in CRC cell lines. Another miRNA with known oncogenic properties that was not altered by butyrate treatment *in vitro*, miR-21, was examined for comparison. An additional miRNA that was not altered by butyrate treatment *in vitro*, and that is generally abundantly and ubiquitously expressed in normal tissue, miR-16, was also examined for comparison (Chang et al 2010).

Upon real-time RT-PCR analysis, levels of miR-17-92 cluster miRNAs in the rectal biopsy samples appeared to increase with the high RM diet compared with the control diet, but not with the high RM + RS diet (Figure 8.4A). The rise in miR-17-92 miRNA levels with the high RM diet alone was approximately 30% (Figure 8.4B). Rectal biopsy miRNA levels for the high RM and RM + RS intervention diets were analysed based on intervention period, for treatment effect, period effect and carry-over effect. miR-17, miR-19a, miR-20a, miR-19b, and miR-92a were significantly increased in the RM diet compared with the RM + RS diet, and there was also a trend towards increased miR-18a in the RM diet compared with the RM + RS diet (Table 8.4). There was no significant carry-over effect for any of the miR-17-92 cluster miRNAs (Table 8.4). The groups-by-periods plots show that for some miRNAs there was no difference between periods for the dietary intervention effects, while for others there were slight differences between intervention period 1 and period 2 (Appendix 3, Figure A3.2); however, statistical analysis showed that the period effect was not significant for any of the miR-17-92 cluster miRNAs (Table 8.4).

As the carry-over effect was not significant, the data from the two periods could be combined and analysed; thus, findings from a pooled analysis are also valid for this outcome variable (Figure 8.4). There was a trend towards increased expression of miR-17-92 cluster miRNAs in the rectal biopsy samples with the high RM diet versus control diet, which was significant for miR-17 ($P = 0.046$), miR-19a ($P = 0.021$), miR-20a ($P = 0.026$), and miR-19b ($P = 0.021$), but not for miR-18a ($P = 0.51$) or miR-92a ($P = 0.09$). Conversely, when the high RM diet was supplemented with RS, the miR-17-92 cluster miRNA levels were lower than with the RM diet alone, which was significant for most

of the miRNAs (P = 0.001 for miR-17; P = 0.16 for miR-18a; P = 0.009 for miR-19a, P = 0.0008 for miR-20a; P = 0.006 for miR-19b; P = 0.006 for miR-92a). There was no significant difference between the control and RM + RS diet for any of the miR-17-92 cluster miRNAs (P = 0.44 for miR-17; P = 0.48 for miR-18a; P = 0.31 for miR-19a, P = 0.14 for miR-20a; P = 0.99 for miR-19b; P = 0.38 for miR-92a). The pooled analysis provided slightly differing estimates of significance than the analysis based on intervention period. Regardless, both showed the majority of miRNAs from the miR-17-92 cluster to be significantly increased with the high RM diet compared with the high RM + RS diet in the rectal biopsy samples, with the exception of miR-18a.

A pooled analysis was also performed for miR-21 and miR-16 levels in the rectal biopsy samples. miR-21 and miR-16 are examples of miRNAs that were not affected by butyrate in the *in vitro* work (Figure 8.5). For miR-16, there was no significant change with the high RM diet compared with the control diet (P = 0.94), the high RM + RS diet compared with the control diet (P = 0.74), or the high RM diet compared with the high RM + RS diet (P = 0.64); thus miR-16 appeared stably expressed regardless of the intervention diet. For miR-21 there was a significant increase with the high RM diet compared with the control diet (P = 0.007), and also a trend towards an increase with the high RM + RS diet compared with the control diet (P = 0.12). There was no significant difference between the high RM and high RM + RS diet for miR-21 (P = 0.76); thus high RM appeared to alter miR-21, but RS supplementation had little protective effect.

Table 8.4: miR-17-92 cluster miRNA levels in rectal biopsies assessed using real-time RT-PCR for high red meat and high red meat + resistant starch intervention diets, with analysis of variance for treatment effect, period effect and carry-over effect

Outcome	RM (Mean ± SD)	RM + RS (Mean ± SD)	Treatment effect (*P* value)	Carry-over effect (*P* value)	Period effect (*P* value)
miR-17	20.2 ± 6.8	15.8 ± 6.8	*P* < 0.01	*P* = 0.12	*P* = 0.32
miR-18a	0.66 ± 0.24	0.57 ± 0.28	*P* = 0.20	*P* = 0.42	*P* = 0.37
miR-19a	9.8 ± 2.9	7.7 ± 3.2	*P* = 0.01	*P* = 0.88	*P* = 0.46
miR-20a	20.0 ± 5.3	16.2 ± 5.9	*P* < 0.01	*P* = 0.66	*P* = 0.18
miR-19b	7.0 ± 2.4	5.0 ± 2.4	*P* < 0.01	*P* = 0.64	*P* = 0.06
miR-92a	25.3 ± 10.1	20.1 ± 9.2	*P* < 0.01	*P* = 0.17	*P* = 0.37

RM: red meat, RM + RS: red meat + resistant starch.

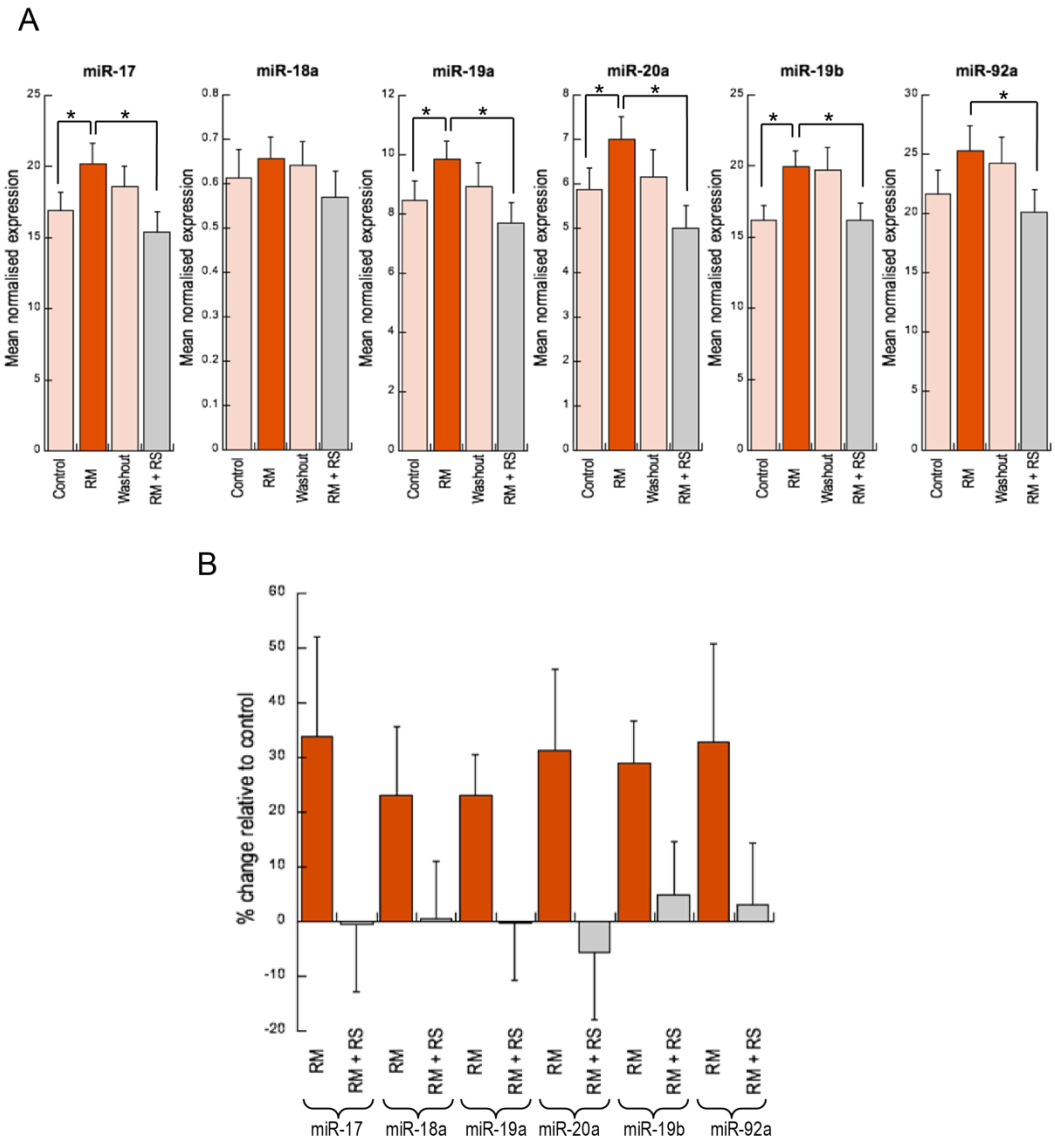

Figure 8.4: Real-time RT-PCR of miR-17-92 cluster levels in rectal biopsies from participants in the high red meat and resistant starch trial

Rectal biopsies collected at the end of each four-week diet (control diet, RM diet, RM + RS diet) (* $P < 0.05$). Expression is normalised to RNU6B levels. (A) Real-time RT-PCR results (mean ± SEM) for the 23 participants shown for each diet. (B) Summary of real-time RT-PCR results for the intervention diets, presented as percent change (mean ± SEM) from control diet. Control: control diet; RM: red meat diet; RM + RS: red meat + resistant starch diet.

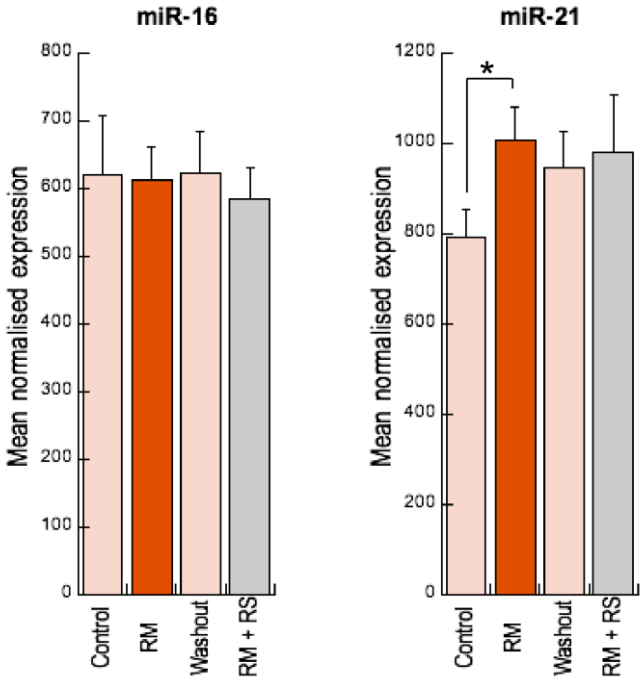

Figure 8.5: Real-time RT-PCR of miR-16 and miR-21 in rectal biopsies from participants in the high red meat and resistant starch trial

Rectal biopsies collected at the end of each four-week diet (control diet, RM diet, RM + RS diet) (* $P < 0.05$). The mean ± SEM of the 23 participants is shown for each diet. Expression is normalised to RNU6B levels. Control: control diet; RM: red meat diet; RM + RS: red meat + resistant starch diet.

8.4.5 Real-time RT-PCR analysis of miR-17-92 target gene mRNA levels in rectal biopsy samples

As discussed in previous Chapters, miRNAs in the miR-17-92 cluster target genes that are important in cell cycle control, including the cell cycle inhibitor *CDKN1A* and the pro-apoptotic genes *PTEN* and *BCL2L11*. To investigate how the diet-induced changes in miR-17-92 cluster miRNA levels influenced these target genes, the total RNA from the rectal biopsy samples was analysed using relative quantitation real-time RT-PCR to detect changes in *CDKN1A*, *PTEN* and *BCL2L11* mRNA levels. There was a trend towards decreased *CDKN1A*, *PTEN* and *BCL2L11* mRNA levels with the high RM diet compared with the control diet, which was statistically significant for *CDKN1A* ($P = 0.02$) (Figure 8.6). There was no significant difference between the control and high RM + RS diet for *PTEN* and *BCL2L11* ($P > 0.05$), although for *CDKN1A* there appeared to be a trend towards decreased mRNA levels with the high RM + RS diet compared with the control diet ($P = 0.008$). *CDKN1A* and *BCL2L11* mRNA levels appeared lower with the washout diet than with the control diet; this was statistically significant for *BCL2L11* ($P = 0.03$)

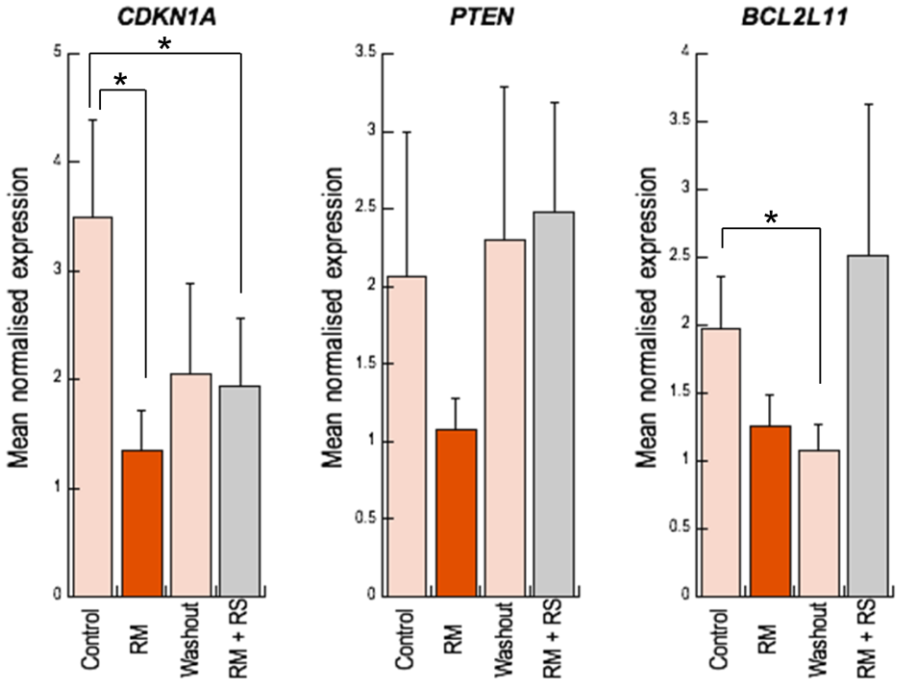

Figure 8.6: Real-time RT-PCR of miR-17-92 target gene expression in rectal biopsies from participants in the high red meat and resistant starch trial

CDKN1A, *PTEN* and *BCL2L11* mRNA levels in rectal biopsies collected at the end of each four-week diet (control diet, RM diet, RM + RS diet) (* $P < 0.05$). The mean ± SEM of the 23 participants is shown for each diet. Expression is normalised to RNU6B levels. Control: control diet; RM: red meat diet; RM + RS: red meat + resistant starch diet.

8.5 Discussion

This Chapter presented miRNA-specific findings from a human randomised cross-over trial designed to examine the effects of a high RM diet, or high RM diet supplemented with butyrylated resistant starch on markers of CRC risk in healthy volunteers aged 50 – 75 years. Epidemiological studies have provided the first evidence for increased CRC risk with high RM intake (WCRF 2007). There are plausible mechanisms for this, including the finding that high RM can increase DNA damage, including an increase in DNA strand breaks and formation of pro-mutagenic DNA adducts (Lewin et al 2006, Toden et al 2006, Toden et al 2007). Now, this Chapter is the first to show that high RM alters miRNA levels in humans, and can significantly increase levels of some miRNAs in rectal biopsy samples, in particular the miR-17-92 cluster of miRNAs, and miR-21, which have known oncogenic properties. This finding was despite the fact that the study was powered to detect changes in primary outcomes not relevant to this Chapter, rather than the secondary outcome of miRNA changes.

While high RM intake potentially increases CRC risk, RS can potentially ameliorate some of these effects. Besides the epidemiological evidence that fibre can decrease CRC risk (WCRF 2007), studies in rodent models has shown that RS supplementation can raise colonic butyrate levels, reduce adenocarcinoma formation in response to a carcinogen, and attenuate RM -induced DNA damage (Le Leu et al 2007a, Le Leu et al 2007b, Toden et al 2007, Le Leu et al 2009, Winter et al 2011). Lewin et al (2006) have also inconclusively suggested that fibre may play a role in modifying DNA adduct formation in humans, in the context of high RM consumption. This study was the first to directly examine the outcomes of supplementing a high RM diet with RS in humans, and the first to examine the influence of these diets on miRNAs in rectal biopsy samples. When the high RM diet was supplemented with RS, this significantly raised faecal butyrate levels. The study identified a novel mechanism by which RS can be beneficial for bowel health, with some of the miRNAs that were elevated in the rectal biopsy samples with RM alone reduced and restored to baseline levels with RS supplementation. In particular, levels of miR-17-92 miRNAs were significantly lower in RM with RS supplementation than with RM alone, while levels of miR-21 were similar in RM with RS supplementation and with RM alone. RS supplementation also did not influence miR-16 levels. This supports the hypothesis that the miR-17-92 cluster miRNA changes with RS supplementation may be due to increased butyrate production; in previous Chapters the miR-17-92 cluster miRNAs, but not miR-21 of miR-16, were influenced by butyrate treatment *in vitro*. As a butyrylated form of RS was used in the

trial, this is likely to have directly administered further butyrate to the colon; and has been previously shown to be more effective in reducing carcinogen damage than standard forms of RS (Bajka et al 2008, Clarke et al 2012).

An important difference between this Chapter and previous Chapters was that the *in vitro* work was performed in CRC cells, while the *in vivo* work in this Chapter was performed in healthy volunteers with normal rectal mucosa tissue. Historically, the response to butyrate in normal cells versus cancer cells has been shown to be different. Referred to as the butyrate paradox, butyrate is a preferred energy source for normal colonic epithelium and assists in maintaining normal proliferation (Roediger 1982); while alternative fuel sources are preferred in CRC cells, and butyrate instead can inhibit proliferation and induce differentiation or apoptosis (Warburg 1956, Mariadason et al 2000). Observations in rat models treated with the carcinogen azoxymethane showed the colon cells to respond to high butyrate levels in a manner more similar to cancer cells; decreased proliferation and enhanced apoptosis were observed in the distal colon with RS feeding and increased butyrate (Le Leu et al 2007a, Le Leu et al 2009). In this Chapter, there was a similar regulation of the miR-17-92 cluster by butyrylated RS in healthy rectal cells *in vivo*, as previously shown with butyrate in CRC cells *in vitro*. This was observed particularly in the context of high RM, with RS only restoring miRNA levels to those of the control, rather than reducing levels lower than baseline. Interestingly, compared to other miR-17-92 miRNAs, there was no significant change between the control, RM and RM + RS diets for one particular miRNA in the cluster, miR-18a. miR-18a may be regulated differently to the other cluster members (Guil & Caceres 2007), and as hypothesised in Chapter 6, may play a homeostatic role in helping to contain oncogenic effects of other miR-17-92 cluster miRNAs. It would be beneficial to also examine the effect of RS (and butyrate) on miR-17-92 cluster miRNA levels in healthy rectal tissue, without the confounding effect of high RM intake.

RS has a potentially protective role in modulating miR-17-92 levels in response to the dysregulation observed with high RM intake. RS was not able to lower miR-21, however, which was also significantly increased with high RM intake. As for the miR-17-92 cluster, miR-21 has similarly been classed as an oncogenic miRNA, and has been shown to regulate tumour suppressor genes such as *PTEN*, *TPM1* and *PDCD4*, and to induce tumourigenesis, invasion and metastasis (Meng et al 2007, Zhu et al 2007, Asangani et al 2008, Medina et al 2010). miR-21 is elevated in CRC, with higher miR-21 expression found in more advanced tumours (Bandres et al 2006, Cummins et al 2006, Volinia et al 2006, Slaby et al 2007, Monzo et al 2008, Chen et al 2009). High miR-21

has been linked to poorer survival and therapeutic outcomes, and can be used as a biomarker for the presence and stage of CRC (Slaby et al 2007, Schetter et al 2008). The finding that this miRNA is elevated with RM intake warrants further investigation to determine any impact on CRC risk.

While this study showed subtle changes in miRNA levels in response to dietary components, as miRNAs can simultaneously target hundreds of mRNAs, even small changes in their expression can have important cellular effects (Hendrickson et al 2009). miR-17-92 and miR-21 are known to promote proliferation (Meng et al 2007, Zhu et al 2007, Asangani et al 2008, Mu et al 2009, Olive et al 2009), and the examination of target gene expression provided preliminary evidence regarding the impact of the detected miRNA changes on cellular function. The increase in levels of miR-17-92 miRNAs with the high RM diet may be one mechanism for the observed decrease in mRNA levels of target genes *CDKN1A*, *PTEN*, and *BCL2L11*, which was statistically significant for the cell cycle inhibitor *CDKN1A*. When the high RM diet was supplemented with resistant starch, there was no significant difference in *PTEN* and *BCL2L11* mRNA levels compared with the control diet, while *CDKN1A* mRNA levels still appeared lower than the control diet. Through target gene regulation, the increase in miR-17-92 miRNAs and miR-21 with the high RM diet may be partly responsible for a corresponding increase in cell proliferation. Another researcher in the trial (Jean Winter) used a proliferating cell nuclear antigen (PCNA) assay as a proliferation marker in the rectal biopsy samples fixed in formalin. There was increased proliferation with the high RM diet compared with the control diet ($P = 0.02$). Proliferation with the high RM + RS diet appeared intermediate between the high RM diet and the control diet, with the high RM + RS diet not significantly different from either the control diet ($P > 0.05$) or high RM diet ($P > 0.05$). Proliferation with the washout diet was significantly higher than with the control diet ($P = 0.02$). The failure of resistant starch supplementation to restore proliferation to baseline could be associated with the observed miR-21 levels, which remained elevated compared with the control diet. Other regulatory factors, including other miRNAs, may also be involved. It should be noted that the length of the washout period may have been insufficient for the examination of target gene expression and cell proliferation; for example, *BCL2L11* mRNA levels and cell proliferation were significantly different in the washout compared with the control diet, indicating a potential carry-over effect. The high variability in mRNA levels in the rectal biopsy samples also limits the ability to draw firm conclusions from these data.

The first evidence to show that high RM and RS have opposing effects on miRNA levels in rectal tissue in humans is presented in this Chapter. Several studies have looked at the effect of dietary components on CRC in other *in vivo* models, particularly rats. As shown in Chapter 1, several studies have examined the miRNA response in rats fed diets containing corn oil or fish oil with pectin or cellulose and injected with azoxymethane or a saline control (Davidson et al 2009, Shah et al 2011). These studies particularly demonstrated the novel role of fish oil in protecting the colon from carcinogen-induced miRNA dysregulation, rather than a role for fibre. Shah et al (2011) did however demonstrate that various dietary combinations and carcinogen exposure modulated a number of key miRNAs, including miR-17-92 cluster miRNAs and miR-21, which were similarly modified by dietary components in this Chapter.

Regulation of miRNA expression by other dietary components has been investigated in cancer types other than CRC, using *in vivo* rat models and cancer cell lines. Some of the food components were shown to have a protective effect on cancer risk. When a rat diet was deficient in folate, hepatocellular carcinomas developed, tumour suppressor miRNAs were decreased, and miRNAs with oncogenic functions were increased (Kutay et al 2006, Pogribny et al 2008, Tryndyak et al 2009, Wang et al 2009a, Starlard-Davenport et al 2010). Curcumin, vitamin E, and retinoic acid were also shown to have protective effects, by increasing levels of miRNAs with tumour suppressive roles (Chapter 1).

There have been no previous human trials that have observed the effect of RM and RS on miRNA expression in colorectal cells. This Chapter presents novel findings, but the trial is not without its limitations. One such limitation is the identification of correlations but not exact causations. It is unclear, for example, what component of the RM is increasing miR-17-92 cluster miRNA levels. High fat or high cholesterol diets, for example, have also been shown to alter miRNA expression in liver cells (Cirera et al 2010, Park et al 2011). It is also not conclusively determined what aspect of the RS is protective, although the use of butyrylated RS to further increase colonic butyrate levels has previously been shown to offer additional protection (Bajka et al 2008, Clarke et al 2012). Offering support for the hypothesis that the miRNA changes with RS supplementation may be due to increased butyrate production, is the *in vivo* replication of *in vitro* findings from previous Chapters where the miR-17-92 cluster of miRNAs but not miR-21 or miR-16 responded to butyrate treatment. The impact of the detected miRNA changes on cellular functions known to be regulated by miR-17-92 and miR-21

miRNAs requires further investigation. How miRNA changes may mediate some of the other observed cellular responses to high RM intake is yet to be determined.

The very high RM intake during the intervention period may limit the applicability of the trial findings to the general population with possibly lower everyday intake of RM. The average intake of RM in the general Australian population remains substantial however, with RM consumption estimates from the National Nutrition Survey in 1995 at 73 g/day for men and 37 g/day for women, and less reliable estimates from production, import, and export data at 136 g/day in 2007/08 (McLennan & Podger 1999, Williams & Droulez 2010). There is also a current trend towards consumption of higher protein diets for weight loss (Noakes & Clifton 2005). The level of RS supplementation used in the dietary intervention could be realistically applied to the general population. Several studies have shown long term supplementation in select populations to be feasible (Burn et al 2008, Burn et al 2011). There has also been a recent expansion in the number of commercially available foods with modifications or supplementation to increase RS content (Landon 2007, Bird et al 2008). The first commercially available RS food ingredient, Hi-maize, was developed in Australia and was introduced into the food supply in 1994 in the form of fibre enriched white bread (Landon 2007). Hi-maize is now added to a range of foods, as are other rich sources of RS, such as BARLEYmax in cereal (Landon 2007, Bird et al 2008). In a global first for a government health authority, Australia's National Health and Medical Research Council now also specify a RS component in their fibre intake recommendations, due to its positive impact on digestive health (NHMRC 2006, Landon 2007).

Chapter 9. General conclusions

9.1 Thesis summary

Epigenetic modifications are important contributors to CRC development and progression. DNA methylation changes including promoter hypermethylation and global hypomethylation are characteristic of CRC development (Toyota et al 1999, Matsuzaki et al 2005, Rodriguez et al 2006, Schuebel et al 2007). Likewise, CRC is also associated with altered patterns of histone modifications, and dysregulation of proteins responsible for these modifications (Zhu et al 2004, Wilson et al 2006, Enroth et al 2011). Disruption of normal miRNA expression levels has also been shown in CRC, with increased levels of some miRNAs with oncogenic potential, and decreased levels of some miRNAs with tumour suppressor roles (Michael et al 2003, Cummins et al 2006, Slaby et al 2007). In addition to genetic mutations, the dysregulation of miRNAs in CRC can occur by epigenetic mechanisms such as altered DNA methylation (Toyota et al 2008, Bandres et al 2009), with more limited evidence to date for histone modification also playing a role (Suzuki et al 2011). While diet and diet-derived compounds such as butyrate can modify CRC cell behaviour through epigenetic mechanisms (Mariadason et al 2000, Della Ragione et al 2001, Daly & Shirazi-Beechey 2006), the role of dietary compounds in modifying miRNA expression in CRC cells and normal colorectal tissue has been less studied. Diet-derived butyrate, with its established mechanism of histone modification, was a plausible candidate for altering miRNA expression through epigenetic changes. It was hypothesised that modification of miRNA expression may contribute to the chemo-protective effect of butyrate and other HDIs.

In this study, the role of butyrate and other HDIs in modulating CRC risk was investigated, by examining the effect of these compounds on miRNA expression in CRC *in vitro*, and in rectal mucosa tissue *in vivo*. The down-stream consequences of these miRNA changes were observed, and the roles of these miRNAs in the context of the anti-proliferative effects of HDIs were determined. In addition to exploring the action of a potentially protective dietary component, the study aimed to determine whether miRNA expression in colorectal cells was also altered by dietary components thought to possibly increase risk of CRC, such as red meat. The major findings of the study, including the dietary regulation of miRNA expression in colorectal cells *in vitro* and *in vivo*, are summarised below.

9.1.1 Butyrate alters microRNA expression in colorectal cancer cell lines.

Chapter 4 demonstrated that treatment with the HDI butyrate decreased proliferation of HT29 and HCT116 CRC cell lines, with the HCT116 cell line showing greater susceptibility to butyrate's anti-proliferative effect. The effect of butyrate treatment on miRNA expression in these CRC cell lines was then examined, through microarray analysis and real-time RT-PCR validation. Expression profiles of miRNAs differ along the gastrointestinal tract (Slattery et al 2011) and are altered in CRC, with this dysregulation often contributing to tumour progression (Michael et al 2003, Lu et al 2005, Cummins et al 2006, Slaby et al 2007, Chen et al 2009). Butyrate was shown to alter the expression of some of the miRNAs that are dysregulated in CRC. Treatment with 5 mM butyrate for 48 h led to a decrease in all miRNAs in the miR-17-92 cluster, including miR-17, miR-18a, miR-19a, miR-20a, miR-19b, and miR-92a, in both the HT29 and HCT116 cells. Other miRNAs that decreased with 5 mM butyrate treatment included miRNAs in the miR-106a-363 cluster, including miR-18b, miR-20b, and miR-106a, and also miR-29b, miR-196a and miR-196b, and miR-301a and miR-301b. These miRNAs have all been shown to be increased in CRC tumour samples (Cummins et al 2006, Volinia et al 2006, Monzo et al 2008, Chen et al 2009, Diosdado et al 2009, Motoyama et al 2009, Luo et al 2012). Some, such as the miR-17-92 cluster and miR-196a, have been shown to promote tumour development, with the miR-17-92 cluster in particular designated oncomir -1 due to its oncogenic potential (He et al 2005a, Schimanski et al 2009). The miR-17-92 cluster of miRNAs promotes proliferation and angiogenesis, inhibit differentiation, and sustain cell survival (Mu et al 2009, Olive et al 2009). Other miRNAs were shown to be increased with butyrate treatment, including miR-23a, miR-23b and miR-1290, which have all been shown to be decreased in CRC (Cummins et al 2006, Chen et al 2009, Luo et al 2012). miR-23b in particular has been identified as having a tumour suppressor role (Zhang et al 2011). miR-210 was also increased with butyrate treatment in both cell lines. The regulation of several miRNAs, including miR-215 and miR-192, was cell-line specific, indicating that genetic variations between cell types influence the butyrate response.

9.1.2 HDI treatment reduces miR-17-92 cluster expression and increases expression of target genes in colorectal cancer cells

In Chapter 5, the effects of the diet-derived HDI butyrate were compared with those of other types of HDIs, in particular the hydroxamic acids TSA and SAHA, to confirm that the dysregulated miRNA expression observed in CRC cells can be altered by

epigenetic mechanisms. Butyrate and these other HDIs were shown to have similar effects on miR-17-92 expression, with all three shown to decrease levels of miRNAs in the miR-17-92 cluster in CRC cell lines, at mM concentrations for butyrate and μM concentrations for TSA and SAHA. No other studies have previously compared the effects of multiple HDIs on miRNA expression in CRC; however, one other study conducted at the same time also found miRNAs from the miR-17-92 cluster and the paralogous cluster miR-106a-363 to be significantly decreased with butyrate treatment in CRC cells (Hu et al 2011). As in Chapter 4, this Chapter showed that the HCT116 cell line had greater susceptibility than the HT29 cell line to the anti-proliferative effects of HDIs, and the decrease in miR-17-92 cluster expression in response to HDI treatment was also greater in the HCT116 cell line. Particularly in the HCT116 cell line, 5 mM butyrate treatment allowed miR-17-92 levels to fall to a level similar to that in normal human rectal mucosa. The difference in response between the two CRC cell lines may be due to various genetic differences; for example, HT29 cells have mutated p53 while HCT116 cells have wild-type p53 (LaBonte et al 2009). Mutations in p53 have previously been shown to reduce response to HDIs such as butyrate (Williams et al 1993, Palmer et al 1997, Emenaker et al 2001, Bandyopadhyay et al 2004).

The butyrate-induced decrease in miR-17-92 cluster miRNA levels may mediate the anti-proliferative and pro-apoptotic effects of butyrate treatment. The miR-17-92 cluster has been shown in mainly lymphoma models to target genes that are important in cell cycle control, including the cell cycle inhibitor *CDKN1A* (p21) and the pro-apoptotic genes *PTEN* and *BCL2L11* (Bim) (Ventura et al 2008, Inomata et al 2009, Mu et al 2009, Olive et al 2009, Wong et al 2010). In Chapter 5, the butyrate-induced decrease in miR-17-92 cluster miRNAs in the CRC cell lines corresponded with an increase in the expression of genes targeted by the cluster, including *CDKN1A*, *PTEN* and *BCL2L11*. Particularly in the HCT116 cells, *CDKN1A*, *PTEN* and *BCL2L11* were restored to levels similar or greater than those detected in normal human rectal mucosa. This regulation could be a result of butyrate-induced chromatin changes, but may be additionally mediated by alteration in miR-17-92 miRNA levels, as investigated in Chapter 6. miR-17-92 is directly activated by C-MYC and by E2F1 and E2F3 (O'Donnell et al 2005, Woods et al 2007). Also in Chapter 5, *E2F1* was shown to be significantly reduced by butyrate in both cell lines, which could play a role in the observed decrease in miR-17-92 levels. Other studies have also shown down-regulation of *E2F1* in response to HDIs (Boutillier et al 2003, Abramova et al 2006, Abramova et al 2010, Noro et al 2010).

9.1.3 Treatment with HDIs reveals competing roles for miR-17-92 cluster members

In Chapter 6, the first evidence was presented for individual miR-17-92 cluster members having opposing effects on proliferation in CRC cells, and support was provided for the concept that miRNAs can mediate the effects of HDIs on gene expression. Decreased miR-17-92 miRNA levels may be partly responsible for the anti-proliferative effects of HDIs, as transfection with miR-17-92 miRNAs reversed this effect. As shown in Chapter 5, in the context of a butyrate-induced reduction in miR-17-92 levels, *CDKN1A*, *PTEN*, and *BCL2L11* mRNA and protein levels were increased. In Chapter 6, transfection with miR-19 (a and b), 17, 20a or 92a mimics reversed this effect and decreased transcript levels of *CDKN1A*, *PTEN*, and *BCL2L11*, with various cluster members targeting different genes. The decrease in miR-17-92 miRNAs and subsequent target gene de-repression is a plausible mechanism to explain some of the anti-proliferative and pro-apoptotic effects of HDIs, which may be additional to direct chromatin-mediated regulation of gene expression.

Chapter 6 identified competing roles of miR-17-92 cluster members in CRC cells, and a potential homeostatic function for miR-18a. miR-19 (a and b) were primarily responsible for promoting proliferation. The HDI-mediated decrease in miR-17-92 levels was associated with decreased proliferation, while transfection with miR-19 (a and b) restored growth to a level closer to that of untreated cells in control medium. Conversely, miR-18a acted against the other miR-17-92 cluster members to decrease proliferation. Several studies are in agreement that among the six miR-17-92 cluster miRNAs, miR-19 (a and b) are the primary oncogenic determinants; these miRNAs were required and largely sufficient for promoting the oncogenic properties of the cluster in lymphoma models (Mu et al 2009, Olive et al 2009). Conversely, there has been little research to date on the role of miR-18a in cancer. Since the completion of research for this Chapter, one study has shown that miR-18a suppressed cell proliferation and targeted Dicer in bladder cancer cells (Tao et al 2012). This could indicate a potential feedback loop where the regulation of Dicer by miR-18a controls miRNA output (Tao et al 2012). In Chapter 6, two novel targets for miR-18a were confirmed, *NEDD9* and *CDK19*. Two previous studies in CRC cell lines have shown that *NEDD9* down-regulation reduced proliferation and in one study also inhibited xenograft tumour growth, while *NEDD9* over-expression increased proliferation and migration (Xia et al 2010, Li et al 2011b). *NEDD9* and *CDK19* were shown in this

Chapter to promote cellular proliferation, with repression of these genes by RNA interference reducing proliferation.

9.1.4 Butyrate alters miR-17-92 cluster transcription via specific histone modifications at the locus of *MIR17HG*, the miR-17-92 host gene.

The mechanisms by which a HDI such as butyrate can alter levels of miR-17-92 cluster miRNAs were further explored in Chapter 7. An initial cycloheximide experiment indicated that the butyrate-induced decrease in miR-17-92 miRNAs in CRC cells may be a combination of a primary transcriptional response, and an indirect response mediated by regulatory proteins. Cycloheximide can be used to block *de novo* protein synthesis in CRC cells (Della Ragione et al 2001, Andoh et al 2002), with this Chapter showing that all of the miR-17-92 cluster miRNAs were significantly down-regulated by 5 mM butyrate, in both standard and cycloheximide-treated HT29 and HCT116 cells, with the exception of miR-17 in the cycloheximide-treated HT29 cells. The decrease in miR-17-92 miRNA levels was greater in the cell lines that were not treated with cycloheximide, with the smaller butyrate-induced decrease in miR-17-92 levels in cycloheximide-treated cells providing an indication that while the inhibition of *de novo* protein synthesis impacted on miR-17-92 regulation, direct regulation of miR-17-92 host gene transcription was also possible.

Possible regulatory mechanisms were explored in Chapter 5, with the butyrate-induced decrease in miR-17-92 regulators like the transcription factor E2F1 one explanation for decreased *MIR17HG* transcription. Further regulatory mechanisms were examined in Chapter 7, with ChIP analysis used to determine how butyrate-induced histone modifications at the miR-17-92 cluster host gene, *MIR17HG*, may lead to altered transcription. The ChIP analysis examined H3K9ac, H3K14ac, H3K27ac, and H3K4me3, which are all generally accepted as activating histone marks (Strahl & Allis 2000, Jenuwein & Allis 2001, Barski et al 2007, Mikkelsen et al 2007, Rodriguez-Paredes & Esteller 2011). Butyrate-treated cells had decreased acetylation of H3K9/H3K14 and H3K27, centred around the proximal promoter and TSS of *MIR17HG*. This was in contrast to the butyrate-treated cells displaying increased acetylation of these lysine residues further upstream and downstream of the TSS. There was also decreased tri-methylation at H3K4 in the butyrate-treated cells, again centred specifically around the proximal promoter and TSS of *MIR17HG*. The decrease in activating histone marks suggests a direct epigenetic mechanism for decreased *MIR17HG* transcription in

response to butyrate. This is in keeping with a study by Rada-Iglesias et al (2007) which showed that butyrate may actually reduce histone H3 and H4 acetylation close to TSSs, and by this mechanism may decrease transcription of some genes. The findings from Chapter 5 and 7 indicate that various mechanisms play a role in miRNA regulation by butyrate in CRC cells, including alterations in transcription factor levels, and modifications in activating histone marks. It is possible that these mechanisms may function cooperatively. HDACs are known to interact with a variety of non-histone proteins, including transcription factors and co-regulators, and their recruitment to specific loci is also assisted by a range of regulatory factors (Ferreira et al 2001).

9.1.5 Red meat and resistant starch alter miR-17-92 cluster expression in rectal mucosa cells of healthy human volunteers

In contrast to the previous Chapters which examined the effect of HDIs such as butyrate on miRNA expression in CRC cells *in vitro*, Chapter 8 explored these effects on rectal mucosa cells *in vivo*. The Chapter presented the first evidence for an effect of dietary compounds on miRNA expression in rectal mucosa cells in humans; miRNA-specific findings were presented from a randomised cross-over trial examining the effects of a high red meat diet, or high red meat diet supplemented with butyrylated resistant starch on markers of CRC risk in healthy volunteers aged 50 – 75 years. Epidemiological studies have provided the first evidence for increased CRC risk with high red meat intake (WCRF 2007). Investigations into the mechanisms surrounding this have shown that red meat can increase DNA damage and induce DNA strand breaks (Toden et al 2006, Toden et al 2007). The generation of potentially carcinogenic N-nitroso compounds can increase DNA alkylation and enhance formation of DNA adducts (Lewin et al 2006). Also, the production of heterocyclic amines and polycyclic aromatic hydrocarbons through cooking at high temperature can induce DNA damage (Rohrmann et al 2009), while the haem iron and free iron in red meat can lead to the production of free radicals, which can also be damaging (Glei et al 2006). In this Chapter, high red meat intake was also shown for the first time to alter miRNA levels in human rectal biopsy samples, and to significantly increase levels of some miRNAs, in particular miR-21 and the miR-17-92 cluster members miR-17, miR-19a, miR-20a and miR-19b, which have known oncogenic properties (Schetter et al 2008, Mu et al 2009, Olive et al 2009).

While high red meat intake may increase CRC risk, resistant starch can potentially ameliorate some of these effects. Besides the epidemiological evidence that fibre can

decrease CRC risk (WCRF 2007), interventional evidence in rodent models has shown that resistant starch supplementation can raise colonic butyrate levels, reduce adenocarcinoma formation in response to carcinogen administration, and attenuate red meat-induced DNA damage (Le Leu et al 2007a, Le Leu et al 2007b, Toden et al 2007, Le Leu et al 2009, Winter et al 2011). One human trial has also suggested inconclusively that fibre may play a role in modifying DNA adduct formation in the context of high red meat consumption (Lewin et al 2006). The study described in Chapter 8 was the first to directly examine the effects of a combined high red meat diet with resistant starch supplementation in humans, and the first to examine the influence of these diets on miRNAs in rectal biopsy samples. When the high red meat diet was supplemented with butyrylated resistant starch, this significantly raised faecal butyrate levels. In Chapter 8, a novel mechanism by which resistant starch may be beneficial for bowel health was displayed, with some of the miRNAs that were elevated with high red meat intake alone reduced and restored to baseline levels with butyrylated resistant starch supplementation. Levels of miR-17-92 miRNAs in particular were significantly lower in red meat with resistant starch supplementation than with red meat alone in the rectal biopsy samples. The elevated miR-17-92 miRNA levels in the high red meat diet corresponded with decreased transcript levels of miR-17-92 target genes such as *CDKN1A*, providing preliminary evidence regarding the impact of the detected miRNA changes on cellular function. Unlike miR-17-92 miRNAs, levels of miR-21 remained similar in red meat with resistant starch supplementation compared with red meat alone, and levels of miR-16 remained stably expressed regardless of diet. This provides support for the hypothesis that the miRNA changes with resistant starch supplementation may be due to increased butyrate production, as in previous Chapters miR-17-92 cluster miRNAs but not miR-21or miR-16 responded to butyrate treatment *in vitro*. Resistant starch, and indirectly butyrate, thus appears to reverse the dysregulation of miR-17-92 miRNAs in human rectal mucosa cells with high red meat exposure *in vivo*.

9.2 Future directions and applications

The decrease in the oncogenic miR-17-92 cluster miRNA levels and increase in target gene expression is a plausible mechanism to explain some of the chemo-protective effects of HDIs like butyrate. Butyrate was shown in this study to reverse the dysregulation of miR-17-92 miRNAs in CRC cells *in vitro*, and potentially also in healthy rectal cells exposed to high levels of red meat *in vivo*. Other butyrate-regulated miRNAs may also play a functional role in contributing to the decreased proliferation and

increased apoptosis in butyrate-treated CRC cells. Characterising the roles of these additional miRNAs represents one area for further study, through functional screens.

Importantly, the *in vitro* findings of a butyrate-induced decrease in miR-17-92 miRNAs were reflected in the *in vivo* human trial with resistant starch supplementation. Global miRNA and associated mRNA expression profiles could also be investigated in an extension of the current trial, to identify important pathways regulated by resistant starch supplementation. Several limitations of this trial are apparent, including a small patient population, and the fact that the study design prevented the determination of the resistant starch effect on colorectal cells without a background of high red meat intake. Further investigation in humans into how high red meat and high resistant starch individually and concomitantly impact on miRNA expression, target gene expression, and CRC development is warranted. While not confirmed, a mechanism for the effect of resistant starch on miRNA expression may be through the displayed increase in butyrate production. Butyrate acts as an energy source for normal colonocytes (Roediger 1982), but reduces proliferation and induces apoptosis in cancer (Mariadason et al 2000). It appears that in the presence of a carcinogen or stress diet, increased butyrate through resistant starch supplementation may have a similar effect on normal colorectal cells as in cancer, by reducing proliferation and increasing apoptosis (Le Leu et al 2007a, Le Leu et al 2009). In this study, resistant starch supplementation leading to increased butyrate levels was also shown to reduce levels of oncogenic miR-17-92 miRNAs in rectal mucosa cells, in the context of high red meat intake. Further exploration of this novel protective mechanism is important in the current environment of high red meat consumption in developed countries, and the concurrent high levels of CRC.

In this study, potential direct and indirect mechanisms were displayed for the regulation of miR-17-92 host gene transcription by butyrate. The altered histone acetylation and methylation observed around the *MIR17HG* TSS suggest a direct epigenetic mechanism for this decrease in response to butyrate, while changes in regulatory proteins such as the transcription factor E2F1 are also likely to play a role. The ChIP analysis presented in Chapter 7 was a preliminary experiment, and was limited to examining several activating histone marks, at one locus. Confirmation of the current finding of butyrate-induced histone modifications around the miR-17-92 cluster using multiple biological replicates is required, and extension to all defined miRNA genes would be beneficial. ChIP-Seq methodology could further assist in identifying the miRNAs that change during the butyrate response and to ascertain which chromatin modifications are

involved in their regulation. Interactions between regulatory proteins, HDACs, and histone modifications could also be explored.

Competing roles of miR-17-92 cluster miRNAs were identified in this study. Most cluster miRNAs inhibited the anti-proliferative effect of HDIs whereas miR-18a enhanced the effect and targeted pro-proliferative genes, *NEDD9* and *CDK19*. While this study focused on the specific effects of these miRNAs on proliferation, future work to assess their specific roles in apoptosis may strengthen the finding that miR-18a has a unique opposing role. The expression of miR-17-92 cluster miRNAs in normal and cancer colorectal cells, their identified target genes, competing roles, and regulation by HDIs are summarised in Figure 9.1. It can be hypothesised that miR-18a may have a homeostatic function in helping to contain the oncogenic effect of the entire miR-17-92 cluster. There is some evidence to suggest that tumour progression may be associated with selection against miR-18a expression (Diosdado et al 2009), creating an imbalance that may favour increased proliferation. It is known that various post-transcriptional regulatory mechanisms can lead to different levels of individual cluster members, with miR-18a specifically processed by hnRNPA1 (Guil & Caceres 2007); this processing may be altered in cancer. Further investigation of the homeostatic role of miR-18a, may be useful, and could include *in vivo* mouse models with manipulated miR-18a levels. Currently the observation that miR-18a acts in opposition to other cluster members is limited to several cancer cell lines, and this hypothesis requires validation in other cell types and contexts. miRNAs can have specific action in various contexts, with positive and negative effects on tumourigenesis (Mendell & Olson 2012).

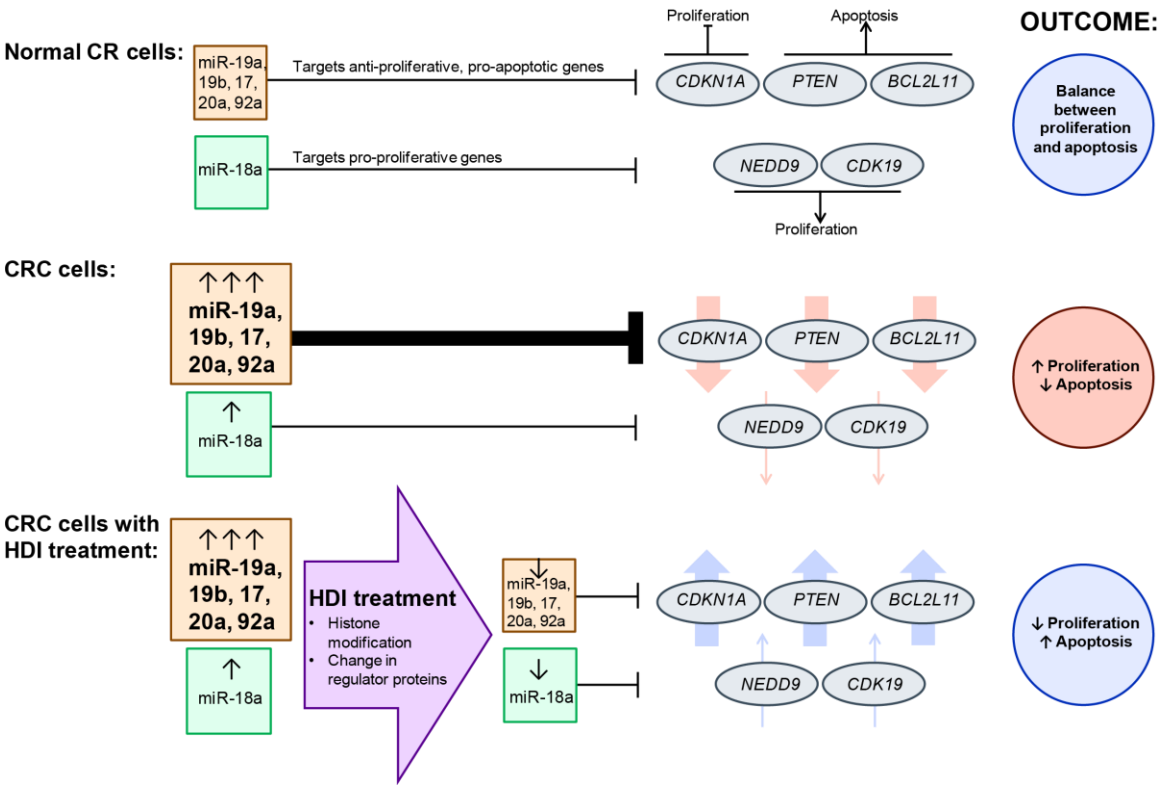

Figure 9.1: Proposed mechanism by which differing levels of miR-17-92 cluster miRNAs in normal cells, CRC cells, and CRC cells with HDI treatment alter identified target genes and cell outcomes.

miR-18a may have a homeostatic function in helping to contain the oncogenic effect of the entire miR-17-92 cluster. Selection against miR-18a expression may occur during tumour progression. This could create an imbalance that favours increased proliferation, through a relative increase in miR-19 (a and b) and other oncogenic miR-17-92 cluster members in CRC. The decrease in these miRNAs with HDI treatment may play a role in decreasing proliferation. HDI: Histone deacetylase inhibitor. While not to scale, the sizes of the boxes in the Figure indicate relative changes in miRNA levels.

There are several potential avenues for therapeutic applications associated with the findings of this project regarding HDI regulation of the miR-17-92 cluster, and competing roles for miR-17-92 cluster members.

HDIs are already under clinical evaluation for their potential as chemotherapeutic agents. Butyrate is rapidly metabolised and has a short half-life *in vivo*, which is not ideal for a systemic chemotherapeutic agent (Miller et al 1987). The HDI SAHA, however, has undergone phase II clinical trials, and was the first of two HDIs to be approved by the FDA for the treatment of cutaneous T-cell lymphoma (Duvic et al 2007, Olsen et al 2007). SAHA is also being investigated for treatment of solid tumours such as CRC. Several small early phase II trials of SAHA in tumours including CRC were mainly concerned with safety and establishing appropriate dosage, and were unable to establish the efficacy of the treatment (Vansteenkiste et al 2008, Wilson et al 2010b). The current evaluations of the clinical effect of HDIs have been performed without a complete understanding of their molecular mechanisms of action (Rada-Iglesias et al 2007). The findings of this study and several other recent studies (Shin et al 2009b, Hu et al 2011) that HDIs modify miRNA expression in CRC cells add to the body of knowledge surrounding their action, and may assist in the refining of treatment strategies and the monitoring of their effect.

Inhibition or delivery of miRNAs may also have therapeutic potential, and may be used to modulate a disease process (Mendell & Olson 2012). A range of miRNA inhibitors has been developed to inhibit specific miRNAs that have pathologic properties, including chemically modified antisense oligonucleotides and miRNA sponges (Krutzfeldt et al 2005, Ebert et al 2007). Preliminary animal studies have highlighted the potential of these miRNA-targeted therapeutics. Krutzfeldt et al (2005), for example, showed that chemically engineered oligonucleotides, termed antagomirs, could silence specific endogenous miRNAs in mice, including miR-122, an abundant liver-specific miRNA. To date, the most advanced miRNA therapeutic remains a miR-122 targeted therapy, specifically a locked nucleic acid antimiR oligonucleotide against miR-122 for treatment of hepatitis C virus infection. Inhibition of miR-122 was shown to suppress viral replication *in vitro* and *in vivo* (Jopling et al 2005, Elmen et al 2008, Lanford et al 2010), and was the first miRNA therapeutic to be tested in humans, with Phase II trials showing viral reduction after treatment without evidence of toxicity (Reesink et al 2012). AntimiRs for members of the miR-17-92 cluster have been used experimentally *in vitro* in several cancer types, including CRC (Matsubara et al 2007, Fontana et al 2008, Tsuchida et al 2011), and have also been used *in vivo* in rodents for other diseases

(Pullamsetti et al 2012). The use of mimics of miRNAs that play beneficial roles in disease has also been explored for its therapeutic potential (Mendell & Olson 2012). The cellular uptake of administered miRNAs is problematic and has been addressed with various strategies, including viral-based delivery or by packaging the miRNAs into lipid nanoparticles for systemic delivery (Kota et al 2009, Pramanik et al 2011). miRNA replacement therapy using miRNAs with tumour suppressor properties has been performed in cancer in rodent models *in vivo*, resulting in tumour suppression without toxicity in normal tissues (Kota et al 2009, Pramanik et al 2011, Trang et al 2011). In the context of the findings of this study, miRNA-based therapy could be used to inhibit miR-19 (a and b) and other oncogenic members of the miR-17-92 cluster using antisense oligonucleotides, or to restore levels of miR-18a using miRNA replacement therapy. For such therapy to be successful, challenges surrounding the tissue-specific effects of miRNAs would require addressing, as miRNAs that promote disease in some tissues may play protective roles in others (Mendell & Olson 2012). One example is miR-26a, which can suppress hepatocellular cancer but may promote glioma formation (Huse et al 2009, Kota et al 2009). miR-17-92 cluster members may also have tissue specific effects. Like other cluster members, miR-92a has an oncogenic role in CRC (Tsuchida et al 2011), while in a non-cancer context miR-92a can decrease angiogenesis (Bonauer et al 2009). Conversely, while miR-18a has been shown in this study to decrease proliferation in CRC, and also to suppress proliferation in bladder cancer (Tao et al 2012), it may also play a role in blood vessel growth (Dews et al 2006). Methods for controlled, tissue-specific delivery are being explored (Mendell & Olson 2012).

Besides HDI treatments or miRNA-based therapeutics which both currently have substantial challenges, the findings of this study confirm the benefits of several proposed CRC prevention strategies. In the human red meat and resistant starch trial, increases in expression of some oncogenic miRNAs were discovered in response to a high red meat diet, with resistant starch, and indirectly high butyrate, to some degree reversing this effect. This provides further evidence to suggest that limiting red meat intake, or ensuring it is consumed in the context of a diet high in fibre and resistant starch, may be beneficial for CRC prevention. Resistant starch supplementation is also a potentially viable strategy for modifying CRC risk, with butyrylated resistant starch offering additional benefits (Bajka et al 2008, Clarke et al 2012). Several studies have shown long term resistant starch supplementation to be feasible (Burn et al 2008, Burn et al 2011). There has also been a recent expansion in the number of commercially available foods with modifications or supplementation to increase resistant starch

content (Landon 2007, Bird et al 2008). In a global first for a government health authority, Australia's National Health and Medical Research Council now also specify a resistant starch component in their fibre intake recommendations, due to its positive impact on digestive health (NHMRC 2006, Landon 2007). Improved understanding at a molecular level of the chemoprotective effects of this dietary component may assist in its dispersion and uptake in the food system.

9.3 Conclusions

This study examined dietary regulation of miRNA expression in colorectal cells, and explored the role of miRNAs in mediating the chemo-protective effects of diet-derived butyrate and other HDIs. Butyrate and other HDIs decrease proliferation and increase apoptosis in CRC cells via epigenetic changes in gene expression, and the dysregulated miRNA expression observed in CRC cells could also be epigenetically altered by HDIs. *In vitro*, a decrease in miR-17-92 cluster miRNA levels was observed in CRC cells with HDI treatment, with a corresponding increase in expression of miR-17-92 target genes, including cell cycle inhibitors and pro-apoptotic genes. The decrease in miR-17-92 expression may be partly responsible for the anti-proliferative effects of HDIs, with introduction of miR-17-92 cluster miRNA mimics reversing this effect and decreasing levels of target gene transcripts. Of the miR-17-92 cluster miRNAs, miR-19a and miR-19b were primarily responsible for promoting proliferation, while in a novel finding, miR-18a acted in opposition to other cluster members to decrease growth. *NEDD9* and *CDK19* were identified as novel miR-18a targets and were shown to be pro-proliferative genes. This study presents the first evidence of competing roles for miR-17-92 cluster members, in the context of HDI-induced changes in CRC.

In addition to the capacity of butyrate to reverse the dysregulation of miR-17-92 miRNAs in CRC cells *in vitro*, this action was also demonstrated with resistant starch supplementation *in vivo*, in the rectal mucosa cells of human volunteers exposed to high levels of red meat. High red meat intake was shown to raise levels of several miRNAs with oncogenic potential, particularly miR-17-92 cluster miRNAs, and also miR-21. In the context of a high red meat diet, resistant starch supplementation to raise butyrate levels was shown to decrease miR-17-92 cluster miRNA levels, restoring them to normal baseline levels. The findings in this study of *in vivo* modulation of rectal cell miRNAs by various dietary compounds have not previously been demonstrated in humans. The regulation of miRNA expression demonstrates a plausible mechanism to explain some of the chemo-protective effects of HDIs, and some of the potentially

carcinogenic properties of other dietary components. Understanding how dietary compounds alter miRNA expression, and how miRNAs modulate the action of HDIs, may provide new opportunities for CRC therapies and prevention strategies.

Appendix 1 – Preliminary experiments showing butyrate-induced microRNA expression changes

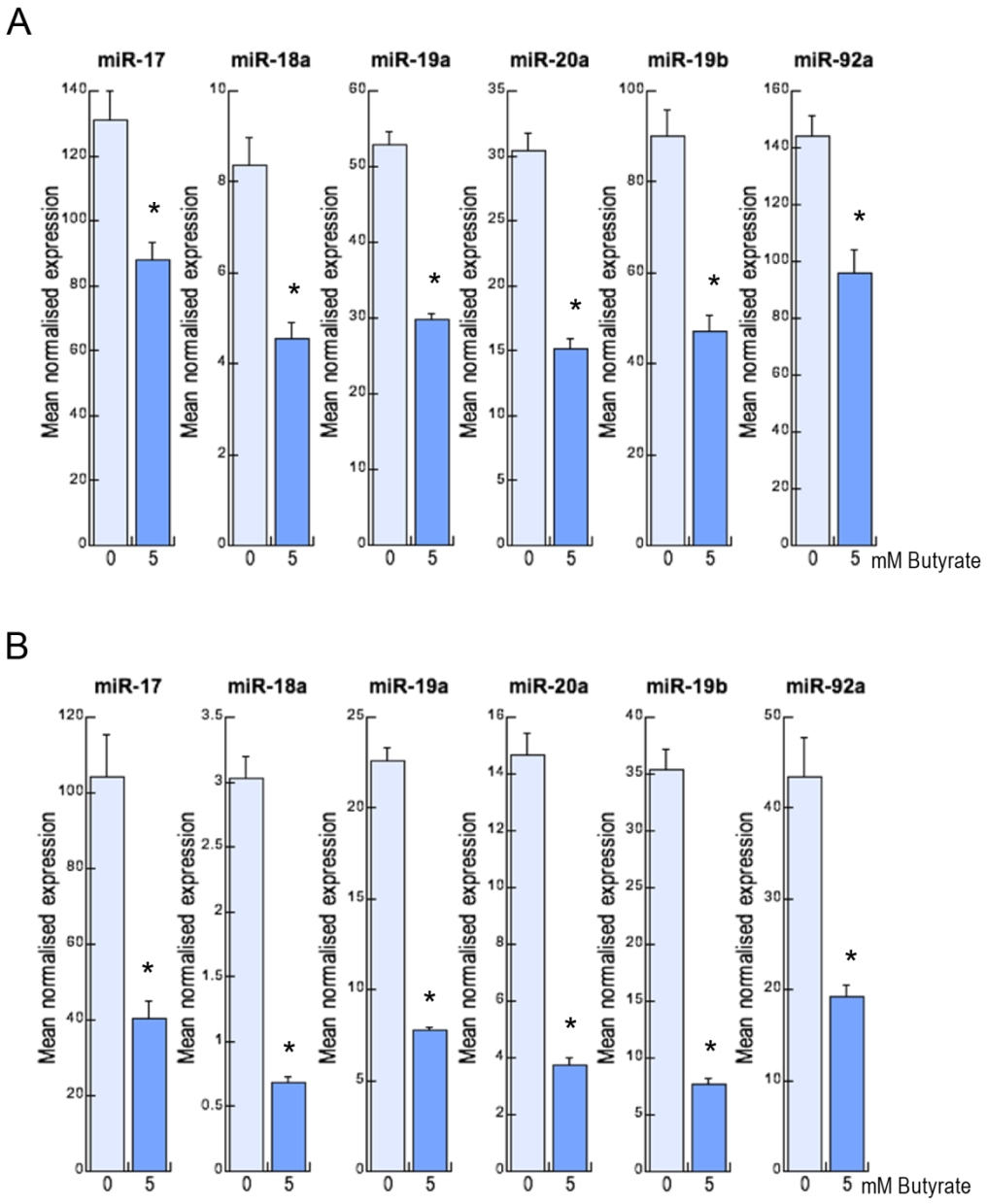

Figure A1.1: Real-time RT-PCR analysis of miR-17-92 levels in HT29 and HCT116 cells with 48 h butyrate treatment.

HT29 (A) and HCT116 (B) cells treated with 5 mM butyrate, compared with cells in control medium (0) (* $P < 0.05$). The mean ± SEM of three cell culture replicates is shown, and expression is normalised to RNU6B levels.

Appendix 2 – Ingenuity Pathway Analysis of miR-18a predicted target genes

Tables A2.1 – A2.3 show the results of the IPA analysis of 91 potential miR-18a target genes (Table A2.4), identified using the intersection of prediction programs in miRGen (Megraw et al 2007). The top IPA networks associated with miR-18a potential targets are listed in Table A2.1. Among the top IPA diseases and disorders associated with the miR-18a potential targets (Table A2.2) is the relevant disorder of 'Cancer'. The top IPA molecular and cellular functions associated with miR-18a potential targets (Table A2.3) included functions which are relevant in cancer development and progression, such as cell cycle and cell death.

Table A2.1: Top IPA networks associated with potential miR-18a target genes

Network number	Associated Network Functions	IPA Score
1	Cardiovascular System Development and Function, Organ Morphology, Skeletal and Muscular System Development and Function	44
2	Cell Signaling, Nucleic Acid Metabolism, Small Molecule Biochemistry	29
3	Connective Tissue Development and Function, Skeletal and Muscular System Development and Function, Tissue Development	19
4	Gene Expression, Embryonic Development, Tissue Development	19
5	Nervous System Development and Function, Cellular Development, Connective Tissue Development and Function	18

Table A2.2: Top IPA diseases and disorders associated with potential miR-18a target genes

Name	*P* value	Number of molecules
Genetic Disorder	5.84E-07 – 1.59E-02	55
Neurological Disease	5.84E-07 – 1.93E-02	38
Psychological Disorders	5.84E-07 – 1.89E-02	25
Respiratory Disease	1.60E-04 – 1.56E-02	3
Cancer	3.18E-04 – 2.03E-02	34

Table A2.3: Top IPA molecular and cellular functions associated with potential miR-18a target genes

Name	*P* value	Number of molecules
Gene Expression	5.64E-10 – 2.07E-02	35
Cellular Development	8.98E-06 – 1.99E-02	30
Cell Death	2.30E-04 – 1.72E-02	30
Cell Cycle	6.15E-04 – 1.98E-02	17
Cellular Movement	6.75E-04 – 2.06E-02	17

Table A2.4: List of potential miR-18a target genes, identified using the intersection of prediction programs in miRGen

Symbol	Gene Name
ACTB	actin, beta
ADD3	adducin 3 (gamma)
AEBP2	AE binding protein 2
ASXL2	additional sex combs like 2 (Drosophila)
ATXN1	ataxin 1
BHLHE22	basic helix-loop-helix family, member e22
BRWD3	bromodomain and WD repeat domain containing 3
BTG3	BTG family, member 3
C1orf9	chromosome 1 open reading frame 9
C5orf13	chromosome 5 open reading frame 13
CAMSAP1L1	calmodulin regulated spectrin-associated protein 1-like 1
CCDC88A	coiled-coil domain containing 88A
CDC42	cell division cycle 42 (GTP binding protein, 25kDa)
CDK19	cyclin-dependent kinase 19
CREBL2	cAMP responsive element binding protein-like 2
CRIM1	cysteine rich transmembrane BMP regulator 1 (chordin-like)
CTDSPL	CTD (carboxy-terminal domain, RNA polymerase II, polypeptide A) small phosphatase-like
CTGF	connective tissue growth factor
DDX42	DEAD (Asp-Glu-Ala-Asp) box polypeptide 42
DPP10	dipeptidyl-peptidase 10 (non-functional)
DUSP16	dual specificity phosphatase 16
EHMT1	euchromatic histone-lysine N-methyltransferase 1
EPB41L1	erythrocyte membrane protein band 4.1-like 1
ESR1	estrogen receptor 1
ETV6	ets variant 6
FCHSD2	FCH and double SH3 domains 2
FNBP1	formin binding protein 1
FOXN1	forkhead box N1
GAB1	GRB2-associated binding protein 1
GAB2	GRB2-associated binding protein 2
GCLC	glutamate-cysteine ligase, catalytic subunit
GIGYF1	GRB10 interacting GYF protein 1
GLRB	glycine receptor, beta
GRHL2	grainyhead-like 2 (Drosophila)
HCN4	hyperpolarization activated cyclic nucleotide-gated potassium channel 4
HDHD2	haloacid dehalogenase-like hydrolase domain containing 2
HIF1A	hypoxia inducible factor 1, alpha subunit (basic helix-loop-helix transcription factor)
HMGCS1	3-hydroxy-3-methylglutaryl-CoA synthase 1 (soluble)
HSF2	heat shock transcription factor 2

IRF2	interferon regulatory factor 2
KDM2A	lysine (K)-specific demethylase 2A
KLHL20	kelch-like 20 (Drosophila)
LIN28A	lin-28 homolog A (C. elegans)
MAN1A2	mannosidase, alpha, class 1A, member 2
MAP7D1	MAP7 domain containing 1
MBNL2	muscleblind-like 2 (Drosophila)
MDGA1	MAM domain containing glycosylphosphatidylinositol anchor 1
MEF2D	myocyte enhancer factor 2D
MEIS1	Meis homeobox 1
MESP1	mesoderm posterior 1 homolog (mouse)
NEDD9	neural precursor cell expressed, developmentally down-regulated 9
NEUROD1	neurogenic differentiation 1
NFAT5	nuclear factor of activated T-cells 5, tonicity-responsive
NR3C1	nuclear receptor subfamily 3, group C, member 1 (glucocorticoid receptor)
PACSIN1	protein kinase C and casein kinase substrate in neurons 1
PAPPA	pregnancy-associated plasma protein A, pappalysin 1
PDE4D	phosphodiesterase 4D, cAMP-specific
PHF2	PHD finger protein 2
PIAS3	protein inhibitor of activated STAT, 3
PLAG1	pleiomorphic adenoma gene 1
PRICKLE2	prickle homolog 2 (Drosophila)
PRKACB	protein kinase, cAMP-dependent, catalytic, beta
PSD3	pleckstrin and Sec7 domain containing 3
PTGFRN	prostaglandin F2 receptor negative regulator
PURB	purine-rich element binding protein B
QKI	quaking homolog, KH domain RNA binding (mouse)
RAB11FIP2	RAB11 family interacting protein 2 (class I)
RAB5C	RAB5C, member RAS oncogene family
RABGAP1	RAB GTPase activating protein 1
REXO2	REX2, RNA exonuclease 2 homolog (S. cerevisiae)
RUNX1	runt-related transcription factor 1
SATB1	SATB homeobox 1
SH3BP4	SH3-domain binding protein 4
SIM2	single-minded homolog 2 (Drosophila)
SLC17A9	solute carrier family 17, member 9
SMAD2	SMAD family member 2
SOCS5	suppressor of cytokine signaling 5
SON	SON DNA binding protein
SOX21	SRY (sex determining region Y)-box 21
STK4	serine/threonine kinase 4
TAOK3	TAO kinase 3
TRIB2	tribbles homolog 2 (Drosophila)
TRIM2	tripartite motif containing 2
UBE2G1	ubiquitin-conjugating enzyme E2G 1 (UBC7 homolog, yeast)
USP6	ubiquitin specific peptidase 6 (Tre-2 oncogene)
VPS54	vacuolar protein sorting 54 homolog (S. cerevisiae)
XYLT2	xylosyltransferase II
YPEL5	yippee-like 5 (Drosophila)
ZBTB4	zinc finger and BTB domain containing 4
ZBTB47	zinc finger and BTB domain containing 47
ZNF367	zinc finger protein 367

Appendix 3 – Period effect analysis for high red meat and resistant starch trial

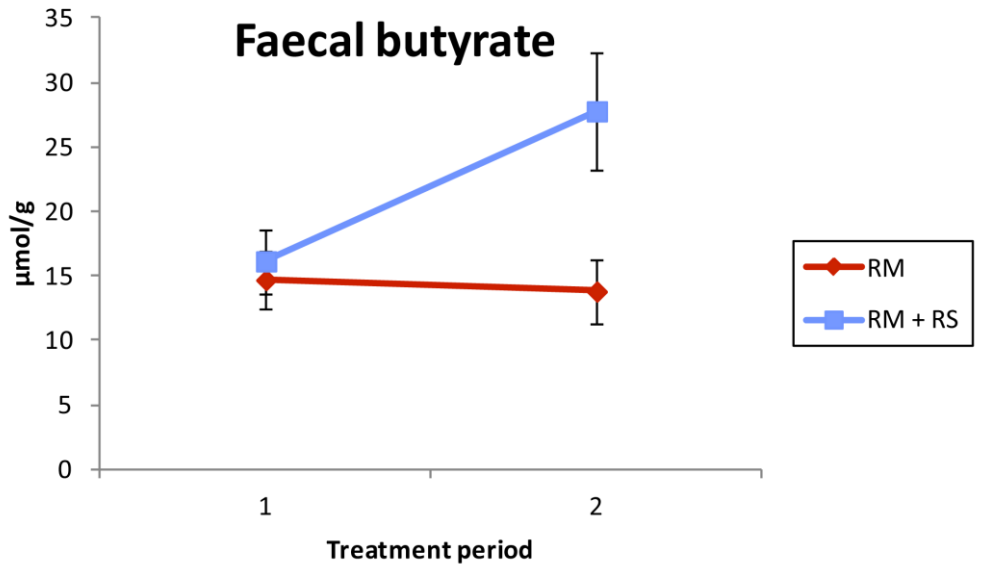

Figure A3.1: Groups-by-periods plot for faecal butyrate levels of participants in the high red meat and resistant starch trial

The mean ± SEM is shown for each diet, in each period. n = 10 in the RM dietary intervention and n = 13 in the RM + RS dietary intervention in the first period. RM: red meat diet; RM + RS: red meat + resistant starch diet.

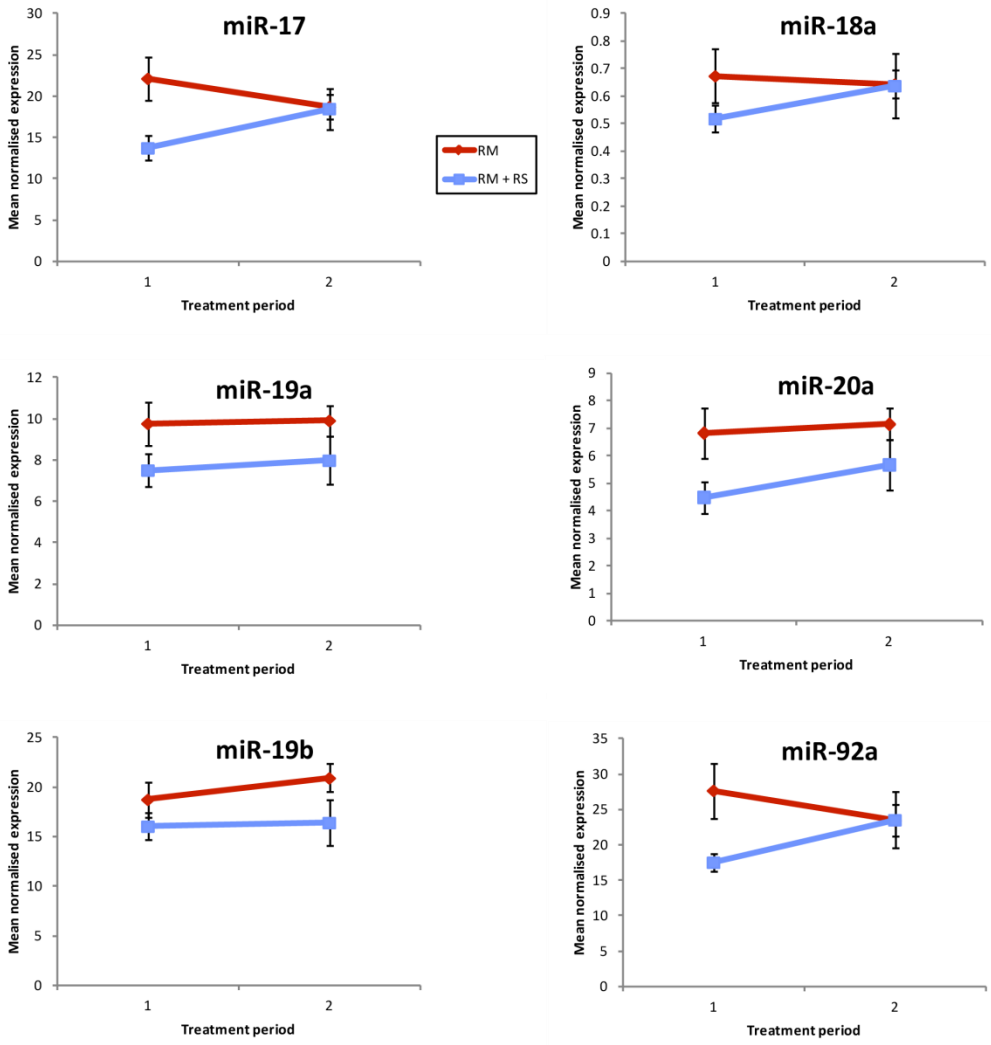

Figure A3.2: Groups-by-periods plot for miR-17-92 cluster miRNA levels in rectal biopsies of participants in the high red meat and resistant starch trial

The mean ± SEM is shown for each diet, in each period. n = 10 in the RM dietary intervention and n = 13 in the RM + RS dietary intervention in the first period. RM = red meat diet; RM + RS = red meat + resistant starch diet.

References

Abrahante JE, Daul AL, Li M, Volk ML, Tennessen JM, Miller EA, et al. The Caenorhabditis elegans hunchback-like gene lin-57/hbl-1 controls developmental time and is regulated by microRNAs. *Dev Cell*. 2003; **4**(5): 625-37.

Abramova MV, Pospelova TV, Nikulenkov FP, Hollander CM, Fornace AJ, Jr., Pospelov VA. G1/S arrest induced by histone deacetylase inhibitor sodium butyrate in E1A + Ras-transformed cells is mediated through down-regulation of E2F activity and stabilization of beta-catenin. *J Biol Chem*. 2006; **281**(30): 21040-51.

Abramova MV, Zatulovskiy EA, Svetlikova SB, Kukushkin AN, Pospelov VA. e2f1 Gene is a new member of Wnt/beta-catenin/Tcf-regulated genes. *Biochem Biophys Res Commun*. 2010; **391**(1): 142-6.

Ach RA, Wang H, Curry B. Measuring microRNAs: comparisons of microarray and quantitative PCR measurements, and of different total RNA prep methods. *BMC Biotechnology*. 2008; **8**: 69.

AIHW. Health expenditure Australia 2003–04. AIHW Cat. no. HWE 32 (Health and Welfare Expenditure Series no. 25). Canberra: Australian Institute of Health and Welfare; 2005.

AIHW. Cancer in Australia: an overview, 2010. Cancer series no. 60. Cat. no. CAN 56. Canberra: Australian Institute of Health and Welfare; 2010.

AIHW. Australian Cancer Incidence and Mortality workbooks, Bowel cancer (ICD10 C18–C20), Australia, 1968–2007. Canberra: Australian Institute of Health and Welfare; 2011.

AIHW. Cancer incidence projections: Australia, 2011 to 2020. Cancer Series no. 66. Cat. no. CAN 62. Canberra: Australian Institute of Health and Welfare; 2012.

AJCC. American Joint Committee on Cancer. Cancer Staging Manual 7th edition. Edge SB, Byrd DR, Compton CC, Fritz AG, Greene FL, Trotti A. New York: Springer; 2010.

Akao Y, Nakagawa Y, Hirata I, Iio A, Itoh T, Kojima K, et al. Role of anti-oncomirs miR-143 and -145 in human colorectal tumors. *Cancer Gene Ther*. 2010; **17**(6): 398-408.

Akao Y, Nakagawa Y, Naoe T. let-7 microRNA functions as a potential growth suppressor in human colon cancer cells. *Biol Pharm Bull*. 2006a; **29**(5): 903-6.

Akao Y, Nakagawa Y, Naoe T. MicroRNAs 143 and 145 are possible common onco-microRNAs in human cancers. *Oncol Rep*. 2006b; **16**(4): 845-50.

Al-Sohaily S, Biankin A, Leong R, Kohonen-Corish M, Warusavitarne J. Molecular pathways in colorectal cancer. *J Gastroenterol Hepatol*. 2012; **27**(9): 1423-31.

Alberts DS, Martinez ME, Roe DJ, Guillen-Rodriguez JM, Marshall JR, van Leeuwen JB, et al. Lack of effect of a high-fiber cereal supplement on the recurrence of colorectal adenomas. Phoenix Colon Cancer Prevention Physicians' Network. *N Engl J Med*. 2000; **342**(16): 1156-62.

Alexander DD, Cushing CA. Red meat and colorectal cancer: a critical summary of prospective epidemiologic studies. *Obes Rev*. 2011; **12**(5): e472-93.

Allis CD, Berger SL, Cote J, Dent S, Jenuwien T, Kouzarides T, et al. New nomenclature for chromatin-modifying enzymes. *Cell*. 2007; **131**(4): 633-6.

Almeida MI, Nicoloso MS, Zeng L, Ivan C, Spizzo R, Gafa R, et al. Strand-Specific miR-28-5p and miR-28-3p Have Distinct Effects in Colorectal Cancer Cells. *Gastroenterology*. 2012; **142**(4): 886-96.

Altonsy MO, Andrews SC. Diallyl disulphide, a beneficial component of garlic oil, causes a redistribution of cell-cycle growth phases, induces apoptosis, and

enhances butyrate-induced apoptosis in colorectal adenocarcinoma cells (HT-29). *Nutr Cancer*. 2011; **63**(7): 1104-13.

Alvarez-Garcia I, Miska EA. MicroRNA functions in animal development and human disease. *Development*. 2005; **132**(21): 4653-62.

Alvaro A, Sola R, Rosales R, Ribalta J, Anguera A, Masana L, et al. Gene expression analysis of a human enterocyte cell line reveals downregulation of cholesterol biosynthesis in response to short-chain fatty acids. *IUBMB Life*. 2008; **60**(11): 757-64.

Ambros V. The functions of animal microRNAs. *Nature*. 2004; **431**(7006): 350-5.

Anderson IH, Levine AS, Levitt MD. Incomplete absorption of the carbohydrate in all-purpose wheat flour. *N Engl J Med*. 1981; **304**(15): 891-2.

Andoh A, Shimada M, Araki Y, Fujiyama Y, Bamba T. Sodium butyrate enhances complement-mediated cell injury via down-regulation of decay-accelerating factor expression in colonic cancer cells. *Cancer Immunol Immunother*. 2002; **50**(12): 663-72.

Annison G, Illman RJ, Topping DL. Acetylated, propionylated or butyrylated starches raise large bowel short-chain fatty acids preferentially when fed to rats. *J Nutr*. 2003; **133**(11): 3523-8.

Archer SY, Johnson J, Kim HJ, Ma Q, Mou H, Daesety V, et al. The histone deacetylase inhibitor butyrate downregulates cyclin B1 gene expression via a p21/WAF-1-dependent mechanism in human colon cancer cells. *Am J Physiol Gastrointest Liver Physiol*. 2005; **289**(4): G696-703.

Archer SY, Meng S, Shei A, Hodin RA. p21(WAF1) is required for butyrate-mediated growth inhibition of human colon cancer cells. *Proc Natl Acad Sci U S A*. 1998; **95**(12): 6791-6.

Arndt GM, Dossey L, Cullen LM, Lai A, Druker R, Eisbacher M, et al. Characterization of global microRNA expression reveals oncogenic potential of miR-145 in metastatic colorectal cancer. *BMC Cancer*. 2009; **9**: 374.

Asangani IA, Rasheed SA, Nikolova DA, Leupold JH, Colburn NH, Post S, et al. MicroRNA-21 (miR-21) post-transcriptionally downregulates tumor suppressor Pdcd4 and stimulates invasion, intravasation and metastasis in colorectal cancer. *Oncogene*. 2008; **27**(15): 2128-36.

Asano T, McLeod RS. Dietary fibre for the prevention of colorectal adenomas and carcinomas. *Cochrane Database Syst Rev*. 2002; (2): CD003430.

Astier A, Manie SN, Law SF, Canty T, Haghayghi N, Druker BJ, et al. Association of the Cas-like molecule HEF1 with CrkL following integrin and antigen receptor signaling in human B-cells: potential relevance to neoplastic lymphohematopoietic cells. *Leuk Lymphoma*. 1997; **28**(1-2): 65-72.

Atmaca A, Al-Batran SE, Maurer A, Neumann A, Heinzel T, Hentsch B, et al. Valproic acid (VPA) in patients with refractory advanced cancer: a dose escalating phase I clinical trial. *Br J Cancer*. 2007; **97**(2): 177-82.

Baffa R, Fassan M, Volinia S, O'Hara B, Liu CG, Palazzo JP, et al. MicroRNA expression profiling of human metastatic cancers identifies cancer gene targets. *J Pathol*. 2009; **219**(2): 214-21.

Bajka BH, Clarke JM, Cobiac L, Topping DL. Butyrylated starch protects colonocyte DNA against dietary protein-induced damage in rats. *Carcinogenesis*. 2008; **29**(11): 2169-74.

Bajka BH, Topping DL, Cobiac L, Clarke JM. Butyrylated starch is less susceptible to enzymic hydrolysis and increases large-bowel butyrate more than high-amylose maize starch in the rat. *Br J Nutr*. 2006; **96**(2): 276-82.

Baker SJ, Markowitz S, Fearon ER, Willson JK, Vogelstein B. Suppression of human colorectal carcinoma cell growth by wild-type p53. *Science*. 1990a; **249**(4971): 912-5.

Baker SJ, Preisinger AC, Jessup JM, Paraskeva C, Markowitz S, Willson JK, et al. p53 gene mutations occur in combination with 17p allelic deletions as late events in colorectal tumorigenesis. *Cancer Res.* 1990b; **50**(23): 7717-22.

Balaguer F, Link A, Lozano JJ, Cuatrecasas M, Nagasaka T, Boland CR, et al. Epigenetic silencing of miR-137 is an early event in colorectal carcinogenesis. *Cancer Res.* 2010; **70**(16): 6609-18.

Balaguer F, Moreira L, Lozano JJ, Link A, Ramirez G, Shen Y, et al. Colorectal cancers with microsatellite instability display unique miRNA profiles. *Clin Cancer Res.* 2011; **17**(19): 6239-49.

Bali P, Pranpat M, Bradner J, Balasis M, Fiskus W, Guo F, et al. Inhibition of histone deacetylase 6 acetylates and disrupts the chaperone function of heat shock protein 90: a novel basis for antileukemia activity of histone deacetylase inhibitors. *J Biol Chem.* 2005; **280**(29): 26729-34.

Bandres E, Agirre X, Bitarte N, Ramirez N, Zarate R, Roman-Gomez J, et al. Epigenetic regulation of microRNA expression in colorectal cancer. *Int J Cancer.* 2009; **125**(11): 2737-43.

Bandres E, Cubedo E, Agirre X, Malumbres R, Zarate R, Ramirez N, et al. Identification by Real-time PCR of 13 mature microRNAs differentially expressed in colorectal cancer and non-tumoral tissues. *Mol Cancer.* 2006; **5**: 29.

Bandyopadhyay D, Mishra A, Medrano EE. Overexpression of histone deacetylase 1 confers resistance to sodium butyrate-mediated apoptosis in melanoma cells through a p53-mediated pathway. *Cancer Res.* 2004; **64**(21): 7706-10.

Barker N, Ridgway RA, van Es JH, van de Wetering M, Begthel H, van den Born M, et al. Crypt stem cells as the cells-of-origin of intestinal cancer. *Nature.* 2009; **457**(7229): 608-11.

Barski A, Cuddapah S, Cui K, Roh T-Y, Schones DE, Wang Z, et al. High-resolution profiling of histone methylations in the human genome. *Cell.* 2007; **129**(4): 823-37.

Bartel DP. MicroRNAs: target recognition and regulatory functions. *Cell.* 2009; **136**(2): 215-33.

Bartley AN, Yao H, Barkoh BA, Ivan C, Mishra BM, Rashid A, et al. Complex patterns of altered MicroRNA expression during the adenoma-adenocarcinoma sequence for microsatellite-stable colorectal cancer. *Clin Cancer Res.* 2011; **17**(23): 7283-93.

Batlle E, Henderson JT, Beghtel H, van den Born MMW, Sancho E, Huls G, et al. Beta-catenin and TCF mediate cell positioning in the intestinal epithelium by controlling the expression of EphB/ephrinB. *Cell.* 2002; **111**(2): 251-63.

Becker C, Fantini MC, Schramm C, Lehr HA, Wirtz S, Nikolaev A, et al. TGF-beta suppresses tumor progression in colon cancer by inhibition of IL-6 trans-signaling. *Immunity.* 2004; **21**(4): 491-501.

Bednar J, Horowitz RA, Grigoryev SA, Carruthers LM, Hansen JC, Koster AJ, et al. Nucleosomes, linker DNA, and linker histone form a unique structural motif that directs the higher-order folding and compaction of chromatin. *Proc Natl Acad Sci U S A.* 1998; **95**(24): 14173-8.

Beitzinger M, Peters L, Zhu JY, Kremmer E, Meister G. Identification of human microRNA targets from isolated argonaute protein complexes. *RNA Biol.* 2007; **4**(2): 76-84.

Bellam N, Pasche B. Tgf-beta signaling alterations and colon cancer. *Cancer Treat Res.* 2010; **155**: 85-103.

Bentwich I, Avniel A, Karov Y, Aharonov R, Gilad S, Barad O, et al. Identification of hundreds of conserved and nonconserved human microRNAs. *Nat Genet.* 2005; **37**(7): 766-70.

Bereshchenko OR, Gu W, Dalla-Favera R. Acetylation inactivates the transcriptional repressor BCL6. *Nat Genet.* 2002; **32**(4): 606-13.

Berger SL. The complex language of chromatin regulation during transcription. *Nature*. 2007; **447**(7143): 407-12.

Bernstein E, Caudy AA, Hammond SM, Hannon GJ. Role for a bidentate ribonuclease in the initiation step of RNA interference. *Nature*. 2001; **409**(6818): 363-6.

Bernstein E, Kim SY, Carmell MA, Murchison EP, Alcorn H, Li MZ, et al. Dicer is essential for mouse development. *Nat Genet*. 2003; **35**(3): 215-7.

Bhaumik SR, Smith E, Shilatifard A. Covalent modifications of histones during development and disease pathogenesis. *Nat Struct Mol Biol*. 2007; **14**(11): 1008-16.

Bingham SA, Day NE, Luben R, Ferrari P, Slimani N, Norat T, et al. Dietary fibre in food and protection against colorectal cancer in the European Prospective Investigation into Cancer and Nutrition (EPIC): an observational study. *Lancet*. 2003; **361**(9368): 1496-501.

Bird A. DNA methylation patterns and epigenetic memory. *Genes Dev*. 2002; **16**(1): 6-21.

Bird AR, Vuaran MS, King RA, Noakes M, Keogh J, Morell MK, et al. Wholegrain foods made from a novel high-amylose barley variety (Himalaya 292) improve indices of bowel health in human subjects. *Br J Nutr*. 2008; **99**(5): 1032-40.

Birkett A, Muir J, Phillips J, Jones G, O'Dea K. Resistant starch lowers fecal concentrations of ammonia and phenols in humans. *Am J Clin Nutr*. 1996; **63**(5): 766-72.

Blais M, Seidman EG, Asselin C. Dual effect of butyrate on IL-1beta--mediated intestinal epithelial cell inflammatory response. *DNA Cell Biol*. 2007; **26**(3): 133-47.

Boffa LC, Gruss RJ, Allfrey VG. Manifold effects of sodium butyrate on nuclear function. Selective and reversible inhibition of phosphorylation of histones H1 and H2A and impaired methylation of lysine and arginine residues in nuclear protein fractions. *J Biol Chem*. 1981; **256**(18): 9612-21.

Boffa LC, Mariani MR, Parker MI. Selective hypermethylation of transcribed nucleosomal DNA by sodium butyrate. *Exp Cell Res*. 1994; **211**(2): 420-3.

Bohnsack MT, Czaplinski K, Gorlich D. Exportin 5 is a RanGTP-dependent dsRNA-binding protein that mediates nuclear export of pre-miRNAs. *Rna*. 2004; **10**(2): 185-91.

Bolden JE, Peart MJ, Johnstone RW. Anticancer activities of histone deacetylase inhibitors. *Nat Rev Drug Discov*. 2006; **5**(9): 769-84.

Bolleyn J, Fraczek J, Vinken M, Lizarraga D, Gaj S, van Delft JH, et al. Effect of Trichostatin A on miRNA expression in cultures of primary rat hepatocytes. *Toxicol In Vitro*. 2011; **25**(6): 1173-82.

Bonauer A, Carmona G, Iwasaki M, Mione M, Koyanagi M, Fischer A, et al. MicroRNA-92a controls angiogenesis and functional recovery of ischemic tissues in mice. *Science*. 2009; **324**(5935): 1710-3.

Boni V, Bitarte N, Cristobal I, Zarate R, Rodriguez J, Maiello E, et al. miR-192/miR-215 influence 5-fluorouracil resistance through cell cycle-mediated mechanisms complementary to its post-transcriptional thymidilate synthase regulation. *Mol Cancer Ther*. 2010; **9**(8): 2265-75.

Bonithon-Kopp C, Kronborg O, Giacosa A, Rath U, Faivre J. Calcium and fibre supplementation in prevention of colorectal adenoma recurrence: a randomised intervention trial. European Cancer Prevention Organisation Study Group. *Lancet*. 2000; **356**(9238): 1300-6.

Booth C, Potten CS. Gut instincts: thoughts on intestinal epithelial stem cells. *J Clin Invest*. 2000; **105**(11): 1493-9.

Borchert GM, Lanier W, Davidson BL. RNA polymerase III transcribes human microRNAs. *Nat Struct Mol Biol*. 2006; **13**(12): 1097-101.

Bostick RM, Potter JD, Kushi LH, Sellers TA, Steinmetz KA, McKenzie DR, et al. Sugar, meat, and fat intake, and non-dietary risk factors for colon cancer incidence in Iowa women (United States). *Cancer Causes Control.* 1994; **5**(1): 38-52.

Bostick RM, Potter JD, Sellers TA, McKenzie DR, Kushi LH, Folsom AR. Relation of calcium, vitamin D, and dairy food intake to incidence of colon cancer among older women. The Iowa Women's Health Study. *Am J Epidemiol.* 1993; **137**(12): 1302-17.

Boutillier AL, Trinh E, Loeffler JP. Selective E2F-dependent gene transcription is controlled by histone deacetylase activity during neuronal apoptosis. *J Neurochem.* 2003; **84**(4): 814-28.

Boyes J, Bird A. DNA methylation inhibits transcription indirectly via a methyl-CpG binding protein. *Cell.* 1991; **64**(6): 1123-34.

Braun CJ, Zhang X, Savelyeva I, Wolff S, Moll UM, Schepeler T, et al. p53-Responsive micrornas 192 and 215 are capable of inducing cell cycle arrest. *Cancer Res.* 2008; **68**(24): 10094-104.

Brennecke J, Stark A, Russell RB, Cohen SM. Principles of microRNA-target recognition. *PLoS Biol.* 2005; **3**(3): e85.

Bressan A, Bigioni M, Bellarosa D, Nardelli F, Irrissuto C, Maggi CA, et al. Induction of a less aggressive phenotype in human colon carcinoma HCT116 cells by chronic exposure to HDAC inhibitor SAHA. *Oncol Rep.* 2010; **24**(5): 1249-55.

Brest P, Lapaquette P, Souidi M, Lebrigand K, Cesaro A, Vouret-Craviari V, et al. A synonymous variant in IRGM alters a binding site for miR-196 and causes deregulation of IRGM-dependent xenophagy in Crohn's disease. *Nat Genet.* 2011; **43**(3): 242-5.

Bronner CE, Baker SM, Morrison PT, Warren G, Smith LG, Lescoe MK, et al. Mutation in the DNA mismatch repair gene homologue hMLH1 is associated with hereditary non-polyposis colon cancer. *Nature.* 1994; **368**(6468): 258-61.

Brummelkamp TR, Bernards R, Agami R. A system for stable expression of short interfering RNAs in mammalian cells. *Science.* 2002; **296**(5567): 550-3.

Burkitt DP. Epidemiology of cancer of the colon and rectum. *Cancer.* 1971; **28**(1): 3-13.

Burn J, Bishop DT, Chapman PD, Elliott F, Bertario L, Dunlop MG, et al. A randomized placebo-controlled prevention trial of aspirin and/or resistant starch in young people with familial adenomatous polyposis. *Cancer Prev Res.* 2011; **4**(5): 655-65.

Burn J, Bishop DT, Mecklin JP, Macrae F, Moslein G, Olschwang S, et al. Effect of aspirin or resistant starch on colorectal neoplasia in the Lynch syndrome. *N Engl J Med.* 2008; **359**(24): 2567-78.

Cabodi S, del Pilar Camacho-Leal M, Di Stefano P, Defilippi P. Integrin signalling adaptors: not only figurants in the cancer story. *Nat Rev Cancer.* 2010; **10**(12): 858-70.

Cai J, Kirlin WG, Chen Y, Yan X, Jones DP, Sartorelli AC. Overexpression of heat shock factor 1 inhibits butyrate-induced differentiation in colon cancer cells. *Cell Stress Chaperones.* 2006; **11**(3): 199-207.

Cai X, Hagedorn CH, Cullen BR. Human microRNAs are processed from capped, polyadenylated transcripts that can also function as mRNAs. *Rna.* 2004; **10**(12): 1957-66.

Calin GA, Dumitru CD, Shimizu M, Bichi R, Zupo S, Noch E, et al. Frequent deletions and down-regulation of micro- RNA genes miR15 and miR16 at 13q14 in chronic lymphocytic leukemia. *Proc Natl Acad Sci U S A.* 2002; **99**(24): 15524-9.

Calin GA, Liu C-G, Sevignani C, Ferracin M, Felli N, Dumitru CD, et al. MicroRNA profiling reveals distinct signatures in B cell chronic lymphocytic leukemias. *Proc Natl Acad Sci U S A.* 2004a; **101**(32): 11755-60.

Calin GA, Sevignani C, Dumitru CD, Hyslop T, Noch E, Yendamuri S, et al. Human microRNA genes are frequently located at fragile sites and genomic regions involved in cancers. *Proc Natl Acad Sci U S A*. 2004b; **101**(9): 2999-3004.

Camacho LH, Olson J, Tong WP, Young CW, Spriggs DR, Malkin MG. Phase I dose escalation clinical trial of phenylbutyrate sodium administered twice daily to patients with advanced solid tumors. *Invest New Drugs*. 2007; **25**(2): 131-8.

Campos EI, Reinberg D. Histones: annotating chromatin. *Annu Rev Genet*. 2009; **43**: 559-99.

Cancer Council Victoria. Dietary Questionnaire for Epidemiological Studies. Victoria: Cancer Council Victoria; 2005.

Cao R, Zhang Y. The functions of E(Z)/EZH2-mediated methylation of lysine 27 in histone H3. *Curr Opin Genet Dev*. 2004; **14**(2): 155-64.

Caplen NJ, Parrish S, Imani F, Fire A, Morgan RA. Specific inhibition of gene expression by small double-stranded RNAs in invertebrate and vertebrate systems. *Proc Natl Acad Sci U S A*. 2001; **98**(17): 9742-7.

Cappell MS. Pathophysiology, clinical presentation, and management of colon cancer. *Gastroenterol Clin North Am*. 2008; **37**(1): 1-24.

Cappell MS, Friedel D. The role of sigmoidoscopy and colonoscopy in the diagnosis and management of lower gastrointestinal disorders: endoscopic findings, therapy, and complications. *Med Clin North Am*. 2002; **86**(6): 1253-88.

Carey MF, Peterson CL, Smale ST. Chromatin immunoprecipitation (ChIP). *Cold Spring Harb Protoc*. 2009; **2009**(9): prot5279.

Carraro G, El-Hashash A, Guidolin D, Tiozzo C, Turcatel G, Young BM, et al. miR-17 family of microRNAs controls FGF10-mediated embryonic lung epithelial branching morphogenesis through MAPK14 and STAT3 regulation of E-Cadherin distribution. *Dev Biol*. 2009; **333**(2): 238-50.

Center MM, Jemal A, Ward E. International trends in colorectal cancer incidence rates. *Cancer Epidemiol Biomarkers Prev*. 2009; **18**(6): 1688-94.

Chakraborty S, Mehtab S, Patwardhan A, Krishnan Y. Pri-miR-17-92a transcript folds into a tertiary structure and autoregulates its processing. *Rna*. 2012; **18**(5): 1014-28.

Chan DSM, Lau R, Aune D, Vieira R, Greenwood DC, Kampman E, et al. Red and processed meat and colorectal cancer incidence: meta-analysis of prospective studies. *PLoS ONE*. 2011; **6**(6): e20456.

Chang KH, Mestdagh P, Vandesompele J, Kerin MJ, Miller N. MicroRNA expression profiling to identify and validate reference genes for relative quantification in colorectal cancer. *BMC Cancer*. 2010; **10**: 173.

Chang KH, Miller N, Kheirelseid EA, Ingoldsby H, Hennessy E, Curran CE, et al. MicroRNA-21 and PDCD4 expression in colorectal cancer. *Eur J Surg Oncol*. 2011a; **37**(7): 597-603.

Chang KH, Miller N, Kheirelseid EA, Lemetre C, Ball GR, Smith MJ, et al. MicroRNA signature analysis in colorectal cancer: identification of expression profiles in stage II tumors associated with aggressive disease. *Int J Colorectal Dis*. 2011b; **26**(11): 1415-22.

Chao A, Thun MJ, Connell CJ, McCullough ML, Jacobs EJ, Flanders WD, et al. Meat consumption and risk of colorectal cancer. *JAMA*. 2005; **293**(2): 172-82.

Chaulk SG, Thede GL, Kent OA, Xu Z, Gesner E, Veldhoen RA, et al. Role of pri-miRNA tertiary structure in miR-17~92 miRNA biogenesis. *RNA Biol*. 2011; **8**(6): 1105-14.

Chen J, Stampfer MJ, Hough HL, Garcia-Closas M, Willett WC, Hennekens CH, et al. A prospective study of N-acetyltransferase genotype, red meat intake, and risk of colorectal cancer. *Cancer Res*. 1998; **58**(15): 3307-11.

Chen L, Fischle W, Verdin E, Greene WC. Duration of nuclear NF-kappaB action regulated by reversible acetylation. *Science*. 2001; **293**(5535): 1653-7.

Chen X, Guo X, Zhang H, Xiang Y, Chen J, Yin Y, et al. Role of miR-143 targeting KRAS in colorectal tumorigenesis. *Oncogene*. 2009; **28**(10): 1385-92.

Chen YX, Fang JY, Zhu HY, Lu R, Cheng ZH, Qiu DK. Histone acetylation regulates p21WAF1 expression in human colon cancer cell lines. *World J Gastroenterol*. 2004; **10**(18): 2643-6.

Chendrimada TP, Gregory RI, Kumaraswamy E, Norman J, Cooch N, Nishikura K, et al. TRBP recruits the Dicer complex to Ago2 for microRNA processing and gene silencing. *Nature*. 2005; **436**(7051): 740-4.

Cheng H, Zhang L, Cogdell DE, Zheng H, Schetter AJ, Nykter M, et al. Circulating plasma MiR-141 is a novel biomarker for metastatic colon cancer and predicts poor prognosis. *PLoS One*. 2011; **6**(3): e17745.

Chi P, Allis CD, Wang GG. Covalent histone modifications--miswritten, misinterpreted and mis-erased in human cancers. *Nat Rev Cancer*. 2010; **10**(7): 457-69.

Chiang Y, Song Y, Wang Z, Chen Y, Yue Z, Xu H, et al. Aberrant expression of miR-203 and its clinical significance in gastric and colorectal cancers. *J Gastrointest Surg*. 2011; **15**(1): 63-70.

Choi WY, Giraldez AJ, Schier AF. Target protectors reveal dampening and balancing of Nodal agonist and antagonist by miR-430. *Science*. 2007; **318**(5848): 271-4.

Choudhry H, Catto JWF. Epigenetic regulation of microRNA expression in cancer. *Methods Mol Biol*. 2011; **676**: 165-84.

Chuang H-C, Chang C-W, Chang G-D, Yao T-P, Chen H. Histone deacetylase 3 binds to and regulates the GCMa transcription factor. *Nucleic Acids Res*. 2006; **34**(5): 1459-69.

Chughtai SA, Crundwell MC, Cruickshank NR, Affie E, Armstrong S, Knowles MA, et al. Two novel regions of interstitial deletion on chromosome 8p in colorectal cancer. *Oncogene*. 1999; **18**(3): 657-65.

Cirera S, Birck M, Busk PK, Fredholm M. Expression profiles of miRNA-122 and its target CAT1 in minipigs (Sus scrofa) fed a high-cholesterol diet. *Comp Med*. 2010; **60**(2): 136-41.

Clarke JD, Hsu A, Yu Z, Dashwood RH, Ho E. Differential effects of sulforaphane on histone deacetylases, cell cycle arrest and apoptosis in normal prostate cells versus hyperplastic and cancerous prostate cells. *Mol Nutr Food Res*. 2011a; **55**(7): 999-1009.

Clarke JM, Bird AR, Topping DL, Cobiac L. Excretion of starch and esterified short-chain fatty acids by ileostomy subjects after the ingestion of acylated starches. *Am J Clin Nutr*. 2007; **86**(4): 1146-51.

Clarke JM, Topping DL, Christophersen CT, Bird AR, Lange K, Saunders I, et al. Butyrate esterified to starch is released in the human gastrointestinal tract. *Am J Clin Nutr*. 2011b; **94**(5): 1276-83.

Clarke JM, Young GP, Topping DL, Bird AR, Cobiac L, Scherer BL, et al. Butyrate delivered by butyrylated starch increases distal colonic epithelial apoptosis in carcinogen-treated rats. *Carcinogenesis*. 2012; **33**(1): 197-202.

Cloonan N, Brown MK, Steptoe AL, Wani S, Chan WL, Forrest AR, et al. The miR-17-5p microRNA is a key regulator of the G1/S phase cell cycle transition. *Genome Biol*. 2008; **9**(8): R127.

Colbert LH, Hartman TJ, Malila N, Limburg PJ, Pietinen P, Virtamo J, et al. Physical activity in relation to cancer of the colon and rectum in a cohort of male smokers. *Cancer Epidemiol Biomarkers Prev*. 2001; **10**(3): 265-8.

Conlon MA, Bird AR. Interactive and individual effects of dietary non-digestible carbohydrates and oils on DNA damage, SCFA and bacteria in the large bowel of rats. *Br J Nutr*. 2009; **101**(8): 1171-7.

Coradini D, Pellizzaro C, Marimpietri D, Abolafio G, Daidone MG. Sodium butyrate modulates cell cycle-related proteins in HT29 human colonic adenocarcinoma cells. *Cell Prolif*. 2000; **33**(3): 139-46.

Craig WJ. Phytochemicals: guardians of our health. *J Am Diet Assoc*. 1997; **97**(10 Suppl 2): S199-204.

Crea F, Nobili S, Paolicchi E, Perrone G, Napoli C, Landini I, et al. Epigenetics and chemoresistance in colorectal cancer: an opportunity for treatment tailoring and novel therapeutic strategies. *Drug Resist Updat*. 2011; **14**(6): 280-96.

Cross SH, Meehan RR, Nan X, Bird A. A component of the transcriptional repressor MeCP1 shares a motif with DNA methyltransferase and HRX proteins. *Nat Genet*. 1997; **16**(3): 256-9.

Cummings JH. Absorption and secretion by the colon. *Gut*. 1975; **16**(4): 323-9.

Cummings JH, Beatty ER, Kingman SM, Bingham SA, Englyst HN. Digestion and physiological properties of resistant starch in the human large bowel. *Br J Nutr*. 1996; **75**(5): 733-47.

Cummings JH, Pomare EW, Branch WJ, Naylor CP, Macfarlane GT. Short chain fatty acids in human large intestine, portal, hepatic and venous blood. *Gut*. 1987; **28**(10): 1221-7.

Cummins JM, He Y, Leary RJ, Pagliarini R, Diaz LA, Jr., Sjoblom T, et al. The colorectal microRNAome. *Proc Natl Acad Sci U S A*. 2006; **103**(10): 3687-92.

Cunningham D, Atkin W, Lenz HJ, Lynch HT, Minsky B, Nordlinger B, et al. Colorectal cancer. *Lancet*. 2010; **375**(9719): 1030-47.

Daly K, Cuff MA, Fung F, Shirazi-Beechey SP. The importance of colonic butyrate transport to the regulation of genes associated with colonic tissue homoeostasis. *Biochem Soc Trans*. 2005; **33**(Pt 4): 733-5.

Daly K, Shirazi-Beechey SP. Microarray analysis of butyrate regulated genes in colonic epithelial cells. *DNA Cell Biol*. 2006; **25**(1): 49-62.

Daroqui MC, Augenlicht LH. Transcriptional attenuation in colon carcinoma cells in response to butyrate. *Cancer Prev Res*. 2010; **3**(10): 1292-302.

Davey CA, Sargent DF, Luger K, Maeder AW, Richmond TJ. Solvent mediated interactions in the structure of the nucleosome core particle at 1.9 a resolution. *J Mol Biol*. 2002; **319**(5): 1097-113.

David CJ, Chen M, Assanah M, Canoll P, Manley JL. HnRNP proteins controlled by c-Myc deregulate pyruvate kinase mRNA splicing in cancer. *Nature*. 2010; **463**(7279): 364-8.

Davidson LA, Wang N, Shah MS, Lupton JR, Ivanov I, Chapkin RS. n-3 Polyunsaturated fatty acids modulate carcinogen-directed non-coding microRNA signatures in rat colon. *Carcinogenesis*. 2009; **30**(12): 2077-84.

Davie JR. Inhibition of histone deacetylase activity by butyrate. *J Nutr*. 2003; **133**(7 Suppl): 2485S-93S.

Davis CD, Ross SA. Evidence for dietary regulation of microRNA expression in cancer cells. *Nutr Rev*. 2008; **66**(8): 477-82.

de Bono JS, Kristeleit R, Tolcher A, Fong P, Pacey S, Karavasilis V, et al. Phase I pharmacokinetic and pharmacodynamic study of LAQ824, a hydroxamate histone deacetylase inhibitor with a heat shock protein-90 inhibitory profile, in patients with advanced solid tumors. *Clin Cancer Res*. 2008; **14**(20): 6663-73.

de Pontual L, Yao E, Callier P, Faivre L, Drouin V, Cariou S, et al. Germline deletion of the miR-17~92 cluster causes skeletal and growth defects in humans. *Nat Genet*. 2011; **43**(10): 1026-30.

de Ruijter AJM, van Gennip AH, Caron HN, Kemp S, van Kuilenburg ABP. Histone deacetylases (HDACs): characterization of the classical HDAC family. *Biochem J*. 2003; **370**(Pt 3): 737-49.

Della Ragione F, Criniti V, Della Pietra V, Borriello A, Oliva A, Indaco S, et al. Genes modulated by histone acetylation as new effectors of butyrate activity. *FEBS Lett*. 2001; **499**(3): 199-204.

Deng G, Nguyen A, Tanaka H, Matsuzaki K, Bell I, Mehta KR, et al. Regional hypermethylation and global hypomethylation are associated with altered chromatin conformation and histone acetylation in colorectal cancer. *Int J Cancer*. 2006; **118**(12): 2999-3005.

Denli AM, Tops BBJ, Plasterk RHA, Ketting RF, Hannon GJ. Processing of primary microRNAs by the Microprocessor complex. *Nature*. 2004; **432**(7014): 231-5.

Deroanne CF, Bonjean K, Servotte S, Devy L, Colige A, Clausse N, et al. Histone deacetylases inhibitors as anti-angiogenic agents altering vascular endothelial growth factor signaling. *Oncogene*. 2002; **21**(3): 427-36.

Dews M, Homayouni A, Yu D, Murphy D, Sevignani C, Wentzel E, et al. Augmentation of tumor angiogenesis by a Myc-activated microRNA cluster. *Nat Genet*. 2006; **38**(9): 1060-5.

Diaz R, Silva J, Garcia JM, Lorenzo Y, Garcia V, Pena C, et al. Deregulated expression of miR-106a predicts survival in human colon cancer patients. *Genes Chromosomes Cancer*. 2008; **47**(9): 794-802.

Dickson MA, Rathkopf DE, Carvajal RD, Grant S, Roberts JD, Reid JM, et al. A phase I pharmacokinetic study of pulse-dose vorinostat with flavopiridol in solid tumors. *Invest New Drugs*. 2011; **29**(5): 1004-12.

Diederichs S, Haber DA. Dual role for argonautes in microRNA processing and posttranscriptional regulation of microRNA expression. *Cell*. 2007; **131**(6): 1097-108.

Diosdado B, van de Wiel MA, Terhaar Sive Droste JS, Mongera S, Postma C, Meijerink WJ, et al. MiR-17-92 cluster is associated with 13q gain and c-myc expression during colorectal adenoma to adenocarcinoma progression. *Br J Cancer*. 2009; **101**(4): 707-14.

Dokmanovic M, Clarke C, Marks PA. Histone deacetylase inhibitors: overview and perspectives. *Mol Cancer Res*. 2007; **5**(10): 981-9.

Dorsett Y, Tuschl T. siRNAs: applications in functional genomics and potential as therapeutics. *Nat Rev Drug Discov*. 2004; **3**(4): 318-29.

Dronamraju SS, Coxhead JM, Kelly SB, Burn J, Mathers JC. Cell kinetics and gene expression changes in colorectal cancer patients given resistant starch: a randomised controlled trial. *Gut*. 2009; **58**(3): 413-20.

Druesne-Pecollo N, Chaumontet C, Pagniez A, Vaugelade P, Bruneau A, Thomas M, et al. In vivo treatment by diallyl disulfide increases histone acetylation in rat colonocytes. *Biochem Biophys Res Commun*. 2007; **354**(1): 140-7.

Druesne N, Pagniez A, Mayeur C, Thomas M, Cherbuy C, Duee P-H, et al. Diallyl disulfide (DADS) increases histone acetylation and p21(waf1/cip1) expression in human colon tumor cell lines. *Carcinogenesis*. 2004; **25**(7): 1227-36.

Duvic M, Talpur R, Ni X, Zhang C, Hazarika P, Kelly C, et al. Phase 2 trial of oral vorinostat (suberoylanilide hydroxamic acid, SAHA) for refractory cutaneous T-cell lymphoma (CTCL). *Blood*. 2007; **109**(1): 31-9.

Earle JS, Luthra R, Romans A, Abraham R, Ensor J, Yao H, et al. Association of microRNA expression with microsatellite instability status in colorectal adenocarcinoma. *J Mol Diagn*. 2010; **12**(4): 433-40.

Easow G, Teleman AA, Cohen SM. Isolation of microRNA targets by miRNP immunopurification. *Rna*. 2007; **13**(8): 1198-204.

Ebert MS, Neilson JR, Sharp PA. MicroRNA sponges: competitive inhibitors of small RNAs in mammalian cells. *Nat Methods*. 2007; **4**(9): 721-6.

Elbashir SM, Harborth J, Lendeckel W, Yalcin A, Weber K, Tuschl T. Duplexes of 21-nucleotide RNAs mediate RNA interference in cultured mammalian cells. *Nature*. 2001; **411**(6836): 494-8.

Elmen J, Lindow M, Schutz S, Lawrence M, Petri A, Obad S, et al. LNA-mediated microRNA silencing in non-human primates. *Nature*. 2008; **452**(7189): 896-9.

Emenaker NJ, Calaf GM, Cox D, Basson MD, Qureshi N. Short-chain fatty acids inhibit invasive human colon cancer by modulating uPA, TIMP-1, TIMP-2, mutant p53, Bcl-2, Bax, p21 and PCNA protein expression in an in vitro cell culture model. *J Nutr*. 2001; **131**(11 Suppl): 3041S-6S.

English DR, MacInnis RJ, Hodge AM, Hopper JL, Haydon AM, Giles GG. Red meat, chicken, and fish consumption and risk of colorectal cancer. *Cancer Epidemiol Biomarkers Prev*. 2004; **13**(9): 1509-14.

Englyst HN, Kingman SM, Cummings JH. Classification and measurement of nutritionally important starch fractions. *Eur J Clin Nutr*. 1992; **46**(Suppl 2): S33-50.

Enroth S, Rada-Iglesisas A, Andersson R, Wallerman O, Wanders A, Pahlman L, et al. Cancer associated epigenetic transitions identified by genome-wide histone methylation binding profiles in human colorectal cancer samples and paired normal mucosa. *BMC Cancer*. 2011; **11**: 450.

Esau C, Davis S, Murray SF, Yu XX, Pandey SK, Pear M, et al. miR-122 regulation of lipid metabolism revealed by in vivo antisense targeting. *Cell Metab*. 2006; **3**(2): 87-98.

Esau C, Kang X, Peralta E, Hanson E, Marcusson EG, Ravichandran LV, et al. MicroRNA-143 regulates adipocyte differentiation. *J Biol Chem*. 2004; **279**(50): 52361-5.

Esteller M. Non-coding RNAs in human disease. *Nat Rev Genet*. 2011; **12**(12): 861-74.

Esteller M, Corn PG, Baylin SB, Herman JG. A gene hypermethylation profile of human cancer. *Cancer Res*. 2001; **61**(8): 3225-9.

Fakih MG, Fetterly G, Egorin MJ, Muindi JR, Espinoza-Delgado I, Zwiebel JA, et al. A phase I, pharmacokinetic, and pharmacodynamic study of two schedules of vorinostat in combination with 5-fluorouracil and leucovorin in patients with refractory solid tumors. *Clin Cancer Res*. 2010; **16**(14): 3786-94.

Fakih MG, Pendyala L, Fetterly G, Toth K, Zwiebel JA, Espinoza-Delgado I, et al. A phase I, pharmacokinetic and pharmacodynamic study on vorinostat in combination with 5-fluorouracil, leucovorin, and oxaliplatin in patients with refractory colorectal cancer. *Clin Cancer Res*. 2009; **15**(9): 3189-95.

Fang JY, Chen YX, Lu J, Lu R, Yang L, Zhu HY, et al. Epigenetic modification regulates both expression of tumor-associated genes and cell cycle progressing in human colon cancer cell lines: Colo-320 and SW1116. *Cell Res*. 2004; **14**(3): 217-26.

Fang WJ, Lin CZ, Zhang HH, Qian J, Zhong L, Xu N. Detection of let-7a microRNA by real-time PCR in colorectal cancer: a single-centre experience from China. *J Int Med Res*. 2007; **35**(5): 716-23.

Fassan M, Pizzi M, Giacomelli L, Mescoli C, Ludwig K, Pucciarelli S, et al. PDCD4 nuclear loss inversely correlates with miR-21 levels in colon carcinogenesis. *Virchows Arch*. 2011; **458**(4): 413-9.

Fazzone W, Wilson PM, Labonte MJ, Lenz HJ, Ladner RD. Histone deacetylase inhibitors suppress thymidylate synthase gene expression and synergize with the fluoropyrimidines in colon cancer cells. *Int J Cancer*. 2009; **125**(2): 463-73.

Fearnhead NS, Wilding JL, Bodmer WF. Genetics of colorectal cancer: hereditary aspects and overview of colorectal tumorigenesis. *Br Med Bull*. 2002; **64**: 27-43.

Fearon ER. Molecular genetics of colorectal cancer. *Annu Rev Pathol*. 2011; **6**: 479-507.

Fearon ER, Vogelstein B. A genetic model for colorectal tumorigenesis. *Cell*. 1990; **61**(5): 759-67.

Ferguson LR, Tasman-Jones C, Englyst H, Harris PJ. Comparative effects of three resistant starch preparations on transit time and short-chain fatty acid production in rats. *Nutr Cancer*. 2000; **36**(2): 230-7.

Ferreira R, Naguibneva I, Mathieu M, Ait-Si-Ali S, Robin P, Pritchard LL, et al. Cell cycle-dependent recruitment of HDAC-1 correlates with deacetylation of histone H4 on an Rb-E2F target promoter. *EMBO Rep*. 2001; **2**(9): 794-9.

Filipowicz W, Bhattacharyya SN, Sonenberg N. Mechanisms of post-transcriptional regulation by microRNAs: are the answers in sight? *Nat Rev Genet*. 2008; **9**(2): 102-14.

Finnin MS, Donigian JR, Cohen A, Richon VM, Rifkind RA, Marks PA, et al. Structures of a histone deacetylase homologue bound to the TSA and SAHA inhibitors. *Nature*. 1999; **401**(6749): 188-93.

Fire A, Xu S, Montgomery MK, Kostas SA, Driver SE, Mello CC. Potent and specific genetic interference by double-stranded RNA in Caenorhabditis elegans. *Nature*. 1998; **391**(6669): 806-11.

Firestein R, Bass AJ, Kim SY, Dunn IF, Silver SJ, Guney I, et al. CDK8 is a colorectal cancer oncogene that regulates beta-catenin activity. *Nature*. 2008; **455**(7212): 547-51.

Fischle W, Wang Y, Jacobs SA, Kim Y, Allis CD, Khorasanizadeh S. Molecular basis for the discrimination of repressive methyl-lysine marks in histone H3 by Polycomb and HP1 chromodomains. *Genes Dev*. 2003; **17**(15): 1870-81.

Fishel R, Lescoe MK, Rao MR, Copeland NG, Jenkins NA, Garber J, et al. The human mutator gene homolog MSH2 and its association with hereditary nonpolyposis colon cancer. *Cell*. 1993; **75**(5): 1027-38.

Flanagan JF, Mi L-Z, Chruszcz M, Cymborowski M, Clines KL, Kim Y, et al. Double chromodomains cooperate to recognize the methylated histone H3 tail. *Nature*. 2005; **438**(7071): 1181-5.

Flood DM, Weiss NS, Cook LS, Emerson JC, Schwartz SM, Potter JD. Colorectal cancer incidence in Asian migrants to the United States and their descendants. *Cancer Causes Control*. 2000; **11**(5): 403-11.

Fodde R, Kuipers J, Rosenberg C, Smits R, Kielman M, Gaspar C, et al. Mutations in the APC tumour suppressor gene cause chromosomal instability. *Nat Cell Biol*. 2001; **3**(4): 433-8.

Fontana L, Fiori ME, Albini S, Cifaldi L, Giovinazzi S, Forloni M, et al. Antagomir-17-5p abolishes the growth of therapy-resistant neuroblastoma through p21 and BIM. *PLoS One*. 2008; **3**(5): e2236.

Ford LP. Using synthetic miRNA mimics for diverting cell fate: a possibility of miRNA-based therapeutics? *Leuk Res*. 2006; **30**(5): 511-3.

Fraga MF, Ballestar E, Paz MF, Ropero S, Setien F, Ballestar ML, et al. Epigenetic differences arise during the lifetime of monozygotic twins. *Proc Natl Acad Sci U S A*. 2005a; **102**(30): 10604-9.

Fraga MF, Ballestar E, Villar-Garea A, Boix-Chornet M, Espada J, Schotta G, et al. Loss of acetylation at Lys16 and trimethylation at Lys20 of histone H4 is a common hallmark of human cancer. *Nat Genet*. 2005b; **37**(4): 391-400.

Fre S, Huyghe M, Mourikis P, Robine S, Louvard D, Artavanis-Tsakonas S. Notch signals control the fate of immature progenitor cells in the intestine. *Nature*. 2005; **435**(7044): 964-8.

Fritsche M, Haessler C, Brandner G. Induction of nuclear accumulation of the tumor-suppressor protein p53 by DNA-damaging agents. *Oncogene*. 1993; **8**(2): 307-18.

FSANZ. Australia New Zealand Food Standards Code (Standard 1.2.8). Canberra: Food Standards Australia New Zealand; 2012.

Fuchs CS, Giovannucci EL, Colditz GA, Hunter DJ, Stampfer MJ, Rosner B, et al. Dietary fiber and the risk of colorectal cancer and adenoma in women. *N Engl J Med*. 1999; **340**(3): 169-76.

Fudenberg G, Getz G, Meyerson M, Mirny LA. High order chromatin architecture shapes the landscape of chromosomal alterations in cancer. *Nat Biotechnol*. 2011; **29**(12): 1109-13.

Fukutomi A, Hatake K, Matsui K, Sakajiri S, Hirashima T, Tanii H, et al. A phase I study of oral panobinostat (LBH589) in Japanese patients with advanced solid tumors. *Invest New Drugs*. 2012; **30**(3): 1096-106.

Fung KY, Lewanowitsch T, Henderson ST, Priebe I, Hoffmann P, McColl SR, et al. Proteomic analysis of butyrate effects and loss of butyrate sensitivity in HT29 colorectal cancer cells. *J Proteome Res*. 2009; **8**(3): 1220-7.

Gaedicke S, Zhang X, Schmelzer C, Lou Y, Doering F, Frank J, et al. Vitamin E dependent microRNA regulation in rat liver. *FEBS Lett*. 2008; **582**(23-24): 3542-6.

Garzon R, Pichiorri F, Palumbo T, Visentini M, Aqeilan R, Cimmino A, et al. MicroRNA gene expression during retinoic acid-induced differentiation of human acute promyelocytic leukemia. *Oncogene*. 2007; **26**(28): 4148-57.

Gaudier E, Forestier L, Gouyer V, Huet G, Julien R, Hoebler C. Butyrate regulation of glycosylation-related gene expression: evidence for galectin-1 upregulation in human intestinal epithelial goblet cells. *Biochem Biophys Res Commun*. 2004; **325**(3): 1044-51.

Gaughan L, Logan IR, Neal DE, Robson CN. Regulation of androgen receptor and histone deacetylase 1 by Mdm2-mediated ubiquitylation. *Nucleic Acids Res*. 2005; **33**(1): 13-26.

Gehrke S, Imai Y, Sokol N, Lu B. Pathogenic LRRK2 negatively regulates microRNA-mediated translational repression. *Nature*. 2010; **466**(7306): 637-41.

Gilbert J, Baker SD, Bowling MK, Grochow L, Figg WD, Zabelina Y, et al. A phase I dose escalation and bioavailability study of oral sodium phenylbutyrate in patients with refractory solid tumor malignancies. *Clin Cancer Res*. 2001; **7**(8): 2292-300.

Gilmour DS, Lis JT. Detecting protein-DNA interactions in vivo: distribution of RNA polymerase on specific bacterial genes. *Proc Natl Acad Sci U S A*. 1984; **81**(14): 4275-9.

Gilmour DS, Lis JT. In vivo interactions of RNA polymerase II with genes of Drosophila melanogaster. *Mol Cell Biol*. 1985; **5**(8): 2009-18.

Gilmour DS, Lis JT. RNA polymerase II interacts with the promoter region of the noninduced hsp70 gene in Drosophila melanogaster cells. *Mol Cell Biol*. 1986; **6**(11): 3984-9.

Giovannucci E, Rimm EB, Stampfer MJ, Colditz GA, Ascherio A, Willett WC. Intake of fat, meat, and fiber in relation to risk of colon cancer in men. *Cancer Res*. 1994; **54**(9): 2390-7.

Git A, Dvinge H, Salmon-Divon M, Osborne M, Kutter C, Hadfield J, et al. Systematic comparison of microarray profiling, real-time PCR, and next-generation sequencing technologies for measuring differential microRNA expression. *Rna-A Publication of the Rna Society*. 2010; **16**(5): 991-1006.

Glei M, Klenow S, Sauer J, Wegewitz U, Richter K, Pool-Zobel BL. Hemoglobin and hemin induce DNA damage in human colon tumor cells HT29 clone 19A and in primary human colonocytes. *Mutat Res*. 2006; **594**(1-2): 162-71.

Glozak MA, Sengupta N, Zhang X, Seto E. Acetylation and deacetylation of non-histone proteins. *Gene*. 2005; **363**: 15-23.

Gobinet J, Carascossa S, Cavailles V, Vignon F, Nicolas J-C, Jalaguier S. SHP represses transcriptional activity via recruitment of histone deacetylases. *Biochemistry*. 2005; **44**(16): 6312-20.

Goldbohm RA, van den Brandt PA, van 't Veer P, Brants HA, Dorant E, Sturmans F, et al. A prospective cohort study on the relation between meat consumption and the risk of colon cancer. *Cancer Res*. 1994; **54**(3): 718-23.

Goljanek-Whysall K, Sweetman D, Abu-Elmagd M, Chapnik E, Dalmay T, Hornstein E, et al. MicroRNA regulation of the paired-box transcription factor Pax3 confers robustness to developmental timing of myogenesis. *Proc Natl Acad Sci U S A*. 2011; **108**(29): 11936-41.

Gope R, Gope ML. Effect of sodium butyrate on the expression of retinoblastoma (RB1) and P53 gene and phosphorylation of retinoblastoma protein in human colon tumor cell line HT29. *Cell Mol Biol*. 1993; **39**(6): 589-97.

Gore L, Rothenberg ML, O'Bryant CL, Schultz MK, Sandler AB, Coffin D, et al. A phase I and pharmacokinetic study of the oral histone deacetylase inhibitor, MS-275, in patients with refractory solid tumors and lymphomas. *Clin Cancer Res*. 2008; **14**(14): 4517-25.

Grady WM, Parkin RK, Mitchell PS, Lee JH, Kim YH, Tsuchiya KD, et al. Epigenetic silencing of the intronic microRNA hsa-miR-342 and its host gene EVL in colorectal cancer. *Oncogene*. 2008; **27**(27): 3880-8.

Gray SG, Qian CN, Furge K, Guo X, Teh BT. Microarray profiling of the effects of histone deacetylase inhibitors on gene expression in cancer cell lines. *Int J Oncol*. 2004; **24**(4): 773-95.

Gregoire S, Xiao L, Nie J, Zhang X, Xu M, Li J, et al. Histone deacetylase 3 interacts with and deacetylates myocyte enhancer factor 2. *Mol Cell Biol*. 2007; **27**(4): 1280-95.

Gregory RI, Yan K-P, Amuthan G, Chendrimada T, Doratotaj B, Cooch N, et al. The Microprocessor complex mediates the genesis of microRNAs. *Nature*. 2004; **432**(7014): 235-40.

Griffiths-Jones S, Grocock RJ, van Dongen S, Bateman A, Enright AJ. miRBase: microRNA sequences, targets and gene nomenclature. *Nucleic Acids Res*. 2006; **34**(Database issue): D140-4.

Gu W, Roeder RG. Activation of p53 sequence-specific DNA binding by acetylation of the p53 C-terminal domain. *Cell*. 1997; **90**(4): 595-606.

Gui CY, Ngo L, Xu WS, Richon VM, Marks PA. Histone deacetylase (HDAC) inhibitor activation of p21WAF1 involves changes in promoter-associated proteins, including HDAC1. *Proc Natl Acad Sci U S A*. 2004; **101**(5): 1241-6.

Guil S, Caceres JF. The multifunctional RNA-binding protein hnRNP A1 is required for processing of miR-18a. *Nat Struct Mol Biol*. 2007; **14**(7): 591-6.

Guil S, Esteller M. DNA methylomes, histone codes and miRNAs: tying it all together. *Int J Biochem Cell Biol*. 2009; **41**(1): 87-95.

Guil S, Long JC, Caceres JF. hnRNP A1 relocalization to the stress granules reflects a role in the stress response. *Mol Cell Biol*. 2006; **26**(15): 5744-58.

Guo C, Sah JF, Beard L, Willson JK, Markowitz SD, Guda K. The noncoding RNA, miR-126, suppresses the growth of neoplastic cells by targeting phosphatidylinositol 3-kinase signaling and is frequently lost in colon cancers. *Genes Chromosomes Cancer*. 2008; **47**(11): 939-46.

Guo H, Ingolia NT, Weissman JS, Bartel DP. Mammalian microRNAs predominantly act to decrease target mRNA levels. *Nature*. 2010; **466**(7308): 835-40.

Guo J, Jin M, Zhang M, Chen K. A Genetic Variant in miR-196a2 Increased Digestive System Cancer Risks: A Meta-Analysis of 15 Case-Control Studies. *PLoS One*. 2012; **7**(1): e30585.

Gururaj AE, Belakavadi M, Salimath BP. Antiangiogenic effects of butyric acid involve inhibition of VEGF/KDR gene expression and endothelial cell proliferation. *Mol Cell Biochem*. 2003; **243**(1-2): 107-12.

Haase AD, Jaskiewicz L, Zhang H, Laine S, Sack R, Gatignol A, et al. TRBP, a regulator of cellular PKR and HIV-1 virus expression, interacts with Dicer and functions in RNA silencing. *EMBO Rep*. 2005; **6**(10): 961-7.

Habold C, Poehlmann A, Bajbouj K, Hartig R, Korkmaz KS, Roessner A, et al. Trichostatin A causes p53 to switch oxidative-damaged colorectal cancer cells from cell cycle arrest into apoptosis. *J Cell Mol Med*. 2008; **12**(2): 607-21.

Hakak Y, Martin GS. Cas mediates transcriptional activation of the serum response element by Src. *Mol Cell Biol*. 1999; **19**(10): 6953-62.

Hake SB, Xiao A, Allis CD. Linking the epigenetic 'language' of covalent histone modifications to cancer. *Br J Cancer*. 2004; **90**(4): 761-9.

Hammill D, Jain N, Armstrong S, Mueller CR. The D-domain of Sp3 modulates its protein levels and activation of the p21(CIP1/WAF1) promoter. *Biochem Biophys Res Commun*. 2005; **335**(2): 377-84.

Han J, Lee Y, Yeom K-H, Kim Y-K, Jin H, Kim VN. The Drosha-DGCR8 complex in primary microRNA processing. *Genes Dev*. 2004; **18**(24): 3016-27.

Han J, Lee Y, Yeom K-H, Nam J-W, Heo I, Rhee J-K, et al. Molecular basis for the recognition of primary microRNAs by the Drosha-DGCR8 complex. *Cell*. 2006; **125**(5): 887-901.

Harada M, Pokrovskaja-Tamm K, Soderhall S, Heyman M, Grander D, Corcoran M. Involvement of miR17 pathway in glucocorticoid-induced cell death in pediatric acute lymphoblastic leukemia. *Leuk Lymphoma*. 2012; **53**(10): 2041-50.

Haring M, Offermann S, Danker T, Horst I, Peterhansel C, Stam M. Chromatin immunoprecipitation: optimization, quantitative analysis and data normalization. *Plant Methods*. 2007; **3**: 11.

Haugen AC, Goel A, Yamada K, Marra G, Nguyen T-P, Nagasaka T, et al. Genetic instability caused by loss of MutS homologue 3 in human colorectal cancer. *Cancer Res*. 2008; **68**(20): 8465-72.

Hawkins N, Norrie M, Cheong K, Mokany E, Ku S-L, Meagher A, et al. CpG island methylation in sporadic colorectal cancers and its relationship to microsatellite instability. *Gastroenterology*. 2002; **122**(5): 1376-87.

Hayashita Y, Osada H, Tatematsu Y, Yamada H, Yanagisawa K, Tomida S, et al. A polycistronic microRNA cluster, miR-17-92, is overexpressed in human lung cancers and enhances cell proliferation. *Cancer Res*. 2005; **65**(21): 9628-32.

He L, Thomson JM, Hemann MT, Hernando-Monge E, Mu D, Goodson S, et al. A microRNA polycistron as a potential human oncogene. *Nature*. 2005a; **435**(7043): 828-33.

He TC, Sparks AB, Rago C, Hermeking H, Zawel L, da Costa LT, et al. Identification of c-MYC as a target of the APC pathway. *Science*. 1998; **281**(5382): 1509-12.

He Y, Brown MA, Rothnagel JA, Saunders NA, Smith R. Roles of heterogeneous nuclear ribonucleoproteins A and B in cell proliferation. *J Cell Sci*. 2005b; **118**(Pt 14): 3173-83.

Hebert SS, Horre K, Nicolai L, Bergmans B, Papadopoulou AS, Delacourte A, et al. MicroRNA regulation of Alzheimer's Amyloid precursor protein expression. *Neurobiol Dis*. 2009; **33**(3): 422-8.

Hebert SS, Horre K, Nicolai L, Papadopoulou AS, Mandemakers W, Silahtaroglu AN, et al. Loss of microRNA cluster miR-29a/b-1 in sporadic Alzheimer's disease correlates with increased BACE1/beta-secretase expression. *Proc Natl Acad Sci U S A*. 2008; **105**(17): 6415-20.

Heilbrun LK, Nomura A, Hankin JH, Stemmermann GN. Diet and colorectal cancer with special reference to fiber intake. *Int J Cancer*. 1989; **44**(1): 1-6.

Hendrickson DG, Hogan DJ, McCullough HL, Myers JW, Herschlag D, Ferrell JE, et al. Concordant regulation of translation and mRNA abundance for hundreds of targets of a human microRNA. *PLoS Biol.* 2009; **7**(11): e1000238.

Herman JG, Umar A, Polyak K, Graff JR, Ahuja N, Issa JP, et al. Incidence and functional consequences of hMLH1 promoter hypermethylation in colorectal carcinoma. *Proc Natl Acad Sci U S A.* 1998; **95**(12): 6870-5.

Heruth DP, Zirnstein GW, Bradley JF, Rothberg PG. Sodium butyrate causes an increase in the block to transcriptional elongation in the c-myc gene in SW837 rectal carcinoma cells. *J Biol Chem.* 1993; **268**(27): 20466-72.

Higginbotham S, Zhang Z-F, Lee IM, Cook NR, Giovannucci E, Buring JE, et al. Dietary glycemic load and risk of colorectal cancer in the Women's Health Study. *J Natl Cancer Inst.* 2004; **96**(3): 229-33.

Hiltunen MO, Alhonen L, Koistinaho J, Myohanen S, Paakkonen M, Marin S, et al. Hypermethylation of the APC (adenomatous polyposis coli) gene promoter region in human colorectal carcinoma. *Int J Cancer.* 1997; **70**(6): 644-8.

Hinnebusch BF, Henderson JW, Siddique A, Malo MS, Zhang W, Abedrapo MA, et al. Transcriptional activation of the enterocyte differentiation marker intestinal alkaline phosphatase is associated with changes in the acetylation state of histone H3 at a specific site within its promoter region in vitro. *J Gastrointest Surg.* 2003; **7**(2): 237-44; discussion 44-5.

Houbaviy HB, Murray MF, Sharp PA. Embryonic stem cell-specific MicroRNAs. *Dev Cell.* 2003; **5**(2): 351-8.

Hu G, Chen D, Li X, Yang K, Wang H, Wu W. miR-133b regulates the MET proto-oncogene and inhibits the growth of colorectal cancer cells in vitro and in vivo. *Cancer Biol Ther.* 2010; **10**(2): 190-7.

Hu S, Dong TS, Dalal SR, Wu F, Bissonnette M, Kwon JH, et al. The microbe-derived short chain fatty acid butyrate targets miRNA-dependent p21 gene expression in human colon cancer. *PLoS One.* 2011; **6**(1): e16221.

Huang J, Papadopoulos N, McKinley AJ, Farrington SM, Curtis LJ, Wyllie AH, et al. APC mutations in colorectal tumors with mismatch repair deficiency. *Proc Natl Acad Sci U S A.* 1996; **93**(17): 9049-54.

Huang PH, Chen CH, Chou CC, Sargeant AM, Kulp SK, Teng CM, et al. Histone deacetylase inhibitors stimulate histone H3 lysine 4 methylation in part via transcriptional repression of histone H3 lysine 4 demethylases. *Mol Pharmacol.* 2011; **79**(1): 197-206.

Huang X, Ding L, Bennewith KL, Tong RT, Welford SM, Ang KK, et al. Hypoxia-inducible mir-210 regulates normoxic gene expression involved in tumor initiation. *Mol Cell.* 2009; **35**(6): 856-67.

Huang Y, Myers SJ, Dingledine R. Transcriptional repression by REST: recruitment of Sin3A and histone deacetylase to neuronal genes. *Nat Neurosci.* 1999; **2**(10): 867-72.

Huang Z, Huang D, Ni S, Peng Z, Sheng W, Du X. Plasma microRNAs are promising novel biomarkers for early detection of colorectal cancer. *Int J Cancer.* 2010; **127**(1): 118-26.

Hubbert C, Guardiola A, Shao R, Kawaguchi Y, Ito A, Nixon A, et al. HDAC6 is a microtubule-associated deacetylase. *Nature.* 2002; **417**(6887): 455-8.

Hublitz P, Albert M, Peters AHFM. Mechanisms of transcriptional repression by histone lysine methylation. *Int J Dev Biol.* 2009; **53**(2-3): 335-54.

Hughes R, Magee EA, Bingham S. Protein degradation in the large intestine: relevance to colorectal cancer. *Curr Issues Intest Microbiol.* 2000; **1**(2): 51-8.

Huse JT, Brennan C, Hambardzumyan D, Wee B, Pena J, Rouhanifard SH, et al. The PTEN-regulating microRNA miR-26a is amplified in high-grade glioma and facilitates gliomagenesis in vivo. *Genes Dev.* 2009; **23**(11): 1327-37.

Hutvagner G, Zamore PD. A microRNA in a multiple-turnover RNAi enzyme complex. *Science*. 2002; **297**(5589): 2056-60.

Iacomino G, Medici MC, Napoli D, Russo GL. Effects of histone deacetylase inhibitors on p55CDC/Cdc20 expression in HT29 cell line. *J Cell Biochem*. 2006; **99**(4): 1122-31.

Iacomino G, Tecce MF, Grimaldi C, Tosto M, Russo GL. Transcriptional response of a human colon adenocarcinoma cell line to sodium butyrate. *Biochem Biophys Res Commun*. 2001; **285**(5): 1280-9.

IARC. Cancer Incidence in Five Continents Vol. IX IARC Scientific Publication No. 160. Curado MP, Edwards B, Shin HR, Storm H, Ferlay J, Heanue M, et al. Lyon: International Agency for Research on Cancer; 2007.

IARC. Globocan 2008 Colorectal Cancer Incidence, Mortality and Prevalence Worldwide in 2008. International Agency for Research on Cancer. 2012. http://globocan.iarc.fr/

Inomata M, Tagawa H, Guo YM, Kameoka Y, Takahashi N, Sawada K. MicroRNA-17-92 down-regulates expression of distinct targets in different B-cell lymphoma subtypes. *Blood*. 2009; **113**(2): 396-402.

Ionov Y, Peinado MA, Malkhosyan S, Shibata D, Perucho M. Ubiquitous somatic mutations in simple repeated sequences reveal a new mechanism for colonic carcinogenesis. *Nature*. 1993; **363**(6429): 558-61.

Ioshikhes IP, Albert I, Zanton SJ, Pugh BF. Nucleosome positions predicted through comparative genomics. *Nat Genet*. 2006; **38**(10): 1210-5.

Ito A, Kawaguchi Y, Lai C-H, Kovacs JJ, Higashimoto Y, Appella E, et al. MDM2-HDAC1-mediated deacetylation of p53 is required for its degradation. *EMBO Journal*. 2002; **21**(22): 6236-45.

Ito K, Yamamura S, Essilfie-Quaye S, Cosio B, Ito M, Barnes PJ, et al. Histone deacetylase 2-mediated deacetylation of the glucocorticoid receptor enables NF-kappaB suppression. *J Exp Med*. 2006; **203**(1): 7-13.

Iwahashi S, Ishibashi H, Utsunomiya T, Morine Y, Ochir TL, Hanaoka J, et al. Effect of histone deacetylase inhibitor in combination with 5-fluorouracil on pancreas cancer and cholangiocarcinoma cell lines. *J Med Invest*. 2011; **58**(1-2): 106-9.

Izawa H, Yamamoto H, Damdinsuren B, Ikeda K, Tsujie M, Suzuki R, et al. Effects of p21cip1/waf1 overexpression on growth, apoptosis and differentiation in human colon carcinoma cells. *Int J Oncol*. 2005; **27**(1): 69-76.

Izumchenko E, Singh MK, Plotnikova OV, Tikhmyanova N, Little JL, Serebriiskii IG, et al. NEDD9 promotes oncogenic signaling in mammary tumor development. *Cancer Res*. 2009; **69**(18): 7198-206.

Janson W, Brandner G, Siegel J. Butyrate modulates DNA-damage-induced p53 response by induction of p53-independent differentiation and apoptosis. *Oncogene*. 1997; **15**(12): 1395-406.

Jass JR. Classification of colorectal cancer based on correlation of clinical, morphological and molecular features. *Histopathology*. 2007; **50**(1): 113-30.

Jemal A, Bray F, Center MM, Ferlay J, Ward E, Forman D. Global cancer statistics. *CA Cancer J Clin*. 2011; **61**(2): 69-90.

Jen J, Kim H, Piantadosi S, Liu ZF, Levitt RC, Sistonen P, et al. Allelic loss of chromosome 18q and prognosis in colorectal cancer. *N Engl J Med*. 1994; **331**(4): 213-21.

Jenuwein T, Allis CD. Translating the histone code. *Science*. 2001; **293**(5532): 1074-80.

Jevnaker AM, Khuu C, Kjole E, Bryne M, Osmundsen H. Expression of members of the miRNA17-92 cluster during development and in carcinogenesis. *J Cell Physiol*. 2011; **226**(9): 2257-66.

Ji R, Cheng Y, Yue J, Yang J, Liu X, Chen H, et al. MicroRNA expression signature and antisense-mediated depletion reveal an essential role of MicroRNA in vascular neointimal lesion formation. *Circ Res*. 2007; **100**(11): 1579-88.

Jiang X, Tsang YH, Yu Q. c-Myc overexpression sensitizes Bim-mediated Bax activation for apoptosis induced by histone deacetylase inhibitor suberoylanilide hydroxamic acid (SAHA) through regulating Bcl-2/Bcl-xL expression. *Int J Biochem Cell Biol*. 2007; **39**(5): 1016-25.

John B, Enright AJ, Aravin A, Tuschl T, Sander C, Marks DS. Human MicroRNA targets. *PLoS Biol*. 2004; **2**(11): e363.

Johnson SM, Grosshans H, Shingara J, Byrom M, Jarvis R, Cheng A, et al. RAS is regulated by the let-7 microRNA family. *Cell*. 2005; **120**(5): 635-47.

Jones SF, Bendell JC, Infante JR, Spigel DR, Thompson DS, Yardley DA, et al. A phase I study of panobinostat in combination with gemcitabine in the treatment of solid tumors. *Clin Adv Hematol Oncol*. 2011; **9**(3): 225-30.

Jopling CL, Yi M, Lancaster AM, Lemon SM, Sarnow P. Modulation of hepatitis C virus RNA abundance by a liver-specific MicroRNA. *Science*. 2005; **309**(5740): 1577-81.

Joseph J, Mudduluru G, Antony S, Vashistha S, Ajitkumar P, Somasundaram K. Expression profiling of sodium butyrate (NaB)-treated cells: identification of regulation of genes related to cytokine signaling and cancer metastasis by NaB. *Oncogene*. 2004; **23**(37): 6304-15.

Kahlert C, Klupp F, Brand K, Lasitschka F, Diederichs S, Kirchberg J, et al. Invasion front-specific expression and prognostic significance of microRNA in colorectal liver metastases. *Cancer Sci*. 2011; **102**(10): 1799-807.

Kalimutho M, Del Vecchio Blanco G, Di Cecilia S, Sileri P, Cretella M, Pallone F, et al. Differential expression of miR-144* as a novel fecal-based diagnostic marker for colorectal cancer. *J Gastroenterol*. 2011a; **46**(12): 1391-402.

Kalimutho M, Di Cecilia S, Del Vecchio Blanco G, Roviello F, Sileri P, Cretella M, et al. Epigenetically silenced miR-34b/c as a novel faecal-based screening marker for colorectal cancer. *Br J Cancer*. 2011b; **104**(11): 1770-8.

Kameue C, Tsukahara T, Ushida K. Alteration of gene expression in the colon of colorectal cancer model rat by dietary sodium gluconate. *Biosci Biotechnol Biochem*. 2006; **70**(3): 606-14.

Kastan MB, Onyekwere O, Sidransky D, Vogelstein B, Craig RW. Participation of p53 protein in the cellular response to DNA damage. *Cancer Res*. 1991; **51**(23 Pt 1): 6304-11.

Kawasaki H, Taira K. Functional analysis of microRNAs during the retinoic acid-induced neuronal differentiation of human NT2 cells. *Nucleic Acids Res*. 2003; (3): 243-4.

Khvorova A, Reynolds A, Jayasena SD. Functional siRNAs and miRNAs exhibit strand bias. *Cell*. 2003; **115**(2): 209-16.

Kim J, Inoue K, Ishii J, Vanti WB, Voronov SV, Murchison E, et al. A MicroRNA feedback circuit in midbrain dopamine neurons. *Science*. 2007a; **317**(5842): 1220-4.

Kim K-M, Shibata D. Methylation reveals a niche: stem cell succession in human colon crypts. *Oncogene*. 2002; **21**(35): 5441-9.

Kim SH, Kim KW, Jeong JW. Inhibition of hypoxia-induced angiogenesis by sodium butyrate, a histone deacetylase inhibitor, through hypoxia-inducible factor-1alpha suppression. *Oncol Rep*. 2007b; **17**(4): 793-7.

Kim VN, Han J, Siomi MC. Biogenesis of small RNAs in animals. *Nat Rev Mol Cell Biol*. 2009; **10**(2): 126-39.

Kinzler KW, Nilbert MC, Su LK, Vogelstein B, Bryan TM, Levy DB, et al. Identification of FAP locus genes from chromosome 5q21. *Science*. 1991; **253**(5020): 661-5.

Kinzler KW, Vogelstein B. Cancer-susceptibility genes. Gatekeepers and caretakers. *Nature*. 1997; **386**(6627): 761, 63.

Kiriakidou M, Nelson PT, Kouranov A, Fitziev P, Bouyioukos C, Mourelatos Z, et al. A combined computational-experimental approach predicts human microRNA targets. *Genes Dev*. 2004; **18**(10): 1165-78.

Knowlton DL, Tang K, Henstock PV, Subramanian RR. miRNA Alterations Modify Kinase Activation In The IGF-1 Pathway And Correlate With Colorectal Cancer Stage And Progression In Patients. *J Cancer*. 2011; **2**: 490-502.

Kobayashi H, Tan EM, Fleming SE. Sodium butyrate inhibits cell growth and stimulates p21WAF1/CIP1 protein in human colonic adenocarcinoma cells independently of p53 status. *Nutr Cancer*. 2003; **46**(2): 202-11.

Kobayashi H, Tan EM, Fleming SE. Acetylation of histones associated with the p21WAF1/CIP1 gene by butyrate is not sufficient for p21WAF1/CIP1 gene transcription in human colorectal adenocarcinoma cells. *Int J Cancer*. 2004; **109**(2): 207-13.

Koch CM, Andrews RM, Flicek P, Dillon SC, Karaoz U, Clelland GK, et al. The landscape of histone modifications across 1% of the human genome in five human cell lines. *Genome Res*. 2007; **17**(6): 691-707.

Kohne C-H, Lenz H-J. Chemotherapy with targeted agents for the treatment of metastatic colorectal cancer. *Oncologist*. 2009; **14**(5): 478-88.

Konings EJM, Goldbohm RA, Brants HAM, Saris WHM, van den Brandt PA. Intake of dietary folate vitamers and risk of colorectal carcinoma: results from The Netherlands Cohort Study. *Cancer*. 2002; **95**(7): 1421-33.

Konishi K, Yamochi T, Makino R, Kaneko K, Yamamoto T, Nozawa H, et al. Molecular differences between sporadic serrated and conventional colorectal adenomas. *Clin Cancer Res*. 2004; **10**(9): 3082-90.

Koralov SB, Muljo SA, Galler GR, Krek A, Chakraborty T, Kanellopoulou C, et al. Dicer ablation affects antibody diversity and cell survival in the B lymphocyte lineage. *Cell*. 2008; **132**(5): 860-74.

Kosinski C, Li VSW, Chan ASY, Zhang J, Ho C, Tsui WY, et al. Gene expression patterns of human colon tops and basal crypts and BMP antagonists as intestinal stem cell niche factors. *Proc Natl Acad Sci U S A*. 2007; **104**(39): 15418-23.

Kota J, Chivukula RR, O'Donnell KA, Wentzel EA, Montgomery CL, Hwang H-W, et al. Therapeutic microRNA delivery suppresses tumorigenesis in a murine liver cancer model. *Cell*. 2009; **137**(6): 1005-17.

Kouzarides T. Chromatin modifications and their function. *Cell*. 2007; **128**(4): 693-705.

Krek A, Grun D, Poy MN, Wolf R, Rosenberg L, Epstein EJ, et al. Combinatorial microRNA target predictions. *Nat Genet*. 2005; **37**(5): 495-500.

Kretzner L, Scuto A, Dino PM, Kowolik CM, Wu J, Ventura P, et al. Combining histone deacetylase inhibitor vorinostat with aurora kinase inhibitors enhances lymphoma cell killing with repression of c-Myc, hTERT, and microRNA levels. *Cancer Res*. 2011; **71**(11): 3912-20.

Krutzfeldt J, Rajewsky N, Braich R, Rajeev KG, Tuschl T, Manoharan M, et al. Silencing of microRNAs in vivo with 'antagomirs'. *Nature*. 2005; **438**(7068): 685-9.

Kuhn DE, Martin MM, Feldman DS, Terry AV, Jr., Nuovo GJ, Elton TS. Experimental validation of miRNA targets. *Methods*. 2008; **44**(1): 47-54.

Kulda V, Pesta M, Topolcan O, Liska V, Treska V, Sutnar A, et al. Relevance of miR-21 and miR-143 expression in tissue samples of colorectal carcinoma and its liver metastases. *Cancer Genet Cytogenet*. 2010; **200**(2): 154-60.

Kunej T, Godnic I, Ferdin J, Horvat S, Dovc P, Calin GA. Epigenetic regulation of microRNAs in cancer: an integrated review of literature. *Mutat Res*. 2011; **717**(1-2): 77-84.

Kutay H, Bai S, Datta J, Motiwala T, Pogribny I, Frankel W, et al. Downregulation of miR-122 in the rodent and human hepatocellular carcinomas. *J Cell Biochem*. 2006; **99**(3): 671-8.

LaBonte MJ, Wilson PM, Fazzone W, Groshen S, Lenz HJ, Ladner RD. DNA microarray profiling of genes differentially regulated by the histone deacetylase inhibitors vorinostat and LBH589 in colon cancer cell lines. *BMC Med Genomics*. 2009; **2**: 67.

Lagos-Quintana M, Rauhut R, Lendeckel W, Tuschl T. Identification of novel genes coding for small expressed RNAs. *Science*. 2001; **294**(5543): 853-8.

Lagos-Quintana M, Rauhut R, Yalcin A, Meyer J, Lendeckel W, Tuschl T. Identification of tissue-specific microRNAs from mouse. *Current Biology*. 2002; **12**(9): 735-9.

Lakner AM, Steuerwald NM, Walling TL, Ghosh S, Li T, McKillop IH, et al. Inhibitory effects of microRNA 19b in hepatic stellate cell-mediated fibrogenesis. *Hepatology*. 2012; **56**(1): 300-10.

Landon S. Resistant starch review. 2007. http://www.resistantstarch.com/NR/rdonlyres/46E5AB79-DABE-4ACA-96A8-1117C99B2ED6/0/Resistant_Starch_Review_Australia.pdf

Lanford RE, Hildebrandt-Eriksen ES, Petri A, Persson R, Lindow M, Munk ME, et al. Therapeutic silencing of microRNA-122 in primates with chronic hepatitis C virus infection. *Science*. 2010; **327**(5962): 198-201.

Lanza G, Ferracin M, Gafa R, Veronese A, Spizzo R, Pichiorri F, et al. mRNA/microRNA gene expression profile in microsatellite unstable colorectal cancer. *Mol Cancer*. 2007; **6**: 54.

Larsson SC, Rafter J, Holmberg L, Bergkvist L, Wolk A. Red meat consumption and risk of cancers of the proximal colon, distal colon and rectum: the Swedish Mammography Cohort. *Int J Cancer*. 2005; **113**(5): 829-34.

Larsson SC, Wolk A. Meat consumption and risk of colorectal cancer: a meta-analysis of prospective studies. *Int J Cancer*. 2006; **119**(11): 2657-64.

Lassen U, Molife LR, Sorensen M, Engelholm SA, Vidal L, Sinha R, et al. A phase I study of the safety and pharmacokinetics of the histone deacetylase inhibitor belinostat administered in combination with carboplatin and/or paclitaxel in patients with solid tumours. *Br J Cancer*. 2010; **103**(1): 12-7.

Lau NC, Lim LP, Weinstein EG, Bartel DP. An abundant class of tiny RNAs with probable regulatory roles in Caenorhabditis elegans. *Science*. 2001; **294**(5543): 858-62.

Law SF, Estojak J, Wang B, Mysliwiec T, Kruh G, Golemis EA. Human enhancer of filamentation 1, a novel p130cas-like docking protein, associates with focal adhesion kinase and induces pseudohyphal growth in Saccharomyces cerevisiae. *Mol Cell Biol*. 1996; **16**(7): 3327-37.

Le Leu RK, Brown IL, Hu Y, Esterman A, Young GP. Suppression of azoxymethane-induced colon cancer development in rats by dietary resistant starch. *Cancer Biol Ther*. 2007a; **6**(10): 1621-6.

Le Leu RK, Brown IL, Hu Y, Morita T, Esterman A, Young GP. Effect of dietary resistant starch and protein on colonic fermentation and intestinal tumourigenesis in rats. *Carcinogenesis*. 2007b; **28**(2): 240-5.

Le Leu RK, Brown IL, Hu Y, Young GP. Effect of resistant starch on genotoxin-induced apoptosis, colonic epithelium, and lumenal contents in rats. *Carcinogenesis*. 2003; **24**(8): 1347-52.

Le Leu RK, Hu Y, Brown IL, Young GP. Effect of high amylose maize starches on colonic fermentation and apoptotic response to DNA-damage in the colon of rats. *Nutr Metab*. 2009; **6**: 11.

Lee EM, Shin S, Cha HJ, Yoon Y, Bae S, Jung JH, et al. Suberoylanilide hydroxamic acid (SAHA) changes microRNA expression profiles in A549 human non-small cell lung cancer cells. *Int J Mol Med*. 2009; **24**(1): 45-50.

Lee NS, Dohjima T, Bauer G, Li H, Li M-J, Ehsani A, et al. Expression of small interfering RNAs targeted against HIV-1 rev transcripts in human cells. *Nat Biotechnol*. 2002; **20**(5): 500-5.

Lee RC, Ambros V. An extensive class of small RNAs in Caenorhabditis elegans. *Science*. 2001; **294**(5543): 862-4.

Lee RC, Feinbaum RL, Ambros V. The C. elegans heterochronic gene lin-4 encodes small RNAs with antisense complementarity to lin-14. *Cell*. 1993; **75**(5): 843-54.

Lee Y, Hur I, Park S-Y, Kim Y-K, Suh MR, Kim VN. The role of PACT in the RNA silencing pathway. *EMBO Journal*. 2006; **25**(3): 522-32.

Lee Y, Kim M, Han J, Yeom K-H, Lee S, Baek SH, et al. MicroRNA genes are transcribed by RNA polymerase II. *EMBO Journal*. 2004; **23**(20): 4051-60.

Lengauer C, Kinzler KW, Vogelstein B. Genetic instability in colorectal cancers. *Nature*. 1997; **386**(6625): 623-7.

Levin B, Lieberman DA, McFarland B, Smith RA, Brooks D, Andrews KS, et al. Screening and surveillance for the early detection of colorectal cancer and adenomatous polyps, 2008: a joint guideline from the American Cancer Society, the US Multi-Society Task Force on Colorectal Cancer, and the American College of Radiology. *CA Cancer J Clin*. 2008; **58**(3): 130-60.

Lewin MH, Bailey N, Bandaletova T, Bowman R, Cross AJ, Pollock J, et al. Red meat enhances the colonic formation of the DNA adduct O6-carboxymethyl guanine: implications for colorectal cancer risk. *Cancer Res*. 2006; **66**(3): 1859-65.

Lewis BP, Burge CB, Bartel DP. Conserved seed pairing, often flanked by adenosines, indicates that thousands of human genes are microRNA targets. *Cell*. 2005; **120**(1): 15-20.

Lewis BP, Shih Ih, Jones-Rhoades MW, Bartel DP, Burge CB. Prediction of mammalian microRNA targets. *Cell*. 2003; **115**(7): 787-98.

Lewis MA, Quint E, Glazier AM, Fuchs H, De Angelis MH, Langford C, et al. An ENU-induced mutation of miR-96 associated with progressive hearing loss in mice. *Nat Genet*. 2009; **41**(5): 614-8.

Li X, Mikkelsen IM, Mortensen B, Winberg JO, Huseby NE. Butyrate reduces liver metastasis of rat colon carcinoma cells in vivo and resistance to oxidative stress in vitro. *Clin Exp Metastasis*. 2004; **21**(4): 331-8.

Li XM, Wang AM, Zhang J, Yi H. Down-regulation of miR-126 expression in colorectal cancer and its clinical significance. *Med Oncol*. 2011a; **28**(4): 1054-7.

Li Y, Bavarva JH, Wang Z, Guo J, Qian C, Thibodeau SN, et al. HEF1, a novel target of Wnt signaling, promotes colonic cell migration and cancer progression. *Oncogene*. 2011b; **30**(23): 2633-43.

Li Y, Zhang X, Polakiewicz RD, Yao T-P, Comb MJ. HDAC6 is required for epidermal growth factor-induced beta-catenin nuclear localization. *J Biol Chem*. 2008; **283**(19): 12686-90.

Lim LP, Lau NC, Weinstein EG, Abdelhakim A, Yekta S, Rhoades MW, et al. The microRNAs of Caenorhabditis elegans. *Genes Dev*. 2003; **17**(8): 991-1008.

Lin J, Gilbert J, Rudek MA, Zwiebel JA, Gore S, Jiemjit A, et al. A phase I dose-finding study of 5-azacytidine in combination with sodium phenylbutyrate in patients with refractory solid tumors. *Clin Cancer Res*. 2009; **15**(19): 6241-9.

Lin WC, Lin FT, Nevins JR. Selective induction of E2F1 in response to DNA damage, mediated by ATM-dependent phosphorylation. *Genes Dev*. 2001; **15**(14): 1833-44.

Link A, Balaguer F, Shen Y, Nagasaka T, Lozano JJ, Boland CR, et al. Fecal MicroRNAs as novel biomarkers for colon cancer screening. *Cancer Epidemiol Biomarkers Prev*. 2010; **19**(7): 1766-74.

Liu J, Carmell MA, Rivas FV, Marsden CG, Thomson JM, Song J-J, et al. Argonaute2 is the catalytic engine of mammalian RNAi. *Science*. 2004; **305**(5689): 1437-41.

Liu K, Li G, Fan C, Zhou X, Wu B, Li J. Increased Expression of MicroRNA-21and Its Association with Chemotherapeutic Response in Human Colorectal Cancer. *J Int Med Res*. 2011a; **39**(6): 2288-95.

Liu L, Chen L, Xu Y, Li R, Du X. microRNA-195 promotes apoptosis and suppresses tumorigenicity of human colorectal cancer cells. *Biochem Biophys Res Commun*. 2010; **400**(2): 236-40.

Liu LT, Chang HC, Chiang LC, Hung WC. Histone deacetylase inhibitor up-regulates RECK to inhibit MMP-2 activation and cancer cell invasion. *Cancer Res*. 2003; **63**(12): 3069-72.

Liu M, Tang Q, Qiu M, Lang N, Li M, Zheng Y, et al. miR-21 targets the tumor suppressor RhoB and regulates proliferation, invasion and apoptosis in colorectal cancer cells. *FEBS Lett*. 2011b; **585**(19): 2998-3005.

Liu RH. Potential synergy of phytochemicals in cancer prevention: mechanism of action. *J Nutr*. 2004; **134**(12 Suppl): 3479S-85S.

Lobjois V, Frongia C, Jozan S, Truchet I, Valette A. Cell cycle and apoptotic effects of SAHA are regulated by the cellular microenvironment in HCT116 multicellular tumour spheroids. *Eur J Cancer*. 2009; **45**(13): 2402-11.

Lodygin D, Tarasov V, Epanchintsev A, Berking C, Knyazeva T, Korner H, et al. Inactivation of miR-34a by aberrant CpG methylation in multiple types of cancer. *Cell Cycle*. 2008; **7**(16): 2591-600.

Long JM, Lahiri DK. MicroRNA-101 downregulates Alzheimer's amyloid-beta precursor protein levels in human cell cultures and is differentially expressed. *Biochem Biophys Res Commun*. 2011; **404**(4): 889-95.

Lu J, Getz G, Miska EA, Alvarez-Saavedra E, Lamb J, Peck D, et al. MicroRNA expression profiles classify human cancers. *Nature*. 2005; **435**(7043): 834-8.

Lu Y, Thomson JM, Wong HY, Hammond SM, Hogan BL. Transgenic over-expression of the microRNA miR-17-92 cluster promotes proliferation and inhibits differentiation of lung epithelial progenitor cells. *Dev Biol*. 2007; **310**(2): 442-53.

Luger K, Mader AW, Richmond RK, Sargent DF, Richmond TJ. Crystal structure of the nucleosome core particle at 2.8 A resolution. *Nature*. 1997; **389**(6648): 251-60.

Lujambio A, Calin GA, Villanueva A, Ropero S, Sanchez-Cespedes M, Blanco D, et al. A microRNA DNA methylation signature for human cancer metastasis. *Proc Natl Acad Sci U S A*. 2008; **105**(36): 13556-61.

Lund E, Guttinger S, Calado A, Dahlberg JE, Kutay U. Nuclear export of microRNA precursors. *Science*. 2004; **303**(5654): 95-8.

Lund EK, Belshaw NJ, Elliott GO, Johnson IT. Recent advances in understanding the role of diet and obesity in the development of colorectal cancer. *Proc Nutr Soc*. 2011; **70**(2): 194-204.

Luo H, Zou J, Dong Z, Zeng Q, Wu D, Liu L. Up-regulated miR-17 promotes cell proliferation, tumor growth and cell cycle progression by targeting RND3 tumor suppressor gene in colorectal carcinoma. *Biochem J*. 2012; **442**(2): 311-21.

Luo J, Su F, Chen D, Shiloh A, Gu W. Deacetylation of p53 modulates its effect on cell growth and apoptosis. *Nature*. 2000; **408**(6810): 377-81.

Ma Y, Zhang P, Wang F, Zhang H, Yang J, Peng J, et al. miR-150 as a potential biomarker associated with prognosis and therapeutic outcome in colorectal cancer. *Gut*. 2012; **61**(10): 1447-53.

MacLennan R, Macrae F, Bain C, Battistutta D, Chapuis P, Gratten H, et al. Randomized trial of intake of fat, fiber, and beta carotene to prevent colorectal adenomas. *J Natl Cancer Inst*. 1995; **87**(23): 1760-6.

Macrae FA, Kilias D, Selbie L, Abbott M, Sharpe K, Young GP. Effect of cereal fibre source and processing on rectal epithelial cell proliferation. *Gut*. 1997; **41**(2): 239-44.

Macrae IJ, Zhou K, Li F, Repic A, Brooks AN, Cande WZ, et al. Structural basis for double-stranded RNA processing by Dicer. *Science*. 2006; **311**(5758): 195-8.

Magnaghi-Jaulin L, Groisman R, Naguibneva I, Robin P, Lorain S, Le Villain JP, et al. Retinoblastoma protein represses transcription by recruiting a histone deacetylase. *Nature*. 1998; **391**(6667): 601-5.

Mal A, Sturniolo M, Schiltz RL, Ghosh MK, Harter ML. A role for histone deacetylase HDAC1 in modulating the transcriptional activity of MyoD: inhibition of the myogenic program. *EMBO Journal*. 2001; **20**(7): 1739-53.

Malumbres M, Harlow E, Hunt T, Hunter T, Lahti JM, Manning G, et al. Cyclin-dependent kinases: a family portrait. *Nat Cell Biol*. 2009; **11**(11): 1275-6.

Mann BS, Johnson JR, Cohen MH, Justice R, Pazdur R. FDA approval summary: vorinostat for treatment of advanced primary cutaneous T-cell lymphoma. *Oncologist*. 2007; **12**(10): 1247-52.

Mariadason JM, Arango D, Corner GA, Aranes MJ, Hotchkiss KA, Yang W, et al. A gene expression profile that defines colon cell maturation in vitro. *Cancer Res*. 2002; **62**(16): 4791-804.

Mariadason JM, Bordonaro M, Aslam F, Shi L, Kuraguchi M, Velcich A, et al. Down-regulation of beta-catenin TCF signaling is linked to colonic epithelial cell differentiation. *Cancer Res*. 2001; **61**(8): 3465-71.

Mariadason JM, Corner GA, Augenlicht LH. Genetic reprogramming in pathways of colonic cell maturation induced by short chain fatty acids: comparison with trichostatin A, sulindac, and curcumin and implications for chemoprevention of colon cancer. *Cancer Res*. 2000; **60**(16): 4561-72.

Marinova Z, Leng Y, Leeds P, Chuang D-M. Histone deacetylase inhibition alters histone methylation associated with heat shock protein 70 promoter modifications in astrocytes and neurons. *Neuropharmacology*. 2011; **60**(7-8): 1109-15.

Marsit CJ, Eddy K, Kelsey KT. MicroRNA responses to cellular stress. *Cancer Res*. 2006; **66**(22): 10843-8.

Mathers JC, Strathdee G, Relton CL. Induction of epigenetic alterations by dietary and other environmental factors. *Adv Genet*. 2010; **71**: 3-39.

Mathew OP, Ranganna K, Yatsu FM. Butyrate, an HDAC inhibitor, stimulates interplay between different posttranslational modifications of histone H3 and differently alters G1-specific cell cycle proteins in vascular smooth muscle cells. *Biomed Pharmacother*. 2010; **64**(10): 733-40.

Mathonnet G, Fabian MR, Svitkin YV, Parsyan A, Huck L, Murata T, et al. MicroRNA inhibition of translation initiation in vitro by targeting the cap-binding complex eIF4F. *Science*. 2007; **317**(5845): 1764-7.

Matsubara H, Takeuchi T, Nishikawa E, Yanagisawa K, Hayashita Y, Ebi H, et al. Apoptosis induction by antisense oligonucleotides against miR-17-5p and miR-20a in lung cancers overexpressing miR-17-92. *Oncogene*. 2007; **26**(41): 6099-105.

Matsuzaki K, Deng G, Tanaka H, Kakar S, Miura S, Kim YS. The relationship between global methylation level, loss of heterozygosity, and microsatellite instability in sporadic colorectal cancer. *Clin Cancer Res*. 2005; **11**(24 Pt 1): 8564-9.

Mavrakis KJ, Wolfe AL, Oricchio E, Palomero T, de Keersmaecker K, McJunkin K, et al. Genome-wide RNA-mediated interference screen identifies miR-19 targets in

Notch-induced T-cell acute lymphoblastic leukaemia. *Nat Cell Biol*. 2010; **12**(4): 372-9.

McKeown-Eyssen GE, Bright-See E, Bruce WR, Jazmaji V, Cohen LB, Pappas SC, et al. A randomized trial of a low fat high fibre diet in the recurrence of colorectal polyps. Toronto Polyp Prevention Group. *J Clin Epidemiol*. 1994; **47**(5): 525-36.

McLennan W, Podger A. National Nutrition Survey. Food Eaten. Australia 1995. ABS Cat No. 4804.0. Canberra: Australian Bureau of Statistics; 1999.

McManus MT, Petersen CP, Haines BB, Chen J, Sharp PA. Gene silencing using micro-RNA designed hairpins. *Rna*. 2002; **8**(6): 842-50.

McOrist AL, Miller RB, Bird AR, Keogh JB, Noakes M, Topping DL, et al. Fecal butyrate levels vary widely among individuals but are usually increased by a diet high in resistant starch. *J Nutr*. 2011; **141**(5): 883-9.

Medina PP, Nolde M, Slack FJ. OncomiR addiction in an in vivo model of microRNA-21-induced pre-B-cell lymphoma. *Nature*. 2010; **467**(7311): 86-90.

Megraw M, Sethupathy P, Corda B, Hatzigeorgiou AG. miRGen: a database for the study of animal microRNA genomic organization and function. *Nucleic Acids Res*. 2007; **35**(Database issue): D149-55.

Meister G, Landthaler M, Patkaniowska A, Dorsett Y, Teng G, Tuschl T. Human Argonaute2 mediates RNA cleavage targeted by miRNAs and siRNAs. *Mol Cell*. 2004; **15**(2): 185-97.

Melo S, Villanueva A, Moutinho C, Davalos V, Spizzo R, Ivan C, et al. Small molecule enoxacin is a cancer-specific growth inhibitor that acts by enhancing TAR RNA-binding protein 2-mediated microRNA processing. *Proc Natl Acad Sci U S A*. 2011; **108**(11): 4394-9.

Melo SA, Moutinho C, Ropero S, Calin GA, Rossi S, Spizzo R, et al. A genetic defect in exportin-5 traps precursor microRNAs in the nucleus of cancer cells. *Cancer Cell*. 2010; **18**(4): 303-15.

Melo SA, Ropero S, Moutinho C, Aaltonen LA, Yamamoto H, Calin GA, et al. A TARBP2 mutation in human cancer impairs microRNA processing and DICER1 function. *Nat Genet*. 2009; **41**(3): 365-70.

Mencia A, Modamio-Hoybjor S, Redshaw N, Morin M, Mayo-Merino F, Olavarrieta L, et al. Mutations in the seed region of human miR-96 are responsible for nonsyndromic progressive hearing loss. *Nat Genet*. 2009; **41**(5): 609-13.

Mendell JT. MicroRNAs: critical regulators of development, cellular physiology and malignancy. *Cell Cycle*. 2005; **4**(9): 1179-84.

Mendell JT. miRiad roles for the miR-17-92 cluster in development and disease. *Cell*. 2008; **133**(2): 217-22.

Mendell JT, Olson EN. MicroRNAs in stress signaling and human disease. *Cell*. 2012; **148**(6): 1172-87.

Meng F, Henson R, Wehbe-Janek H, Ghoshal K, Jacob ST, Patel T. MicroRNA-21 regulates expression of the PTEN tumor suppressor gene in human hepatocellular cancer. *Gastroenterology*. 2007; **133**(2): 647-58.

Michael MZ, O'Connor SM, van Holst Pellekaan NG, Young GP, James RJ. Reduced accumulation of specific microRNAs in colorectal neoplasia. *Mol Cancer Res*. 2003; **1**(12): 882-91.

Michels KB, Fuchs CS, Giovannucci E, Colditz GA, Hunter DJ, Stampfer MJ, et al. Fiber intake and incidence of colorectal cancer among 76,947 women and 47,279 men. *Cancer Epidemiol Biomarkers Prev*. 2005; **14**(4): 842-9.

Michlewski G, Guil S, Semple CA, Caceres JF. Posttranscriptional regulation of miRNAs harboring conserved terminal loops. *Mol Cell*. 2008; **32**(3): 383-93.

Mikkelsen TS, Ku M, Jaffe DB, Issac B, Lieberman E, Giannoukos G, et al. Genome-wide maps of chromatin state in pluripotent and lineage-committed cells. *Nature*. 2007; **448**(7153): 553-60.

Miller AA, Kurschel E, Osieka R, Schmidt CG. Clinical pharmacology of sodium butyrate in patients with acute leukemia. *Eur J Cancer Clin Oncol*. 1987; **23**(9): 1283-7.

Milner JA. Molecular targets for bioactive food components. *J Nutr*. 2004; **134**(9): 2492S-98S.

Mimori K, Ogawa K, Okamoto M, Sudo T, Inoue H, Mori M. Clinical significance of enhancer of zeste homolog 2 expression in colorectal cancer cases. *Eur J Surg Oncol*. 2005; **31**(4): 376-80.

Minegishi M, Tachibana K, Sato T, Iwata S, Nojima Y, Morimoto C. Structure and function of Cas-L, a 105-kD Crk-associated substrate-related protein that is involved in beta 1 integrin-mediated signaling in lymphocytes. *J Exp Med*. 1996; **184**(4): 1365-75.

Miyoshi K, Miyoshi T, Siomi H. Many ways to generate microRNA-like small RNAs: non-canonical pathways for microRNA production. *Mol Genet Genomics*. 2010; **284**(2): 95-103.

Miyoshi Y, Nagase H, Ando H, Horii A, Ichii S, Nakatsuru S, et al. Somatic mutations of the APC gene in colorectal tumors: mutation cluster region in the APC gene. *Hum Mol Genet*. 1992; **1**(4): 229-33.

Monzo M, Navarro A, Bandres E, Artells R, Moreno I, Gel B, et al. Overlapping expression of microRNAs in human embryonic colon and colorectal cancer. *Cell Res*. 2008; **18**(8): 823-33.

Morelli MP, Tentler JJ, Kulikowski GN, Tan AC, Bradshaw-Pierce EL, Pitts TM, et al. Preclinical Activity of the Rational Combination of Selumetinib (AZD6244) in Combination with Vorinostat in KRAS Mutant Colorectal Cancer Models. *Clin Cancer Res*. 2012; **18**(4): 1051-62.

Morita S, Horii T, Kimura M, Goto Y, Ochiya T, Hatada I. One Argonaute family member, Eif2c2 (Ago2), is essential for development and appears not to be involved in DNA methylation. *Genomics*. 2007; **89**(6): 687-96.

Morita S, Oizumi S, Minami H, Kitagawa K, Komatsu Y, Fujiwara Y, et al. Phase I dose-escalating study of panobinostat (LBH589) Administered intravenously to Japanese patients with advanced solid tumors. *Invest New Drugs*. 2011.

Mosakhani N, Sarhadi VK, Borze I, Karjalainen-Lindsberg ML, Sundstrom J, Ristamaki R, et al. MicroRNA profiling differentiates colorectal cancer according to KRAS status. *Genes Chromosomes Cancer*. 2012; **51**(1): 1-9.

Moss EG, Lee RC, Ambros V. The cold shock domain protein LIN-28 controls developmental timing in C. elegans and is regulated by the lin-4 RNA. *Cell*. 1997; **88**(5): 637-46.

Motiwala T, Ghoshal K, Das A, Majumder S, Weichenhan D, Wu Y-Z, et al. Suppression of the protein tyrosine phosphatase receptor type O gene (PTPRO) by methylation in hepatocellular carcinomas. *Oncogene*. 2003; **22**(41): 6319-31.

Motoyama K, Inoue H, Takatsuno Y, Tanaka F, Mimori K, Uetake H, et al. Over- and under-expressed microRNAs in human colorectal cancer. *Int J Oncol*. 2009; **34**(4): 1069-75.

Mourelatos Z, Dostie J, Paushkin S, Sharma A, Charroux B, Abel L, et al. miRNPs: a novel class of ribonucleoproteins containing numerous microRNAs. *Genes Dev*. 2002; **16**(6): 720-8.

Mu P, Han YC, Betel D, Yao E, Squatrito M, Ogrodowski P, et al. Genetic dissection of the miR-17~92 cluster of microRNAs in Myc-induced B-cell lymphomas. *Genes Dev*. 2009; **23**(24): 2806-11.

Muller PY, Janovjak H, Miserez AR, Dobbie Z. Processing of gene expression data generated by quantitative real-time RT-PCR. *Biotechniques*. 2002; **32**(6): 1372-4, 76, 78-9.

Munster P, Marchion D, Bicaku E, Lacevic M, Kim J, Centeno B, et al. Clinical and biological effects of valproic acid as a histone deacetylase inhibitor on tumor and surrogate tissues: phase I/II trial of valproic acid and epirubicin/FEC. *Clin Cancer Res.* 2009a; **15**(7): 2488-96.

Munster P, Marchion D, Bicaku E, Schmitt M, Lee JH, DeConti R, et al. Phase I trial of histone deacetylase inhibition by valproic acid followed by the topoisomerase II inhibitor epirubicin in advanced solid tumors: a clinical and translational study. *J Clin Oncol.* 2007; **25**(15): 1979-85.

Munster PN, Marchion D, Thomas S, Egorin M, Minton S, Springett G, et al. Phase I trial of vorinostat and doxorubicin in solid tumours: histone deacetylase 2 expression as a predictive marker. *Br J Cancer.* 2009b; **101**(7): 1044-50.

Murphy M, Ahn J, Walker KK, Hoffman WH, Evans RM, Levine AJ, et al. Transcriptional repression by wild-type p53 utilizes histone deacetylases, mediated by interaction with mSin3a. *Genes Dev.* 1999; **13**(19): 2490-501.

Muto T, Bussey HJ, Morson BC. The evolution of cancer of the colon and rectum. *Cancer.* 1975; **36**(6): 2251-70.

Myzak MC, Dashwood WM, Orner GA, Ho E, Dashwood RH. Sulforaphane inhibits histone deacetylase in vivo and suppresses tumorigenesis in Apc-minus mice. *FASEB Journal.* 2006a; **20**(3): 506-8.

Myzak MC, Hardin K, Wang R, Dashwood RH, Ho E. Sulforaphane inhibits histone deacetylase activity in BPH-1, LnCaP and PC-3 prostate epithelial cells. *Carcinogenesis.* 2006b; **27**(4): 811-9.

Myzak MC, Karplus PA, Chung F-L, Dashwood RH. A novel mechanism of chemoprotection by sulforaphane: inhibition of histone deacetylase. *Cancer Res.* 2004; **64**(16): 5767-74.

Myzak MC, Tong P, Dashwood W-M, Dashwood RH, Ho E. Sulforaphane retards the growth of human PC-3 xenografts and inhibits HDAC activity in human subjects. *Exp Biol Med.* 2007; **232**(2): 227-34.

Nagel R, le Sage C, Diosdado B, van der Waal M, Oude Vrielink JA, Bolijn A, et al. Regulation of the adenomatous polyposis coli gene by the miR-135 family in colorectal cancer. *Cancer Res.* 2008; **68**(14): 5795-802.

Nakajima G, Hayashi K, Xi Y, Kudo K, Uchida K, Takasaki K, et al. Non-coding MicroRNAs hsa-let-7g and hsa-miR-181b are Associated with Chemoresponse to S-1 in Colon Cancer. *Cancer Genomics Proteomics.* 2006; **3**(5): 317-24.

Nakano K, Mizuno T, Sowa Y, Orita T, Yoshino T, Okuyama Y, et al. Butyrate activates the WAF1/Cip1 gene promoter through Sp1 sites in a p53-negative human colon cancer cell line. *J Biol Chem.* 1997; **272**(35): 22199-206.

Nan X, Campoy FJ, Bird A. MeCP2 is a transcriptional repressor with abundant binding sites in genomic chromatin. *Cell.* 1997; **88**(4): 471-81.

Nan X, Ng HH, Johnson CA, Laherty CD, Turner BM, Eisenman RN, et al. Transcriptional repression by the methyl-CpG-binding protein MeCP2 involves a histone deacetylase complex. *Nature.* 1998; **393**(6683): 386-9.

Natarajan M, Stewart JE, Golemis EA, Pugacheva EN, Alexandropoulos K, Cox BD, et al. HEF1 is a necessary and specific downstream effector of FAK that promotes the migration of glioblastoma cells. *Oncogene.* 2006; **25**(12): 1721-32.

Ng EK, Chong WW, Jin H, Lam EK, Shin VY, Yu J, et al. Differential expression of microRNAs in plasma of patients with colorectal cancer: a potential marker for colorectal cancer screening. *Gut.* 2009a; **58**(10): 1375-81.

Ng EK, Tsang WP, Ng SS, Jin HC, Yu J, Li JJ, et al. MicroRNA-143 targets DNA methyltransferases 3A in colorectal cancer. *Br J Cancer.* 2009b; **101**(4): 699-706.

NHMRC. Nutrient Reference Values for Australia and New Zealand Including Recommended Dietary Intakes. Canberra: National Health and Medical Research Council; 2006.

Nicolaides NC, Littman SJ, Modrich P, Kinzler KW, Vogelstein B. A naturally occurring hPMS2 mutation can confer a dominant negative mutator phenotype. *Mol Cell Biol.* 1998; **18**(3): 1635-41.

Nicolas FE. Experimental validation of microRNA targets using a luciferase reporter system. *Methods Mol Biol.* 2011; **732**: 139-52.

Nie J, Liu L, Zheng W, Chen L, Wu X, Xu Y, et al. microRNA-365, down-regulated in colon cancer, inhibits cell cycle progression and promotes apoptosis of colon cancer cells by probably targeting Cyclin D1 and Bcl-2. *Carcinogenesis.* 2012; **33**(1): 220-5.

Noakes M, Clifton PM. The CSIRO Total Wellbeing Diet. Melbourne: Penguin; 2005.

Norat T, Bingham S, Ferrari P, Slimani N, Jenab M, Mazuir M, et al. Meat, fish, and colorectal cancer risk: the European Prospective Investigation into cancer and nutrition. *J Natl Cancer Inst.* 2005; **97**(12): 906-16.

Noro R, Miyanaga A, Minegishi Y, Okano T, Seike M, Soeno C, et al. Histone deacetylase inhibitor enhances sensitivity of non-small-cell lung cancer cells to 5-FU/S-1 via down-regulation of thymidylate synthase expression and up-regulation of p21(waf1/cip1) expression. *Cancer Sci.* 2010; **101**(6): 1424-30.

Nystrom M, Mutanen M. Diet and epigenetics in colon cancer. *World J Gastroenterol.* 2009; **15**(3): 257-63.

O'Callaghan NJ, Toden S, Bird AR, Topping DL, Fenech M, Conlon MA. Colonocyte telomere shortening is greater with dietary red meat than white meat and is attenuated by resistant starch. *Clin Nutr.* 2012; **31**(1): 60-4.

O'Donnell KA, Wentzel EA, Zeller KI, Dang CV, Mendell JT. c-Myc-regulated microRNAs modulate E2F1 expression. *Nature.* 2005; **435**(7043): 839-43.

O'Keefe SJ, Kidd M, Espitalier-Noel G, Owira P. Rarity of colon cancer in Africans is associated with low animal product consumption, not fiber. *Am J Gastroenterol.* 1999; **94**(5): 1373-80.

O'Neill GM, Seo S, Serebriiskii IG, Lessin SR, Golemis EA. A new central scaffold for metastasis: parsing HEF1/Cas-L/NEDD9. *Cancer Res.* 2007; **67**(19): 8975-9.

Ogawa H, Rafiee P, Fisher PJ, Johnson NA, Otterson MF, Binion DG. Butyrate modulates gene and protein expression in human intestinal endothelial cells. *Biochem Biophys Res Commun.* 2003; **309**(3): 512-9.

Ogino S, Nosho K, Kirkner GJ, Kawasaki T, Chan AT, Schernhammer ES, et al. A cohort study of tumoral LINE-1 hypomethylation and prognosis in colon cancer. *J Natl Cancer Inst.* 2008; **100**(23): 1734-8.

Okamoto R, Tsuchiya K, Nemoto Y, Akiyama J, Nakamura T, Kanai T, et al. Requirement of Notch activation during regeneration of the intestinal epithelia. *Am J Physiol Gastrointest Liver Physiol.* 2009; **296**(1): G23-35.

Olive V, Bennett MJ, Walker JC, Ma C, Jiang I, Cordon-Cardo C, et al. miR-19 is a key oncogenic component of mir-17-92. *Genes Dev.* 2009; **23**(24): 2839-49.

Olive V, Jiang I, He L. mir-17-92, a cluster of miRNAs in the midst of the cancer network. *Int J Biochem Cell Biol.* 2010; **42**(8): 1348-54.

Olsen EA, Kim YH, Kuzel TM, Pacheco TR, Foss FM, Parker S, et al. Phase IIb multicenter trial of vorinostat in patients with persistent, progressive, or treatment refractory cutaneous T-cell lymphoma. *J Clin Oncol.* 2007; **25**(21): 3109-15.

Olsen PH, Ambros V. The lin-4 regulatory RNA controls developmental timing in Caenorhabditis elegans by blocking LIN-14 protein synthesis after the initiation of translation. *Dev Biol.* 1999; **216**(2): 671-80.

Ono S, Oue N, Kuniyasu H, Suzuki T, Ito R, Matsusaki K, et al. Acetylated histone H4 is reduced in human gastric adenomas and carcinomas. *J Exp Clin Cancer Res.* 2002; **21**(3): 377-82.

Orchel A, Molin I, Dzierzewicz Z, Latocha M, Weglarz L, Wilczok T. Quantification of p21 gene expression in Caco-2 cells treated with sodium butyrate using real-time reverse transcription-PCR (RT-PCR) assay. *Acta Pol Pharm*. 2003; **60**(2): 103-5.

Ota A, Tagawa H, Karnan S, Tsuzuki S, Karpas A, Kira S, et al. Identification and characterization of a novel gene, C13orf25, as a target for 13q31-q32 amplification in malignant lymphoma. *Cancer Res*. 2004; **64**(9): 3087-95.

Ozawa Y, Towatari M, Tsuzuki S, Hayakawa F, Maeda T, Miyata Y, et al. Histone deacetylase 3 associates with and represses the transcription factor GATA-2. *Blood*. 2001; **98**(7): 2116-23.

Ozsolak F, Poling LL, Wang Z, Liu H, Liu XS, Roeder RG, et al. Chromatin structure analyses identify miRNA promoters. *Genes Dev*. 2008; **22**(22): 3172-83.

Ozsolak F, Song JS, Liu XS, Fisher DE. High-throughput mapping of the chromatin structure of human promoters. *Nat Biotechnol*. 2007; **25**(2): 244-8.

Paddison PJ, Caudy AA, Bernstein E, Hannon GJ, Conklin DS. Short hairpin RNAs (shRNAs) induce sequence-specific silencing in mammalian cells. *Genes Dev*. 2002; **16**(8): 948-58.

Palmer DG, Paraskeva C, Williams AC. Modulation of p53 expression in cultured colonic adenoma cell lines by the naturally occurring lumenal factors butyrate and deoxycholate. *Int J Cancer*. 1997; **73**(5): 702-6.

Pang M, Ma L, Liu N, Ponnusamy M, Zhao TC, Yan H, et al. Histone deacetylase 1/2 mediates proliferation of renal interstitial fibroblasts and expression of cell cycle proteins. *J Cell Biochem*. 2011; **112**(8): 2138-48.

Papadopoulos N, Nicolaides NC, Wei YF, Ruben SM, Carter KC, Rosen CA, et al. Mutation of a mutL homolog in hereditary colon cancer. *Science*. 1994; **263**(5153): 1625-9.

Park J-H, Kim S-H, Choi M-C, Lee J, Oh D-Y, Im S-A, et al. Class II histone deacetylases play pivotal roles in heat shock protein 90-mediated proteasomal degradation of vascular endothelial growth factor receptors. *Biochem Biophys Res Commun*. 2008; **368**(2): 318-22.

Park JH, Ahn J, Kim S, Kwon DY, Ha TY. Murine hepatic miRNAs expression and regulation of gene expression in diet-induced obese mice. *Mol Cells*. 2011; **31**(1): 33-8.

Pasquinelli AE, Reinhart BJ, Slack F, Martindale MQ, Kuroda MI, Maller B, et al. Conservation of the sequence and temporal expression of let-7 heterochronic regulatory RNA. *Nature*. 2000; **408**(6808): 86-9.

Patnaik A, Rowinsky EK, Villalona MA, Hammond LA, Britten CD, Siu LL, et al. A phase I study of pivaloyloxymethyl butyrate, a prodrug of the differentiating agent butyric acid, in patients with advanced solid malignancies. *Clin Cancer Res*. 2002; **8**(7): 2142-8.

Patry C, Bouchard L, Labrecque P, Gendron D, Lemieux B, Toutant J, et al. Small interfering RNA-mediated reduction in heterogeneous nuclear ribonucleoparticule A1/A2 proteins induces apoptosis in human cancer cells but not in normal mortal cell lines. *Cancer Res*. 2003; **63**(22): 7679-88.

Paul CP, Good PD, Winer I, Engelke DR. Effective expression of small interfering RNA in human cells. *Nat Biotechnol*. 2002; **20**(5): 505-8.

Pelisch F, Khauv D, Risso G, Stallings-Mann M, Blaustein M, Quadrana L, et al. Involvement of hnRNP A1 in the matrix metalloprotease-3-dependent regulation of Rac1 pre-mRNA splicing. *J Cell Biochem*. 2012; **113**(7): 2319-29.

Pellizzaro C, Coradini D, Daidone MG. Modulation of angiogenesis-related proteins synthesis by sodium butyrate in colon cancer cell line HT29. *Carcinogenesis*. 2002; **23**(5): 735-40.

Petrocca F, Visone R, Onelli MR, Shah MH, Nicoloso MS, de Martino I, et al. E2F1-regulated microRNAs impair TGFbeta-dependent cell-cycle arrest and apoptosis in gastric cancer. *Cancer Cell*. 2008; **13**(3): 272-86.

Pickering MT, Stadler BM, Kowalik TF. miR-17 and miR-20a temper an E2F1-induced G1 checkpoint to regulate cell cycle progression. *Oncogene*. 2009; **28**(1): 140-5.

Piekarz RL, Frye R, Turner M, Wright JJ, Allen SL, Kirschbaum MH, et al. Phase II multi-institutional trial of the histone deacetylase inhibitor romidepsin as monotherapy for patients with cutaneous T-cell lymphoma. *J Clin Oncol*. 2009; **27**(32): 5410-7.

Pietinen P, Malila N, Virtanen M, Hartman TJ, Tangrea JA, Albanes D, et al. Diet and risk of colorectal cancer in a cohort of Finnish men. *Cancer Causes Control*. 1999; **10**(5): 387-96.

Pili R, Salumbides B, Zhao M, Altiok S, Qian D, Zwiebel J, et al. Phase I study of the histone deacetylase inhibitor entinostat in combination with 13-cis retinoic acid in patients with solid tumours. *Br J Cancer*. 2012; **106**(1): 77-84.

Pillai RS, Artus CG, Filipowicz W. Tethering of human Ago proteins to mRNA mimics the miRNA-mediated repression of protein synthesis. *Rna*. 2004; **10**(10): 1518-25.

Pitts TM, Morrow M, Kaufman SA, Tentler JJ, Eckhardt SG. Vorinostat and bortezomib exert synergistic antiproliferative and proapoptotic effects in colon cancer cell models. *Mol Cancer Ther*. 2009; **8**(2): 342-9.

Pogribny IP, Tryndyak VP, Ross SA, Beland FA. Differential expression of microRNAs during hepatocarcinogenesis induced by methyl deficiency in rats. *Nutr Rev*. 2008; **66 Suppl 1**: S33-5.

Poliseno L, Salmena L, Riccardi L, Fornari A, Song MS, Hobbs RM, et al. Identification of the miR-106b~25 microRNA cluster as a proto-oncogenic PTEN-targeting intron that cooperates with its host gene MCM7 in transformation. *Sci Signal*. 2010; **3**(117): 29.

Pool-Zobel BL, Selvaraju V, Sauer J, Kautenburger T, Kiefer J, Richter KK, et al. Butyrate may enhance toxicological defence in primary, adenoma and tumor human colon cells by favourably modulating expression of glutathione S-transferases genes, an approach in nutrigenomics. *Carcinogenesis*. 2005; **26**(6): 1064-76.

Portanova P, Russo T, Pellerito O, Calvaruso G, Giuliano M, Vento R, et al. The role of oxidative stress in apoptosis induced by the histone deacetylase inhibitor suberoylanilide hydroxamic acid in human colon adenocarcinoma HT-29 cells. *Int J Oncol*. 2008; **33**(2): 325-31.

Pospisil V, Vargova K, Kokavec J, Rybarova J, Savvulidi F, Jonasova A, et al. Epigenetic silencing of the oncogenic miR-17-92 cluster during PU.1-directed macrophage differentiation. *EMBO J*. 2011; **30**(21): 4450-64.

Powell AE, Wang Y, Li Y, Poulin EJ, Means AL, Washington MK, et al. The pan-ErbB negative regulator Lrig1 is an intestinal stem cell marker that functions as a tumor suppressor. *Cell*. 2012; **149**(1): 146-58.

Power DG, Gloglowski E, Lipkin SM. Clinical genetics of hereditary colorectal cancer. *Hematol Oncol Clin North Am*. 2010; **24**(5): 837-59.

Pramanik D, Campbell NR, Karikari C, Chivukula R, Kent OA, Mendell JT, et al. Restitution of tumor suppressor microRNAs using a systemic nanovector inhibits pancreatic cancer growth in mice. *Mol Cancer Ther*. 2011; **10**(8): 1470-80.

Prasanna Kumar S, Thippeswamy G, Sheela ML, Prabhakar BT, Salimath BP. Butyrate-induced phosphatase regulates VEGF and angiogenesis via Sp1. *Arch Biochem Biophys*. 2008; **478**(1): 85-95.

Pullamsetti SS, Doebele C, Fischer A, Savai R, Kojonazarov B, Dahal BK, et al. Inhibition of microRNA-17 improves lung and heart function in experimental pulmonary hypertension. *Am J Respir Crit Care Med*. 2012; **185**(4): 409-19.

R Development Core Team. R: A language and environment for statistical computing. Vienna, Austria: R Foundation for Statistical Computing; 2011.

Rada-Iglesias A, Enroth S, Ameur A, Koch CM, Clelland GK, Respuela-Alonso P, et al. Butyrate mediates decrease of histone acetylation centered on transcription start sites and down-regulation of associated genes. *Genome Res*. 2007; **17**(6): 708-19.

Rafter J, Bennett M, Caderni G, Clune Y, Hughes R, Karlsson PC, et al. Dietary synbiotics reduce cancer risk factors in polypectomized and colon cancer patients. *Am J Clin Nutr*. 2007; **85**(2): 488-96.

Ramalingam SS, Kummar S, Sarantopoulos J, Shibata S, LoRusso P, Yerk M, et al. Phase I study of vorinostat in patients with advanced solid tumors and hepatic dysfunction: a National Cancer Institute Organ Dysfunction Working Group study. *J Clin Oncol*. 2010; **28**(29): 4507-12.

Ray S, Lee C, Hou T, Boldogh I, Brasier AR. Requirement of histone deacetylase1 (HDAC1) in signal transducer and activator of transcription 3 (STAT3) nucleocytoplasmic distribution. *Nucleic Acids Res*. 2008; **36**(13): 4510-20.

Ree AH, Dueland S, Folkvord S, Hole KH, Seierstad T, Johansen M, et al. Vorinostat, a histone deacetylase inhibitor, combined with pelvic palliative radiotherapy for gastrointestinal carcinoma: the Pelvic Radiation and Vorinostat (PRAVO) phase 1 study. *Lancet Oncol*. 2010; **11**(5): 459-64.

Reesink HW, Janssen HLA, Zeuzem S, Lawitz E, Rodriguez-Torres M, Patel K, et al. Final Results - Randomized, Double-blind, Placebo-controlled Safety, Anti-viral Proof-of-Concept Study of Miravirsen, an Oligonucleotide Targeting miR-122, in Treatment-naive Patients with Genotype 1 Chronic HCV Infection. *47th International Liver Congress (EASL 2012). Barcelona, April 18-22*. 2012; (Abstract 58).

Reinhart BJ, Slack FJ, Basson M, Pasquinelli AE, Bettinger JC, Rougvie AE, et al. The 21-nucleotide let-7 RNA regulates developmental timing in Caenorhabditis elegans. *Nature*. 2000; **403**(6772): 901-6.

Reinhart BJ, Weinstein EG, Rhoades MW, Bartel B, Bartel DP. MicroRNAs in plants.]. *Genes Dev*. 2002; **16**(13): 1616-26.

Rhodes LV, Nitschke AM, Segar HC, Martin EC, Driver JL, Elliott S, et al. The histone deacetylase inhibitor trichostatin A alters microRNA expression profiles in apoptosis-resistant breast cancer cells. *Oncol Rep*. 2012; **27**(1): 10-6.

Richly H, Aloia L, Di Croce L. Roles of the Polycomb group proteins in stem cells and cancer. *Cell Death Dis*. 2011; **2**: e204.

Robertson KD, Ait-Si-Ali S, Yokochi T, Wade PA, Jones PL, Wolffe AP. DNMT1 forms a complex with Rb, E2F1 and HDAC1 and represses transcription from E2F-responsive promoters. *Nat Genet*. 2000; **25**(3): 338-42.

Rodriguez-Paredes M, Esteller M. Cancer epigenetics reaches mainstream oncology. *Nat Med*. 2011; **17**(3): 330-9.

Rodriguez A, Griffiths-Jones S, Ashurst JL, Bradley A. Identification of mammalian microRNA host genes and transcription units. *Genome Res*. 2004; **14**(10A): 1902-10.

Rodriguez J, Frigola J, Vendrell E, Risques R-A, Fraga MF, Morales C, et al. Chromosomal instability correlates with genome-wide DNA demethylation in human primary colorectal cancers. *Cancer Res*. 2006; **66**(17): 8462-9468.

Roediger WE. Utilization of nutrients by isolated epithelial cells of the rat colon. *Gastroenterology*. 1982; **83**(2): 424-9.

Rohrmann S, Hermann S, Linseisen J. Heterocyclic aromatic amine intake increases colorectal adenoma risk: findings from a prospective European cohort study. *Am J Clin Nutr*. 2009; **89**(5): 1418-24.

Ropero S, Fraga MF, Ballestar E, Hamelin R, Yamamoto H, Boix-Chornet M, et al. A truncating mutation of HDAC2 in human cancers confers resistance to histone deacetylase inhibition. *Nat Genet*. 2006; **38**(5): 566-9.

Roy S, Tenniswood M. Site-specific acetylation of p53 directs selective transcription complex assembly. *J Biol Chem*. 2007; **282**(7): 4765-71.

Ruppin H, Bar-Meir S, Soergel KH, Wood CM, Schmitt MG, Jr. Absorption of short-chain fatty acids by the colon. *Gastroenterology*. 1980; **78**(6): 1500-7.

Sachdeva M, Zhu S, Wu F, Wu H, Walia V, Kumar S, et al. p53 represses c-Myc through induction of the tumor suppressor miR-145. *Proc Natl Acad Sci U S A*. 2009; **106**(9): 3207-12.

Saito Y, Liang G, Egger G, Friedman JM, Chuang JC, Coetzee GA, et al. Specific activation of microRNA-127 with downregulation of the proto-oncogene BCL6 by chromatin-modifying drugs in human cancer cells. *Cancer Cell*. 2006; **9**(6): 435-43.

Sampson VB, Rong NH, Han J, Yang Q, Aris V, Soteropoulos P, et al. MicroRNA let-7a down-regulates MYC and reverts MYC-induced growth in Burkitt lymphoma cells. *Cancer Res*. 2007; **67**(20): 9762-70.

Sankar N, Baluchamy S, Kadeppagari RK, Singhal G, Weitzman S, Thimmapaya B. p300 provides a corepressor function by cooperating with YY1 and HDAC3 to repress c-Myc. *Oncogene*. 2008; **27**(43): 5717-28.

Sarver AL, French AJ, Borralho PM, Thayanithy V, Oberg AL, Silverstein KA, et al. Human colon cancer profiles show differential microRNA expression depending on mismatch repair status and are characteristic of undifferentiated proliferative states. *BMC Cancer*. 2009; **9**: 401.

Sauer J, Richter KK, Pool-Zobel BL. Physiological concentrations of butyrate favorably modulate genes of oxidative and metabolic stress in primary human colon cells. *J Nutr Biochem*. 2007; **18**(11): 736-45.

Schaefer A, O'Carroll D, Tan CL, Hillman D, Sugimori M, Llinas R, et al. Cerebellar neurodegeneration in the absence of microRNAs. *J Exp Med*. 2007; **204**(7): 1553-8.

Schatzkin A, Lanza E, Corle D, Lance P, Iber F, Caan B, et al. Lack of effect of a low-fat, high-fiber diet on the recurrence of colorectal adenomas. Polyp Prevention Trial Study Group. *N Engl J Med*. 2000; **342**(16): 1149-55.

Schatzkin A, Mouw T, Park Y, Subar AF, Kipnis V, Hollenbeck A, et al. Dietary fiber and whole-grain consumption in relation to colorectal cancer in the NIH-AARP Diet and Health Study. *Am J Clin Nutr*. 2007; **85**(5): 1353-60.

Schepeler T, Reinert JT, Ostenfeld MS, Christensen LL, Silahtaroglu AN, Dyrskjot L, et al. Diagnostic and prognostic microRNAs in stage II colon cancer. *Cancer Res*. 2008; **68**(15): 6416-24.

Scheppach W, Bartram P, Richter A, Richter F, Liepold H, Dusel G, et al. Effect of short-chain fatty acids on the human colonic mucosa in vitro. *JPEN J Parenter Enteral Nutr*. 1992; **16**(1): 43-8.

Schetter AJ, Leung SY, Sohn JJ, Zanetti KA, Bowman ED, Yanaihara N, et al. MicroRNA expression profiles associated with prognosis and therapeutic outcome in colon adenocarcinoma. *JAMA*. 2008; **299**(4): 425-36.

Schimanski CC, Frerichs K, Rahman F, Berger M, Lang H, Galle PR, et al. High miR-196a levels promote the oncogenic phenotype of colorectal cancer cells. *World J Gastroenterol*. 2009; **15**(17): 2089-96.

Schneider-Poetsch T, Ju J, Eyler DE, Dang Y, Bhat S, Merrick WC, et al. Inhibition of eukaryotic translation elongation by cycloheximide and lactimidomycin. *Nat Chem Biol*. 2010; **6**(3): 209-17.

Schones DE, Cui K, Cuddapah S, Roh T-Y, Barski A, Wang Z, et al. Dynamic regulation of nucleosome positioning in the human genome. *Cell*. 2008; **132**(5): 887-98.

Schuebel KE, Chen W, Cope L, Glockner SC, Suzuki H, Yi J-M, et al. Comparing the DNA hypermethylome with gene mutations in human colorectal cancer. *PLoS Genet*. 2007; **3**(9): 1709-23.

Schuettengruber B, Chourrout D, Vervoort M, Leblanc B, Cavalli G. Genome regulation by polycomb and trithorax proteins. *Cell*. 2007; **128**(4): 735-45.

Schulte JH, Horn S, Otto T, Samans B, Heukamp LC, Eilers UC, et al. MYCN regulates oncogenic MicroRNAs in neuroblastoma. *Int J Cancer*. 2008; **122**(3): 699-704.

Schulz KF, Altman DG, Moher D, Group C. CONSORT 2010 Statement: updated guidelines for reporting parallel group randomised trials. *BMC Med*. 2010; **8**: 18.

Schwarz DS, Hutvagner G, Du T, Xu Z, Aronin N, Zamore PD. Asymmetry in the assembly of the RNAi enzyme complex. *Cell*. 2003; **115**(2): 199-208.

Segal E, Fondufe-Mittendorf Y, Chen L, Thastrom A, Field Y, Moore IK, et al. A genomic code for nucleosome positioning. *Nature*. 2006; **442**(7104): 772-8.

Shah MS, Schwartz SL, Zhao C, Davidson LA, Zhou B, Lupton JR, et al. Integrated microRNA and mRNA expression profiling in a rat colon carcinogenesis model: effect of a chemo-protective diet. *Physiol Genomics*. 2011; **43**(10): 640-54.

Shen L, Kondo Y, Rosner GL, Xiao L, Hernandez NS, Vilaythong J, et al. MGMT promoter methylation and field defect in sporadic colorectal cancer. *J Natl Cancer Inst*. 2005; **97**(18): 1330-8.

Shi B, Sepp-Lorenzino L, Prisco M, Linsley P, deAngelis T, Baserga R. Micro RNA 145 targets the insulin receptor substrate-1 and inhibits the growth of colon cancer cells. *J Biol Chem*. 2007; **282**(45): 32582-90.

Shibuya H, Iinuma H, Shimada R, Horiuchi A, Watanabe T. Clinicopathological and prognostic value of microRNA-21 and microRNA-155 in colorectal cancer. *Oncology*. 2010; **79**(3-4): 313-20.

Shin D, Shin J-Y, McManus MT, Ptacek LJ, Fu Y-H. Dicer ablation in oligodendrocytes provokes neuronal impairment in mice. *Ann Neurol*. 2009a; **66**(6): 843-57.

Shin JH, Li RW, Gao Y, Baldwin Rt, Li CJ. Genome-wide ChIP-seq mapping and analysis reveal butyrate-induced acetylation of H3K9 and H3K27 correlated with transcription activity in bovine cells. *Funct Integr Genomics*. 2012; **12**(1): 119-30.

Shin S, Lee EM, Cha HJ, Bae S, Jung JH, Lee SM, et al. MicroRNAs that respond to histone deacetylase inhibitor SAHA and p53 in HCT116 human colon carcinoma cells. *Int J Oncol*. 2009b; **35**(6): 1343-52.

Siavoshian S, Blottiere HM, Cherbut C, Galmiche JP. Butyrate stimulates cyclin D and p21 and inhibits cyclin-dependent kinase 2 expression in HT-29 colonic epithelial cells. *Biochem Biophys Res Commun*. 1997; **232**(1): 169-72.

Siavoshian S, Segain JP, Kornprobst M, Bonnet C, Cherbut C, Galmiche JP, et al. Butyrate and trichostatin A effects on the proliferation/differentiation of human intestinal epithelial cells: induction of cyclin D3 and p21 expression. *Gut*. 2000; **46**(4): 507-14.

Simonsson M, Heldin C-H, Ericsson J, Gronroos E. The balance between acetylation and deacetylation controls Smad7 stability. *J Biol Chem*. 2005; **280**(23): 21797-803.

Singh PN, Fraser GE. Dietary risk factors for colon cancer in a low-risk population. *Am J Epidemiol*. 1998; **148**(8): 761-74.

Siu LL, Pili R, Duran I, Messersmith WA, Chen EX, Sullivan R, et al. Phase I study of MGCD0103 given as a three-times-per-week oral dose in patients with advanced solid tumors. *J Clin Oncol*. 2008; **26**(12): 1940-7.

Slaby O, Svoboda M, Fabian P, Smerdova T, Knoflickova D, Bednarikova M, et al. Altered expression of miR-21, miR-31, miR-143 and miR-145 is related to clinicopathologic features of colorectal cancer. *Oncology*. 2007; **72**(5-6): 397-402.

Slattery ML, Wolff E, Hoffman MD, Pellatt DF, Milash B, Wolff RK. MicroRNAs and colon and rectal cancer: differential expression by tumor location and subtype. *Genes Chromosomes Cancer*. 2011; **50**(3): 196-206.

Smyth GK. Limma: Linear models for microarray data. Gentleman R, Carey V, Dudoit S, Irizarry R, Huber W. Bioinformatics and computational biology solutions using R and bioconductor. New York: Springer; 2005.

Snippert HJ, van der Flier LG, Sato T, van Es JH, van den Born M, Kroon-Veenboer C, et al. Intestinal crypt homeostasis results from neutral competition between symmetrically dividing Lgr5 stem cells. *Cell*. 2010; **143**(1): 134-44.

Solomon MJ, Larsen PL, Varshavsky A. Mapping protein-DNA interactions in vivo with formaldehyde: evidence that histone H4 is retained on a highly transcribed gene. *Cell*. 1988; **53**(6): 937-47.

Song Y, Xu Y, Wang Z, Chen Y, Yue Z, Gao P, et al. MicroRNA-148b suppresses cell growth by targeting cholecystokinin-2 receptor in colorectal cancer. *Int J Cancer*. 2012; **131**(5): 1042-51.

Spring KJ, Zhao ZZ, Karamatic R, Walsh MD, Whitehall VLJ, Pike T, et al. High prevalence of sessile serrated adenomas with BRAF mutations: a prospective study of patients undergoing colonoscopy. *Gastroenterology*. 2006; **131**(5): 1400-7.

Stark GR, Kerr IM, Williams BR, Silverman RH, Schreiber RD. How cells respond to interferons. *Annu Rev Biochem*. 1998; **67**: 227-64.

Starlard-Davenport A, Tryndyak V, Kosyk O, Ross SR, Rusyn I, Beland FA, et al. Dietary methyl deficiency, microRNA expression and susceptibility to liver carcinogenesis. *J Nutrigenet Nutrigenomics*. 2010; **3**(4-6): 259-66.

Stathis A, Hotte SJ, Chen EX, Hirte HW, Oza AM, Moretto P, et al. Phase I study of decitabine in combination with vorinostat in patients with advanced solid tumors and non-Hodgkin's lymphomas. *Clin Cancer Res*. 2011; **17**(6): 1582-90.

Staton AA, Giraldez AJ. Use of target protector morpholinos to analyze the physiological roles of specific miRNA-mRNA pairs in vivo. *Nat Protoc*. 2011; **6**(12): 2035-49.

Steele NL, Plumb JA, Vidal L, Tjornelund J, Knoblauch P, Rasmussen A, et al. A phase 1 pharmacokinetic and pharmacodynamic study of the histone deacetylase inhibitor belinostat in patients with advanced solid tumors. *Clin Cancer Res*. 2008; **14**(3): 804-10.

Stephen AM, Haddad AC, Phillips SF. Passage of carbohydrate into the colon. Direct measurements in humans. *Gastroenterology*. 1983; **85**(3): 589-95.

Strahl BD, Allis CD. The language of covalent histone modifications. *Nature*. 2000; **403**(6765): 41-5.

Sturlan S, Kapitanovic S, Kovacevic D, Lukac J, Spaventi S, Spaventi R, et al. Loss of heterozygosity of APC and DCC tumor suppressor genes in human sporadic colon cancer. *J Mol Med*. 1999; **77**(3): 316-21.

Suarez Y, Fernandez-Hernando C, Yu J, Gerber SA, Harrison KD, Pober JS, et al. Dicer-dependent endothelial microRNAs are necessary for postnatal angiogenesis. *Proc Natl Acad Sci U S A*. 2008; **105**(37): 14082-7.

Suh N, Blelloch R. Small RNAs in early mammalian development: from gametes to gastrulation. *Development*. 2011; **138**(9): 1653-61.

Sui G, Soohoo C, Affar EB, Gay F, Shi Y, Forrester WC, et al. A DNA vector-based RNAi technology to suppress gene expression in mammalian cells. *Proc Natl Acad Sci U S A*. 2002; **99**(8): 5515-20.

Sun K, Wang W, Zeng JJ, Wu CT, Lei ST, Li GX. MicroRNA-221 inhibits CDKN1C/p57 expression in human colorectal carcinoma. *Acta Pharmacol Sin*. 2011; **32**(3): 375-84.

Sun M, Estrov Z, Ji Y, Coombes KR, Harris DH, Kurzrock R. Curcumin (diferuloylmethane) alters the expression profiles of microRNAs in human pancreatic cancer cells. *Mol Cancer Ther*. 2008; **7**(3): 464-73.

Sun PC, Tzao C, Chen BH, Liu CW, Yu CP, Jin JS. Suberoylanilide hydroxamic acid induces apoptosis and sub-G1 arrest of 320 HSR colon cancer cells. *J Biomed Sci*. 2010; **17**: 76.

Sung MW, Waxman S. Combination of cytotoxic-differentiation therapy with 5-fluorouracil and phenylbutyrate in patients with advanced colorectal cancer. *Anticancer Res*. 2007; **27**(2): 995-1001.

Suraweera N, Duval A, Reperant M, Vaury C, Furlan D, Leroy K, et al. Evaluation of tumor microsatellite instability using five quasimonomorphic mononucleotide repeats and pentaplex PCR. *Gastroenterology*. 2002; **123**(6): 1804-11.

Suto RK, Clarkson MJ, Tremethick DJ, Luger K. Crystal structure of a nucleosome core particle containing the variant histone H2A.Z. *Nat Struct Biol*. 2000; **7**(12): 1121-4.

Suzuki H, Takatsuka S, Akashi H, Yamamoto E, Nojima M, Maruyama R, et al. Genome-wide profiling of chromatin signatures reveals epigenetic regulation of MicroRNA genes in colorectal cancer. *Cancer Res*. 2011; **71**(17): 5646-58.

Svoboda P, Stein P, Hayashi H, Schultz RM. Selective reduction of dormant maternal mRNAs in mouse oocytes by RNA interference. *Development*. 2000; **127**(19): 4147-56.

Sylvestre Y, De Guire V, Querido E, Mukhopadhyay UK, Bourdeau V, Major F, et al. An E2F/miR-20a autoregulatory feedback loop. *J Biol Chem*. 2007; **282**(4): 2135-43.

Tagawa H, Karube K, Tsuzuki S, Ohshima K, Seto M. Synergistic action of the microRNA-17 polycistron and Myc in aggressive cancer development. *Cancer Sci*. 2007; **98**(9): 1482-90.

Takakura S, Mitsutake N, Nakashima M, Namba H, Saenko VA, Rogounovitch TI, et al. Oncogenic role of miR-17-92 cluster in anaplastic thyroid cancer cells. *Cancer Sci*. 2008; **99**(6): 1147-54.

Taniguchi T, Iwashita J, Murata J, Ueda K, Abe T. The histone deacetylase inhibitor trichostatin A induces cell cycle arrest and rapid upregulation of gadd45β in LS174T human colon cancer cells. *ABC*. 2012; **2**: 43-50.

Tanzer A, Stadler PF. Molecular evolution of a microRNA cluster. *J Mol Biol*. 2004; **339**(2): 327-35.

Tao J, Wu D, Li P, Xu B, Lu Q, Zhang W. microRNA-18a, a member of the oncogenic miR-17-92 cluster, targets Dicer and suppresses cell proliferation in bladder cancer T24 cells. *Mol Med Report*. 2012; **5**(1): 167-72.

Tazawa H, Tsuchiya N, Izumiya M, Nakagama H. Tumor-suppressive miR-34a induces senescence-like growth arrest through modulation of the E2F pathway in human colon cancer cells. *Proc Natl Acad Sci U S A*. 2007; **104**(39): 15472-7.

Terry P, Giovannucci E, Michels KB, Bergkvist L, Hansen H, Holmberg L, et al. Fruit, vegetables, dietary fiber, and risk of colorectal cancer. *J Natl Cancer Inst*. 2001; **93**(7): 525-33.

Tetsu O, McCormick F. Beta-catenin regulates expression of cyclin D1 in colon carcinoma cells. *Nature*. 1999; **398**(6726): 422-6.

Thiagalingam S, Cheng K-H, Lee HJ, Mineva N, Thiagalingam A, Ponte JF. Histone deacetylases: unique players in shaping the epigenetic histone code. *Ann N Y Acad Sci*. 2003; **983**: 84-100.

Thiagalingam S, Laken S, Willson JK, Markowitz SD, Kinzler KW, Vogelstein B, et al. Mechanisms underlying losses of heterozygosity in human colorectal cancers. *Proc Natl Acad Sci U S A*. 2001; **98**(5): 2698-702.

Thibodeau SN, Bren G, Schaid D. Microsatellite instability in cancer of the proximal colon. *Science*. 1993; **260**(5109): 816-9.

Thomson JM, Newman M, Parker JS, Morin-Kensicki EM, Wright T, Hammond SM. Extensive post-transcriptional regulation of microRNAs and its implications for cancer. *Genes Dev*. 2006; **20**(16): 2202-7.

Thomson JM, Parker J, Perou CM, Hammond SM. A custom microarray platform for analysis of microRNA gene expression. *Nat Methods*. 2004; **1**(1): 47-53.

Thorne AW, Kmiciek D, Mitchelson K, Sautiere P, Crane-Robinson C. Patterns of histone acetylation. *Eur J Biochem*. 1990; **193**(3): 701-13.

Tiemersma EW, Kampman E, Bueno de Mesquita HB, Bunschoten A, van Schothorst EM, Kok FJ, et al. Meat consumption, cigarette smoking, and genetic susceptibility in the etiology of colorectal cancer: results from a Dutch prospective study. *Cancer Causes Control*. 2002; **13**(4): 383-93.

Toden S, Bird AR, Topping DL, Conlon MA. Resistant starch prevents colonic DNA damage induced by high dietary cooked red meat or casein in rats. *Cancer Biol Ther*. 2006; **5**(3): 267-72.

Toden S, Bird AR, Topping DL, Conlon MA. High red meat diets induce greater numbers of colonic DNA double-strand breaks than white meat in rats: attenuation by high-amylose maize starch. *Carcinogenesis*. 2007; **28**(11): 2355-62.

Topping DL, Clifton PM. Short-chain fatty acids and human colonic function: roles of resistant starch and nonstarch polysaccharides. *Physiol Rev*. 2001; **81**(3): 1031-64.

Torlakovic E, Skovlund E, Snover DC, Torlakovic G, Nesland JM. Morphologic reappraisal of serrated colorectal polyps. *Am J Surg Pathol*. 2003; **27**(1): 65-81.

Toyota M, Ahuja N, Ohe-Toyota M, Herman JG, Baylin SB, Issa JP. CpG island methylator phenotype in colorectal cancer. *Proc Natl Acad Sci U S A*. 1999; **96**(15): 8681-6.

Toyota M, Suzuki H, Sasaki Y, Maruyama R, Imai K, Shinomura Y, et al. Epigenetic silencing of microRNA-34b/c and B-cell translocation gene 4 is associated with CpG island methylation in colorectal cancer. *Cancer Res*. 2008; **68**(11): 4123-32.

Tran DH, Satou K, Ho TB. Finding microRNA regulatory modules in human genome using rule induction. *BMC Bioinformatics*. 2008; **9 Suppl 12**: S5.

Trang P, Wiggins JF, Daige CL, Cho C, Omotola M, Brown D, et al. Systemic delivery of tumor suppressor microRNA mimics using a neutral lipid emulsion inhibits lung tumors in mice. *Mol Ther*. 2011; **19**(6): 1116-22.

Tryndyak VP, Ross SA, Beland FA, Pogribny IP. Down-regulation of the microRNAs miR-34a, miR-127, and miR-200b in rat liver during hepatocarcinogenesis induced by a methyl-deficient diet. *Mol Carcinog*. 2009; **48**(6): 479-87.

Tsang WP, Kwok TT. The miR-18a* microRNA functions as a potential tumor suppressor by targeting on K-Ras. *Carcinogenesis*. 2009; **30**(6): 953-9.

Tsang WP, Ng EK, Ng SS, Jin H, Yu J, Sung JJ, et al. Oncofetal H19-derived miR-675 regulates tumor suppressor RB in human colorectal cancer. *Carcinogenesis*. 2010; **31**(3): 350-8.

Tsuchida A, Ohno S, Wu W, Borjigin N, Fujita K, Aoki T, et al. miR-92 is a key oncogenic component of the miR-17-92 cluster in colon cancer. *Cancer Sci*. 2011; **102**(12): 2264-71.

Tsuchiya S, Fujiwara T, Sato F, Shimada Y, Tanaka E, Sakai Y, et al. MicroRNA-210 regulates cancer cell proliferation through targeting fibroblast growth factor receptor-like 1 (FGFRL1). *J Biol Chem*. 2011; **286**(1): 420-8.

Tsuji N, Kobayashi M, Nagashima K, Wakisaka Y, Koizumi K. A new antifungal antibiotic, trichostatin. *J Antibiot*. 1976; **29**(1): 1-6.

Turner BM. Histone acetylation as an epigenetic determinant of long-term transcriptional competence. *Cell Mol Life Sci*. 1998; **54**(1): 21-31.

Ushigome M, Ubagai T, Fukuda H, Tsuchiya N, Sugimura T, Takatsuka J, et al. Up-regulation of hnRNP A1 gene in sporadic human colorectal cancers. *Int J Oncol*. 2005; **26**(3): 635-40.

Valeri N, Gasparini P, Braconi C, Paone A, Lovat F, Fabbri M, et al. MicroRNA-21 induces resistance to 5-fluorouracil by down-regulating human DNA MutS homolog 2 (hMSH2). *Proc Natl Acad Sci U S A*. 2010; **107**(49): 21098-103.

van de Wetering M, Sancho E, Verweij C, de Lau W, Oving I, Hurlstone A, et al. The beta-catenin/TCF-4 complex imposes a crypt progenitor phenotype on colorectal cancer cells. *Cell*. 2002; **111**(2): 241-50.

Van Lint C, Emiliani S, Verdin E. The expression of a small fraction of cellular genes is changed in response to histone hyperacetylation. *Gene Expr*. 1996; **5**(4-5): 245-53.

van Rooij E. The art of microRNA research. *Circ Res*. 2011; **108**(2): 219-34.

van Rooij E, Sutherland LB, Liu N, Williams AH, McAnally J, Gerard RD, et al. A signature pattern of stress-responsive microRNAs that can evoke cardiac hypertrophy and heart failure. *Proc Natl Acad Sci U S A*. 2006; **103**(48): 18255-60.

van Seventer GA, Salmen HJ, Law SF, O'Neill GM, Mullen MM, Franz AM, et al. Focal adhesion kinase regulates beta1 integrin-dependent T cell migration through an HEF1 effector pathway. *Eur J Immunol*. 2001; **31**(5): 1417-27.

Vanhoutvin SA, Troost FJ, Hamer HM, Lindsey PJ, Koek GH, Jonkers DM, et al. Butyrate-induced transcriptional changes in human colonic mucosa. *PLoS One*. 2009; **4**(8): e6759.

Vansteenkiste J, Van Cutsem E, Dumez H, Chen C, Ricker JL, Randolph SS, et al. Early phase II trial of oral vorinostat in relapsed or refractory breast, colorectal, or non-small cell lung cancer. *Invest New Drugs*. 2008; **26**(5): 483-8.

Ventura A, Young AG, Winslow MM, Lintault L, Meissner A, Erkeland SJ, et al. Targeted deletion reveals essential and overlapping functions of the miR-17 through 92 family of miRNA clusters. *Cell*. 2008; **132**(5): 875-86.

Venturini L, Battmer K, Castoldi M, Schultheis B, Hochhaus A, Muckenthaler MU, et al. Expression of the miR-17-92 polycistron in chronic myeloid leukemia (CML) CD34+ cells. *Blood*. 2007; **109**(10): 4399-405.

Vickers MM, Bar J, Gorn-Hondermann I, Yarom N, Daneshmand M, Hanson JE, et al. Stage-dependent differential expression of microRNAs in colorectal cancer: potential role as markers of metastatic disease. *Clin Exp Metastasis*. 2012; **29**(2): 123-32.

Vogelstein B, Fearon ER, Hamilton SR, Kern SE, Preisinger AC, Leppert M, et al. Genetic alterations during colorectal-tumor development. *N Engl J Med*. 1988; **319**(9): 525-32.

Volinia S, Calin GA, Liu CG, Ambs S, Cimmino A, Petrocca F, et al. A microRNA expression signature of human solid tumors defines cancer gene targets. *Proc Natl Acad Sci U S A*. 2006; **103**(7): 2257-61.

Wallace K, Grau MV, Levine AJ, Shen L, Hamdan R, Chen X, et al. Association between folate levels and CpG Island hypermethylation in normal colorectal mucosa. *Cancer Prev Res*. 2010; **3**(12): 1552-64.

Wang B, Majumder S, Nuovo G, Kutay H, Volinia S, Patel T, et al. Role of microRNA-155 at early stages of hepatocarcinogenesis induced by choline-deficient and amino acid-defined diet in C57BL/6 mice. *Hepatology*. 2009a; **50**(4): 1152-61.

Wang CJ, Zhou ZG, Wang L, Yang L, Zhou B, Gu J, et al. Clinicopathological significance of microRNA-31, -143 and -145 expression in colorectal cancer. *Dis Markers*. 2009b; **26**(1): 27-34.

Wang H, Wu J, Meng X, Ying X, Zuo Y, Liu R, et al. MicroRNA-342 inhibits colorectal cancer cell proliferation and invasion by directly targeting DNA methyltransferase 1. *Carcinogenesis*. 2011; **32**(7): 1033-42.

Wang S, Aurora AB, Johnson BA, Qi X, McAnally J, Hill JA, et al. The endothelial-specific microRNA miR-126 governs vascular integrity and angiogenesis. *Dev Cell*. 2008; **15**(2): 261-71.

Wang X, Tournier C. Regulation of cellular functions by the ERK5 signalling pathway. *Cell Signal*. 2006; **18**(6): 753-60.

Wang YX, Zhang XY, Zhang BF, Yang CQ, Chen XM, Gao HJ. Initial study of microRNA expression profiles of colonic cancer without lymph node metastasis. *J Dig Dis*. 2010; **11**(1): 50-4.

Wang Z. The guideline of the design and validation of MiRNA mimics. *Methods Mol Biol*. 2011; **676**: 211-23.

Wang Z, Cummins JM, Shen D, Cahill DP, Jallepalli PV, Wang T-L, et al. Three classes of genes mutated in colorectal cancers with chromosomal instability. *Cancer Res*. 2004; **64**(9): 2998-3001.

Wang Z, Zhang X, Yang Z, Du H, Wu Z, Gong J, et al. MiR-145 regulates PAK4 via the MAPK pathway and exhibits an antitumor effect in human colon cells. *Biochem Biophys Res Commun*. 2012; **427**(3): 444-9.

Warburg O. On the origin of cancer cells. *Science*. 1956; **123**(3191): 309-14.

Watamoto K, Towatari M, Ozawa Y, Miyata Y, Okamoto M, Abe A, et al. Altered interaction of HDAC5 with GATA-1 during MEL cell differentiation. *Oncogene*. 2003; **22**(57): 9176-84.

WCRF. Food, Nutrition, Physical Activity and the Prevention of Cancer: a Global Perspective. Washington DC: World Cancer Research Fund / American Institute for Cancer Research; 2007.

Weisenberger DJ, Siegmund KD, Campan M, Young J, Long TI, Faasse MA, et al. CpG island methylator phenotype underlies sporadic microsatellite instability and is tightly associated with BRAF mutation in colorectal cancer. *Nat Genet*. 2006; **38**(7): 787-93.

Whitehead RP, Rankin C, Hoff PMG, Gold PJ, Billingsley KG, Chapman RA, et al. Phase II trial of romidepsin (NSC-630176) in previously treated colorectal cancer patients with advanced disease: a Southwest Oncology Group study (S0336). *Invest New Drugs*. 2009; **27**(5): 469-75.

Whittaker SJ, Demierre M-F, Kim EJ, Rook AH, Lerner A, Duvic M, et al. Final results from a multicenter, international, pivotal study of romidepsin in refractory cutaneous T-cell lymphoma. *J Clin Oncol*. 2010; **28**(29): 4485-91.

Wianny F, Zernicka-Goetz M. Specific interference with gene function by double-stranded RNA in early mouse development. *Nat Cell Biol*. 2000; **2**(2): 70-5.

Wightman B, Ha I, Ruvkun G. Posttranscriptional regulation of the heterochronic gene lin-14 by lin-4 mediates temporal pattern formation in C. elegans. *Cell*. 1993; **75**(5): 855-62.

Willett WC, Stampfer MJ, Colditz GA, Rosner BA, Speizer FE. Relation of meat, fat, and fiber intake to the risk of colon cancer in a prospective study among women. *N Engl J Med*. 1990; **323**(24): 1664-72.

Williams AC, Browne SJ, Hague A, Collard T, Palmer G, Paraskeva C. Apoptosis, differentiation, and the control of colonic cell numbers. Domschke W, Stoll R,

Brasitus TA, Kagnoff MF. Intestinal Mucosa and its Diseases - Pathophysiology and Clinics. New York: Springer; 1999.

Williams AC, Hague A, Manning AM, Van der Stappen JW, Paraskeva C. In vitro models of human colorectal cancer. *Cancer Surv.* 1993; **16**: 15-29.

Williams AH, Valdez G, Moresi V, Qi X, McAnally J, Elliott JL, et al. MicroRNA-206 delays ALS progression and promotes regeneration of neuromuscular synapses in mice. *Science.* 2009; **326**(5959): 1549-54.

Williams EA, Coxhead JM, Mathers JC. Anti-cancer effects of butyrate: use of micro-array technology to investigate mechanisms. *Proc Nutr Soc.* 2003; **62**(1): 107-15.

Williams P, Droulez V. Australian red meat consumption - implications of changes over 20 years on nutrient composition. *Food Australia.* 2010; **62**(3): 87-94.

Wilson AJ, Byun DS, Popova N, Murray LB, L'Italien K, Sowa Y, et al. Histone deacetylase 3 (HDAC3) and other class I HDACs regulate colon cell maturation and p21 expression and are deregulated in human colon cancer. *J Biol Chem.* 2006; **281**(19): 13548-58.

Wilson AJ, Chueh AC, Togel L, Corner GA, Ahmed N, Goel S, et al. Apoptotic sensitivity of colon cancer cells to histone deacetylase inhibitors is mediated by an Sp1/Sp3-activated transcriptional program involving immediate-early gene induction. *Cancer Res.* 2010a; **70**(2): 609-20.

Wilson PM, El-Khoueiry A, Iqbal S, Fazzone W, LaBonte MJ, Groshen S, et al. A phase I/II trial of vorinostat in combination with 5-fluorouracil in patients with metastatic colorectal cancer who previously failed 5-FU-based chemotherapy. *Cancer Chemother Pharmacol.* 2010b; **65**(5): 979-88.

Winawer SJ, Zauber AG, Fletcher RH, Stillman JS, O'Brien MJ, Levin B, et al. Guidelines for colonoscopy surveillance after polypectomy: a consensus update by the US Multi-Society Task Force on Colorectal Cancer and the American Cancer Society. *CA Cancer J Clin.* 2006; **56**(3): 143-59; quiz 84-5.

Winawer SJ, Zauber AG, Ho MN, O'Brien MJ, Gottlieb LS, Sternberg SS, et al. Prevention of colorectal cancer by colonoscopic polypectomy. The National Polyp Study Workgroup. *N Engl J Med.* 1993; **329**(27): 1977-81.

Winter J, Nyskohus L, Young GP, Hu Y, Conlon MA, Bird AR, et al. Inhibition by resistant starch of red meat-induced promutagenic adducts in mouse colon. *Cancer Prev Res.* 2011; **4**(11): 1920-8.

Witt O, Deubzer HE, Milde T, Oehme I. HDAC family: What are the cancer relevant targets? *Cancer Lett.* 2009; **277**(1): 8-21.

Wong P, Iwasaki M, Somervaille TC, Ficara F, Carico C, Arnold C, et al. The miR-17-92 microRNA polycistron regulates MLL leukemia stem cell potential by modulating p21 expression. *Cancer Res.* 2010; **70**(9): 3833-42.

Woods K, Thomson JM, Hammond SM. Direct regulation of an oncogenic micro-RNA cluster by E2F transcription factors. *J Biol Chem.* 2007; **282**(4): 2130-4.

Workman JL. Nucleosome displacement in transcription. *Genes Dev.* 2006; **20**(15): 2009-17.

Worthley DL, Le Leu RK, Whitehall VL, Conlon M, Christophersen C, Belobrajdic D, et al. A human, double-blind, placebo-controlled, crossover trial of prebiotic, probiotic, and synbiotic supplementation: effects on luminal, inflammatory, epigenetic, and epithelial biomarkers of colorectal cancer. *Am J Clin Nutr.* 2009; **90**(3): 578-86.

Wu JT, Archer SY, Hinnebusch B, Meng S, Hodin RA. Transient vs. prolonged histone hyperacetylation: effects on colon cancer cell growth, differentiation, and apoptosis. *Am J Physiol Gastrointest Liver Physiol.* 2001; **280**(3): G482-90.

Wu L, Fan J, Belasco JG. MicroRNAs direct rapid deadenylation of mRNA. *Proc Natl Acad Sci U S A.* 2006; **103**(11): 4034-9.

Xi Y, Formentini A, Chien M, Weir DB, Russo JJ, Ju J, et al. Prognostic Values of microRNAs in Colorectal Cancer. *Biomark Insights*. 2006; **2**: 113-21.

Xia D, Holla VR, Wang D, Menter DG, DuBois RN. HEF1 is a crucial mediator of the proliferative effects of prostaglandin E(2) on colon cancer cells. *Cancer Res*. 2010; **70**(2): 824-31.

Xia X-G, Zhou H, Samper E, Melov S, Xu Z. Pol II-expressed shRNA knocks down Sod2 gene expression and causes phenotypes of the gene knockout in mice. *PLoS Genet*. 2006; **2**(1): e10.

Xiao C, Srinivasan L, Calado DP, Patterson HC, Zhang B, Wang J, et al. Lymphoproliferative disease and autoimmunity in mice with increased miR-17-92 expression in lymphocytes. *Nat Immunol*. 2008; **9**(4): 405-14.

Xiao H, Hasegawa T, Isobe K. p300 collaborates with Sp1 and Sp3 in p21(waf1/cip1) promoter activation induced by histone deacetylase inhibitor. *J Biol Chem*. 2000; **275**(2): 1371-6.

Xu WS, Parmigiani RB, Marks PA. Histone deacetylase inhibitors: molecular mechanisms of action. *Oncogene*. 2007; **26**(37): 5541-52.

Yamakuchi M, Yagi S, Ito T, Lowenstein CJ. MicroRNA-22 regulates hypoxia signaling in colon cancer cells. *PLoS One*. 2011; **6**(5): e20291.

Yamamichi N, Shimomura R, Inada K, Sakurai K, Haraguchi T, Ozaki Y, et al. Locked nucleic acid in situ hybridization analysis of miR-21 expression during colorectal cancer development. *Clin Cancer Res*. 2009; **15**(12): 4009-16.

Yan HL, Xue G, Mei Q, Wang YZ, Ding FX, Liu MF, et al. Repression of the miR-17-92 cluster by p53 has an important function in hypoxia-induced apoptosis. *EMBO J*. 2009; **28**(18): 2719-32.

Yang WM, Inouye C, Zeng Y, Bearss D, Seto E. Transcriptional repression by YY1 is mediated by interaction with a mammalian homolog of the yeast global regulator RPD3. *Proc Natl Acad Sci U S A*. 1996; **93**(23): 12845-50.

Yang Z, Chang Y-J, Miyamoto H, Yeh S, Yao JL, di Sant'Agnese PA, et al. Suppression of androgen receptor transactivation and prostate cancer cell growth by heterogeneous nuclear ribonucleoprotein A1 via interaction with androgen receptor coregulator ARA54. *Endocrinology*. 2007; **148**(3): 1340-9.

Yao YL, Yang WM, Seto E. Regulation of transcription factor YY1 by acetylation and deacetylation. *Mol Cell Biol*. 2001; **21**(17): 5979-91.

Yatabe Y, Tavare S, Shibata D. Investigating stem cells in human colon by using methylation patterns. *Proc Natl Acad Sci U S A*. 2001; **98**(19): 10839-44.

Yi R, Qin Y, Macara IG, Cullen BR. Exportin-5 mediates the nuclear export of pre-microRNAs and short hairpin RNAs. *Genes Dev*. 2003; **17**(24): 3011-6.

Yin J, Kong D, Wang S, Zou TT, Souza RF, Smolinski KN, et al. Mutation of hMSH3 and hMSH6 mismatch repair genes in genetically unstable human colorectal and gastric carcinomas. *Hum Mutat*. 1997; **10**(6): 474-8.

Yoshida M, Beppu T. Reversible arrest of proliferation of rat 3Y1 fibroblasts in both the G1 and G2 phases by trichostatin A. *Exp Cell Res*. 1988; **177**(1): 122-31.

Yoshida M, Kijima M, Akita M, Beppu T. Potent and specific inhibition of mammalian histone deacetylase both in vivo and in vitro by trichostatin A. *J Biol Chem*. 1990; **265**(28): 17174-9.

Yoshida M, Nomura S, Beppu T. Effects of trichostatins on differentiation of murine erythroleukemia cells. *Cancer Res*. 1987; **47**(14): 3688-91.

Young GP, Hu Y, Le Leu RK, Nyskohus L. Dietary fibre and colorectal cancer: a model for environment--gene interactions. *Mol Nutr Food Res*. 2005; **49**(6): 571-84.

Young GP, Le Leu RK. Resistant starch and colorectal neoplasia. *J AOAC Int*. 2004; **87**(3): 775-86.

Yu G, Tang JQ, Tian ML, Li H, Wang X, Wu T, et al. Prognostic values of the miR-17-92 cluster and its paralogs in colon cancer. *J Surg Oncol*. 2012; **106**(3): 232-7.

Yu J-Y, DeRuiter SL, Turner DL. RNA interference by expression of short-interfering RNAs and hairpin RNAs in mammalian cells. *Proc Natl Acad Sci U S A*. 2002; **99**(9): 6047-52.

Yuan Z-L, Guan Y-J, Chatterjee D, Chin YE. Stat3 dimerization regulated by reversible acetylation of a single lysine residue. *Science*. 2005; **307**(5707): 269-73.

Zamore PD, Tuschl T, Sharp PA, Bartel DP. RNAi: double-stranded RNA directs the ATP-dependent cleavage of mRNA at 21 to 23 nucleotide intervals. *Cell*. 2000; **101**(1): 25-33.

Zampetaki A, Kiechl S, Drozdov I, Willeit P, Mayr U, Prokopi M, et al. Plasma microRNA profiling reveals loss of endothelial miR-126 and other microRNAs in type 2 diabetes. *Circ Res*. 2010; **107**(6): 810-7.

Zeng Y, Cullen BR. Sequence requirements for micro RNA processing and function in human cells. *Rna*. 2003; **9**(1): 112-23.

Zeng Y, Yi R, Cullen BR. Recognition and cleavage of primary microRNA precursors by the nuclear processing enzyme Drosha. *EMBO Journal*. 2005; **24**(1): 138-48.

Zerbe LK, Pino I, Pio R, Cosper PF, Dwyer-Nield LD, Meyer AM, et al. Relative amounts of antagonistic splicing factors, hnRNP A1 and ASF/SF2, change during neoplastic lung growth: implications for pre-mRNA processing. *Mol Carcinog*. 2004; **41**(4): 187-96.

Zhang CL, McKinsey TA, Olson EN. Association of class II histone deacetylases with heterochromatin protein 1: potential role for histone methylation in control of muscle differentiation. *Mol Cell Biol*. 2002; **22**(20): 7302-12.

Zhang H, Hao Y, Yang J, Zhou Y, Li J, Yin S, et al. Genome-wide functional screening of miR-23b as a pleiotropic modulator suppressing cancer metastasis. *Nat Commun*. 2011; **2**: 554.

Zhang S, Cai X, Huang F, Zhong W, Yu Z. Effect of trichostatin a on viability and microRNA expression in human pancreatic cancer cell line BxPC-3. *Exp Oncol*. 2008; **30**(4): 265-8.

Zhang Y, Ng HH, Erdjument-Bromage H, Tempst P, Bird A, Reinberg D. Analysis of the NuRD subunits reveals a histone deacetylase core complex and a connection with DNA methylation. *Genes Dev*. 1999; **13**(15): 1924-35.

Zhao J-J, Sun D-G, Wang J, Liu S-R, Zhang C-Y, Zhu M-X, et al. Retinoic acid downregulates microRNAs to induce abnormal development of spinal cord in spina bifida rat model. *Childs Nerv Syst*. 2008; **24**(4): 485-92.

Zhao Y, Lu S, Wu L, Chai G, Wang H, Chen Y, et al. Acetylation of p53 at lysine 373/382 by the histone deacetylase inhibitor depsipeptide induces expression of p21(Waf1/Cip1). *Mol Cell Biol*. 2006; **26**(7): 2782-90.

Zheng G, Yang Y-C. Sumoylation and acetylation play opposite roles in the transactivation of PLAG1 and PLAGL2. *J Biol Chem*. 2005; **280**(49): 40773-81.

Zheng H, Pritchard DM, Yang X, Bennett E, Liu G, Liu C, et al. KLF4 gene expression is inhibited by the notch signaling pathway that controls goblet cell differentiation in mouse gastrointestinal tract. *Am J Physiol Gastrointest Liver Physiol*. 2009; **296**(3): G490-8.

Zhu P, Martin E, Mengwasser J, Schlag P, Janssen KP, Gottlicher M. Induction of HDAC2 expression upon loss of APC in colorectal tumorigenesis. *Cancer Cell*. 2004; **5**(5): 455-63.

Zhu S, Si M-L, Wu H, Mo Y-Y. MicroRNA-21 targets the tumor suppressor gene tropomyosin 1 (TPM1). *J Biol Chem*. 2007; **282**(19): 14328-36.